



University
of Naples
Federico II

Faculty of
Engineering

Seismic Retrofitting and Restoration
of Historical Buildings
Using Innovative Materials:
the Case of Carmine's Bell Tower
in Naples

Simona Voto



Ph.D. Programme in Materials and Structures

UNIVERSITY OF NAPLES FEDERICO II
Faculty of Engineering

PH.D. PROGRAMME in MATERIALS and STRUCTURES
COORDINATOR PROF. DOMENICO ACIERNO
XXII CYCLE



SIMONA VOTO

PH.D. THESIS

**Seismic Retrofitting and Restoration of Historical
Buildings Using Innovative Materials:
the Case of Carmine's Bell Tower in Naples**

TUTOR PROF. GAETANO MANFREDI
CO-TUTOR DR. FRANCESCA CERONI

A Mena e Claudio

Acknowledgments

At the end of my training cycle and scientific investigation I would like to thank all the people who accompanied me on this professional pathway and who played a key role not only for my professional education, but mainly for my human experience.

I wish to express my most sincere appreciations to Prof. Gaetano Manfredi for his tutorship and Prof. Domenico Acierno, the Ph.D. course coordinator, for making this work possible and for giving me the opportunity to investigate a research topic so attracting for me.

I wish to heartily thank Dr. Francesca Ceroni who with her patient and constant supervision guided me in this job. Thanks Francesca to have accompanied me in an extra adventure on the Carmine Church's Bell Tower.

I wish to congratulate Ing. Palmaccio for his terrific help in the project numerical analysis.

I would like to thank all friends and colleagues in the Department of Structural Engineering who contributed in numerous ways to make this programme an enjoyable one.

This work would not have been possible without the willingness of Superintendence for Architectural Heritage and Culture of Naples, in the person of the architect Tobia di Ronza, who made available all the material in their possession and allowed to conduct all necessary inspections and surveys.

A special wish to the people of the historical Archive of Simancas for their invaluable support in the historical reconstruction of the Carmine complex

A deeply felt thank to the Friars of the Carmine Complex that opened the doors of their home and their private archives to me

A particularly strong kiss to Maestro Maurizio Rea, the Carmine Church's organist, that stroke the sentimental notes of my heart with his celestial art.

Many thanks to Geom. De Lorenzo of Restauro&Recuperi S.p.A for his key support during all the different phases of the project.

I would like to thanks also the TECNOIN srl and STRAGO srl for performing the experimental tests and the dynamic structural investigation.

Finally a special thank to my parents: to my father for teaching me equilibrium and rationality and for transmitting me the passion for the research and to my mother that was so sympathetic with me always ready to offer me a smile in my darkest hours. Thanks both of you for believing in me every single day of my

life. The love and the admiration I feel for them cannot be described in so few words.

I would like to express my deep love to my beloved brother and sister for being so close to me with their love.

Last but not least, I wish to express my deep gratitude to my dear Morten André, for the encouragement and support constantly offered to me during the research

My heartily thanks to André's whole family: without the fabulous support of the Helland's, the elaboration of this thesis would not have been possible. Thanks to all of them.

A special thank to Per Arne for being so sympathetic in encouraging me to go ahead on this effort.

Finally thanks to myself that realized all this.

Index

ACKNOWLEDGMENTS

CHAPTER I

INTRODUCTION

1.1	GENERAL REMARKS	3
1.2	OBJECTIVE AND SCOPE OF THE THESIS	11
1.3	REFERENCES	15

CHAPTER II

HISTORICAL INVESTIGATION

2.1	URBAN FRAMING	17
2.2.	THE “MERCATO” DISTRICT AND ITS HISTORICAL DEVELOPMENT	19
2.2.1	Origins	19
2.2.2	The Angevin Reign	20
2.2.3	The suburb in the Aragonese and Spanish period	22

2.2.4	From the Austrian reign to the Risanamento	24
2.2.5	Post Second World War	25
2.3	HISTORICAL EVOLUTION OF THE CHURCH OF “SANTA MARIA DEL CARMINE MAGGIORE” AND ITS BELL TOWER	29
2.3.1	The foundation	29
2.3.2	The Gothic structure	32
2.3.3	The Aragonese structure	36
2.3.4	The Spanish structure	39
2.4	REFERENCES	47

CHAPTER III

ARCHITECTURAL INVESTIGATION

3.1	HISTORICAL-CRITICAL ANALYSIS OF ARCHITECTURAL AND STRUCTURAL CHANGES OF THE CARMINE BELL TOWER	49
3.1.1	Cross linking between the history and the structure	49
3.1.2	Overview of the restoration carried out on the Bell Tower	60
3.2	GEOMETRIC SURVEY	66
3.3	DAMAGE SURVEY IN NON- STRUCTURAL ELEMENTS	72
3.4	REFERENCES	77

CHAPTER IV***STRUCTURAL INVESTIGATION***

4.1	MATERIAL SURVEY	79
4.1.1	Building techniques for masonry structures in Southern Italy	79
4.1.2	Analysis of material and wall textures of the Bell Tower	84
4.2	DAMAGE SURVEY IN STRUCTURAL ELEMENTS	86
4.3	IN SITU EXPERIMENTAL TESTS TO EVALUATE MECHANICAL PROPERTIES OF MATERIALS	91
4.3.1	Destructive test	92
4.3.1.1	<i>Stratigraphic logs and Visual examinations</i>	92
4.3.1.2	<i>Double flat jacks</i>	96
4.3.2	Non destructive test	99
4.3.2.1	<i>Sonic tests. Analysis with impact-echo technique</i>	99
4.4	EVALUATION OF STRESS DISTRIBUTION IN THE MATERIALS	104
4.4.1	Destructive test	104
4.4.1.1	<i>Single flat jacks</i>	104
4.4.1.2	<i>Measurement of steel tie-rod strain</i>	107
4.5	DINAMIC CHARACTERIZATION OF THE BELL TOWER	109
4.5.1	Strumentation and test procedure	109
4.5.2	Natural dynamic behaviour of the Bell Tower	113
4.5.3	Bell effects	116

4.5.4	Variability of dynamic parameters during the test	123
4.6	REFERENCES	126

CHAPTER V

ANALYSIS OF THE STRUCTURAL BEHAVIOR OF THE BELL TOWER OF CARMINE

5.1	STRUCTURAL BEHAVIOUR OF THE BELL TOWER	129
5.2	GLOBAL ANALYSIS OF THE STRUCTURE	131
5.2.1	The FEM model	131
5.2.2	Linear analysis for vertical loads	135
5.2.3	Modal dynamic analysis	142
5.2.4	Non linear static analysis	149
5.2.4.1	<i>Evaluation of the displacement capacity</i>	149
5.2.4.2	<i>Evaluation of displacement demand</i>	154
5.2.4.3	<i>Comparison between displacement capability and displacement demand</i>	157
5.3	ANALYSIS OF LOCAL MECHANISMS	161
5.3.1	Typologies of local mechanisms of masonry structures	162
5.3.2	Identification of local mechanisms in the bell tower	166
5.3.3	Verification of mechanisms according to the Italian Seismic Code	172
5.4	REFERENCES	177

CHAPTER VI***REHABILITATION WORKS***

6.1	DESIGN OF SEISMIC THREAT REHABILITATION	179
6.1.1	DESIGN AND INSTALLATION OF THE NEW TIES	184
6.1.1.1	<i>Choice and design criteria of innovative material for new ties</i>	184
6.1.1.2	<i>The scaffolding</i>	191
6.1.1.3	<i>Sequence of installation of new ties</i>	193
6.1.1.4	<i>Monitoring system</i>	196
6.2	RESTORATION OF NON-STRUCTURAL ELEMENTS	200
6.3	REFERENCES	207

CHAPTER VII

<i>CONCLUSIONS</i>	209
Appendix I	213
Appendix II	221
Appendix III	229
Appendix IV	231
Appendix V	253
Appendix VI	261
Appendix VII	271
Appendix VIII	283
Appendix IX	289
Appendix X	291

Chapter I

Introduction

1.1 GENERAL REMARKS

The evaluation of the state and the design of a restoration project for an historical construction recall technical and historical investigations involving various types of competences, in order to assess its main architectural features and effects superimposed by its history.

In Italy large part of the country is classified as seismic zone (OPCM 3431, 2005) [1]. For this reason the evaluation of the seismic vulnerability of existing historical masonry buildings requires the definition of an appropriate methodology that, in case of structural retrofit, will also be able to minimize the impact (Linee Guida, 2006) [2].

Many historical buildings located in the Mediterranean area are masonry constructions. Masonry is an assembly of heterogeneous materials (mortar, stones and filling material) with an intrinsic variability due to their particular origin. Most of them are hard to fit into specific categories, insofar as they present peculiarities that make them “one-offs” both in architectural and structural terms.

The current configuration of monuments is the result of interventions undergone in the course of their history that have changed the original structural

and architectural configuration. The several events that the historical heritage building has been subjected to over the time may have altered its original “unicum” imprinting. Changes have usually been introduced to repair damages caused by accidental events (earthquakes, wars, and fires), continuous actions (wind, rain, traffic) or functional and architectural reasons. Such changes over time of the original layout can have an impact on the local and global resistance mechanisms. This status amplifies the uncertainty about geometry, materials and interaction with other buildings. This implies that the assessment of the structural behaviour has to be approached through an assessment of the current condition of the structure and through the analysis of its history in terms of material properties, construction techniques, structural details, crack pattern, damage map, and material decay. Such aspects make each monumental building unique. So, its study should adequately incorporate multi-disciplinary investigations at local and global levels.

Seismic assessment of historical constructions is a difficult task due to the complexity of several factors involved, including the heterogeneity and uncertainty typical of the constituent materials, the intricate geometry configurations, and the cultural and artistic importance of this type of structure. The latter aspects entail a deep knowledge of the history of the construction and the design of retrofitting interventions according to two principles: *adjusting the structural safety to code standards* and *preserving the cultural heritage significance in order to hand it down to posterity*.

According to the International Council on Monuments and Sites (ICOMOS) recommendations (ICOMOS, 1964; ICOMOS, 2005) [3 & 4]:

“Diagnosis is based on historical, qualitative and quantitative approaches. The qualitative approach is mainly based on direct observation of the structural damage and material decay, as well as historical and archaeological research; whereas, the quantitative approach is mainly based on material and structural tests, monitoring and structural analysis”.

The main aim is to perform a diagnosis to characterize the current conditions of

the structure and identify the causes of the damage state (Lagomarsino et al., 2004 [5]; Modena et al., 2004 [6]). Only a well assessed diagnosis of the building can be the basis to perform safety evaluation and to plan interventions compatible with “minimum impact” requirements. Diagnosis of building and design of maintenance therapy and/or retrofitting need a detailed anamnesis phase based on both qualitative and quantitative approaches. A first important differentiation is identifying damages due to accidental events (i.e. earthquakes, fire, explosions, inappropriate functional additions and restorations) and damages caused by the normal use of the structure due to the loading conditions and the degradation of mechanical properties of materials. Evaluation of damage condition of a masonry structure should be aimed at establishing if the damage pattern is stable or if there is an evolution leading to a structural collapse.

This analysis useful to develop a reliable theoretical model and to design the correct interventions (Modena et al., 2002) [7]), may be grouped in three different categories:

- *Historical;*
- *Architectural;*
- *Structural.*

All the collected data from this analysis must be interpreted considering that “*conservation, reinforcement and restoration of architectural heritage artefacts require a multi-disciplinary approach*” (ICOMOS Recommendations, 2005) [4].

Historical, archival and bibliographical investigations are useful for a historical-critical analysis necessary to characterize, analyze and record the origin of the structure and the vicissitudes during its history, its characteristic and anomalous elements, its structural morphology and its static conditions. Historical inquiries and archival research can clarify the reasons for interventions done in the past and can be very useful for understanding structural lack and deficiencies of the investigated structures. Important information may be drawn from studying the influence of neighbouring

buildings, in terms of constraint conditions, pushing actions, or contribution to mass participation for seismic actions.

A detailed geometrical survey (Binda et al., 2000) [8] makes possible the detection of characteristic features such as alignments, wall configurations, micro-cracks and construction details (Carpinteri et al., 2005) [9]. The structural performance of a masonry building may be dependent on all these parameters, both in terms of local and global behaviour. Usually heritage masonry constructions are characterized by a wide variability of wall texture, degree and quality of connections, type (i.e. stone blocks, bricks, mortar), size and assembling modes of constituent elements (i.e. arrangement and size of blocks), physical and mechanical properties of materials (i.e. unit weight, strength, elastic modulus). Furthermore mechanical properties are strictly dependent on their geological history and can be variable for stones of the same typology derived from different sites. The knowledge of different construction typologies and masonry texture is important to define the structural behaviour of buildings made of natural stone. The global performance of the structure depends on the local behaviour at the stone-mortar interfaces in the single element and on the interaction amongst different elements. Construction techniques in the past were often related to the available materials (i.e. tuff, calcareous stones, mortar) and to the social-economic asset of the area. These factors can give very peculiar and strictly local characteristics to the masonry buildings. This implies the need of detailed inspection and monitoring of materials decay.

Each structure is a singular case and a detailed *in situ* experimental analysis is required. The importance of evaluating existing masonry buildings by means of *in situ* non-destructive investigations has been mentioned by many authors (Binda et al., 2000) [8]; Carpinteri et al., 1991 [10]).

The goals of non-destructive techniques can be various as:

- Detection of hidden structural elements, such as floor structures, arches, piers;
- Definition of masonry typology;

- Mapping the non-homogeneity of the materials;
- Evaluation of the extent of the mechanical damage;
- Discovery of the presence of voids and flaws;
- Evaluation of surface decay;
- Mechanical and physical properties.

Structural inquiries are fundamental to identify the current state of the structure and the mechanical properties of the materials, to evaluate the local (i.e. deformations and stresses computed by means of hydraulic jacks, sonic tests and cylinder cuttings) and global behaviour through surveys (out-of-straightness, rotations, deflections, settlements) and health monitoring. The latter one, based on environmental vibrations (traffic, wind, man-induced vibrations) or even caused artificially by hydraulic jacks, represents often an important instrument to collect information about the dynamic behaviour of the structure. Experimental in situ inquiries and measures, best performed using modern non-destructive tests (Uomoto, 2000) [11] can solve most of the uncertainties related to a multidisciplinary knowledge of the building and can be useful also to calibrate Finite Element (FEM) models that describe the static and dynamic behaviour in the linear field. The experimental tests that can be carried out on site are numerous and many of them are semi or non-destructive, using non contact measurements or having minimum interactions with the structure. Usually these types of tests should be extensively realized in the structure and their results calibrated and/or correlated with the ones coming from few destructive tests. However, in situ tests, performed with low invasive technique agree with the “minimum impact” and reversibility items requested for retrofitting intervention complying with the Recommendations of ICOMOS, 2005 [4]. Most codes underline the philosophy that as larger and detailed is the knowledge of structure as safe is the diagnosis and less invasive the retrofitting. To this aim the safety factors tend to be lowered whenever the knowledge of the design increases. Conversely, the use of more refined numerical provisional models may give rise to less cumbersome interventions for the requested design structural performance, but this aim should be based on affordable experimental

results. The reliability of the numerical simulation depends significantly on the quality and the quantity of information available and used to implement the models. For heritage buildings, experimental modal analysis is often conducted using continuous environmental vibrations which are either natural (wind) or man-made (road or rail traffic, nearby building sites, bells, etc.).

Dynamic identification, performed in situ by using environmental sources or vibrations induced by additional sources (Cosenza and Iervolino, 2007) [12], can be a useful tool to better calibrate the properties of the constituent materials (unit weight, elastic modulus), to clarify the interaction with surrounding buildings by evaluating the degree of constraints supplied, and to highlight any damage conditions in the building (i.e. diffuse cracking, decay of material) influencing global deformability. In these cases the processing techniques to be used are rather complex, insofar as they have to operate with only output data. The instruments required for surveying must have high resolution to capture very low levels of acceleration. In this respect, this test has the considerable advantage of not being invasive and not requiring the installation of activators, which, for applications on a heritage structure, is even more beneficial. Information about dynamic behaviour is essential to establish the response of the construction under an earthquake action (Eurocode 8–Part 1, 2005) [13].

Based on detailed information about history, geometry and materials of masonry constructions, refined three-dimensional (3D) models by finite elements can be useful to understand the structural behaviour for the present actions, to identify the original causes of the damage pattern detected and the resisting mechanisms and to predict behaviour for exceptional action (i.e. earthquakes). To this aim the empirical evidence obtained by in situ surveys can be used to calibrate the analytical models. After their validation, they can predict structural performance for different actions and also reveal the reasons for past structural behaviour. The static and dynamic analyses can be performed by Finite-Element Models (Lourenço, 2002 [14]; Curti et al., 2006 [15]; Ivorra and Pallarés, 2006 [16]). To this aim dynamic-based model updating techniques (Roca, 2006) [17] can be performed to adjust the main structural

parameters by comparison between experimental and theoretical modal shapes and frequencies. Furthermore some information about the stress distribution in the structure (i.e. local values of in situ compressive stress supplied by flat-jacks) under the current gravity loads represents a target for analytical modelling to calibrate the mechanical properties of materials (unit weight, elastic modulus, strength). However, assessment of a reliable model is not simple, since the usual hypothesis of isotropy. Homogeneity and linear elastic behaviour are not always applicable to masonry which, by definition, is a heterogeneous assembly of several materials. In addition, historical constructions were built in the past on the behaviour of traditional rules often far from the current seismic design standards. In this way the application of standard methods to evaluate the structural safety could lead to plan invasive retrofitting which is not respectful of the preservation requirements for heritage buildings (ICOMOS Recommendations, 2005 [4]; Modena et al., 2006 [18].; Roca, 2006 [17]). Assessment of masonry structures is complicated by the variation of structural properties and depends on the type of assemblage of the materials (masonry blocks, bricks, mortar and filling) with characteristics that may vary statistically. Data from experimental tests (i.e. density of materials, geometrical assessment of architectonic and structural elements) used in numerical models can be verified and calibrated comparing the theoretical stress distribution with local measures obtained by in situ loading test (i.e. flat jacks) or with observation of global damage state. The experimental dynamic identification on site can assume an important role in defining the behaviour of the structure under seismic loads. Moreover, the use of the data collected with dynamic health monitoring is not straightforward and requires “ad hoc” assessment methods.

The comparisons between the theoretical dynamic behaviour and the experimental in situ identification allows to verify the reliability of physical parameters (density, geometry, elastic properties) used in the models. Furthermore the influence of several factors on the global behaviour (interaction with surrounding buildings, connections amongst constituent

elements, stability of foundations, damage state of materials) and uncertainty about the construction techniques can be identified. An improved knowledge of the materials and geometry can result also useful to collect more detailed information to set up numerical models performing nonlinear analyses which may lead to higher safety factors at ultimate limit states. In particular the nonlinear static analysis (Push over, Eurocode 8, 2005) [13] seems to be sufficiently reliable to evaluate the seismic vulnerability of the masonry buildings. It is strongly based on the dynamic identification of the structure to describe accurately the force distributions that matches the fundamental modes. In the specific case of towers (Cosenza and Iervolino, 2007) [12], the “vertical” nature of this type of structure, often tall and slender, makes them more vulnerable to settlements and movements induced by earthquake actions. In addition, their slenderness and the boundary condition of cantilever, often typical of towers, make them unsuitable for redistributing stresses and dissipating energy. The characteristic limited ductility of the masonry accentuates this brittle structural behaviour. It is often accompanied by a concentration of stresses at the basement because of the “cantilever” shape and can be amplified by the brittleness of deteriorated masonry. Effects of sustained service loads like wind or bell vibrations should not be underestimated in evaluating deformations and displacements of slender elements like towers, because they can cause a permanent damage state (Anzani et al., 2000) [19]. Seismic actions could worsen the existing damage state, leading to a collapse, or could activate new failure mechanisms. Furthermore, observation of damage earthquake-induced in ancient bell towers evidenced that a vulnerable architectural element is often the belfry, considering that the seismic input acting at the high level, where the belfry is usually positioned, can be considerably different from that acting at ground level due to the filtering effect of the entire structure (Curti et al., 2006) [15].

1.2 OBJECTIVE AND SCOPE OF THE THESIS

Following the previously introduced principles, the Bell Tower of “Santa Maria del Carmine” sited in Naples (Italy) has been studied and restoration procedures and achieved results are presented in this doctoral thesis.

This case can represent a “case study” of a generalized methodology to approach the study of an historical building starting from the preliminary investigations up to device solutions to improve the safety of the structure.

The Bell Tower has been deeply examined by the Author performing detailed experimental and theoretical analyses. The analyses followed a multidisciplinary approach to identify:

- The architectural and structural features;
- The materials that characterized the structure;
- The state of damage;
- The interventions made in various periods;
- The stress state in the masonry under gravity loads;
- The dynamic behaviour.

The multidisciplinary approach is necessary to collect information coming from different types of inquiries. It should be the primary step to approach a verification process for a masonry heritage building finalized to a restoration intervention able to warrant both “lowest impact” requirements (ICOMOS 2005) [4] and acceptable safety conditions for the structure.

The Bell Tower of “Santa Maria del Carmine” church is an ancient (XVII century) historical masonry building located in the city of Naples (Italy). The Tower is 68.0m high and is made by faced yellow tuff masonry along the initial 41.0m of height and by clay bricks along the upper levels. Internal and external walls are covered by decorative dark stone (Piperno) along the first nine meters.

Detailed historical, architectural and structural inquiries have been developed on the Bell Tower. This analysis has been necessary to clarify the

sequence of changes that were introduced in the structure during the centuries mainly to eliminate damages caused either by accidental events like earthquakes, or by the continuous actions of acting loads.

An in-depth survey was carried out in situ on the masonry. Detailed experimental in situ investigations have been performed to define the geometry, to find the composing materials, to characterize their mechanical properties, to analyze damage condition and to identify the dynamic behaviour of the structure. An experimental dynamic characterization of the Bell Tower was also realized considering the environment vibrations due to wind, traffic and bells. The collected information represents the starting point for designing a seismic upgrade to meet the standards applied to historic monuments.

The experimental results have been successively used to develop a numerical 3-D FE model. This model has been used to perform a linear static analysis under gravity loads, to calibrate the mechanical parameters given by experimental results (i.e. the density of materials) and to check the safety condition for the vertical loads usually acting on the structure. Then, a linear dynamic analysis has been also accomplished to assess the values of Young's modulus of materials and the constraint conditions offered by the surrounding buildings, based on parametric comparisons with the experimental results (natural frequencies and corresponding modal shapes obtained by dynamic in situ tests). This last study has been useful to understand the behaviour of the Tower under horizontal actions like an earthquake, considering that the structure is located in a medium risk seismic area. Therefore with the assumption of a "global behaviour" of the Tower, a non linear static analysis (Push - over) was carried out based on the results of the previous inquiries, pointing out a low risk condition for the expected seismic actions (peak ground acceleration of 0.168g). Considering that previous numerical analysis evidenced that the Tower satisfied global checks for the expected seismic actions, in this thesis attention is focussed on the study of local out-of-plane mechanisms activated by those actions. In order to avoid such mechanisms, design, application and monitoring procedure of innovative connective systems with tie

rods made of glass FRP laminates have been applied.

To understand the role of the different “investigation tiles”, the following paragraphs summarize the development of the different investigation categories applied to the Bell Tower of the “Santa Maria del Carmine” Church. Information derived from the different categories of investigations does not appear to be independent of each other, but they must be integrated to support a reliable assessment of the available data. ICOMOS recommendations strongly underline the requirement of a multidisciplinary approach to be operated on heritage building restoration. Diagnosis of the structural safety of the building has to be based on different kind of inquiries, both qualitative and quantitative. Anamnesis of the structure starts from preliminary qualitative inquiries aimed at identifying, by a visual survey, geometry, materials typology, and decay and damage pattern, to recognize the critical aspect of the building and give a direction to the quantitative ones. Inquiry typologies that were analyzed from the author can be summarized as follows:

- Historical inquiries to assess the structural and architectural evolution over the time, to collect information about the building manufacturing technique and materials used.
- Geometrical and material survey to define geometrical parameters defining the structural asset of the building and to distinguish the architectural elements from the structural ones.
- Planning and execution of in situ tests to characterize the mechanical properties of materials by semi and non-destructive tests, to estimate the stress distribution in masonry under gravity loads.
- Experimental dynamic identification to individuate the main natural frequencies and modal shapes of the building to be successively compared with more or less refined numerical provisions, to evidence eventual effects of several phenomena on the dynamic behaviour (i.e. constraints effects offered by surrounding buildings and foundation systems, relevant decay of materials causing reduction of stiffness of the structure, anomalous participation of mass due to incorrect evaluation of

geometry or contribution of not considered elements).

- Modelling of the structure by more or less refined numerical and analytical approaches based on the collected information in order to, firstly, calibrate parameters influencing the local and global structural behaviour and, then, to estimate safety vs. vertical and horizontal actions.
- Estimation of vulnerability of the structure and design of a “minimum impact” retrofitting.

1.3 REFERENCES

- [1] OPCM 3431, 2005. Ordinanza del Presidente del Consiglio dei ministri - *Primi elementi in materia di criteri generali per la classificazione sismica del territorio nazionale e di normative tecniche per le costruzioni in zona sismica* (in Italian).
- [2] *Linee Guida per la valutazione e riduzione del rischio sismico del patrimonio culturale con riferimento alle norme tecniche per le costruzioni*, Luglio 2006 (in Italian).
- [3] ICOMOS, 1964. *International Charters for the Conservation and Restoration of Monuments and Sites*. II International Congress of Architects and Technicians of Historic Monuments, the Venice Charter.
- [4] ICOMOS, 2005. “*International Council on Monument and sites, Recommendations for the analysis, conservation and Structural restoration of Architectural Heritage*”. Document approved in the Committee meeting in Barcelona the 15th June 2005.
- [5] Lagomarsino S., Podestà S., Resemin S., 2004. “*Observational and mechanical models for the vulnerability assessment of monumental buildings*”. Proc. of the 13th World Conference on Earthquake Engineering, Vancouver BC, Canada.
- [6] Modena C., Valluzzi M.R., Binda L., Cardani G., Saisi A., 2004. “*Vulnerability of historical centres in seismic area: reliability of assessment methods for different building typologies*”. Proc. of 13th International Brick/Blocks Masonry Conference RAI, Amsterdam, July 4-7, CD ROM.
- [7] Modena C., Valluzzi M.R., Tognini Folli R., Binda L., 2002. “*Design choices and intervention techniques for repairing and strengthening of the Monza Cathedral Bell Tower*”. *Construction and Building Materials*; 16: 385-395.
- [8] Binda L., Saisi A., Tiraboschi C., 2000 “*Investigation procedures for the diagnosis of historic masonries*”. *Construction and Building Materials*; 14:199-233
- [9] Carpinteri A., Invernizzi S., Lacidogna G., 2005. “*In situ damage assessment and non linear modelling of historical masonry towers*”. *Engineering Structures*; 27:387–395.
- [10] Carpinteri A., Bocca P., 1991. “*Damage and diagnosis of materials and structures*”. Proc. of DDMS 91. Politecnico di Torino, Bologna: Pitagora.
- [11] Uomoto T., 2000. “*Non-Destructive Testing in Civil Engineering*”. Elsevier Science. ISBN-10: 0080437176.
- [12] Cosenza E., Iervolino I., 2007. “*Case Study. Seismic retrofitting of a medieval bell tower by FRP*”. *ASCE Journal of Composites for Construction*; 11(3): 319-327.
- [13] CEN. Eurocode 8, 2005. “*Design provisions for earthquake resistance of structures, Part 1: General rules. Specific rules for various materials and elements*”. EN 1998-3:2005, Committee for Standardization. Brussels, Belgium.

-
- [14] Lourenco P. B., 2002. “*Computations on historic masonry structures*”. Structural Engineering and Materials 4(3): 301–319.
- [15] Curti E., Lagomarsino S., Podestà S., 2006. “*Dynamic models for the seismic analysis of ancient bell tower*”. In Proceedings of Structural Analysis of Historical Constructions, New Delhi, India, eds., P. B. Lourenco, P. Roca, C. Modena, S. Agrawal. CD-ROM.
- [16] Ivorra S., Pallare’ s J. F., 2006. “*Dynamic investigations on a masonry bell tower*”. Engineering Structures; 28: 660-667.
- [17] Roca P., 2006. “*The study and restoration of historical structures: from principle to practice.*”, Proc. of Structural Analysis of Historical Constructions, New Delhi, P.B. Lourenco, P. Roca, C. Modena, S. Agrawal S. Eds, CD ROM.
- [18] Modena C., Casarini F., Valluzzi M.R., Da Porto, F., 2006. “*Codes of Practice for Architectural Heritage in seismic zones*”. Proc. of Structural Analysis of Historical Constructions, New Delhi, P.B. Lourenco, P. Roca, C. Modena, S. Agrawal S. Eds, CD ROM.
- [19] Anzani A., Binda L., Mirabella R. G., 2000. “*The effect of heavy persistent actions into the behaviour of ancient masonry*”. Materials and Structures; 33: 251–61.

Chapter II

Historical investigation

2.1 URBAN FRAMING

The Bell Tower of “Santa Maria del Carmine Maggiore” is a 17th century structure located in Naples, Italy. The Bell Tower is part of the “Complex of Carmine”, composed by the church, the monastery, the cloister and a Brotherhood (Fig.1). Until the last century, a fort with the same name was also part of this complex, until it was destroyed to allow the realization of Via Marina (*Marina Street*). Only two towers of the ancient fort still survive today. The complex is located in the “Mercato” neighbourhood of the city, adjacent to the original city wall, near the main gate carrying the same name as well.

The public square was the heart of the city during the Angevin and Borbonic periods, and the Carmine Complex was, until the end of the seventeenth century, a symbolic image for all Neapolitan inhabitants. Compromised by many reconstructions during the “Risanamento” period and the post Second World War period, it testifies an interrupted and not concluded destiny. The Carmine Complex is today one of the few elements of remarkable architectonic interest in a very degraded area, including on one side the ancient but disintegrated neighbourhood area, and on the other one a recent construction (Ottieri’s building) built in abnormal dimensions that completely alter the

original atmosphere and all the contest around. In fact after the construction of this new building, the large and elegant Carmine Bell Tower silhouette, which has always been visible from most parts of the city, remains partially hidden.



Fig.1. Aerophotogrammetry. "Mercato" Square

2.2 THE “MERCATO” DISTRICT AND ITS HISTORICAL DEVELOPMENT

2.2.1 Origins

The “Mercato” neighbourhood, although not belonging to the system of foundation of the Greek Naples, has always been closely connected to the Greek-Roman city, representing the main contact with the sea. It consolidated this role when, in medieval age, the more ancient nucleus was connected to the sea area through that coastal wraps defined “*junctura civitatis*”. Originally it was only a marsh (palus neapolitana) that the Normans fenced off with walls. This area was previously called the “Arena”, and later “Field of Moricino”. No one knows exactly where this name came from, but perhaps it was by the traffickers of different nationalities and religions living there, including many Jews that were known generically as “Mori”. Until the thirteenth century, residential and religious constructions were only occasionally built in this area. Along the beach there were only a few small fishing villages. It could not be otherwise because the ancient inhabitants had preferred to locate the city on the hilly areas, which allowed better defences against possible marine incursions. A similar approach was also followed in the medieval period. Under Valentinian III, Narses and Belisarius, the city walls were not extended. There were realized simply reconstruction and consolidation of existing fortifications. During the Dukedom age, Naples still continued to grow up, while retaining the size of the Greek-Roman period. Only the new economic progress under the Angevin period determined the conditions for a significant urban development. The merchant area, in direct contact with the harbour, was where, more than any other place, it was felt the need to rationalize the land.

2.2.2 The Angevin period

In 1189 Naples became part of the Hohenstaufen Empire. The Hohenstaufens were a highly powerful Germanic royal house of Swabian origins. Conflict between the Hohenstaufen house and the Papacy led, in 1266, to Pope Innocent IV crowning Duke Charles I, from the Angevin Dynasty, as the King of Naples. With Charles I d'Anjou, Naples was elevated to capital of the kingdom and the official market of the city was transferred to the "Mercato" area. At that time, the square was called the "Great Hole" (*Foro Magno*) or simply "Market". In 1267, Charles I had to face a new attack from Konradin von Hohenstaufen who revenged his reign. At the end, Konradin was beheaded in the bloom of his youth in "Piazza Mercato" (*Mercato Square*).

The history of the Complex of Carmine began then, in that distant morning of 26 October 1269 when Konradin was carried in the square in a box enclosure not far from Carmine's Castle, so Charles I and his court, who lived there, could watch the executions well. Friedrich of Austria, who had accompanied Konradin in his expedition, went onto the scaffold first and then, immediately after, the blond Swabian Prince.

In a few years, the new reign transformed the face of the city. Noble French families, and many artists and merchants, moved to Naples following the King. The city at that time was divided into three distinct areas, the first foundation from the Greek-Roman age, the second from the medieval age, and the third "junctura civitatis", constituted through the implementation of the villages on the beach. This area was subjected to several interventions during the Angevin kingdom. In particular, Charles I wanted to incorporate in the new walls the villages of "Field of Moricino" and therefore, gave impetus to the development of the city in the south-east zone. Within the new expanded walls, new roads were planned and the construction of residences and religious buildings was begun. The system of fortifications was reinforced with the construction of new castles. The last bulwark of the town was built by Charles III de Durazzo in 1382, just on the south-eastern side of the city walls behind the established

structure of the church and the convent of Carmine who gave it the name (the Bulwark of Carmine). The new area of development of the city immediately acquired the functions that have been conserved until now. The King ordered the transfer of the market, earlier located in the ancient square of “San Lorenzo”, to this area. The proximity to the port and the rationalization of all the commercial areas for the foreign merchants that had moved to Naples made the traffic and the communications easier. The Field of “Moricino”, as described above, became one of the most active life-centres within the new port facilities. Charles I d’Anjou ruled absolute inalienability of land bordering the port area, allowing only the realization of religious buildings or enhancement of existing ones (Fig.2).



Fig.2. Micco Spadaro, “Mercato Square”. Largo Mercato, Oil on canvas, cm 80x145, Fundacion Casa Ducal de Medinaceli, Spagna

Naples became the most important city of Italy at that time because of the wise economic policy pursued through the promotion of trade, appropriate measures taken by the King at the time of the great famines, and also the lowering of prices of essential items.

Although during the Angevin age the new urban area got a great role and became the object of many interventions. The development of housing was very limited in those years, and the quality of housing was very poor. The area of the port was degraded because of the narrow streets and smelly air. The square so defined, will remain unchanged in later centuries. From the beginning of the thirteenth century, the Field of “Moricino” and the “Mercato” Square were the scene of the executions of those condemned to death. The history of this square is a story often macabre, even if sometimes glorious.

2.2.3 The suburb in Aragonese and Spanish period

In 1452, with Alfonso I de Aragón, the Aragonese dominion in Naples began, paving the way for a civil and economic development of the city and the flourishing of Renaissance art and ideals. With Fernando I de Aragón in 1484 a program of urban expansion and restoration of the city walls began. According to Celano (Celano, Chiarini, 1974) [1] a new gate was built in this period. It was called “Porta del Carmine” (Fig.3) because it was built near the convent.

In 1503, Spain conquered Naples at the Battle of Garigliano and, as a result, Naples fell under direct rule of the Spanish Empire throughout the entire Habsburg period. With the definition “Spanish vice-kingdom” we refer to a period of almost two centuries of colonialist domination. Between 1503 and 1707, the crown of Madrid exerted its power on Naples. A host of viceroys took regency of the city and proved to be devoted to vexations; they also stole works of art and imposed heavy taxes.

The most important of the viceroys was don Pedro Álvarez de Toledo. He introduced heavy taxation and favored the Inquisition, but at the same time improved the conditions of Naples. He opened the main street, which still bears

his name today, paved other roads, strengthened and expanded the walls, restored old buildings, and erected new buildings and fortresses. The city of Naples turned, by 1560, into the largest and best fortified city in the Spanish empire. During this period Naples became Europe's second largest city behind Paris only.

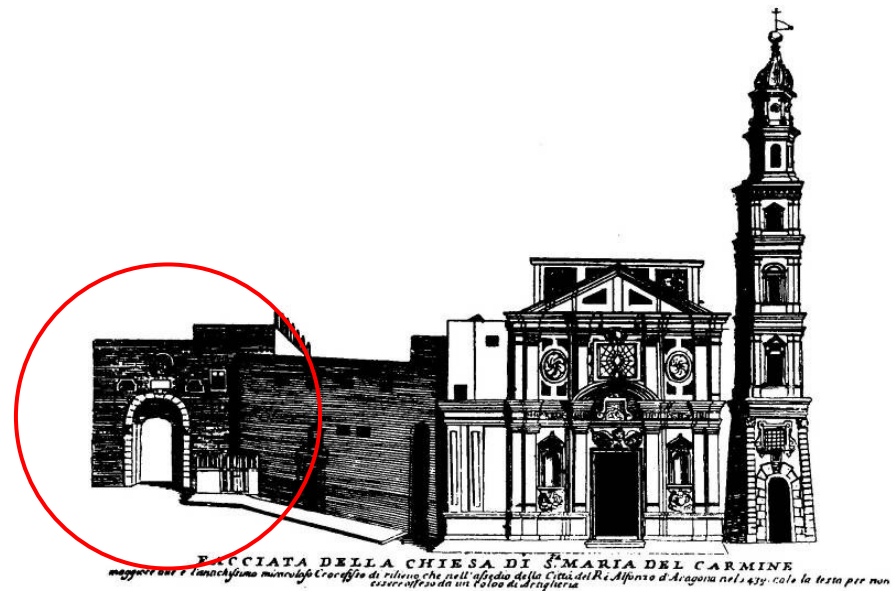


Fig.3. The Church and the Gate of Carmine in the Petrini engraving reported in Celano, Chiarini, 1974

During the Spanish domination, Baroque period, there were only few signs of a formal architectural language. The Bell Tower of Carmine imposed its strong presence not only in the architectural landscape of the square but in the environmental implications of the whole city.

To complete the framework of transformations of the seventeenth century, we must remember the conclusion of the construction of “Castle of Carmine”. The construction began during the kingdom of Charles III de Durazzo when the

ancient city walls were enriched with new defensive towers along the Marina. At that time in the far eastern section of the city the tower called the “Sperone” (Spur) was built, the first part of the later “Castle of Carmine”. Through the direction of Viceroy Parafan de Ribera, Duke of Alcala, the Spur was enlarged in 1484, rebuilt and reinforced in 1512. The result was the transformation of the tower from a round to a square shape.

2.2.4 From the Austrian reign to the Risanamento

In 1734 the Kingdom of Naples and the Kingdom of Sicily were united under a single independent crown (*Utriusque Siciliarum*), that of Carlos de Bourbon. The last years of the Bourbon Kingdom and the first of the Unification of Italy were characterized by the need to rationalize the port area and sea links to the service of industrialization, now of considerable size. The cholera of 1884 allowed the rationalization of urban intervention of great size, which impacted considerably on the transformation of the village. The epidemic was of such magnitude as to force the government to operate and for the first time since the Unification of Italy, the possibility of financing sanitation and housing was considered. A special law was promulgated. This law for the rehabilitation of the city of Naples was enacted in 1885 and the works began in 1889. For the “Mercato” area, the organization of the roads and the new urban structure from one side improved the hygienic conditions, but from the other side did not yield the expected benefits. The rationalization of the roads was not followed by valuable residential interventions. The only remarkable element was characterized by the realization of the “Villa del Popolo” in the “Marina” area (Fig.4). The cutting of the medieval blocks that represented the link between the ancient town and the market area increased the effect of separation determined by the brutal “Rettifilo” street construction. Furthermore, the opening of 14 sleepers, 12 meters wide, which connected the “Rettifilo” with the “Marina” street, completely destroyed the continuity of the curtain wall construction along the sea. A few years later, the transformation of the area was

completed by removing the small cloister of the Carmine monastery and the demolition of the bastion of the seventeenth-century castle.



Fig.4. Carmine Square, “Villa del Popolo”, photo of 1880

2.2.5 Post Second World War

“Piazza del Carmine” (Carmine’s Square) and the village of “Moricino” continued to suffer changes until the late nineteenth century and also during the events of the First and Second World Wars. In 1906, the Carmine bulwark (Fig.5), located at the intersection of “Nuova Marina” street and “Garibaldi” street, was removed. The bulwark was an important witness to the political and urban history of the city, and in its place was built a mediocre neo-Renaissance building, used as a military store, and called barracks “G. Sani”. The resettlement planning following the reconstruction plan after the Second World

War determined the current configuration of the square. Compared with other Italian cities, Naples was hardly hit by air raids during the Second World War, and the historical and artistic heritage was not spared, resulting in heavy damage. The reconstruction of housing was the primary problem of the post-war period.

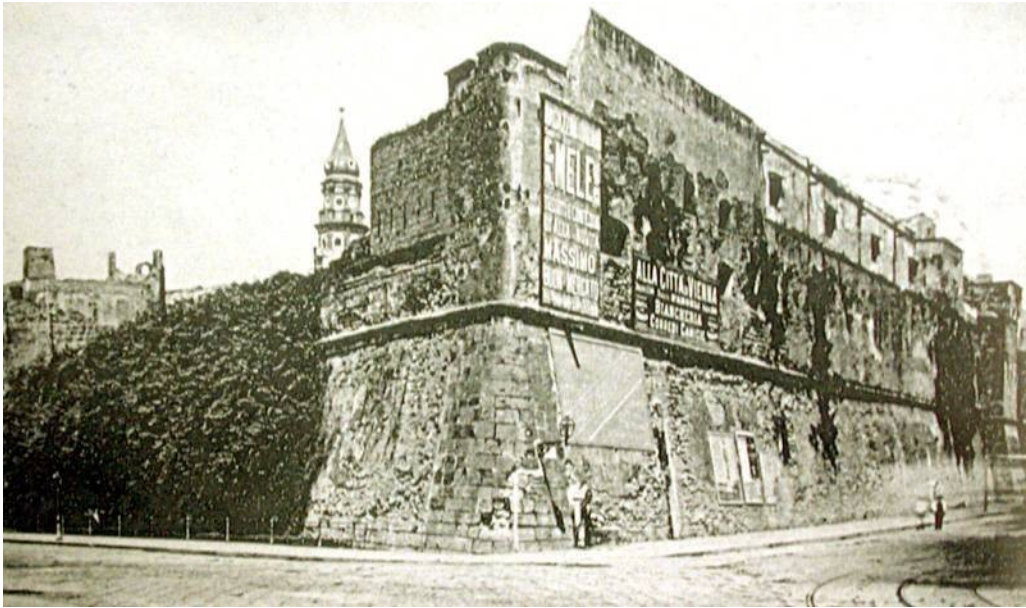


Fig.5. The Carmine bulwark in a photo of 1880

In 1944, the City Council appointed a committee to prepare a reconstruction town-planning scheme. The plan was delivered ten months later, but the administrative process was very troubled and long years were spent between adoptions, referrals, comments and debates. The result was a legislation gap that facilitated speculation and the first irreversible damage was inflicted to the city. The “Mercato” Square highlights the catastrophic effects that can be produced when the quality of projects is very poor and intentions of traders are highly speculative. In the early sixty of the twentieth century, Mr Ottieri, the

builder, became responsible of demeaning the “Largo Mercato” architectural look raising a building with no design quality and the worst post Second World War public housing standards, which acts like a curtain that plugs the southern side of the street. (Cajati, 1998) [2] (Fig.6).



Fig.6. Ottieri building and the Bell Tower of Carmine (Roberto Pane picture).

Further damage was achieved with the development of the new street “Via Marittima”. This made possible the realization of the dual carriageway with a central reserved lane and consequently, the isolation of the “Vado del Carmine” door, built by the architect Bonpiè in 1748. This gate, realized under Carlos de Bourbon, was one of the most representative gates of the city. Not only the port lost its function, but also the second cloister of the Carmine monastery was cut off and a side of the arcade was left exposed along the new road of the “Marina” (Fig.7). In addition, two of the towers of “Torrione del Carmine” (Carmine Stronghold) have been moved forward and incorporated in the traffic divider along the ancient fifteenth city wall (Fig.8). This urban disfigurement

further marginalized the “Mercato” Square, breaking the continuity between the monastery complex and the Towers of the Carmine’s Fortress. The original configuration has been completely compromised and any intention of future rehabilitation has been made impossible.



Fig.7. Rest of the second cloister



Fig.8. The two stronghold towers today

2.3 HISTORICAL EVOLUTION OF THE “SANTA MARIA DEL CARMINE” CHURCH AND ITS BELL TOWER

2.3.1 The foundation

The monumental complex of the “Carmine Maggiore” is located on the outskirts of the ancient city, along the original city walls, and close to the old main gate called “Vado”. It is situated in the old area of the market (Fig.9). To the north of the building is the Egiziaca Church, and to the west there is a stream that goes into the sea nearby. On the east side was the ancient church of the Carmelitan friars. We do not have documentation about the foundation of this complex. According to the Carmelitan author, the Dominican Father Da Montorio, and the text “Chronistoria del Carmine Maggiore” [3], composed from 1690 to 1699 by Father Pier Tommaso Moscarella, and continued by other Friars in the next centuries, the foundation of the monastery is reported before the twelfth century. Father Moscarella says:

“...because of the continuous traffic trip that the Amalfitans made in Syria, and their piety and devotion, I can believe that probably in their voyages, on which they have left their immortal name for being the inventors of riding the waves with the magnet, and govern the route with that both during day and night they have also moved our religious people from the Amalfi coast to the shores of Naples since there is just a few hours walk in between. And finally I conclude that our Royal Convent was first created as a hermitage, not only because at that time the place was far away from the city, but also lonely and remote since only after many centuries we see this as at present, enclosed within the walls... So, considering all these circumstances both together and separately, I can probably assume that not only is it absurd to believe that our Royal Convent was founded in the year one thousand of the Lord, but even a lot of time ahead, due to be immemorial the coming of our religious people, and unknown to the earliest records of our City”.

Other writers, such as Celano (1974) [1], Clemente (1875) [4], Galante (1873) [5] state that the first historical document that certifies the existence of the church, around 1150, is a papal bill of Pope Sixtus IV, written in 1475. This Pope bill granted Ferrante de Aragón indulgences and privileges for the church, where we read that *“populus neapolitanus a trecentis annis et ultra dictam ecclesiam visitare consuevit”*.



Fig.9. Carmine's complex (June 2005)

This would confirm the hypothesis that the church already existed around the year one thousand. Salvatore Di Giacomo (1892) [6] in the opera *“Napoli Nobilissima”*, describing the sanctuary, says:

“...a small church, entitled to the Bishop of Mira, St. Nicola of Bari, was at the beginning of the seventh century near by the marina outside the city... at that time a hospice had been built on the shore for the old continuers in the profession of St. Andrea and next to the hospice a small church was founded for the religious occurrences of the invalid fishermen”.

Di Giacomo continued:

“...Once arrived in Naples, fleeing from persecution by the Saracens, some of the hermits of Mount Carmelo, were transferred the hospice and the church, as they asked. An old image of St. Maria of Carmelo that had saved them from persecution took place in the church of the old sailors and gave it a new name”.

Following the hypothesis of this illustrious writer, we could confirm the existence of a small church near the Marina that was to be composed of a crypt with a Greek cross plant. The votive image of the Virgin Bruna was kept inside the crypt and on the top it was built a small chapel named “Santa Maria della Grotticella”, because of the presence of a hypogeum.

Another historical document that certainly confirms the hypothesis of the existence of the church in the Middle Ages is linked to the beheading of Konradin of Svevia and his cousin, Duke Frederik of Austria, in the “Mercato” Square, in 1268. Their bodies were put in pits and buried in the square itself. De Blasiis (1886-1887) [7] mentions that the beheading happened “*in the market of Naples along the stream of water that runs near by the church of the brothers of Carmelo*”. Queen Elisabeth von Bayern, arrived in Naples with large amounts of money for the ransom of his son Konradin, found him dead and donated the treasure to the Carmelitan brothers to enlarge the existing church close to where Konradin was executed and to give a proper burial to his son and nephew. The first transformation of the church and the monastery was then performed with Svevian money under the Angevin domination. Confirmed by Monaco (1975) [8], when Charles I died, his son Charles II allowed the current church to be built over the mounds of Konradin and Frederik. Konradin

and his cousin's bones were placed in the temple. It was built on the banks of the stream that flowed through Morocino field, and very close to running water, which was required to be crossed through a bridge (Quagliarella, 1932) [9].

2.3.2 The Gothic structure

The work for the new church began in 1283 and came to an end only early in next century when the large cloister was completed. The start date is derived from two manuscripts preserved in the monastery of San Gregorio Maggiore in Naples. As Quagliarella (1932) [9] says, the new church had a very simple form, with a nave and without lateral chapels, which began to appear in the fifteenth century with the spread of devotion to the Virgin of Carmelo. The large cloister and, on the east side, a more comfortable dormitory were built. The dormitory was no longer than fifty meters and extended up to the nearby beach (Fig.10).

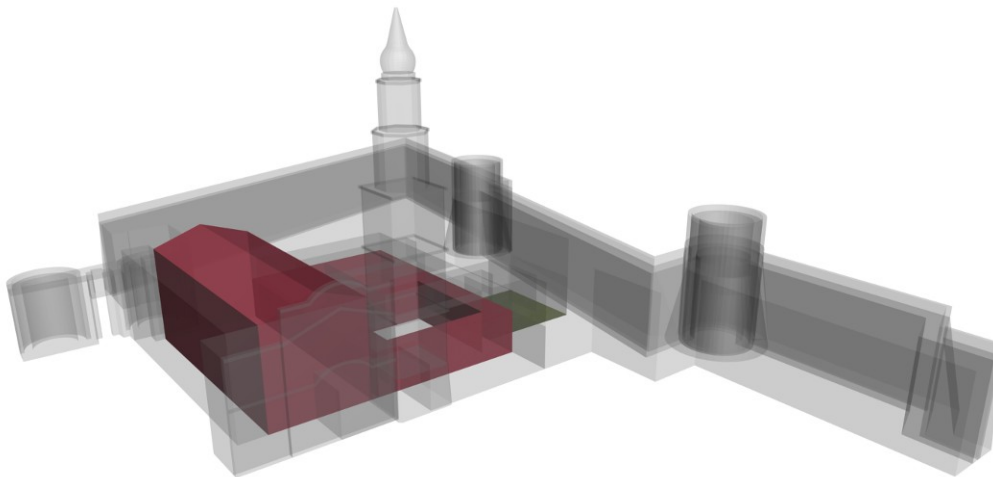


Fig.10. The Church during the XIII century, large cloister and dormitory

This consisted of a long superior corridor, flanked by cells on the right and on the left, about twenty-four in number, with laboratories in the underground

floor. Originally, the large cloister served the men as a place of recreation. Partial remains of Gothic structures are still visible in the cloister. Today, the cloister (Fig.11) appears configured in the lower order by a massive and heavy system of rectangular pillars and round arches, over which there are two rows of rough windows. Behind the pillars, near the surgery, we can perceive octagonal cross section “piperno” pillars, topped by pointed arches. The Angevin monastery should be characterized by a series of hollow structures, the testimony of which remains in a large room called “Salone” (Fig.13). This is the room that was used as refectory and is preceded by a now plugged pointed arch portal (perceivable under the plaster) (Fig.14), and in the cross vault on the main entrance (Fig.15). This cross vault is the most interesting element of that original support which confirms a sequence of vaults of this kind on each side of the ambulatory (Fig.12).



Fig.11. Aerial view. The Large Cloister



Fig.12. Arcade. North view

The Angevin cloister was held in a single order of arches, concluded by an upstairs terrace for use as cells. While of the original structure is easy to read the ogival arches (Fig.16), in the overlapping along the sides of the cloister, it is not so easy to recognize the Angevin “support”. Only two thin pillars of this remain visible (Figs.17&18), those fixed into the corner piers that terminate the

series of arches of the arcade to the north. A third one, similar to the others, emerges in the corner of a wall shared with the church, located passing the entrance hall.



Fig.13. Old refectory openings



Fig.14. Remains of the old "Salone" portal



Fig.15. Covering vault of the Bell Tower entry



Fig.16. Partial remains of the original ogival arches



Fig.17. Angevin column on the Bell Tower basement



Fig.18. Angevin pillar

Finally, on the walls of the cloister arcade running aside the adjacent church, the cross vaults, with same frescoes as those painted on the walls, lay on granite brackets resembling a hanging capital. It's legitimate to identify in these elements the capitals of the Angevin's pillars, then walled, that were located at a higher elevation than the springing line of the following reinforcement arches. When in 1382 King Charles III de Durazzo became King of Naples he started a project of reinforcement of the city walls. He repaired the old city walls and built new towers along the sea. In the place called Palus Neapolitana, and later Field of Moricino, a tower was built for the defence of the city and harbour and it was called, because of its shape, the "Spur" (Fig.19).

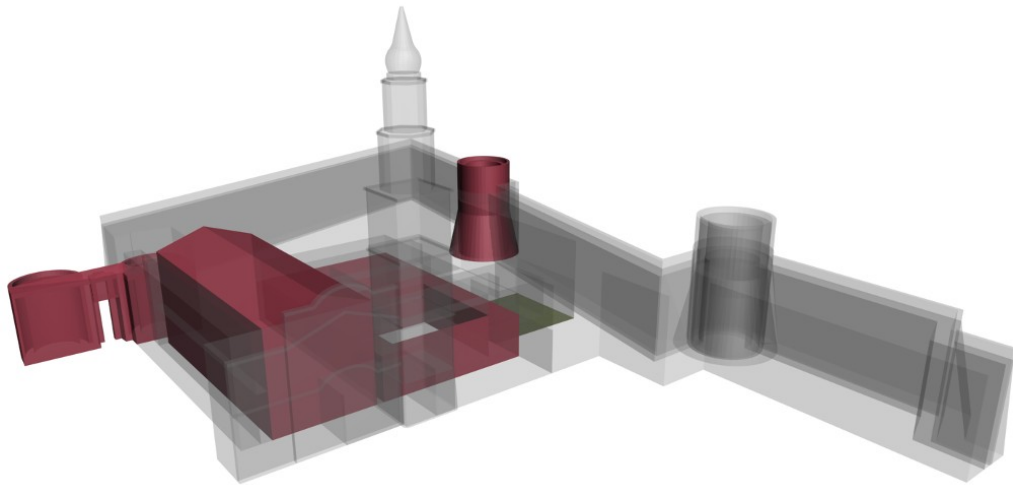


Fig.19. Carmine main gate and the "Spur"

2.3.3 The Aragonese structure

In 1441 Alfonso V de Aragón conquered Naples, reunifying the territory of the ancient Norman- Swabian reign with the title of rex Utriusque Siciliae, and

established the capital in the Neapolitan town. Alfonso de Aragón taking besieged Naples, strokes the city in correspondence of the Suburb of “S. Maria Loreto”. During the siege against the Aragonese, the Angevins had placed their artillery on the Bell Tower of the Carmine’s church to hinder the entry of the Aragonese forces. The Bell Tower, with the attached monastery, became in this period a real fortress. The Aragonese were trying to destroy these batteries and flush out those centres of resistance that were seriously endangering their advance. From the Aragonese camp on the banks of “Sebeto” towards the Suburb of “Loreto”, don Pedro, the Castille Infant and captain-general of the army, directed the fire of his mortars against the Bell Tower and the church, and it is said that a bullet, breaking the apse, fell on the famous crucifix which is still kept inside the church and that avoided the stroke. According to Celano (1974) [1], during the Aragonese reign, the Carmine complex was enlarged and completely transformed. It’s possible to assume that in this period the reversal of apse and entry was made. Near the church the Carmine Gate was built, replacing the Angevin Gate. It is possible that the transformation of all the monastery complex, began with the work of consolidation and restructuring carried out since 1439, when the whole Carmine complex was hit during the Aragonese siege. The first bibliographic citation of the existence of a Bell Tower near the “Carmine Maggiore” church dates back to the fifteenth century. In this period, the beautiful Renaissance altar of St. Barbara, the patron of lightning, was realized. It was placed at the foot of the Tower so as to be able to protect the Tower itself from lightnings (Fig.20). The citation is in the text “Chronistoria Real Convento del Carmine Maggiore” [3], concerning the political events of 1439. At that time, the Bell Tower was important in the defence of the city against the Aragonese. We know from history that in 1456 a violent earthquake knocked the highest part of it and destroyed the rostrum of the church and part of the large dormitory. It was necessary to demolish the remaining part of the Tower and rebuild a new one. In 1458, the construction of the new Bell Tower by Palamidessa was begun. From the Chronistoria, we note that in 1459 the construction of the new Bell Tower was not yet finished. The

Bell Tower was certainly incomplete throughout the sixteenth century. In 1466, Father Giovanni from Siena built the second cloister of the monastery. This was built on the area of the garden of the monks that stretched up to the sea, in conjunction with the Carmine military tower (the Spur). The smaller cloister, unfortunately sacrificed in the twentieth century to the route of the “Nuova Marina” street, had a square shape with a side of twenty meters, and consisted of six arches on pillars of “piperno”, with three upper floors, as evidenced by residual stumps. The increased number of monks and the damage caused by various earthquakes imposed the raising of the large cloister.

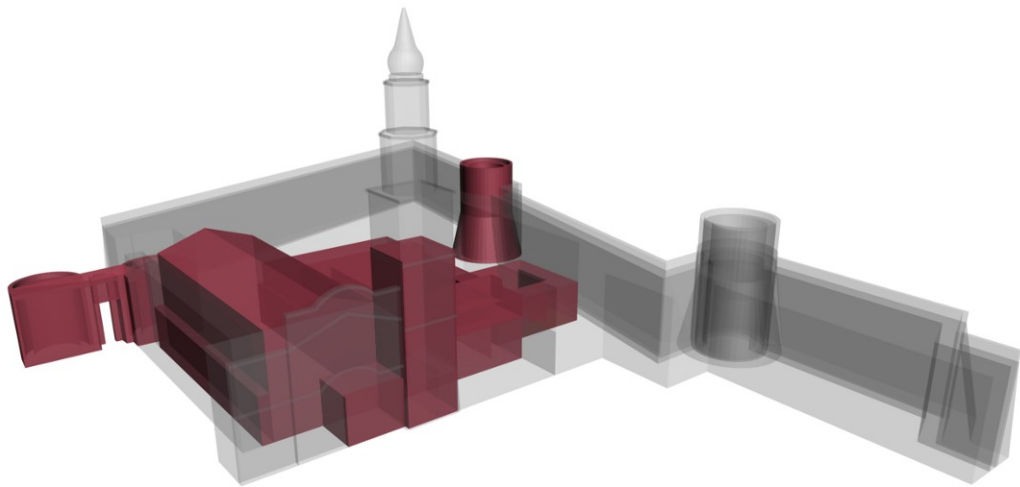


Fig.20. Saint Barbara Chapel to the foot of the Bell Tower

The works were made from 1466 to 1517 and imposed raising of large cloister that was conducted leaving the original pillars in place and including them inside new ones of larger cross section and different shape (Figs.21 a-b-c-d). So the original octagonal granite columns were incorporated into the masonry of the pillars and made almost square. The raising occurred in two different time spans. The first consisted of increasing by one floor the height of all wings of the cloister.

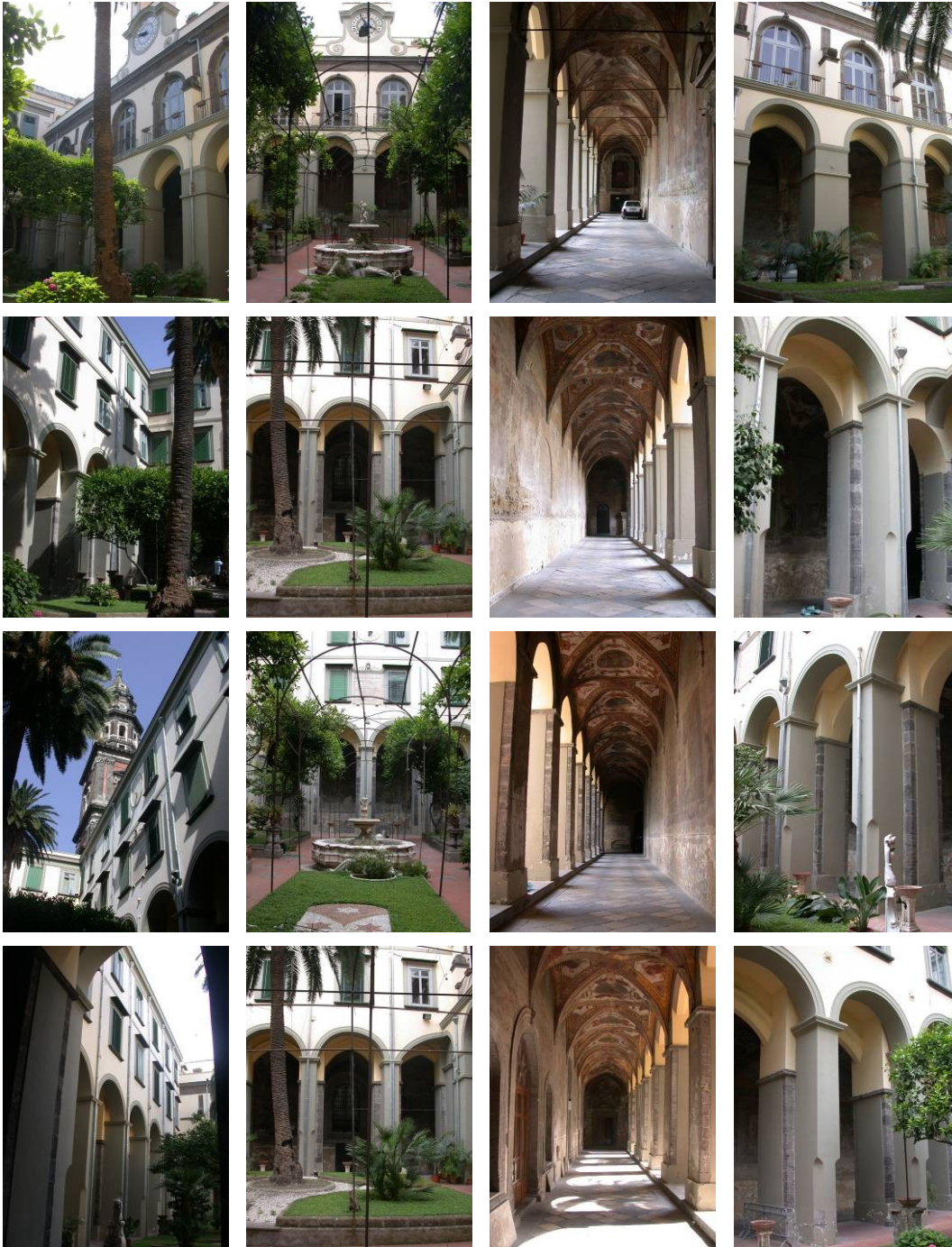


Fig.21a. North arcade

Fig.21b. South arcade

Fig.21c. East arcade

Fig.21d. West arcade

The second was to build a second floor only on three wings of the cloister: the eastern, western and northern. This second elevation imposed a further reinforcement of the piers which was implemented by placing smaller pillars in place, connected by arches. This explains the difference between the pillars of the three sides compared to the fourth.

The previous structure, therefore, has been reinforced by a new structural skeleton, with new foundations, creating a different perspective with proportions very far from canonical. The visual effect that we receive is one in which the original structure seems to “crimp” to the two overlapping structures. In this period, the Friars and the military inhabited the monastery at the same time. The Friars were in the northern and eastern sides of the corridor, up to the original entry to the Tower (second level of the monastery). The military occupied the remaining part of the corridor. Until 1866, the entire eastern part of the second floor formed the apartment of the governor General of the Fortress, as stated in the *Cronistoria* [3]. The Carmelites remained in the monastery until 1866, leaving it for military purposes until 1922. When they returned, they occupied only two sides of the cloister. The other part of the smaller cloister of the monastery was used over time for different functions: prison, barracks and finally police school.

2.3.4 The Spanish structure

During the sixteenth century no big changes were done in the monastery complex. In 1537 the enlargement of the city wall by don Pedro Álvarez de Toledo was begun. This works were involved also the walls near the Carmine. In 1566 the “Torrione of Carmine” (Stronghold tower) (Fig.22) was damaged by a terrible flood. In this occasion, the Duke of Alcalà, understanding the importance of defence of the Stronghold, expanded and remade it into a square shape. In 1611 the walls of the monastery did not touch those of the city. Between these and the convent there was a vacuum. In this year, the Friars of the church granted, by a Court of Fortification of the Most Excellent city of

Naples, to extended up on those walls of the city both the Dormitory that the adjoining ex apartment of the governor General of the castle. Under this concession was built the factory and the large and lovely balcony that overlooks the sea. Below that were fabricated rooms and laboratories for servicing the convent (Chronistoria del Carmine Maggiore) [3]

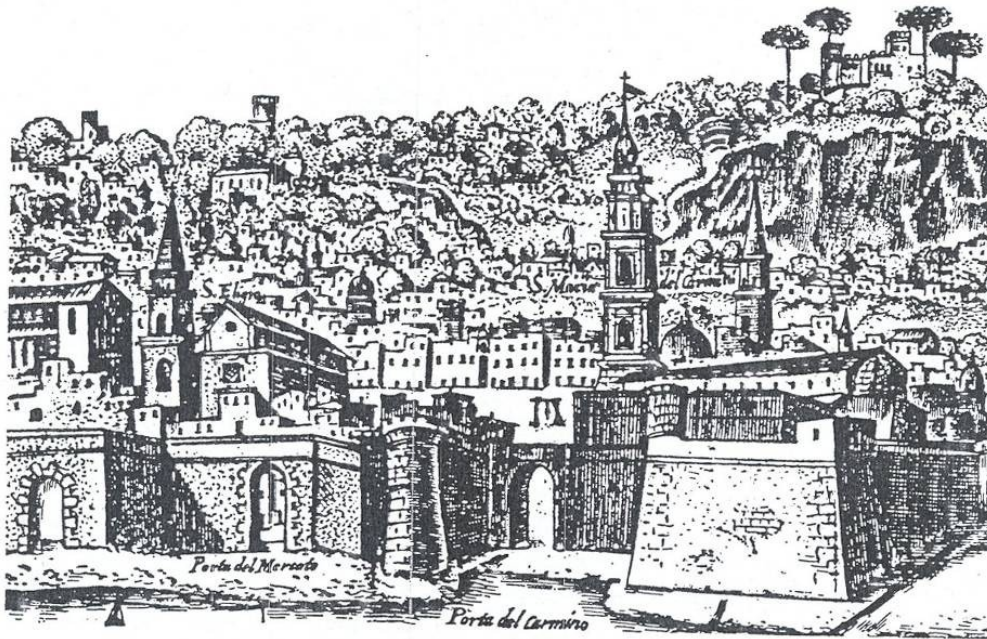


Fig.22. *Fidelissima Urbis Neapolitanae*, Baratta (1629). Copper engraving (48,5 X 212,5)cm. Italian Commercial Bank, Rome

The Cronistoria is very frugal in recounting the events of the 1647. It said this:

“In the early days of the uprising, the populace broke, to be able to enter in the convent, the exteriors doors of the Church, the small door of the church that gets inside the large cloister, and that one of the pulpit, the door of the

monastery on the seaside (Carrese Gate), and also smashed the door of the oven ... ”.

During the Spanish dominion all the strains of an increasingly over-populated city exploded in July 1647, when the legendary Masaniello (a local fisherman) led the populace in violent rebellion against the oppressive rule of the Spanish. Neapolitans declared a Republic and asked France for support, but the Spaniards suppressed the insurrection in April of the following year. In the middle of the period of popular rebellions against the ruling Spanish, the heads of the people, even after the death of Masaniello, were mostly home and resided in the convent. The “Chronistoria of Santa Maria del Carmine” [3] says:

“Gennaro Annese, after the death of Prince Francesco Toraldo di Massa D., by the people elected Captain General and Governor of the tower, was residing in the monastery and caused various damages. A cannon targeted the monastery and fortified Stronghold tower from a ships and destroyed a window of the dormitory. One bullet hit the Bell Tower.”

After the events of the revolution of Masaniello, the Spanish returned to reign supreme. The convent was occupied by soldiers who lived there for sixteen years at the expense of regular observance of the poor friars. In 1648, the convent that was the headquarters of the insurgents guided by Gennaro Annese, fell to the hands of Don Giovanni of Austria and the Conde de Oñate. They decided to enlarged and fortify the “Square tower”, laying on the troops of Spain. Unable to contain the entire garrison, one part of it was placed in the cells of the monks and in the cloister. The Stronghold tower became Castle (Figs.23&24) and remained a barracks until 1664. In this period the large cloister become the parade ground of the castle (drill ground of the castle). Then, after the revolutionaries exiting the stronghold tower, the defence structure restructured by the Conde de Oñate became a true castle. The protest of the Carmelites for the occupation of monastery premises was very strong but without any positive effects. In 1662, fourteen years after the renovation, a new intervention gave the definitive asset to the fort.

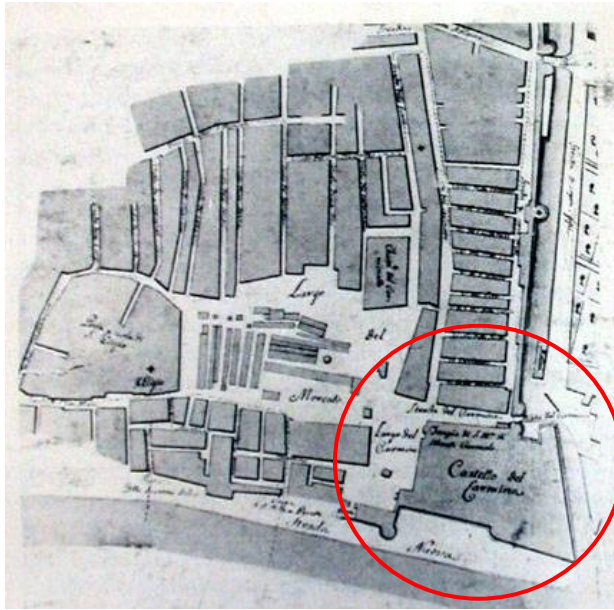
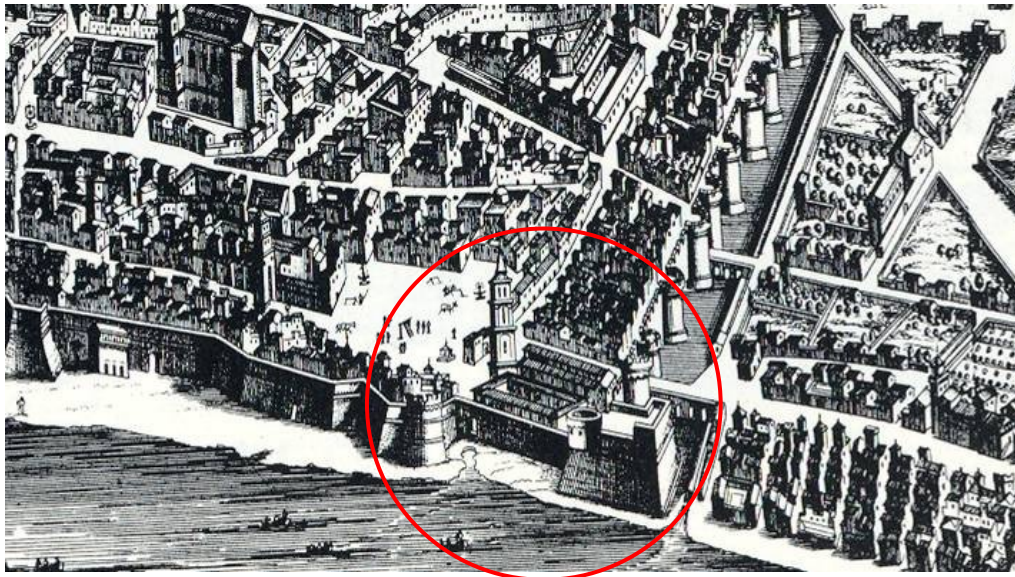


Fig.23. Lay out of the sites under the venue of the Carmine Castle, Naples, State Archive, Drawing Section

Fig.24. Napoli, B. Stopendael (1663), copper engraving, (42 X 102)cm. Grimaldi Collection, Naples



On this occasion, the Spanish government decided to make the convent a real fortress, as would have happened if the brothers had decided to move, but they refused and stayed.

The “Cronistoria” [3] says:

“The church and monastery were almost incorporated within the new Castle...in addition a long corridor paved with Vesuvius lava, ensured a connection between the church and the bastion of the castle (Fig.25). The corridor was running on the on the north side church chapel roof and behind the choir of monks”.

Apparently was intended for the easy transport of artillery from the castle in the Mercato Square. This walkway allowed better defence on one of the city gates, the Carmine one. In fact the soldiers were not obliged to cross the square where they could have been attacked.

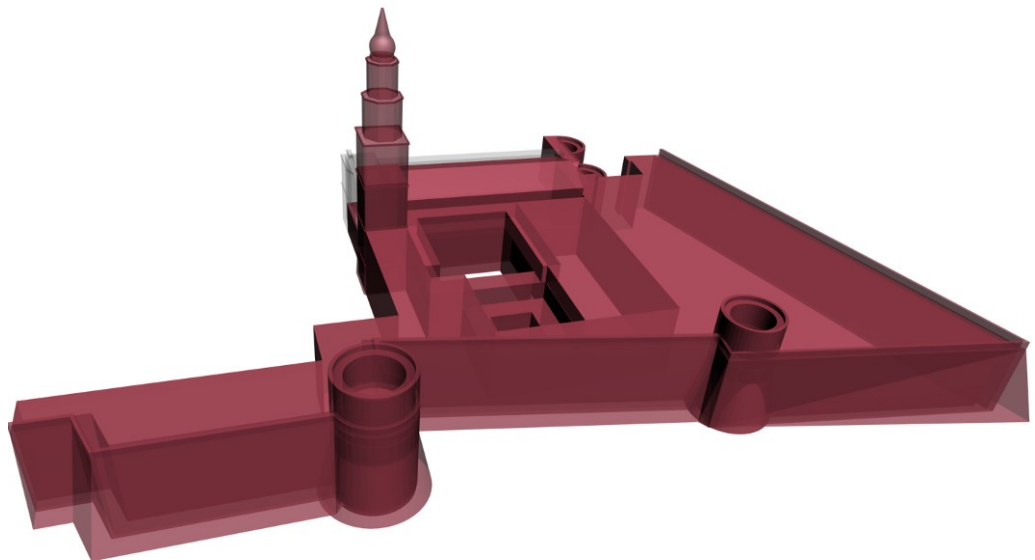


Fig.25. The Carmine Castle

The Viceroy Conde de Peñaranda wished that the castle had a capacity to accommodate a large garrison, and felt obliged to completely separate the

military structure from the religious one, although the gap between the two complexes would have to be very large. If necessary, the troops could go through it and enter into the monastery. The Viceroy gave assignment to two of the major architects working in those years, Francesco Picchiati and Domenico Antonio Cafaro, to provide for the resettlement area in front of the church and the convent of Carmine, and to give a more logical configuration of the castle and to the religious complex. The cost to the monastery was 30,000 scudi of which over half were bestowed by the brothers Francesco and Bartolomeo Pinto, Carmelite friars, and the remaining amount was bestowed by the Prince of Cellamare.

The work was begun in 1662. The difficulty consisted of reducing the communication between the castle and the monastery, but not closing it. In this way, when needed, the troops could not immediately occupy it.

- Was raised a wall that prevented any communication between the defensive zone and convent.
- To separate the two structures, this was equipped with a corridor in which the soldiers could go through in case of defense.

From Celano's letter:

Following the 1647 popular revolt (Masaniello), at the beginning of April 1648 the Spanish troops at the orders of Don John of Austria and the Viceroy Comte D'Ognatte occupied the Carmine Monastery, transforming it into a true drill ground. The Carmine friars, to send the soldiers off the Monastery, were obliged to pay between 1663-1664 the sum of 30.000 ducati to build the ring road of the Royal Carmine Monastery with the fortification of the tower on a plan arrived from Spain. To protect the corridor built all around the first story of the monastery, to allow the crossing of the soldiers through the Bell Tower and to locate guns, it was cut at the bottom the first story window south of the Bell Tower. The correspondent façade was lined with a double band of tuff wall

hiding the upper portion of the window. In fact from inside it can be observed the arch shape.

Confirmation of the realization and existence of this corridor was found by the writer in two documents discovered at the Simancas Archive in Spain with two attached drawings (one of those unplubished) from the original design by Picchiati and Cafaro. In Appendix I the copy of the two plans is reported.

Additionally from the Coppola's paint representing the 1656 plague it's possible to glimpse the sheltered communication trench running alongside the church (Fig.26).



Fig.26. Carlo Coppola, "Pest happened in the Kingdom of Naples in 1656", Oil on canvas, Storage Capodimonte Museum, Naples

For two centuries, the Bell Tower was unfinished, until 1615 when construction was resumed. Designs by Giovan Giacomo di Conforto were made, above the ancient basement, consisting of three orders of quadrilateral shape. Because of the sudden death of the architect, the work was interrupted in 1620. The work was resumed two years later by the Dominican Father Giuseppe Donzelli (Father Nuvolo), who completed the Bell Tower with an octagonal cell and a pyramidal spire. The tower was covered in polychrome, majolica tiles, with a

typical “pear shaped” form. The work on the new building was completed in 1631 (Fig.27). Between 1659 and 1664 the third expansion of the square was realized in front of the convent and the castle, under the vice-royalty of the Conde de Peñaranda. The church had different adaptations and transformations. The most important was the reduction in Baroque style between 1753 and 1766. The work was made by the architect Tagliacozzi-Canale, who was helped by the masons and the plasterers brothers Cimmafonti Gargiulo.

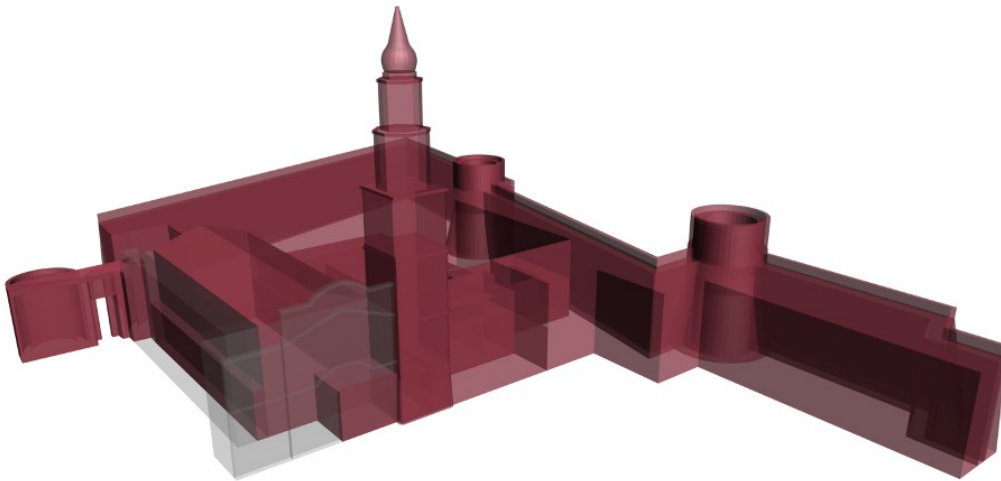


Fig.27. The Bell Tower and the Castle

In Appendix II is reported the entire historical document that have been consulted during the research.

2.4 REFERENCES

- [1] Celano C., Chiarini G.B., 1974. *“Notizie del bello dell’antico e del curioso della città di Napoli”*, Edizioni Scientifiche Italiane (in Italian).
- [2] Cajati C., Pastore R., 1998. *“Il Chiostrò e la Piazza: Il Mercato da Sant’Eligio al Carmine”*, Giannini Editore, Napoli (in Italian).
- [3] Moscarella P.T., *“Chronistoria del Carmine Maggiore di Napoli”*, written by Pier Tommaso Moscarella until 1589 and continued by alii until 1825, Bibl. Naz. Sez. Misc.X AA2 (in Italian).
- [4] Clemente D., 1875. *“Il Santuario della Bruna o la Chiesa del Carmine Maggiore”*, Tip. Editrice già del Fibreno, Napoli (in Italian).
- [5] Galante A., 1873. *“Guida Sacra della Città’ di Napoli”*, Fausto Fiorentino, Napoli, 1967, Edizione Fibrebo, Napoli (in Italian).
- [6] Di Giacomo S., 1892. *“Le Chiese di Napoli: Santa Maria del Carmine Maggiore”*, Napoli Nobilissima Per 40 Vol. I,ff. 1-2, 4 Gen/Feb-Apr 1892: 18-32, 56-60, 97 (in Italian).
- [7] De Blasiis G., 1886-1887. *“Le Case dei Principi Angioini nella Piazza Di Castelnuovo”*, In Archivio Storico per le provincie napoletane pubblicato a cura della Società di Storia Patria Napoli presso Federico Furchheim, Libraio (in Italian).
- [8] Monaco G., 1975. *“Santa Maria del Carmine detta “La Bruna” Storia-Culto-Folklore”*, Laurenziana, Napoli (in Italian).
- [9] Quagliarella P. T., 1932. *“Guida Storico-Artistica del Carmine Maggiore”*, Napoli, Taranto (in Italian).

Chapter III

Architectural investigation

3.1 HISTORICAL-CRITICAL ANALYSIS OF ARCHITECTURAL AND STRUCTURAL CHANGES

3.1.1 Cross linking between the history and the structure

The historical investigation has been conducted by consulting historical reference material at public and private libraries, in the state archives and in the Superintendency archives. This investigation has helped to establish the evolution of construction from the fifteenth century up to the present day. A particular attention has been made in understanding the various phases of realization which influence the used materials and techniques and the development of the surrounding constructions that could represent restraints in the structural behaviour as well.

The monumental set of constructions constituting the Carmine Complex (Fig.1) is located at the extreme periphery of the ancient city of Naples. The monumental complex consists in: the Church of Santa Maria del Carmine, the Bell Tower, the Brotherhood of SS. Rosario and the monastery with the large cloister (Fig.2)

The Bell Tower is 68.0m high (additional 4.5m including the cross at the tip) and is made of six storeys plus the basement level. The first historical citation of the Bell Tower is reported in the opera called “Chronistoria del Real Convento del Carmine Maggiore” (Moscarella et al., 1589-1825) [1]. This text reports that during an earthquake in 1456 the upper section of the building fell down, making it necessary to demolish the remaining part. In 1458 the construction of a new Bell Tower started but only in 1615 the construction was completed. According to the design of Giovan Giacomo di Conforto, three levels having quadrilateral layout were built above the ancient base (Clemente, 1875 - Filangieri, 1885) [2&3].



Fig.1. The complex today

The works stopped in 1620 because of the sudden death of the architect Conforto. They were resumed only two years later by the Dominican monk-architect Giuseppe Donzelli (Father Nuvolo) who completed the Bell Tower with octagonal additional levels and with a characteristic “peared” shaped pyramidal dome covered by polychromatic glazed tiles. The new construction was finished within 1631 (Figs.3&4).

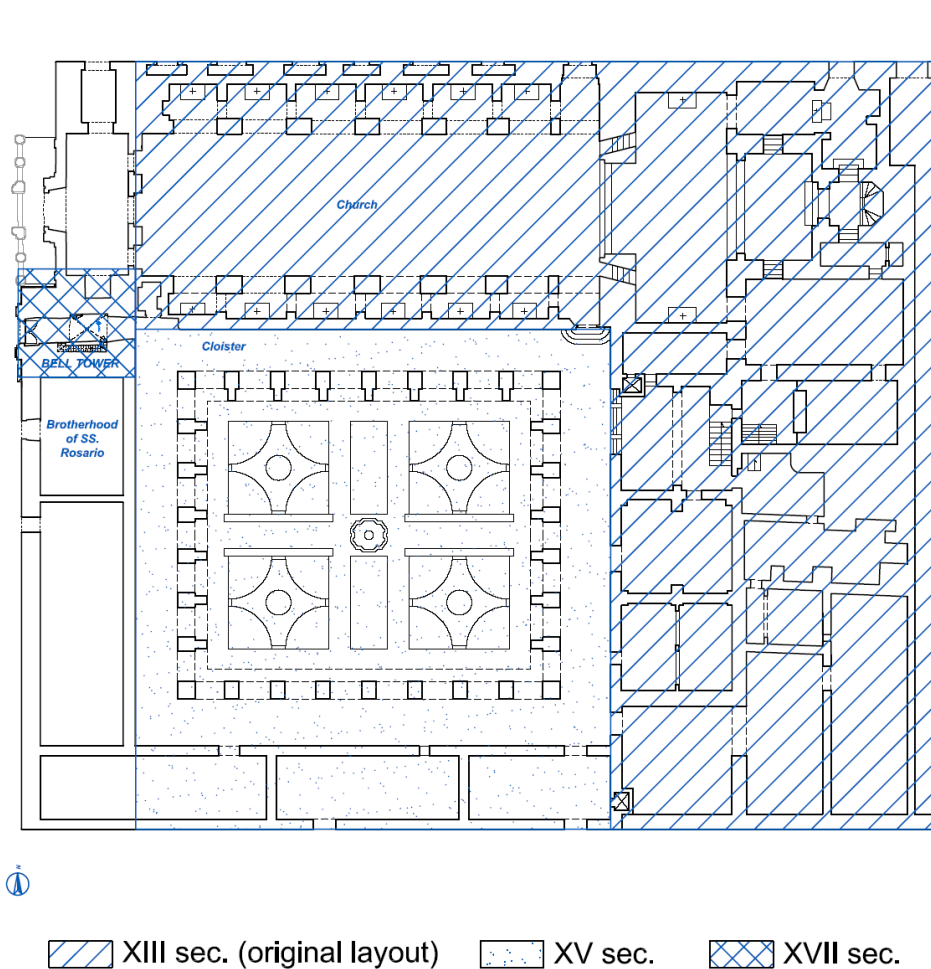


Fig.2. The complex overall layout

The first two levels are surrounded by adjacent buildings (the church, the brotherhood building and the monastery), while the upper ones are free on every side. The plan is variable along the height of the Tower changing from a rectangular section up to the +40.0m level, to an octagonal layout until +57.0m level, where the peared dome starts covering the top of the Bell Tower. In the past the Tower has been subjected to several changes wich have contributed to make it very discontinuous both under architectural and structural aspects.



Fig.3. The Bell Tower Cusp



Fig.4. Rear view of the Bell Tower

The Bell Tower is not an isolated structure, but is part of a building assy that experienced architectural and structural modifications during the centuries. These, may have influenced its behaviour concerning the interactions with adjacent structures. In fact the northern and southern side of the Bell Tower are

constrained between two other buildings: The Church of the Carmine the Major on the northern side up to a height of about +19.0m and the Brotherhood of SS. Rosario named “del Cappuccio” in the southern side up to a height of about +16.0m, as shown in Fig.2. The western side is open on the main square and is completely free, while the eastern side is bordering the cloister of the Church. Therefore the interactions with the adjacent church and monastery were modified from the initial configuration to nowadays.

Through the analysis of the ancient views of the Petrini’s engraving (Fig.4) dating from the 18th century referenced by Celano and Chiarini [4] and the Antonio Joli’s painting (Fig.5) dated from 17th century and kept at National Motor Museum, Beulieu, England, it is possible to confirm that probably the Bell Tower was a structure isolated from the rest of the complex and free on all fronts. Joli’s painting, which dates to the end of XVIII century, clearly shows a space between the two buildings (Fig.5). In these iconographic fonts, it is possible to see the presence of two windows (one at the first level, another at the second level) similar to the side ones in the upper storeys that are nowadays completely sheltered. At the end of the XVIII century the church got many modifications (Celano, 1974; Quagliarella, 1932) [4&5]. The most important one is that the original Renaissance styled façade reproduced in the iconographic sources was modified in the current baroque styled façade. The new façade was moved forward with respect to the original ones. This is the reason why the Bell Tower side adjacent to the body of the church is hidden. The pre-existing windows were plugged and the room in between filled with different material to enhance the homogeneity of the complex. In fact inside the first level of the Bell Tower it can be seen the track of an opening that very probably corresponds to the pre-existing window.

The degree of the interactions amongst the three structures (Bell Tower, church and congregation), resulting from the modifications done through the centuries, has been more in depth verified through the survey on materials, geometry, structure and the dynamic characterization of the structure.



Fig.4. The Church and the Gate of Carmine in the Petrini engraving reported in Celano Chiarini, 1974



Fig.5. Antonio Joli, Piazza del Carmine, particolare. Beaulieu, National Motor Museum

The understanding of the connections between these three structures is paramount to establish the constraints of the surrounding buildings on the Bell Tower in order to design a structural model and to evaluate reciprocal actions under static and seismic loads.

The current structure of the Carmine Bell Tower is installed on the structure of the original fourteenth century Bell Tower. To-days' only the basement part, made with piperno rusticated ashlar is still there. Remains of the original structure can be observed also inside. This can be stated with confidence since the door opening the Friars dormitory into the Tower appears in a late fourteenth century style. This clearly demonstrates that it is part of the ancient Bell Tower. These walls must have remained intact after the collapse of the tower caused by the earthquake described above. This door probably was the main entrance for the original Bell Tower. Historical sources therefore enable us to state with confidence that the construction of the church comes before the construction of the Bell Tower. It has been necessary to assess the extent of the scarfing accomplished "a posteriori" between the two structures through the filling material and to examine the various structural modifications done on the façade of the church during the centuries. It was also considered necessary to conduct an in situ investigation in order to further assess the texture of the walls by removing the plaster for a first visual assessment and subsequently to proceed with wall coring to map their properties. The plaster was removed and test cylindrical samples were extracted from the wall adjacent the church (Fig.6a, Fig.6c) and from the original wall of the structure dating back to the XIV century (Fig.6a, 6b). It has been deduced that the two walls have exactly the same geometric and tipologic characteristic. In the wall adjacent the church it has been detected also the presence of a plugged opening. So it was possible to confirm that the basement wall of the Bell Tower that today is sheltered by the structure of the church was originally free.

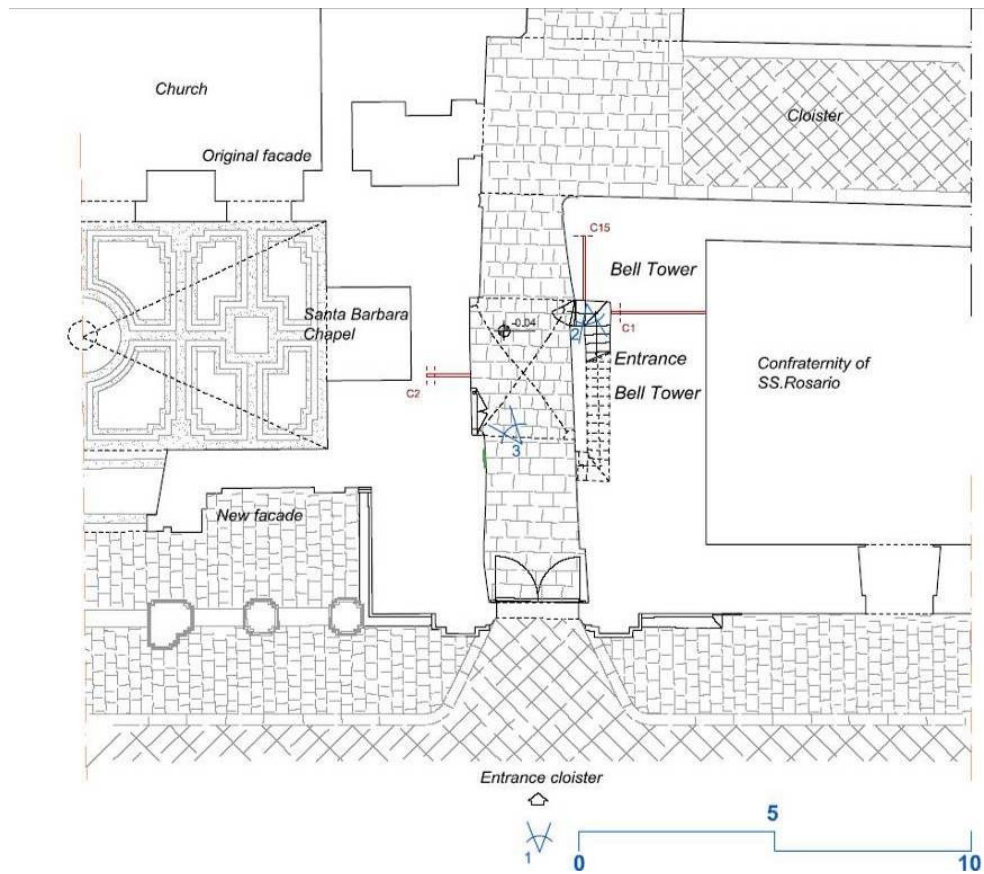


Fig.6a. 1 level Plan



Fig.6b. External part of the Bell Tower basement



Fig.6c. Pipern coating inside the basement area



Fig.6d. Removing of plaster on the wall adjoining the church

On this wall today (on the church side) we find the Saint Barbara Chapel. As we have read in the historical investigation, this chapel was positioned at the foot of the Bell Tower to protect it from lightnings. This can still confirm that this wall was part of the Bell Tower and that probably close to the chapel there was the previous entry into the cloisters (the plugged opening). (Figs.6a-b-c-d). From this viewpoint it was noted that the plugged opening in place at the first floor was the passage into the corridor that connects the tower with the current level of the church choir (Fig.7).

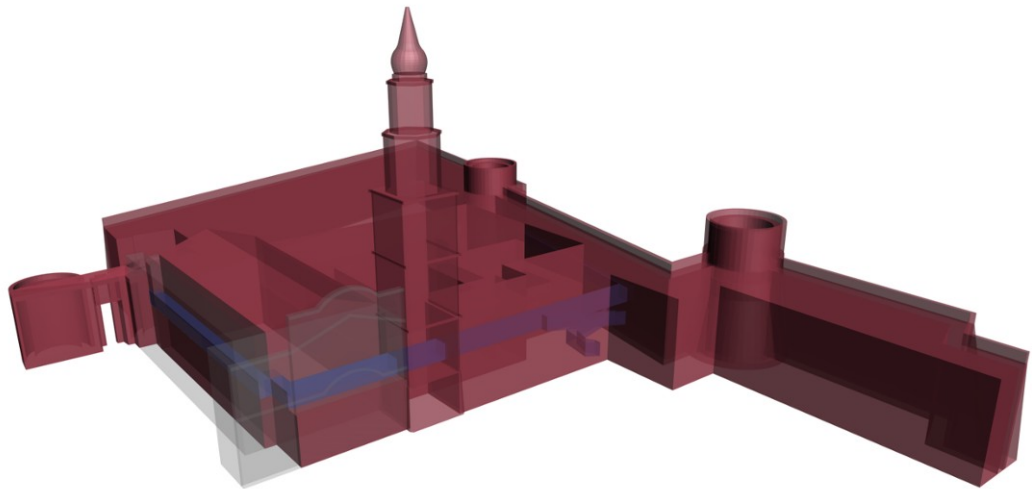


Fig.7. Military corridor

As mentioned above, the corridor was originally designed to allow a faster and more efficient transition of soldiers from the rooms of the adjoining Castle to the door of Carmine (Fig.8a, Fig.8d).

In a private archive it was also found a 1906 document (Appendix III) which reports about the closing “*of the old road to the castle behind the organ*” (Fig.8a, Fig.8c). Since the late nineteenth century, the new organ was placed behind the wall bordering the Tower and the church.

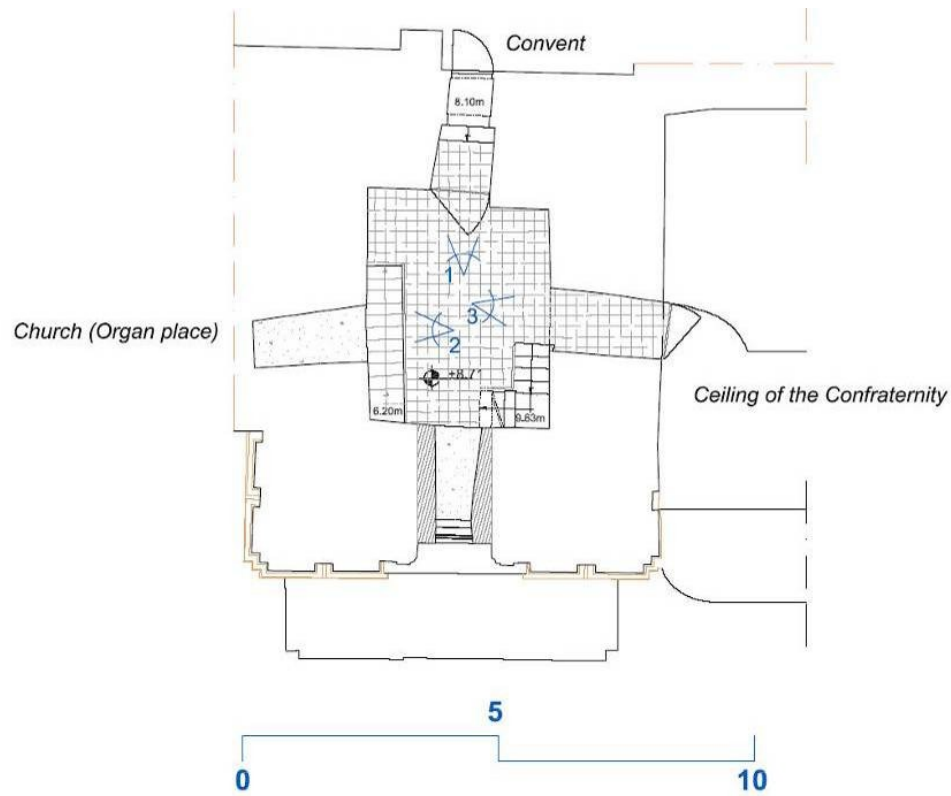


Fig.8a. First level plan, elevation 8,71m

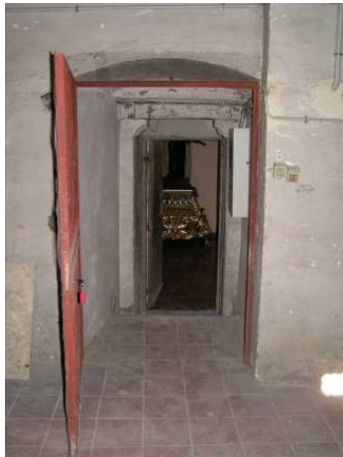


Fig.8b. Monastery's entrance to the Bell Tower



Fig.8c. Plugged Opening in correspondence of the organ level



Fig.8d. Passage to the Castle

Currently next to this wall, a plugged opening is located in the Bell Tower on the first floor. Note that the transit of the soldiers happened through the Tower while it was still possible to access this surroundings even from the monastery area (Fig.8a, Fig.8b). In this we see the will to create a separation zone between the monastic and military zone.

Historical surveys found that the Congregation was built at a later time than the Bell Tower without any structural connection with the pre-existing walls. Regarding the interaction with the building of the Congregation, from visual examination of the roofing level of the Congregation it appears that the floor does not unload on the wall bordering the Tower. As evident in the Figs.9&10, the beams are in fact positioned perpendicular to the outside wall of the congregation that overlooks the Piazza del Carmine and not on the one adjacent to the Tower. It was necessary to make samples to verify if for constructing the Brotherhood structure either it was necessary to build a wall adjacent to the one of the Tower or the structure was simply built in adherence.



Fig.9. Roofing floor of the Brotherhood



Fig.10. Roofing floor supported by the wall bordering the Tower

3.1.2 Overview of the restoration carried out on the Bell Tower

The knowledge of the history of the factory, conducted at public and private libraries, has backed the consolidation of the operations performed on the same. The bibliographical investigation showed that during the last centuries the Bell Tower was accessible only from the first level of the convent. To allow the access to the structure from the cloister, a stair was later realized in the basement part of the Bell Tower. Very probably this was accomplished in the middle of the twentieth century, at the same time of the construction of the reinforced concrete stair that is present at the upper storeys.

After the Second World War, the Bell Tower presented several damages and it was necessary to reconstruct a structure allowing the access to different levels. From the first to the last level the original wooden stairs have been replaced by RC stairs with slabs (Fig.11) well inserted (thickness about 250.0mm) into the masonry walls.



Fig.11. View of the reinforced concrete stair

A diffuse system of steel reinforced inclined mortar injections was realized to

better join the RC stairs to the masonry walls. This stairs probably does not follow a pattern similar to the original wooden staircase. Infact, by comparison with types of towers of the same era, the access to different levels was garantited by vertical wooden stairs that went to higher levels probably through openings in the vaults of masonry.

In addition it was found from the superficial investigation of matter that some original walls of the perimeter of the Tower are lined with tuff bricks. Probably this was required for the realization of RC stairs. Most of these interventions are not documented and so it is not simple to find their rationale as for the presence of reinforced concrete pads in some points of the walls and the elimination of the original masonry vaults of the floor (Figs.12a-b).



Fig.12a. Exterior concrete slab



Fig.12b. Inside view of the Tower: remains of the demolished vault

The Tower today has six floors in addition to the ground level, while historical sources recall approximately 14 floors made by slender vaults realized with tuff stones and clay bricks.

The original old masonry vaulted ceiling and the wooden floors were partially removed and modified recently by adding reinforced concrete (RC) slabs (Fig.13&14) probably for structural and functional reasons.

In particular at the third level the floor is totally made by an R.C. slab, while at the other levels R.C. slabs have been realized on the original vaults. Furthermore, partial remains of the XIV century vault are visible at level +13.2m (Fig.14) and a wooden truss is still visible at the level of bells (Fig.15).

R.C. stairs with slab inserted in the masonry walls allow to reach the last floor of the Tower and sometimes is realized through the vault (Fig.16).



Fig.13. Reinforced concrete plate



Fig.14. Demolished vault



Fig.15. Wooden beams



Fig.16. Reinforced concrete stair

Some recent interventions, at the end of the 1970's and the 1980's, to remedy damages caused by previous seismic actions, consisted in application of steel chains additional to the existing ones. In fact some systems of steel bars at the upper levels go back to the end of the XIX century, while the strands and the bars through the stairs (Fig.17) were located in the 1920's-1930's, before the construction of the RC stair in 1950's and the demolition of existing vaults and wooden floors. For the strand, only the anchoring plates are visible from the outside (Fig.18), since the cables runs through the walls, while the steel bars (diameter 30.0-50.0mm) are visible from the inside of the Bell Tower and their anchoring systems are generally made of vertical bars or outside semi-horizontal bars. A lot of them are ineffective at the anchorage or present a diffuse superficial corrosion and probably are not efficient anymore.



Fig.17. Bars through the stairs



Fig.18. Anchoring plates of strands and bars

Before the 1980's in the structure were present, therefore, longitudinal and transverse chains arranged above and below the belfry. Surveys carried out in

the 1980's, certified the ineffectiveness of these chains and the need to intervene in the same area with the reinforced stitching to make the belfry and the part below unitary and monolithic. After the earthquake of 1980, mortar injection reinforced with steel bars were realized in the corners of most floors lower than the fourth level to increase the connection between walls and improve the monolithic behavior of the structure. Only qualitative indications about the position and the realization of this type of interventions have been founded as illustrated in Fig.19.

Furthermore, the intervention of consolidation of the 1980's also provides for the implementation at various levels of horizontal stiffening frames in order to obtain a proper stabilization of the walls. Finally, the arches of the structure were consolidated with the perforations arranged radially.

Those interventions are documented in the Archives of the SuperIntendency as mandatory because of the increasing of the earthquake damages and are simply classified as "highest urgency" interventions, without any documented project. Consequently the structural damages in the Bell Tower justifying these interventions are unknown. Furthermore it can be assumed that in the past a certain level of disconnections amongst walls was assessed, requiring the improvement of the rigidity of the box structure through insertion of steel bars connecting opposite walls and injections in the corners. Anyway the visual assessment of the corrosion of strands and bars, worsened by the proximity of the structure to the sea, leads to consider some of these interventions not effective any more.

Therefore between the surveys to be carried on the structure has been provide to realize tests to assess the stress state of the chains.

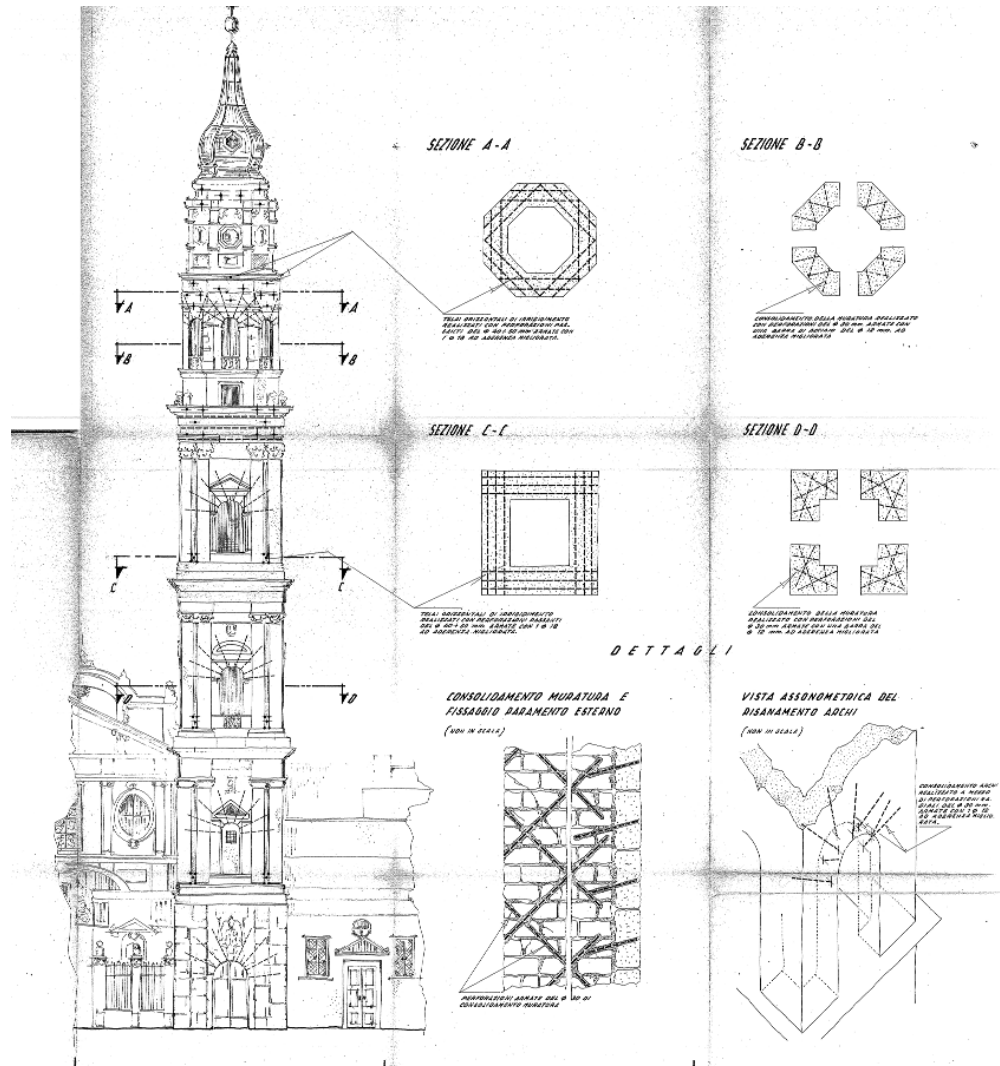


Fig.19. Project of reinforced injection

3.2 GEOMETRIC SURVEY

Generally the evaluation of structures requires an in-depth knowledge of its geometry. This is even truer in the case of monumental masonry buildings. Only the evaluation of the geometry, coupled to the historical analysis allows us to reconstruct all the modifications on the building during its history. The second step in gaining knowledge of the structure is the definition of geometry of the structural elements. For this purpose two surveys are necessary: on the geometry and on the material characteristics. However the structural survey can be considered complete only if the damage situation is understood.

The restoration project requires an in-depth knowledge of the historical construction. In fact this makes it possible to detect the highly characteristic features that only the structure can disclose (alignments, wall configurations, microcracks, construction details, etc.). The study of the structure through historical, archival and bibliographical documentations was accompanied by a historical-critic survey necessary to understand the materiality of the manufacturing as much close to the original configuration as possible. The historical analysis supported by the survey allowed me to characterize, analyze and record the origin of the structure and the vicissitudes during its history, its characteristic elements, the anomalous ones, the structural morphology and its static conditions. The survey operation was an important element in the process of acquiring a complete assessment of the architectonic work.

This process was developed in several steps:

- acquaintance with the structure to find and chose the best suitable survey techniques;
- survey;
- graphical reproduction;
- reading of the structure through the field survey, its direct evaluation, analysis of the historical documentation, the bibliographical sources of the archives.

A punctual and detailed graphical reproduction was realized, able to represent all the elements characterizing the structure of the building. From the geometrical point of view, a topographic survey of some key points and a following photogrammetric survey was realized, through which the graphical reproduction of 12 plan views, 4 vertical views and 4 sections of the Bell Tower were obtained. From the carried out survey it was possible to derive the thicknesses of the walls that vary from a maximum of 4.0m to a minimum of 1.0m. In particular the survey clarified the entity of the structural wall thickness at the different levels, the thickness and configuration of the floors (wooden floors, masonry vaults, reinforced concrete slabs), the horizontal and vertical layout of the stairs, the in plane and vertical interactions with surrounding structures, the position of the relative openings, the positions of steel bars and strands. In Figs.20-24, a front prospect, a longitudinal section of the Tower with three plan views respectively at the ground level, +19.0m and +40.0m are reported. Up to +40.0m the plan have a rectangular layout, even if the plan is rather irregular in the first metres because of the uncertainty in the definition at the basement of the contours of the Bell Tower, Church and the Brotherhood. Above +40.0m the plan assumes an octagonal shape with decreasing wall thickness and larger amount of openings. The relief survey has been designed so as to provide detailed information on the geometry of structural parts such as coverings, windows and entrances, stairs in order to clarify:

- Thickness of masonry at different levels;
- Thickness and typology of floor (R.C. slabs, wooden slabs and beams)
- Planimetric and altimetric development of the stairs;
- Position of hollows, windows, doors and accesses to surrounding structures;
- Interaction with the surrounding structures (church, monastery);
- Position of steel chains.

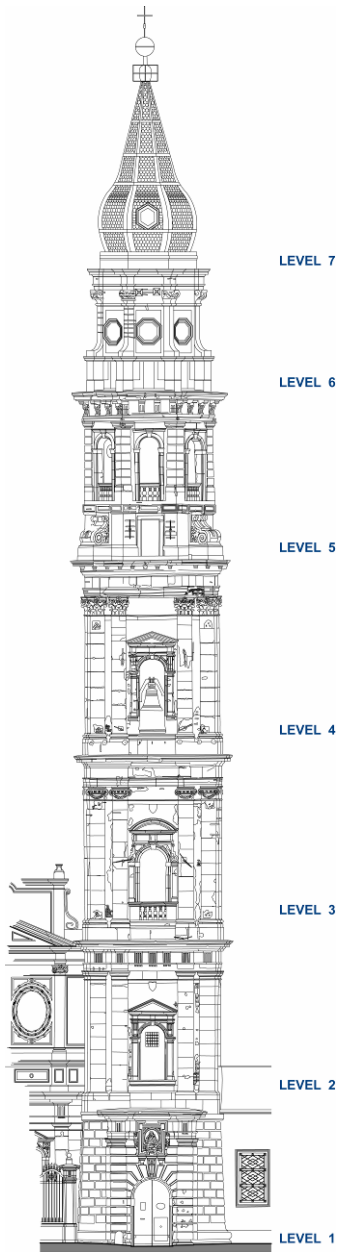


Fig.20. Front prospect of the Tower

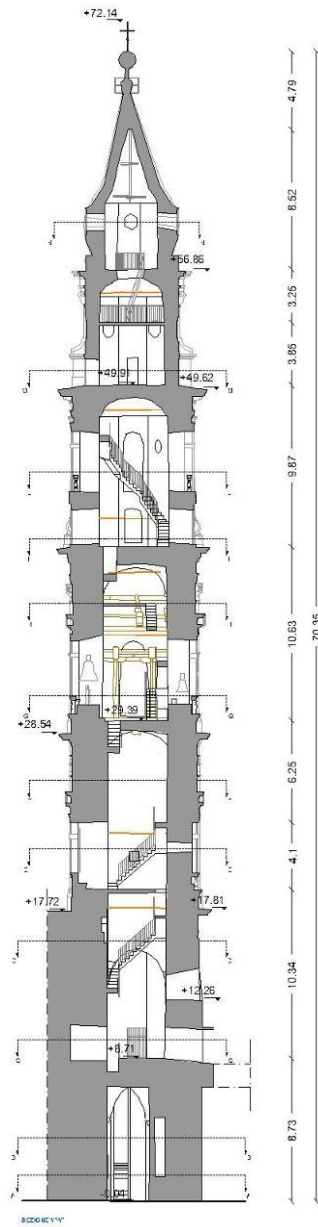


Fig.21. Longitudinal section of the Tower

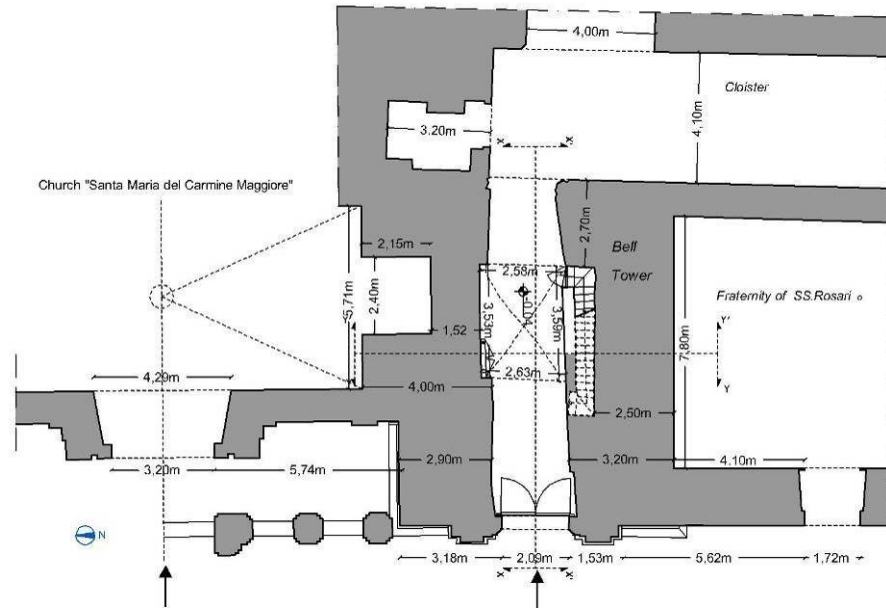


Fig.22. Plan view at ground floor +0.00m

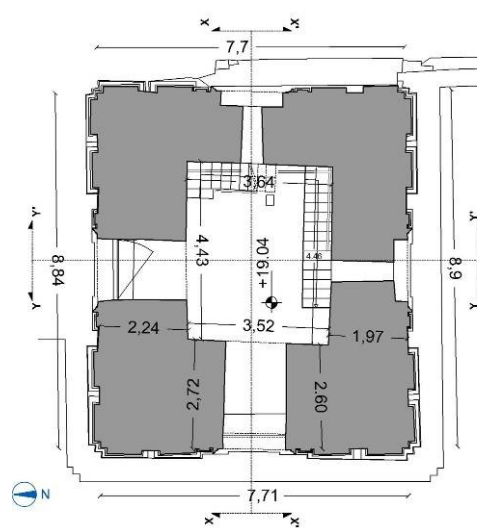


Fig.23. Plan view at +19.00m

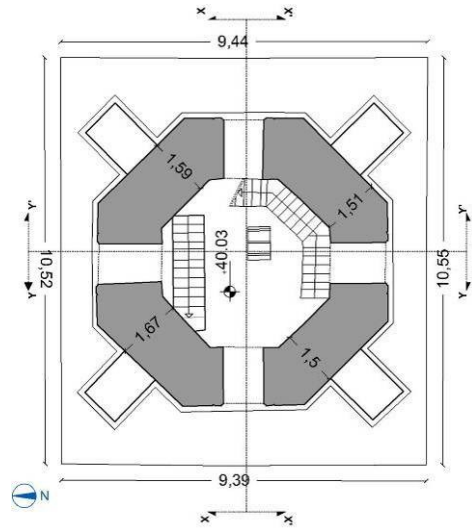


Fig.24. Plan view at +40.00m

It has to be underlined the difficulty to define exactly the contours of the Tower for the first +19.0m, considering the presence of the surrounding buildings. Up to +40.0m the plan has a rectangular layout. Above +40.0m the plans take an octogonal shape with decreasing wall thickness and larger amount of openings. The rectangular structure of the Tower is made of tuff masonry while the remaining upper part is made of solid brick. In the belfry houses 5 bells, of which the largest has a diameter of 1.47m. At the top of the cross stands on a globe of copper with a diameter of 110.0cm. The entire amount is protected by as many as 30 points of platinum against possible electric shock. The external face is in Piperno while the steps are in slate.

A detailed survey of the complex system of steel chains connecting orthogonal walls in the Tower has been performed: totally there are 55 chains with the first ones applied at about +18.0m and the last ones at about +56.0m. At each level the connective system is made of four chains placed symmetrically and parallel to the walls. Various types of chains are present in the Tower. At four levels the single chain is realized by a system of 6 steel strands (probably dated XIX century), each of them made by seven wires having diameter 4mm: the cables pass across the masonry walls and have an external plate anchorage fixing the 6 strands all together. Therefore the chains visible inside are made of steel bars with diameter variable in the range 35.0-50.0mm and having transversal or horizontal bar as external anchorage.

They are characterized by different types of anchorage systems such as horizontal or vertical elements for bars (Fig.25a-b) or a plate for strands passing through the walls and not visible from inside (Figs.26). Separately from the different anchorage system, the driving principle in the design of the steel ties was to realize, at each level, a connecting system made of four orthogonal ties parallel to the walls. The steel chains at +56.0m have an internal system to preload in tension the bars and external steel plates as anchorage. The presence of several steel ties and reinforced injections realized in the past to secure the global behaviour of the Bell Tower is a clear indication of the potential that local phenomena could be activated in the structure due to ineffective

connections amongst its walls. The survey pointed out that many of them are presently ineffective due to either a damaged anchorage or a diffused superficial corrosion that has strongly reduced their resisting area making them close to being ineffective

In Appendix IV is reported all the geometric survey made for the Bell Tower.

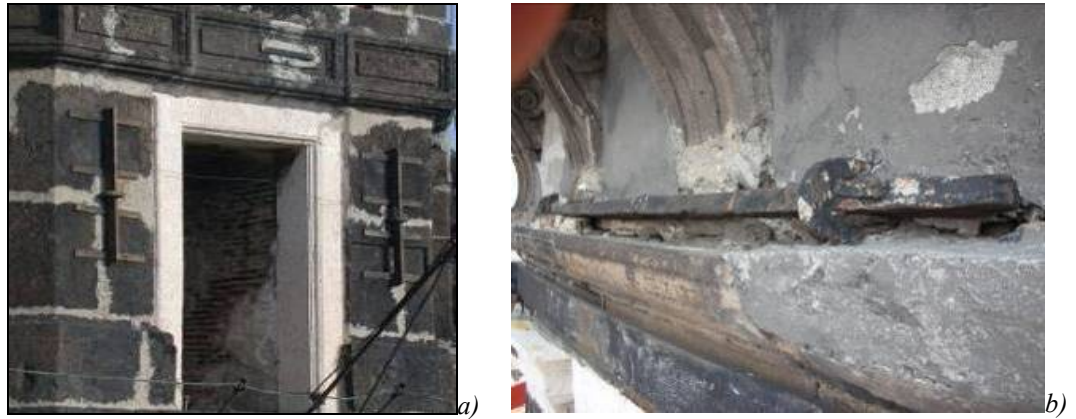


Fig.25. Anchorage of bars: a) vertical; b) horizontal

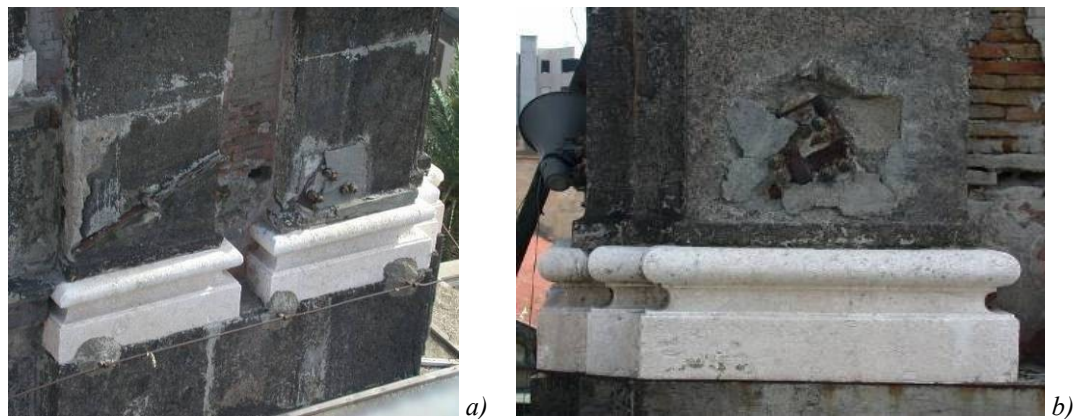


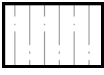
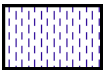
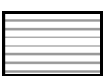
Fig.26. Particulars of ties: a)anchorage of strand; b) anchorage of bars

3.3 DAMAGE SURVEY IN NON- STRUCTURAL ELEMENTS

In the last couple of decades the role of the description in the architectural restoration design took larger place, both in relation to the assessment of the condition of the historical artefact and the graphic return of the design phases and methods. Recently there's been a stronger interest for a restoration design not being limited to a description before and after the operation. Attention must be paid to materials, to their distribution and processing, to their decay so to arrive at a pre-diagnosis and to define an operation planning and a series of conservation procedures. The attention for the formulation of graphic procedures brought out the editing of the Normal Code 1/88 (regulation for stone materials) that describes macroscopic alterations and decays of stone materials prepared by a special Committee appointed at the Central Restoration Institute. This graphic methodology for the identification, lessening and control of the stone material decay is based on experiences run within different disciplinary sectors, like chemistry, physics and technical physics applied to the field of cultural heritage. Within this frame the graphic presentation took a paramount importance in the restoration design, both in the preliminary assessment phase (i.e. thorough survey of the artefacts from the formal, material and decay viewpoint) and the description of the phases of the design and conservation procedures. The geometric and material survey of the artefact to be restored became a privileged survey tool to read the building thoroughly assessing its consistency, noting characteristics and peculiarities like alignments, differences in the wall thicknesses, gaps, texture variations. These parameters are significant of a choice that can be either historical-artistic or simply technical-constructive, to be studied in depth. This way the survey phase interlaces with the historical research, confirming or voiding its assumptions. It's possible to talk of a triad design-history-restoration where each element is strengthened by the other ones and brings in new incentives and investigations. An overall survey was run on the outside surfaces of the Bell Tower to assess

the general condition and appearance of the masonry structure. It appears evident the lack of maintenance through detached spot of plaster, presence of vegetation, presence of corrosion but there was no particular evidence of severe decay. The survey assessment is reported in Table 1 and in Fig.27.

Table 1. Different case of decay present on the facades of the Bell Tower

Materials	Symbology	Phenomenon description	Causes
Peperino		Fault: Fall and loss of parts	Lack of maintenance, environmental agents and not accurate introduction of brackets, strands and tie-bars
Marble		Detachment: Discontinuity within material surface or with the substrate: this term is used particularly for plaster layers and mosaics	Natural ageing, lack of maintenance, atmospheric agents
Plaster		Detachment: Discontinuity within material surface or with the substrate: this term is used particularly for plaster layers and mosaics	Natural ageing, lack of maintenance, atmospheric agents
Peperino		Presence of vegetation: term used in presence of lichens, musks and plants	Lack of maintenance, atmospheric agents
Peperino		Patina: natural modification of the material surface causing a change of the original colour	Natural ageing, lack of maintenance, atmospheric agents, atmospheric pollution
Peperino		Surface deposit: accumulation of foreign materials of different nature	Presence of powder deposits, debris, dove guano, dark patina caused by the deposition of atmospheric particles
Marble		Surface deposit: accumulation of foreign materials of different nature	Presence of powder deposits, debris, dove guano, dark patina caused by the deposition of atmospheric particles
Plaster		Tie-bar and strand sockets, brackets	Corrosion of sockets due to humidity, action of rains, lack of maintenance
Peperino		Cracking: presence of continuity solution in the material with relative displacement of the parts	Light cracking and failure, lack of maintenance
Marble		Deformation: shape variation through the thickness. Appears evident mainly in plate elements	Light cracking and failure, lack of maintenance
Peperino		Anthropical decay	

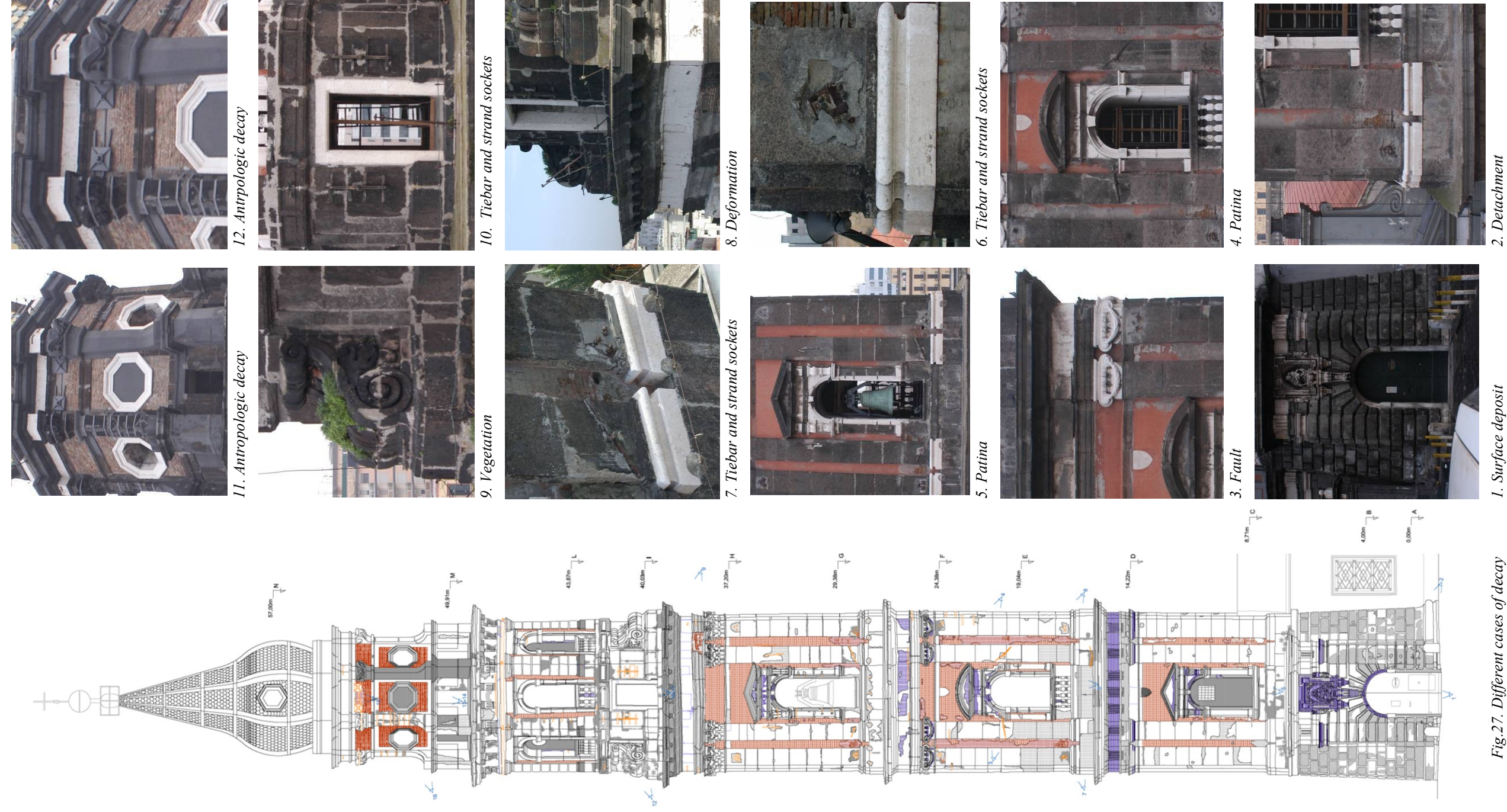


Fig.27. Different cases of decay

3.4 REFERENCES

- [1] Moscarella P.T., “*Chronistoria del Carmine Maggiore di Napoli*”, written by Pier Tommaso Moscarella until 1589 and continued by alii until 1825, Bibl. Naz. Sez. Misc.X AA2 (in Italian).
- [2] Clemente D., 1875. “*Il Santuario della Bruna o la Chiesa del Carmine Maggiore*”. Tip. Editrice già del Fibreno, Napoli, Bibl. Naz. Sez. Nap. Misc. VI A 4(8) (in Italian).
- [3] Filangieri G., 1885. “*Chiesa e Convento del Carmine Maggiore in Napoli*”, Descrizione storica e artistica. Tipografia dell’Accademia Reale delle Scienze, Napoli, Bibl. Naz. Sez. Nap. Misc. IX B 2 (in Italian).
- [4] Clano C., Chiarini G.B., 1974. “*Notizie del bello, dell’antico e del curioso della città di Napoli, divise dall’autore in dieci giornate per guida e comodo de’ viaggiatori, con aggiunzioni di Giovan Battista Chiarini*”. Naples, Edizioni Scientifiche Italiane (in Italian).
- [5] Qagliarella P.T., 1932. “*Guida storico-artistica del Carmine Maggiore*”, Taranto, Bibl. Naz. Sez.Nap. VIB 1026 (in Italian).

Chapter IV

Structural investigation

4.1 MATERIAL SURVEY

4.1.1 Building techniques for masonry structures in Southern Italy

Existing masonry historical buildings represent a large percentage of the existing residential and monumental building blocks in Italy; such structures possess mainly traditional configurations. Nevertheless, the assessment of the configuration type may result rather complex and not suitable for simplified modelling (Lourenço & Roque, 2006) [1]. There are a number of historical centres in the South of Italy which are characterized by a variety of masonry structures employing different materials, construction techniques, urban and architectural features. Different local needs, such as the urban environment, site condition, local climate, topography and the availability of construction materials render each historical building unique and hence, different from any other. Many of the historical masonry buildings currently present on Italian territory date back to the Middle Ages. The building techniques of walls in the medieval period differ, depending on economic potential, social aspects and local material availability and evolved over time according to different solutions depending also on the size of the stone used. The heritage buildings of Middle

and Southern Italy are mainly stone masonry structures made of tuff of different origin.

Tuff is a natural stone with volcanic origin and physical and mechanical characteristics widely variable from place to place. It has been used extensively as a construction material because of its lightness and good workability. It has good mechanical properties in compression and low unit weight due to a very porous structure. The mechanical parameters of tuff can vary appreciably according to the original quarry and depend on the structure of the internal system of microscopic voids. In particular, among all the different kinds, the yellow Neapolitan quality is one of the most used because of its larger availability and relevant variability of mechanical properties as demonstrated in experimental tests by Dell'Erba, 1923 [2]. Dell'Erba classified this kind of tuff as low (<2MPa), poor (2-3MPa), middle (3-4MPa), good (4-5MPa), high (5-7.5MPa) and elevated compressive strength (>7.5MPa).

The extent of diagenesis (temperature and trapped gas present at the time of sedimentation), the average size of pumice inclusions, saturation degree and porosity are the main physical parameters influencing the compressive strength. Furthermore the average strength of saturated tuff is approximately 75% of the dry one, while it may suffer a substantial mechanical degradation over 105°C. The tensile strength generally varies between 0.5MPa and 5.0MPa, while the elastic modules vary from 800MPa to 3000MPa; mainly (80% of the cases) between 1000 and 2000MPa (Ceroni, Voto et al., 2004)[3].

Because of its extremely good workability, this material has always been dug out over the centuries and formed into blocks, taking an absolute primary role as both structural and decorative finishing in the sacral, civil and military architecture of the Southern Italy regions like Lazio, Campania, Puglia and Sicily.

Tuff shows good characteristics for both structural behaviour and thermal insulation, but decays rather easily when exposed to atmospheric agents. For this reason, the external masonry walls are often shielded with plaster cladding or more resistant stones.

Depending on the particular geo-lithological and historical-cultural conditions of the areas under evaluation (Fiengo et al., 1994) [4], the walls textures of the tuff can be classified as:

- Squared tuff stones with irregular or isodome textures;
- Faced tuff masonry (Fig.1) filled with demolition material, scraps of either crushed ashlar or chopped block stones extracted from quarries;
- Mixed masonry with tuff stones and rows of bricks to better distribute loads.

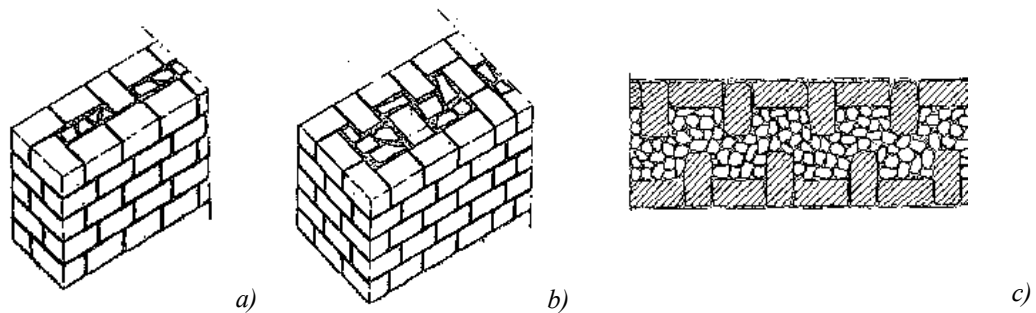


Fig.1. Faced tuff walls: a) thickness < 0.7m; b) thickness > 1.0m; c) connection by orthogonal stones (reported in Fiengo. et al., 1994 [4])

The elements resulting from the joining of the stones behave like a monolithic block, showing cohesion with no interruptions. This is due to the staggered layout of the joints, in addition to the regularity of the block faces, the careful selection of materials (strength, durability, toughness, workability) and the good composition of the mortar. The regularity of the faces and the parallelism in their assembly guarantee the uniform transmission of the loads, due also to the mortar that fills the gaps between the various elements. The building techniques used in Southern Italy do not vary greatly from place to place. Most ancient masonry structures used the facing technique for the economic advantages associated with such materials, availability of manpower and also speed of execution. In the faced masonry texture, two parallel stone panels are separated by a void

filled with demolition material, scraps of either crushed ashlar or chopped block stones. Unfortunately this kind of technique has often shown a weakness in the link between the two front surfaces. To avoid this problem, sometimes the two front surfaces were connected by orthogonal stones called diatones (Ceroni & Voto, 2008) [5]. The faced block system was often sized on the basis of experience. The walls had a minimum thickness of 50.0cm, depending on the type of building. The frequency of transversal elements generally increased with the wall thickness (Fig.2). Over time, the wall assembling techniques improved focussing attention also into avoiding corresponding vertical joints between adjacent stones. The structural response of a building in fact depends strictly on the mutual connections between the stones in the same walls and between the resistant elements (horizontal and/or vertical). Particularly, if the walls constituting the building are not well connected to each other in the corners, they can behave independently without developing a global, collaborating resistant mechanism, under horizontal actions, such as an earthquake. So, the response of each wall is mainly related to its behaviour out of the plane. Antique masonry buildings are frequently subject to local failures, characterized by single parts involved in out-of-plane mechanisms, activated by horizontal actions when the connections among them and/or with the horizontal elements are lacking or are not effective anymore. These phenomena have already been observed in the past and were usually avoided by applying some “good construction principles”, such as:

- Strengthening of connections in the corners of orthogonal walls by performing crossing textures (Fig.3);
- Insertion of steel ties (bars, cables, wires) giving a punctual connection between orthogonal walls (Fig.4);
- Attention to avoid preferential failure lines by a proper assembling of stones and alternating layout of mortar joints (Fig.5).

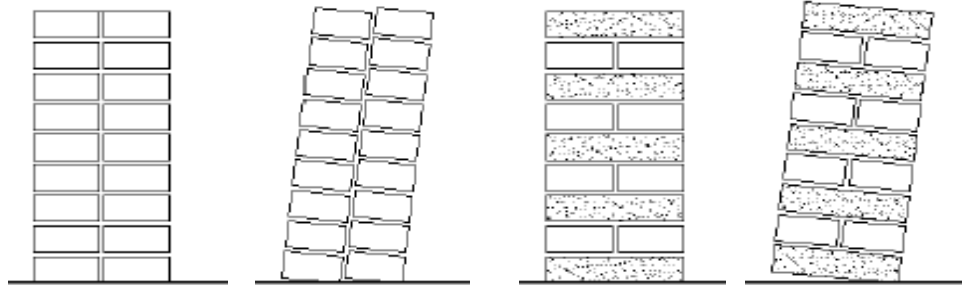


Fig.2. Effect of transversal connection of diatons between walls in faced masonry



Fig.3. Strengthening of corners by more resistant elements

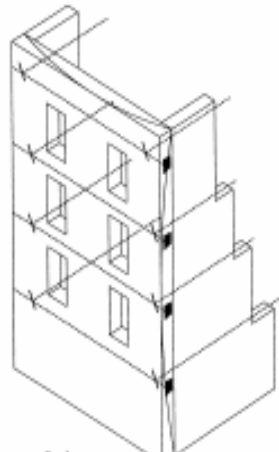


Fig.4. Connection between orthogonal walls by steelrods

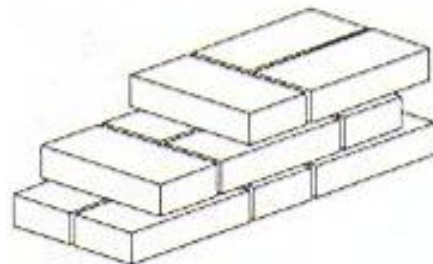


Fig.5. Alternated layout of mortar joints

4.1.1 Analysis of material and wall textures of the Bell Tower

The broad variability and heterogeneity of the mechanical properties affecting historical masonry buildings (Binda et al., 1992) [6], makes the material survey a primary and fundamental step to carry out proper analysis of their structural behaviour. As introduced in the previous paragraph, the geometrical survey enabled us to determine the geometry of both structural and architectonic decorative elements. The structural behaviour of masonry buildings however, is not only dependent on the geometry of the elements, but also on the texture of the walls and the mechanical properties of constituent materials. The behaviour of masonry elements is associated with the geometry and mechanical properties of the masonry blocks and the mortar and the way they are assembled. For faced masonry walls, the typology of filling materials and the degree of connection between the external walls are further parameters that influence the structural behaviour and have to be investigated.

Therefore, a preliminary visual survey of the materials was made, that allowing a definition of the variability of materials and texture in the Bell Tower, with the aim to classify all the materials of the structure (Appendix V). For each material, the exact nature, typology (i.e. squared stones, roughly cut stones, solid or perforated bricks, fired or sun-dried bricks), dimensions and utilization modalities have been identified. When possible, it was desirable in this phase to distinguish the original materials corresponding to the first construction phase from the ones introduced in later periods. Surface plaster, without historical value, was removed in various internal points to discover the masonry texture (frame with dimensions about 50cm x 50cm).

A comparison of the wall textures and the materials found inside the Bell Tower with typologies and construction techniques typical of Neapolitan area, defined on the basis of bibliographical historical surveys, let us identify the periods of construction of the different parts of the structure, showing also the overlapping of construction phases going back to different ages.

The Tower is made of faced masonry (Fig.6) of Neapolitan yellow tuff up to the

+40.0m level. The faced tuff wall texture is produced by roughly squared tuff stones, with a regular shape and thick mortar joints (approximately 3.0cm). Stone sizes are 16c x 23cm alternating with 20 x 20cm stones. The tuff walls are covered on the outer sides by piperno and the inner sides by peperino for approximately the first +7.5m. Piperno and peperino are other types of natural volcanic dark stones with higher mechanical properties than tuff and are generally used in the part of the structure where more resistance to external actions is necessary. The internal covering in peperino (Fig.7) is made by well-squared and aligned rectangular shaped stones 20cm thick, with thin mortar joints (1.5cm). This texture is typical of Neapolitan fifteenth century architecture and confirms the hypothesis that the seventeenth-century structure was built atop the original basement made in the fifteenth century. The level having a squared layout are built with a tuff wall texture, characterized by roughly squared tuff stones, with a regular shape and thick mortar joints (about 3.0cm). Stone dimensions are 16 x 23cm alternated with 20 x 20cm stones. For the levels characterized from a squared layout, the maximum and minimum dimensions of the entire wall thickness are 3.4m and 2.6m, respectively. The mortar joints and the filling material between the faced tuff walls are of pozzolanic nature. Above +40.0m, the Tower has an octagonal layout with walls made of red and yellow clay bricks (Fig.8). The total thickness of walls above +41.0m decreases from 1.8m to 0.9m.



Fig.6. Tuff wall texture



Fig.7. Peperino cover stones



Fig.8. Clay bricks wall texture

In Appendix VI a report of the material survey is presented.

4.2 DAMAGE SURVEY IN STRUCTURAL ELEMENTS

The research accomplished in the archives of the Superintendency revealed that the structure was damaged several times by seismic events (1656, 1728, 1745, 1762, 1866, 1877), up to the recent 1980 earthquake. Examination of the current cracks distribution however, showed no special damages to the structural elements, whereas, the major analysis of interventions and changes made over time, especially in the last century, gave us reason to assume a number of weaknesses in the overall behaviour of the structure. This had also been identified by experts who had examined the Tower previously. Since its construction, various interventions have altered the original configuration of the Bell Tower, complicating the analysis of its effective conditions. Most of the cracks in the building still have belonged to various disturbing causes, such as age of the property, shock caused by war bombs, earthquakes, manipulations of some frames made in previous transformations, and the constant stress of the structures due to the vibrations produced by the bells. These cases have generated over the years, a complex damage distribution characterized by the presence of vertical cracks and buckling cracks that made necessary appropriate interventions of consolidation.

Visual inspection of the external facades of the Tower revealed the presence of degradation of coatings. For some of them, it is necessary to understand if the level of degradation is linked to the external face only or to what extent it may instead be the result of problems in the internal masonry. In Fig.9 some details of external wall disruptions are reported. The buckling of the piperno cladding in the vicinity of a corner is quite apparent in this picture. Fig.10 shows a deformation of the frame at the level where the tuff rectangular layout changes to an octagonal layout in the brick structure.

The R.C. stairs built in the fifties of the twentieth century, is realized of slabs in R.C. inserted into the wall through a curb in R.C. The presence of stairs can have a beneficial effect of confinement. It can be a good connection for the walls and can improve the global “box behaviour” of the Tower, especially at

higher levels where the walls are less thick. It can also have a favourable effect on the confinement of the Tower in particular, in the upper parts where the structure is more slender.



Fig.9. Damage on lateral and main front of the Bell Tower. Stone buckling



Fig.10. Damage on lateral and main front of the Bell Tower. Frame deformation

It is assumed that past survey detected a lack of linkages between walls. This

made necessary to stabilize the structure and to connect opposite walls by insertion of tie-bars plus injections in the angles. The presence of inclined injections in correspondence of the curbs and the angles would confirm the need to scarf the staircase within the masonry both to guarantee the static resistance of the slab and to improve the extent of connection between the staircase and the masonry walls, improving the restraint effect. Furthermore already in the past, the structure showed a high deformability confirmed by the fact that at the upper levels, beyond +40.0m where the plant is octagonal and the structure is slender, some original symmetrical openings were closed during the years by clay brick walls (Fig.11). At the fifth floor (+40.0m level) some cracks were closed by mortar injections. The cracks probably were formed at the interfaces between different materials where tuff curtains had been used to close the windows. Some of these closures may be related to periods just after the completion of the structure and were necessary to stiffen the structure in the presence of loads of exercise (wind, not negligible vibration due to the operation of the bells).

Steel bars are located at the various levels of the Tower, while all along its outside perimeter and for its entire height a series of plates of iron cage are put in place. Their purpose is to tie up the façade piperno lining and to avoid its detaching and falling down. Moreover, almost all ornamental stone parts protruding outside of the Tower have prompted a reinforcement of the constraint, made by means of collars, ties, brackets, etc. The presence of chains and strands, were made also in order to prevent and/or compensate the outside opening of the walls of the Tower and to exercise a kind of containment on the structure favouring the box behaviour. The high numbers of reinforced injections in the angles also appear to reiterate the need for containment and better mutual seam of the walls of the structure. In fact in some parts of the Tower was found as some of the walls actually seem to present a tendency to deflect outward.

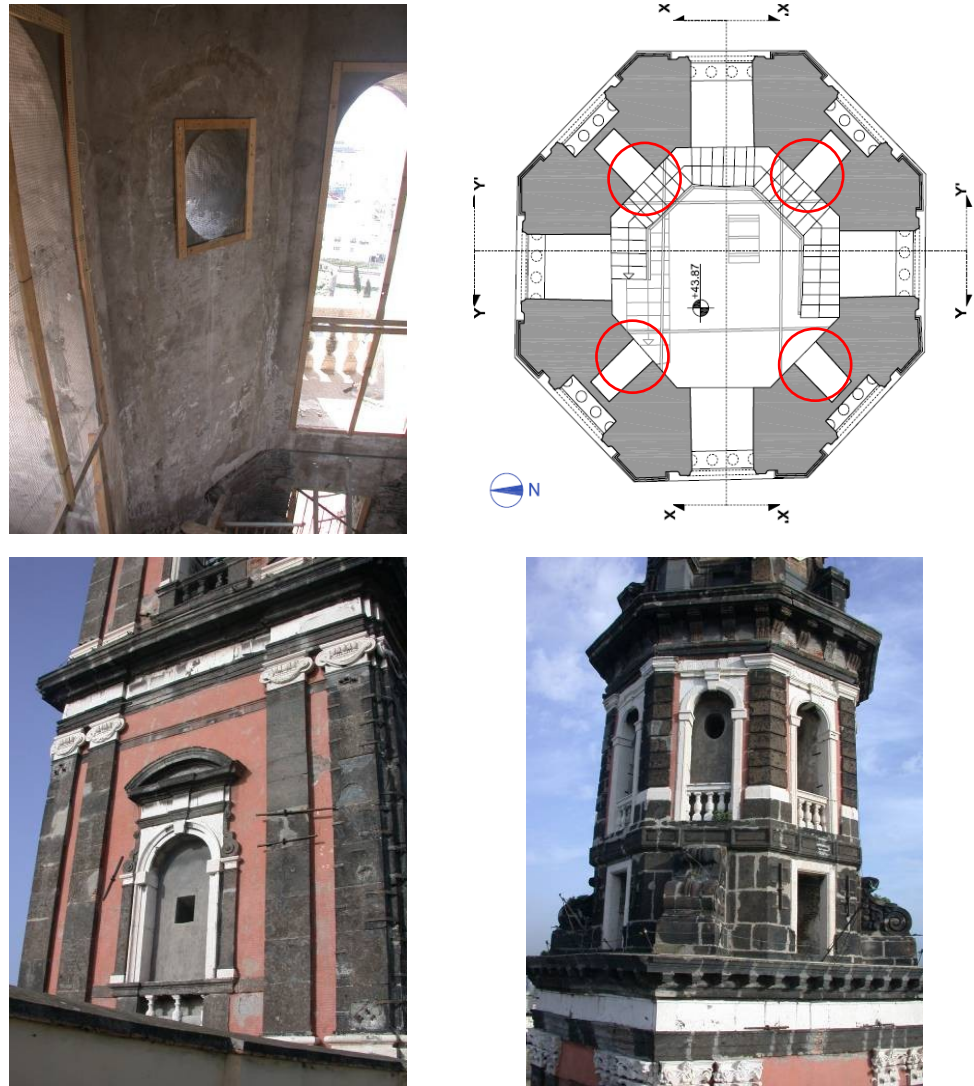


Fig.11. Inside and outside view of closet opening

The demolition of the original vaults, whether due to an aggravation of their state of damage could be another symptom of the tendency of the structure to have a behaviour characterized by inflection of the side walls out of their plan.

In the first assessment of the actual conditions of the Bell Tower and the type of interventions made over time, it would appear that the structure suffers from problems of confinement of the walls with a tendency to open outwards. It should also be noted that the dynamic effects are configured not only as seismic actions, but also as actions due to wind, vibrations induced by traffic and significant movement of the system bells as well. These actions, occurring repeatedly, may have triggered mechanisms subsequently made worse by accidental more severe actions due to the earthquake.

Damage was defined by surveying crack patterns and irregularities in the masonry texture. Assessment of the current crack distribution, however, evidenced no particular damage to the structure. On the other hand, previous retrofitting works including the thick layer of plaster dated from the 1970s-1980s and jacketing the masonry walls at most of the levels, have covered earlier damage conditions. Identification and analysis of the various interventions and alterations carried out over the years, particularly during the last century, suggested some weaknesses in the global behaviour of the structure. Many chains present diffuse superficial corrosion or local damage and are probably no longer fully effective. The visual examination of the state of corrosion of strands and chains probably aggravated by the proximity to the sea of the structure, making it likely that many of these interventions are not currently most active. In spite of these interventions, no particular damage has been observed in the connections between orthogonal walls and no out-of-plane mechanism is currently visible. In contrast, a slight eccentricity of the highest part of the Tower, made of clay brick walls placed according to the octagonal layout, is visible and is also confirmed by the geometrical survey.

4.3 IN SITU EXPERIMENTAL TESTS TO EVALUATE MECHANICAL PROPERTIES OF MATERIALS

Based on the preliminary surveys, a detailed program of experimental in situ tests has been designed and executed (Ceroni, Voto et al., 2009) [7] to characterize geometrical, mechanical and structural aspects useful to develop a numerical model of the Tower. The assessment of the safety conditions of a structure and the design of a reinforcement intervention for static and dynamical loads requires an in depth knowledge of the actual conditions of the structure. This appeared to be rather complicated for the Carmine Bell Tower due to the different interventions accomplished in different times with techniques and materials (steel, reinforced concrete) different from the original ones and to the interactions with the adjacent structures (Church and the Brotherhood). Tests to evaluate mechanical properties of the materials and prospecting by TV probes within the walls, allowed us to determine the thickness of walls, texture, distinguishing covering and structural thickness. In particular the following tests were planned:

- Cores in the wall (sample diameter 40, 60 and 100mm) to identify the materials and the wall typology;
- Sonic tests by ultrasound scanner to evaluate the homogeneity of the materials qualitatively and to determine the modulus of elasticity quantitatively;
- Stratigraphical mapping of the wall thicknesses through TV prospecting;
- Double flat jacks to evaluate the compressive strength of the masonry and the modulus of elasticity by the use of the constitutive law for the investigated portions of material.

In general the tests plan is devised in order to accomplish a few destructive and quantitative tests and many non destructive tests to evaluate qualitatively the homogeneity of the materials inside the structure. Experimental tests have been

performed to obtain a good knowledge about the type and the mechanical properties of materials constituting the Tower and to have information about its dynamic behaviour. In the following the meaningful results are presented dividing the test results in two categories according to destructive and non destructive techniques. In Appendix VII position and extension of realized cores, single and double flat jacks, sonic waves points, are reported on the plants of all the level. In particular, single flat-jack tests were conducted on four floors to evaluate the in situ stress levels. In addition, double flat-jack tests were done at the same locations to estimate the compressive strength, constitutive relationship and elastic modulus.

4.3.1 Destructive tests

4.3.1.1 Stratigraphic cores and Visual examinations

Basing on the geometrical and the material survey, 15 cylinders with diameter 60mm were cores at different levels. The position and extension of the logs accomplished at two levels (indicated with the “C” label) are reported in Fig.12. Endoscope inspections by using a colour microcamera were also accomplished through the logs holes. The extracted samples (Fig.13) allowed us to confirm the identification of materials and texture constituting the walls also along the thickness. The samples confirmed that the Tower is made of faced tuff masonry walls up to +41.40m level and that the base of the Tower has a peperino covering the tuff walls. Therefore the logs samples showed that the filling material between the two faced tuff walls is made by pozzolanic mortar and tuff bricks. Up to the level +41.40m, the walls are made of solid clay bricks for the entire thickness, even if at some levels original symmetrical openings have been closed with tuff curtains covered by a layer of clay bricks. The log samples evidenced that also in this texture the joint mortars are of pozzolanic nature. Basing on the samples extracted at different locations, mean values of density of tuff and clay bricks were estimated as 15kN/m³ and

17kN/m³, the stone specimens being weighed by a hydrostatic method (CNR 40/70, 1973) [8]. To estimate the actual unit weight of the tuff masonry, the panels should be considered as consisting on average of two wall faces which may be attributed with good approximation a unit weight close to that of stone and of infill.

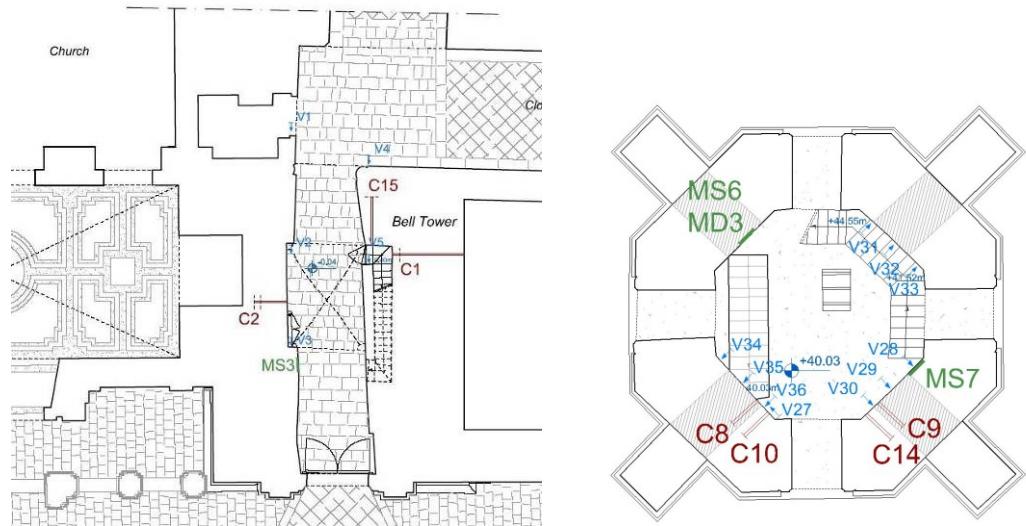


Fig.12. Example of the location of in situ tests a) plant +19.00m; b) plant +40.00m

These values for the stones correspond to a density of the masonry assembling of 12kN/m³ until the first floor (about +9.0m), 11kN/m³ for the higher levels for the tuff and 16kN/m³ for the clay bricks. These lower values take into account the presence of voids, mortar, filling material in the masonry assembly, especially for the faced tuff masonry. Density of tuff is estimated slightly higher for the lower levels to take into account the presence of covering in piperno of the basement. In addition, with the material extracted from the cores were derived cylindrical samples of yellow tuff on which we have made in laboratory compression tests. These gave a compressive strength of about 2.6MPa, value in the range of variability relieved in the literature (Dell'Erba, 1923) [2].



Basament: Tuff faced wall with peperino covering (20cm).

Squared layout: Faced tuff wall

Octagonal layout: Bricks regular wall

Mortar: Pozzolanic type

Density Tuff: 15kN/m³

Density Bricks: 17kN/m³

Fig.13. Test cores examples



Experimental tests on specimens of a similar yellow Neapolitan tuff (Ceroni et al., 2004) [3] gave compressive strength of 3.7MPa and secant Young modulus of about 1800MPa. In particular the C2 log was accomplished at the ground level along the wall of Tower facing the church to clarify the connection between the two structures. The sample showed the presence of piperno with a thickness of 20cm at a distance of 92cm from the internal edge of the wall. The use of this material, generally applied in the past as outer facing, confirms the hypothesis that the side of the Bell Tower adjacent to the church was originally separate from it. As shown by the historical sources and from iconography of the seventeenth and eighteenth century and as reported in the images of Joli and Petrini (Figs.4-5 Chapter III).

Results of coring and visual prospecting are reported in Table 1.

Table 1. Results of coring and drilling stratigraphic visual

Acronym	Identification	Comments
C1	South wall Elevation +1.70m	Hole length: 207cm - Diameter: 40.0mm From 0 to 23cm: Peperino From 100 to 207cm: Faced tuff wall
C2	North wall Elevation +0.90m	Hole length: 93cm - Diameter: 60.0mm From 0 to 85 cm: Faced tuff wall From 85 to 93cm: Peperino
C3	North wall Elevation +9.90m	Hole length: 93cm - Diameter: 60.0mm From 0 to 93 cm: Faced tuff wall
C4	South wall Elevation +10.50m	Hole length: 93cm - Diameter: 60.0mm From 0 to 93cm: Faced tuff wall
C5	East wall Elevation +14.00m	Hole length 150cm - Diameter: 60.0mm From 0 to 145cm: Faced tuff wall
C6	West wall Elevation +20.20m	Hole length: 145cm - Diameter: 60.0mm From 0 to 145 cm: Faced tuff wall
C7	South wall Elevation +31.00m	Hole length: 97cm - Diameter: 60.0mm From 0.0 to 97.0cm: Faced tuff wall
C8	North-west wall Elevation +41.40m	Hole length: 105.0cm - Diameter: 60.0mm From 0.0 to 105.0 cm: Faced tuff wall
C9	North-West wall Elevation +41.40m	Hole length: 85cm - Diameter: 60.0mm From 0 to 16 cm: Bricks wall From 16 to 85.0 cm: Tuff wall
C10	Nord-west wall Elevation +41.40m	Hole length: 50cm - Diameter: 60.0mm From 0 to 50 cm: Bricks wall with regular texture
C11	North-West wall Elevation +50.75m	Hole length: 50cm - Diameter: 60.0mm From 0 to 50 cm: Tuff wall with regular texture
C12	South wall Elevation +9.90m	Hole length: 38cm - Diameter: 100.0mm From 0 to 38cm: Tuff wall with regular texture
C13	North wall Elevation +20.20m	Hole length: 220cm - Diameter: 60.0mm From 0 to 220 cm: Faced tuff wall
C14	South-west wall Elevation +41.40m	Hole length 110cm - Diameter: 60mm From 0 to 110 cm: Bricks wall with regular texture
C15	East wall Elevation +1.90m	Hole length: 145cm - Diameter: 60mm From 0 to 22 cm: Piperno From 22 to 145 cm: Faced tuff wall

4.3.1.2 *Double flat jacks*

Double flat-jack test allows us to determine the constitutive solid mechanics relationship and the compressive strength of the investigated masonry (dimensions about 40 x 50cm for a depth of 26cm). The test is carried out by inserting two flat-jacks into parallel slots, posed along the height of the wall. Their applied pressure is gradually increased, inducing uniform compressive stress in the masonry block between them. The test can be carried out until the local failure of the block happens and allows us to define the compressive strength of the investigated masonry. The stress–strain relationship can be obtained relieving the deformation of the masonry block by measuring the distance between fixed reference points. Additionally the secant elastic modulus may be derived from the solid mechanics relationship assuming linear-elastic behaviour up to 1/3 of the failure stress, defined by the start point of non linearity of the curve. Three double flat-jack tests (Fig.14) on three different levels were realized in correspondence of three single flat-jack tests (+8.7m, +19.00m, +40.00m) that will be discussed in the next paragraph. Their locations are reported in Figs.15a-b and individual by the label “MD”.



Fig.14. MD1 realized on the first level

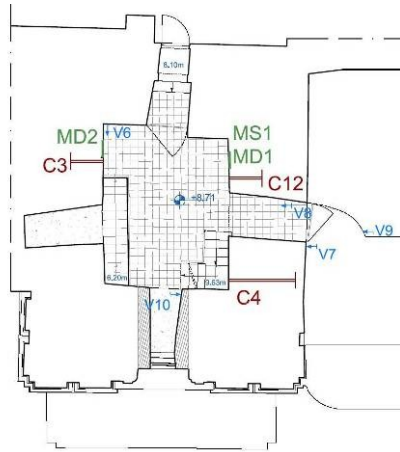


Fig.15a. Location of in situ tests.
I level +8.71m

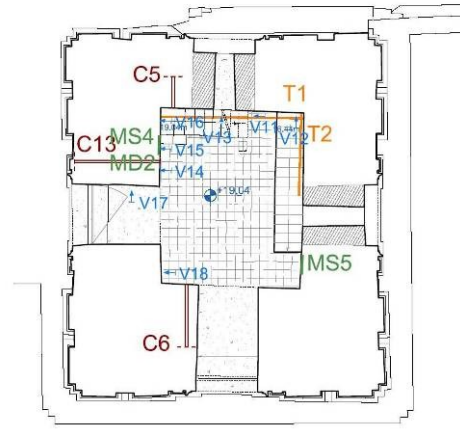


Fig.15b. Location of in situ tests.
II level +19.04m

The stress–strain relationships obtained by double flat-jack tests are reported in Figs.16a-b for the faced tuff and the investigated clay brick masonry, pointing out, after the first charge-discharge cycle, the linear trend until local failure happened. The values of compressive strengths, f_m , given by the three double flat-jacks are reported in Table 2, together with the elastic modulus, E , calculated as secant modulus between 0 and a stress equal to one-third of the ultimate strength. The elastic modulus given by the flat jack MD2 is anomalous, probably because it was realized in a inhomogeneous masonry portion. On the contrary the flat jack MD3 gives a value of elastic modulus similar to the tuff, evidencing that was realized in a tuff curtain closing an original opening of the clay brick wall. Since these tests on masonry take into account the properties of the constituent materials (mortar, stones) and texture (thickness of mortar, size and positioning of blocks), the elastic modulus and strength are lower than those of the stones (for tuff masonry, the mean compressive strength measured by MD1 and MD2 is 1.47MPa versus 2.6MPa of the stone measured by the compression test).

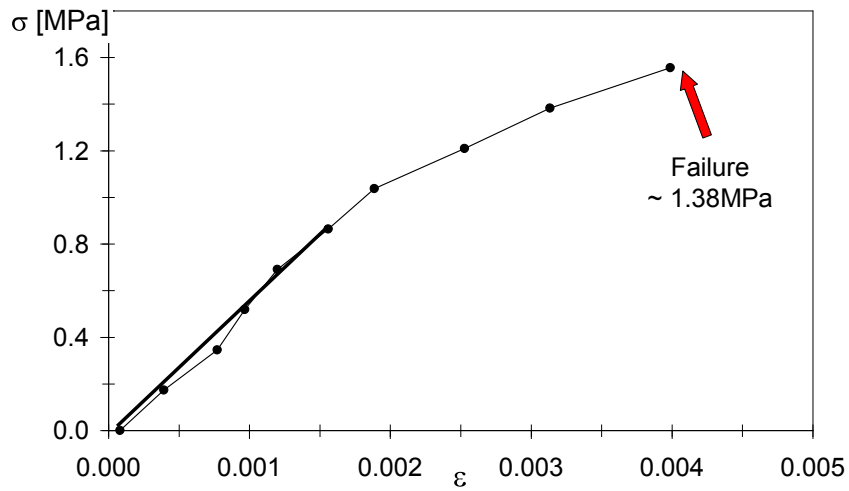


Fig.16a. Stress-strain relationship in faced tuff (MD1)

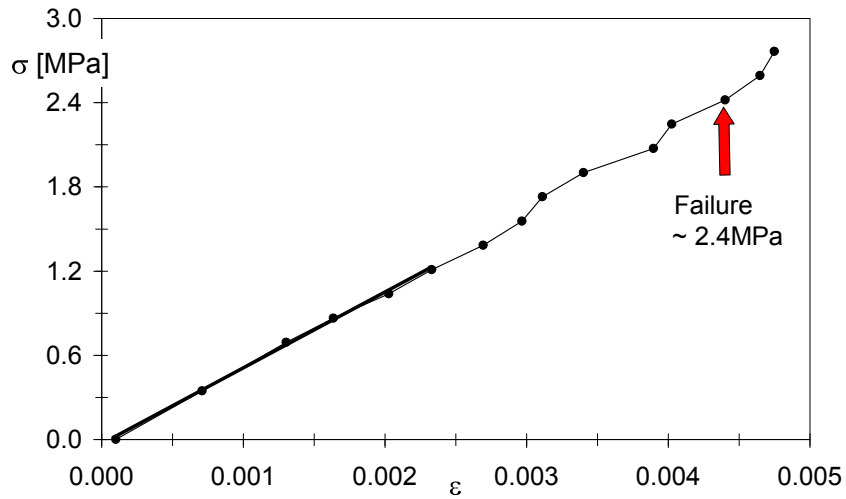


Fig.16b. Stress-strain relationship in faced tuff in clay bricks-tuff (MD3)

Table 2. Results of double flat-jacks

Acronym	Level	Material	f_m [MPa]	E [MPa]
MD1	+8.70m	Tuff	1.38	530
MD2	+19.0m	Tuff	1.56	340
MD3	+40.0m	Clay brick- Tuff	2.40	530

Also the deformability of the stone-mortar assembly can be influenced by the mechanical properties of the single materials, from the geometry (thickness and texture of mortar layers, dimensions and position of blocks), from microcracks and slip at the interfaces. In fact the elastic modulus of tuff masonry resulted lower than the one evaluated in experimental test for the single tuff blocks (Ceroni et al., 2004) [3]. The MD3 test was carried out where an original window had been closed by a tuff wall. Therefore it has to be underlined that both single materials and masonry assembling can have been subjected in the past to a damage process due to long time loading or environmental attacks (wind erosion, chlorine attacks near to the sea, acid attack due to pollution and traffic) that could have caused a decreasing of the original mechanical properties.

4.3.2 Non destructive tests

4.3.2.1 *Sonic tests. Analysis with impact-echo technique*

Non-destructive tests were performed on the principle of wave transmission according to the impact-echo technique, which is essentially a modification of ultrasonic testing techniques. In this method an impulse force is applied to the object, usually by a hammer. Its response is monitored by a transducer, that can also be mounted on the same surface as the source of the impulse with the advantage that it is not necessary to have access to both the surfaces of the structure that is being inspected. Once the impact is made, the stress waves produced propagate in the material and are reflected back and forth by free boundaries and by internal defects. Because the wavelength of the sound is inversely proportional to the frequency, the high frequencies used in ultrasonic tests tend to be scattered very easily in heterogeneous materials, such as concrete or masonry. So that if the wavelength is larger than the object to be detected, then it may be undetected (Reese & Kawahara, 1993) [9]. The impact-echo technique generally uses smaller frequencies (0.5–25kHz) with respect to

ultrasonic tests (more than 25kHz), because the defects, flaws, and thickness to be investigated are greater. Sonic tests, measuring the velocity of volume waves propagation within a material, allow us to have some qualitative information about the homogeneity and the degree of compactness of the crossed material. Evaluation of elastic properties is based on the principle that the phase velocity of longitudinal waves, V_L , often called compressive waves, in a continuous body is directly proportional to its elastic modulus, E_d , to the unit weight (ρ) and Poisson's ratio (ν) of the investigated solid, according to the following relation:

$$V_L = \left[\frac{E_d}{\rho} \cdot \frac{1-\nu}{(1+\nu) \cdot (1-\nu)} \right]^{1/2} \quad (1)$$

Therefore knowing density and Poisson's ratio (ρ and ν) of the investigated material, the dynamic elastic modulus can be evaluated. When the waves intersect a discontinuity within the material they're crossing (micro-cracks, voids, change of materials) the distance between the source and the receiver increases compared to the geometric dimension, because the wave should cross the discontinuity, so that the apparent speed falls down. The instrumentation necessary for this type of test is made of a sonic emitter (generally an instrumented hammer), by a receiver and a data acquisition station (Figs.17a-b). Measurement were performed by direct transmission (Fig.18a), when source and receiving points are on the opposite sides of wall, by indirect transmission, when source and receiving point are placed on the same surface of the investigated element; and by semi-direct transmission(Fig.18b), when source and receiving point are placed on adjacent walls, often orthogonal. Approximately 60 measurements were performed by hitting the surface at different points of the Tower with a hammer. In Figs.19a-b the locations where the tests were carried out at two levels (+19.04m and +49.91m) are reported, also indicating the direction of wave transmission (label "V") using a direct and/or semi-direct procedures, depending on the possibility to access the external side of investigated walls.



Fig.17a. Receiver



Fig.17b. Instrumented hammer

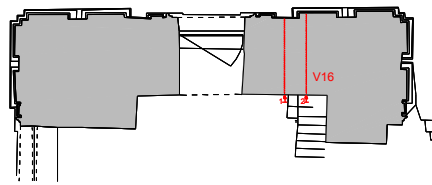


Fig.18a. Illustration of the impact-echo test by direct wave transmission

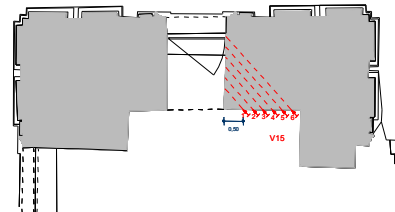


Fig.18b. Illustration of the impact-echo test by semi-direct wave transmission.

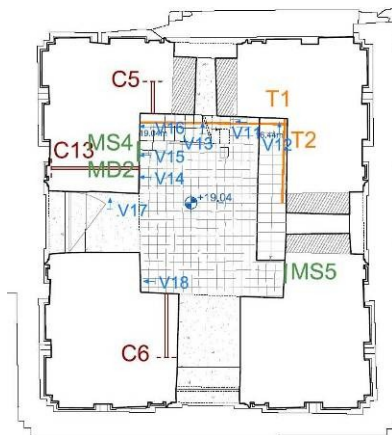


Fig.19a. Location of the in situ tests. II level +19.04m

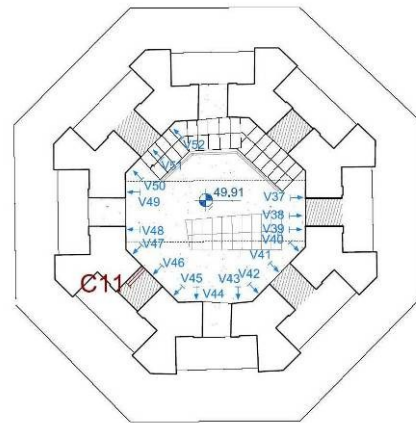


Fig.19a. Location of the in situ tests. VI level +49.91m

In particular, at +19.04m (Fig.19a) all tests have been realized by direct procedure (Fig.18a) with exception of test V15 realized according to the indirect one (Fig.19b), while at +40,91m, all tests are realized using the indirect procedure due to the difficulty to access outside at this level. In Appendix VIII there are reported all the values for the 60 measurements. Using the values of density measured for the stones, mean values (E_m) standard deviation (s_E) and covariance coefficient on all the measures are obtained and reported in Table 3 together with the local values calculated at the same points where the double flat-jacks (MD1, MD2, MD3) were realized.

In the brackets the number of measurements for each material is also reported. The values given by the two types of tests are in very good agreement. The compressive strength of the tuff stone was evaluated by compressive tests on cylindrical dry samples. The mean value on three tests is about 2.6MPa, which lies in the range of variability found in the technical literature (Dell'Erba, 1923) [2]. This value is really close to the values determined by the double flat jacks (Table 4) MD1 and MD3 (530MPa for both) that are also pretty close to the local values determined with the sonic tests (555MPa e 486MPa).

Table 3. Results of sonic inquires

Material	Elastic modulus [MPa]					
	E_m	s_E	Cov.	Local measures		
				MD1	MD2	MD3
Tuff	527 (16)	87	0.17	555	341	486
Clay brick	852 (19)	129	0.15	-	-	-

Table 4. Results of double flat-jacks and sonic inquires

Acronym	Level	Material	f_m [MPa]	E [MPa]	E [MPa] by local impact – echo measures
MD1	+8.70m	Tuff	1.38	530	555
MD2	+19.0m	Tuff	1.56	340	341
MD3	+40.0m	Clay brick- Tuff	2.40	530	486

The correlation between the elastic modulus determined in the sonic tests with the MD3 jack and the typical tuff value would confirm the existence of a tuff plugged opening within a brick-made wall. The anomalous value given by the MD2 jack was determined also in the sonic tests, confirming the existence in that point of discontinuity in the tuff masonry. In fact the point MD3 was realized in correspondence of a closed opening and the results of both tests (486MPa of wave vs. 530MPa of flat-jack) furnish values typical of tuff, while sensible higher values have been obtained (about 850MPa) in correspondence of effective clay brick masonry. For levels up +40.0m, because the clay bricks in some cases are replaced by tuff curtains, the elastic modulus is variable depending on the locations where the waves are transmitted. The values are higher for clay brick walls and more similar to tuff where the walls have been reassembled. In some cases, higher wave speeds are due to the presence of steel reinforced mortar injections, covering stones or decorative elements of piperno. Dispersion of results is also related to the heterogeneity of the filling material. In general, the sonic inquiries have shown a certain homogeneity of results where walls are made of clay bricks. Greater variability has been observed, however, in the case of faced tuff masonry. Irregularity and inhomogeneity of filling materials, presence of covering, injections and steel chains, make the masonry assembly more heterogeneous and the elastic modulus variable.

4.4 EVALUATION OF THE STRESS DISTRIBUTION IN MATERIALS

Experimental in situ tests by single flat jacks have been performed to evaluate the stress distribution in the masonry and measures of strain in steel chains have been also performed.

4.4.1 Destructive tests

4.4.1.1 *Single flat jacks*

Single flat-jack tests allow estimations of compressive stresses of existing masonry structures (Fig.20). A stress–strain relationship can be obtained relieving the deformation of the portion of investigated masonry by measuring the distance between fixed reference points. Results are acceptable assuming a linear behaviour of the material. This assumption as a good level of accuracy if the stress level is not high.



Fig.20. MS1 realized on the first level

Eight single flat-jack tests were carried out at four levels (+0.0m, +8.7m, +19.0m, +40.0m) where materials and plan layout show substantial variation. These were done on opposite walls to show asymmetry in stress distribution. Levels were chosen basing on the previous geometrical and material surveys. In Figs.21a-b-c-d are reported the position of six of them indicated with the label “MS”.

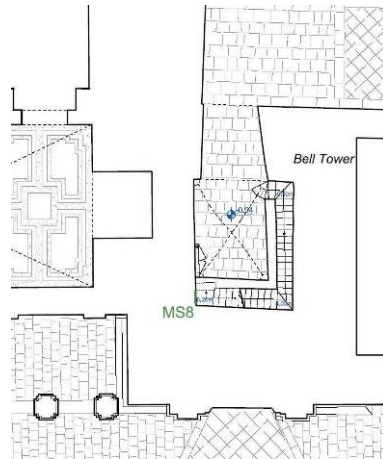


Fig.21a. I level+ 0.04m

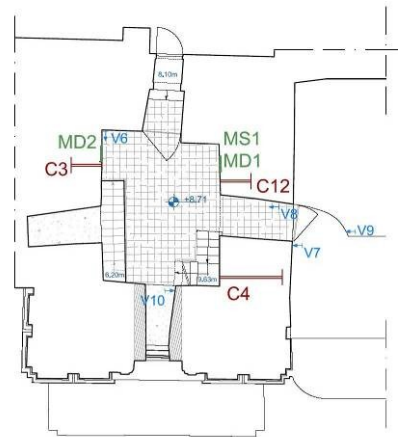


Fig.21b. I level+ 8.71m

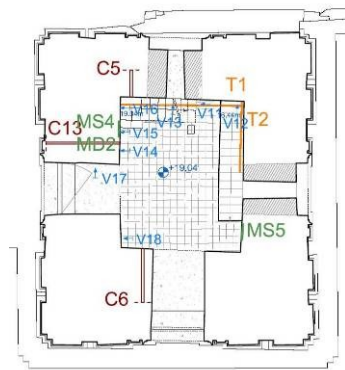


Fig.21c. II level +19.04m

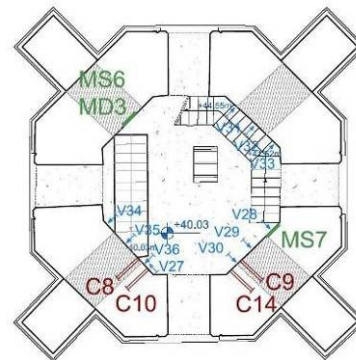


Fig.21d. IV level +40.03m

In Table 5 a summary of the results of flat-jacks are reported, showing a good uniformity of the stress distribution with a progressive reduction along the height. The results show that for the first level (+8.7m), there is a substantial uniformity in the stress distribution in the evaluated sections, with a progressive reduction of the stress with the increase of elevation. The highest stress values are found at the base (entry at elevation +8.7m).

Table 5. Results of single flat-jacks

Flat Jack	Level	Material	Experimental stress [MPa]	Theoretical stress [MPa]
MS3	+0.0m	Tuff	0.35	0.50
MS8	+8.0m	Tuff	0.17	0.41
MS1	+8.70m	Tuff	0.35	0.40
MS2	+8.70m	Tuff	0.30	0.40
MS4	+19.0m	Tuff	0.26	0.31
MS5	+19.0m	Tuff	0.26	0.31
MS6	+40.0m	Clay bricks	0.17	0.17
MS7	+40.0m	Clay bricks	0.17	0.15

The flat jack MS8 gives an anomalous value. This value is not very significant because was realized in a very discontinuous portion of masonry, in the division wall between Tower and Church, where the individuation of the perimeter of the two structures is not clear. A simple evaluation of the dead loads with the values of density estimated through the in situ tests (i.e. 11-12kN/m³ for tuff and 16kN/m³ for clay bricks masonry) allowed us to obtain the theoretical values of compressive stresses. These results are reported in the last column of Table 4 and are very near to the effective ones, with exception of MS8. The flat-jacks showed that the maximum stresses were registered at the basis of the Tower, pointing out a correct progressive reduction of the wall thickness along the height. Fig.22 shows the relation stress-displacement as determined in a single flat jack test.

Considering the results of the single and double flat-jacks, the vertical stresses were under 25% of the compressive strength, showing that for the permanent vertical loads the Tower appears to be in good condition. The experimental stresses relieved in situ can be directly compared with the results of numerical static analysis adopting linear-elastic behaviour of materials.

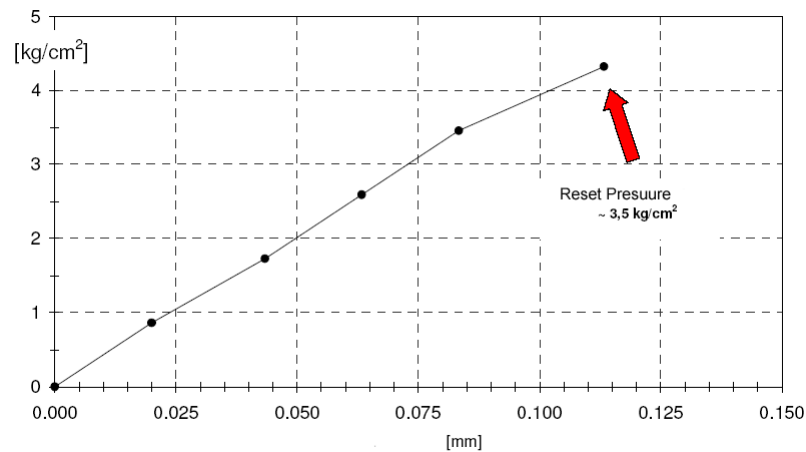


Fig.22. Relation stress-displacement as determined in a single flat jack test

4.4.1.2 Measurement of steel tie-rod strain

Considering the corrosion of some steel chains, the effectiveness of the ties were tested by measuring the strain levels of steel by vibration sources. To measure the strain levels of steel, 22 tie rods were monitored. In particular, after applying a strain gauge on each of the chains in question, a small incision with a diameter of 0.8mm and a depth of 1.0mm was made close to the strain gauge. On the basis of the principle of tension release, the tensile stresses of each chain were calculated with the strain gauge measurement (Fig.23). The measured strains show that most of them bear tensile stresses varying between 27MPa and 99MPa and eight chains are very low stressed. In Fig.24 is reported the

position of some chain that have been analysed at the fourth level. Some of the chains that have been investigated have also corrosion problems that in some cases lead to a local failure of the anchorage (Fig.25) making the tie action ineffective.

In Appendix IX the results of the analysis for all the 22 chains is reported.



Fig.23. Measurement of steel tie-rod strain 15,16, 17, 18 and 19

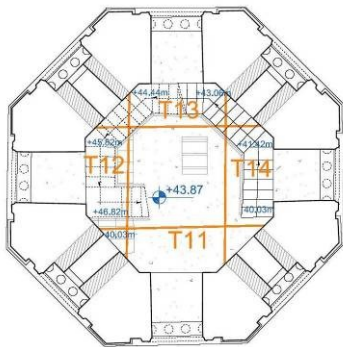


Fig.24. V level +43.87m



Fig.25. Damage of anchorage of steel chain

4.5 DYNAMIC CHARACTERIZATION OF THE BELL TOWER

Knowledge of a building's dynamic characteristics is essential for various engineering purposes, such as estimation of seismic vulnerability, assessment and possible monitoring of behaviour during an earthquake and design of restoration works. The dynamic characteristics of the Carmine Bell Tower were investigated after a series of diagnostic interventions, with a view to supplying useful information for calibrating the finite element model. Even the most advanced modelling may not take into account uncertainties concerning the execution of structural parts, the weight of non-structural parts, the constraints of nearby buildings, and the level of damage of materials. This means that modelling should always be accompanied by dynamic test identification. In this case, starting from the measurement of the dynamic input on the structure and its response, the structure's dynamic parameters have been identified (fundamental vibration, frequencies and relative modal shapes). As regards the procedure normally followed in developing a finite element model, in which, once the structure is known, its response is sought. In the experimental approach a reverse path is followed: the response is known as well as the cause behind it, and this is the basis for seeking knowledge on the structure.

4.5.4 Strumentation and test procedure

A dynamic characterization of the structure has been performed considering environmental source vibrations as traffic, wind and bell for three days. This type of test is based on processing the signals generated by continuous environmental disturbances which are either natural (wind) or man-made (road or rail traffic, nearby building sites, bells, etc.). The elaboration techniques to be used are rather complex, insofar as they have to operate with only output data, i.e., responses recorded at measuring points to environmental stresses. Hence the tools required for surveying must be high resolution to capture very

low levels of acceleration. In this respect, this test has the considerable advantage of not being invasive and not requiring the installation of activators, which, for applications on a monument, in this case with little room to manoeuvre inside and bounded by other structures, is even more beneficial. Extra vibrations were also produced by localized impulses given by an instrumented hammer in order to clarify uncertainty related to low acceleration levels. The hammer used is able to supply an impulse with a maximum peak of 22kN, which can be controlled with a load cell and displayed with an acquirer and with a frequency range varying both according to the type of tip adopted and the material on which the strain is applied. Structural monitoring and data processing were carried out under the supervision of the author.

Several pairs of mono-axial accelerometer sensors were positioned at different heights (levels 2-7) according to various measurement schemes. Sensors were fixed in the corner of the floor to check eventual asymmetric behaviours of these nodes. The accelerometers used were servo-balanced mono-axial with a capacitive transducer, whose response, appropriately modulated and treated, is converted into Volts. This sensor is used chiefly for engineering applications of various types, although the wide scale range (from $\pm 0.25g$ to $\pm 4g$) makes it also suited for recording earthquakes. In Table 6 the technical specifications of the accelerometers are reported.

Table 6. Accelerometer specifications

Dynamic range	145 dB+
Band width	DC to 200 Hz
Output	Single-end; differential
Bottom scale range	± 2 g; $1/4$ g
Bottom scale output	± 10 V single
Sensitivity	5 V/g; 40V/g
Feed	12 V

Four tests were carried out according to the following scheme:

Test 1. Four pairs of sensors X/Y were positioned respectively at the sixth (+49.0m) and fourth level (+29.0m, the bell floor) in the corners (Fig.26a); vibrations due to environmental effects for about 12 hours were recorded.

Test 2. Four pairs of sensors X/Y were kept at the sixth level, while four other pairs were placed at the third level (+19.0m, Fig.26b), that is, the last level where the Tower is laterally restrained by the other buildings.

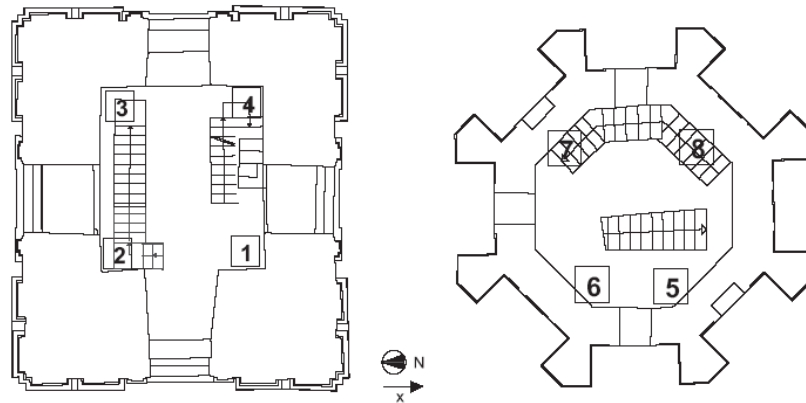


Fig.26a. Location of four pairs of accelerometers X/Y at fourth (+29.0m) and sixth levels (+49.0m) for test 1

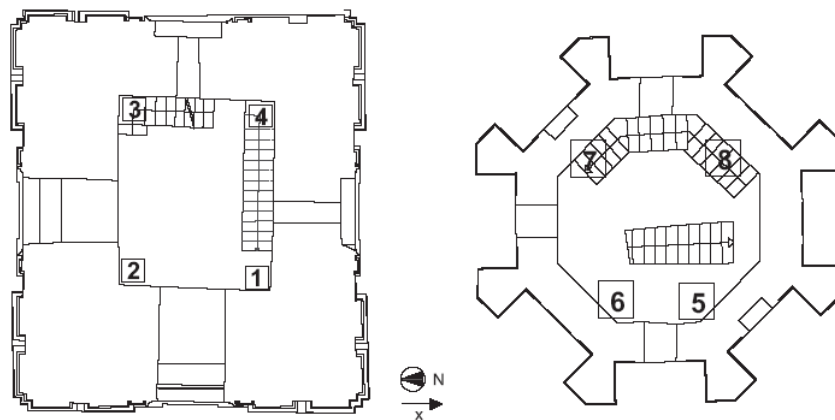


Fig.26b. Map of location of four pairs of accelerometers X/Y at third (+19.0m) and sixth levels (+49.0m) for Test 2.

Test 3. Six couples of sensors X/Y were positioned along the same vertical from the second to the seventh level according to the correspondence reported in Table 7. The environmental vibrations have been registered continuously for 32 hours (from 6:30p.m. of 17/03/06 until 1:30a.m of 19/03/07). Acquisition of displacements in x and y directions was performed in real time as integration of accelerations. The entire height has been monitored using a couple of sensors X/Y at each level (from the II to VII) to have a representation of the modal shapes.

Test 4. Finally the same set up of instruments as at Step 3 has been used by adding another couple of sensors at level V and at the basement to measure vibrations at the base of the building.

Table 7. Instrumented levels for dynamic in situ test

Level	Level (m)	Sensor x	Sensor y
1	+0.0	1 x	1 y
2	+8.7	2 x	2 y
3	+19.0	3 x	3 y
4	+29.4	4 x	4 y
5	+40.0	5 x	5 y
6	+49.9	6 x	6 y
7	+57.0	7 x	7 y

For some tests the effects of impulses (about 7kN) produced by the hammer at the fifth and sixth levels were also registered. The length of the time window used for the modal identification was 3 minutes on average, that is a sufficient interval to analyze both the effects induced by environmental continuous noise and singular impulses (bells ringing for about 1 minute or hammer impact).

Modal analysis with unknown input on the structure is generally carried out adopting operational modal analysis (OMA) (Zhang et al., 2005) [10]. The modal parameters of the structure were evaluated in output-only condition

through the use of the frequency domain decomposition technique (Brincker et al., 2000) [11]. This method is able to take into account several modal shapes at the same frequency by decomposing the cross-spectral matrix. A lot of applications of these techniques have been proposed recently for the assessment of the dynamic behaviour of masonry structures (Ivorra and Pallare's, 2007; Benedettini and Gentile, 2007) [12&13]. Data recorded on the structure are processed after a preliminary classification and validation of them in order to assess the stationary presence of spurious harmonic components and to evaluate significant parameters as peak or mean accelerations by filtering and signal extractions. The identification of the first natural frequencies was based on the examination of the power spectra of accelerations measured during the performed experimental tests. Successively the same results have also been obtained following the procedure developed in (Rainieri et al., 2007) [14]

4.5.4 Natural dynamic behaviour of the Bell Tower

In Table 8 the experimental values of frequencies, f , periods, T , and damping, D , of the first five modal shapes are reported. Totally seven levels have been monitored following the correspondence reported in Table 7 with couples of mono-axial accelerometer sensors recording signal in x and y direction. The first four modal shapes are flexural along the two principal axis of the structure (axis x = axis North-South; axis y = axis East-West), while the fifth is torsional, even if the latter one is not well identified. For the first and the third modal shapes, displacements happen along the x axis, while according to the second and fourth modal shapes, displacements are along the y axis. The modal shapes along the two directions seem to be uncoupled and have similar values of frequencies (lightly greater in y direction). Displacements in directions x and y were acquired in real time as integration of accelerations. Fig.27 illustrates the first four normalized modal shapes of the Bell Tower assuming the maximum at the highest monitored level of the structure (level seven at +57.0m). For each direction the first and second modal shapes show no change in curvature sign

along the Tower, whereas for the third and fourth modal shape, there is a point where the curvature sign changes, confirming the normal and expected behaviour of a cantilever.

Table 8. Dynamic characterization

Mode	Type	f [hz]	T [s]	D [%]
1	Flex. X	0.69	1.45	1.0
2	Flex. Y	0.76	1.32	1.2
3	Flex. X	2.28	0.44	1.7
4	Flex. Y	2.35	0.43	1.9
5	Torsional	2.76	0.36	1.1

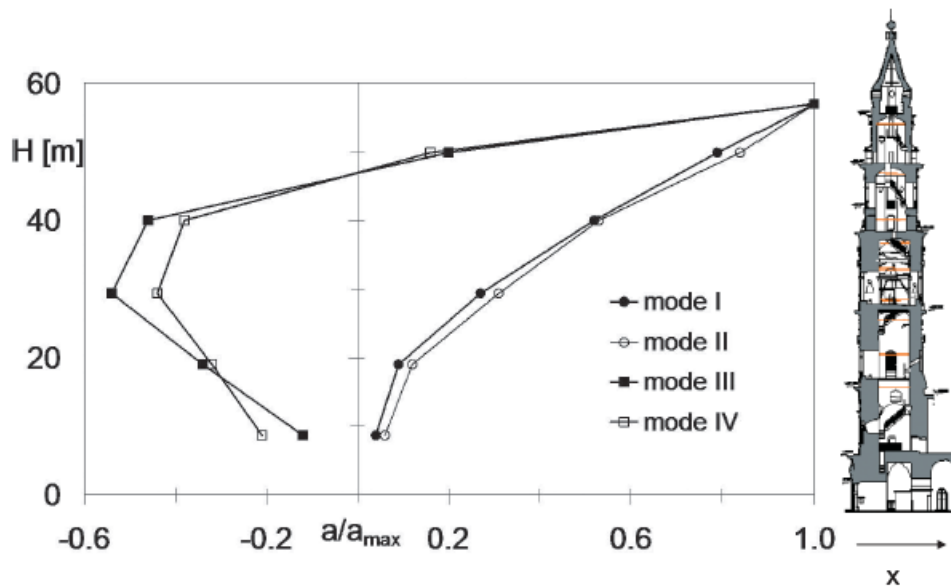


Fig. 27. Graph and schematic illustration of experimental normalized modal shapes.

Also the analyses of the modal shape in terms of displacement show that the first two modal shapes are predominant respect the following ones.

The three days data acquisition highlighted a greater deformability along the x direction (axis North-South), except for the levels where the dynamic effects can be partially influenced by the surrounding structures.

In Fig.28 the mean maximum values of displacements, referred to measurements recorded for three minutes during Test 3, are reported. A greater deformability in direction x is evidenced when the Tower is vibrating around the vertical position.

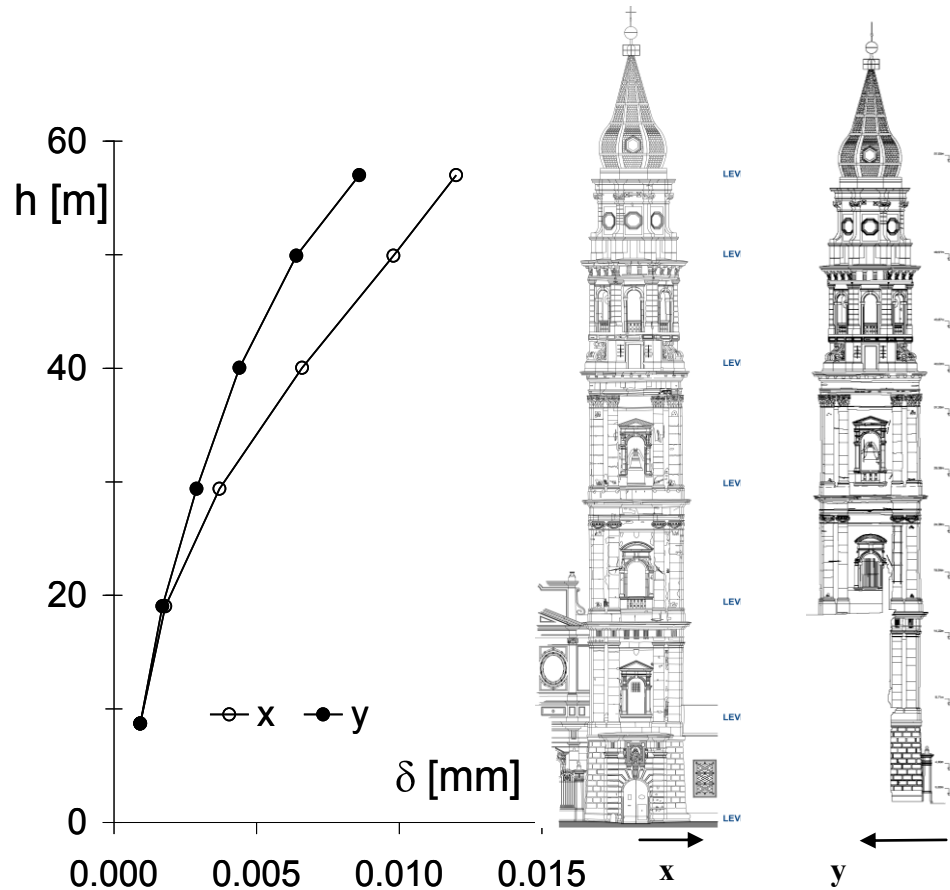


Fig.28. Graph and schematic illustration the distribution of mean maximum displacement

4.5.3 Bell effects

During Test 3, three relevant peaks were noticed when bells rang (2-3 minutes according to time of day) with effects varying according to the time of ringing due to the different shape of the sound. At the fourth level (+40.0) there are five bells, four lateral having growing values of radius from about 0.50–0.80m placed in symmetrical windows in the walls (Figs.29a-b) and one central (Fig.30) with radius of about 1.50m. Bells tilt on their axis with swing angle in the range of 60° – 80° that is typical of the Central-European system (Ivorra and Pallare's, 2006) [15]. Bell yokes are light and do not act as counterweights, so that bell swinging is characterized by quick oscillations with durable vibrations.

Usually on working days, only the smallest bell swings at 10a.m. with nine tolls. On Saturday, that is the day for which sensors have measured vibrations, bells ring three times a day at 10a.m, 12 noon, and 6p.m with different modalities: at 10a.m. only the smallest lateral bell swings with nine tolls, at 12 noon three lateral bells (the smaller ones, Fig.29b) swing together in similar way, and at 6p.m the same three bells are in full peal continuously for approximately 2 minutes. On Sunday and holy days, the smaller three bells swing at 8a.m, 9:30a.m, 12 noon, and 6p.m, always in full peal, but it must be underlined that, in respect to this schedule, some variations may happen due to specific events.

In particular in Figs.31a-b, the peak acceleration measured by sensors and the displacements, calculated by integrating acceleration, for six instrumented levels (from second to seventh) are reported when the bells ring at three times (10a.m, 12 noon, 6p.m). Graphs show that for each level the bell swinging at 6p.m. is the most significant in terms of displacement, followed by that at 10a.m and then at 12 noon (Fig.31b), whereas in terms of peak acceleration the impulse decreases from 12 noon to 6p.m. (Fig.31a).

The differential accelerations induced on the structure are probably due to the swinging modalities previously explained. At 6p.m three bells are in full peal with a continuous movement during 2 minutes, while at 10a.m and 12 noon one or three bells swing with nine tolls.

Single tolls probably give higher impulses to the structure with respect to the continuous movement. The trend is different for displacements that depend also on the frequency of the signal. In particular, the analysis in frequency domain evidenced for bell swinging at 6p.m peaks at low frequencies with amplified displacements.



Fig.29. Photographs of the bell located at lateral windows of the Santa Maria del Carmine Bell Tower on: a) east side; and b) west side



Fig.30. Central bell

Furthermore, effects are observed by the sensors applied at the levels where the bells are positioned especially in x directions (fourth level, +30.0m, sensors 4x in Fig.31a) and at the nearest ones (third and fifth levels, sensors 3x, 3y, 5x, 5y). In particular at the level of the bells (fourth level, +30.0m) the maximum displacement when the bells ring at noon increases approximately 35-fold with respect to the environmental conditions (Fig.31c), whereas, at the levels further from the bells, the displacement increase is lower (levels two, six, seven, as shown in Fig.31d).

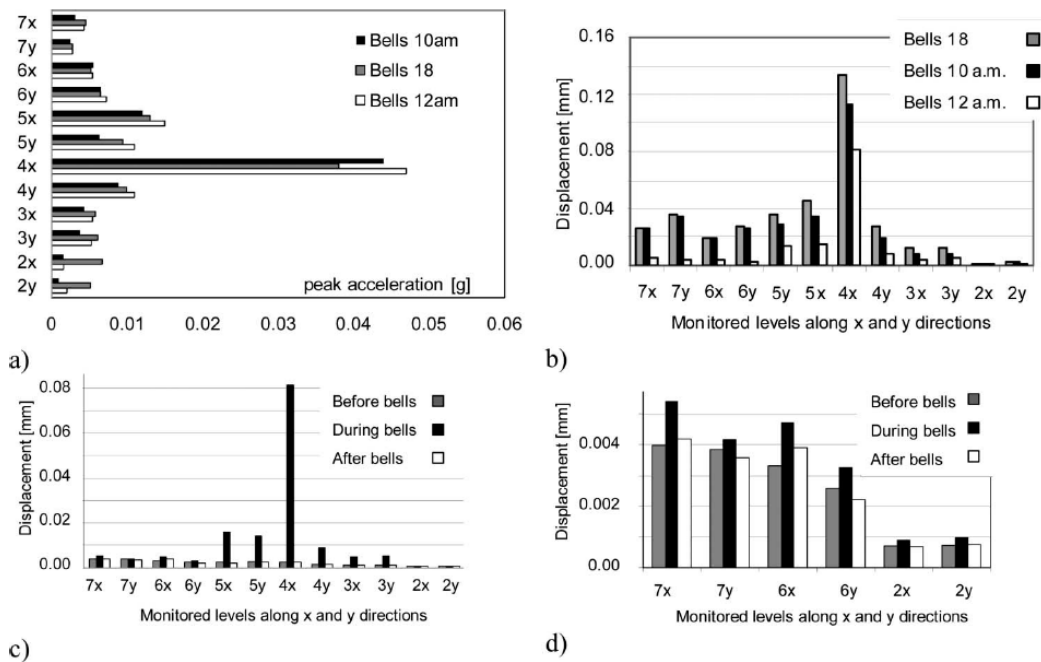


Fig.31. Graphs of the effects of bells at different hours at various levels: a) peak acceleration at each level for three bell ringing times; b) displacement at each level for three bell ringing times; c) displacement at each level before, during and after bell ringing at 12 noon; d) displacement at second, sixth, and seventh levels before, during, and after bell ringing at 12 noon

However, the behaviour of the entire Tower is influenced by bell ringing. The maximum acceleration registered each hour at the seventh level for the period of 25

hours during Test 3 is shown in Fig.32. It is evident that there are peaks when the bells usually swing (10a.m, 12 noon, 6p.m) and also at 8p.m, not corresponding to the usual swinging times. Fig.32 shows that at the seventh level, peaks in x direction are moderately higher than y, whereas for the fourth level, where the bells are located, much higher effects in x direction were observed (Figs.31a& 31b). This larger deformability in x direction, already evidenced for the mean displacement (Fig.28) distribution, should be accentuated by the swinging modalities of the bells, considering that two of the three bells tilt on their axis along the x direction.

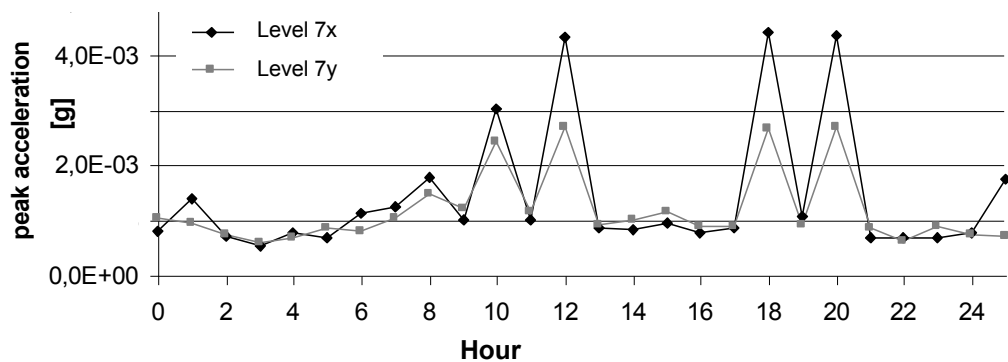


Fig.32. Effects of bells at various levels for different hours during the day: peak acceleration during 25hours for the 7th level

Furthermore, regarding the effect of bells ringing, a variation in the frequency response was registered. Acceleration peaks were observed in ranges of frequencies other than natural ones and may well be associated to forced oscillations due to movement of the bells or their supports. When the bells stop, some peaks corresponding to the natural frequencies of the Tower become discernible again and when the bells definitively stop the residual effects are recorded at the natural frequencies. In Fig.33, the power spectral responses obtained for the y direction are reported for four conditions: environmental

vibrations, during bell swinging at 12 noon, during attenuation of bell swinging and after stopping bell swinging.

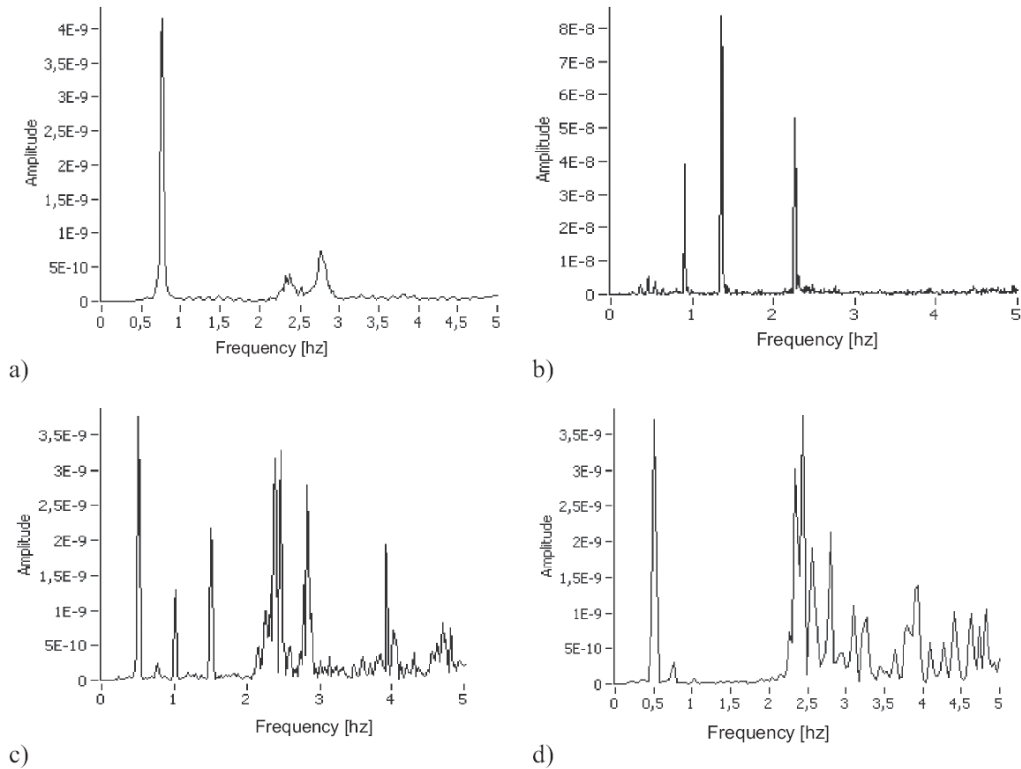


Fig.33. Graphs of the power spectrum of the Santa Maria del Carmine Tower in y direction: a) without bell swinging; b) during bell swinging at 12 noon; c) during attenuation of bell swinging at 12 noon; and d) after stopping bell swinging at 12 noon.

In Table 9 the values of frequencies evidenced during bell swinging are reported. Considering the major effects produced by bells ringing, the measures corresponding to these peaks were subsequently neglected to calculate the mean value of acceleration (RMS) in the single interval (1 hour) to evidence if the global behaviour was influenced by other phenomena for the entire duration of Test 3.

Table 9. Natural frequencies during bell swinging at 12noon

Modal shape	f [hz]
1 Flexural X	0.52
2 Flexural Y	0.49
3 Flexural X	0.96
4 Flexural Y	0.91
5 Flexural X	1.44
6 Flexural Y	1.36

In Figs.34a-b the mean accelerations for directions x and y are reported for the third and fifth levels positioned immediately below and above the floor with bells. Interestingly, for the fifth level, as for all the others, accelerations in direction x were greater than those recorded in direction y, whereas for only the third level they are comparable or lower with respect to direction y. The third level (+19.0m) is the last level of the Tower surrounded by buildings and it could be more restrained in direction x than the second level due to the presence of the church roof. To better analyse the effect of other phenomena on the dynamic behaviour of the Tower, in Fig.34c the mean values of acceleration in x direction during Test 3 at the six instrumented levels are graphed. It is possible to notice that the mean values of acceleration can be correlated to the hour of the day. During the evening and at night-time, starting at 9p.m. of Friday, the accelerations are lower than those recorded at the same time on Saturday. Then, the values remain constant until 1a.m. due to the greater traffic movement for the week end.

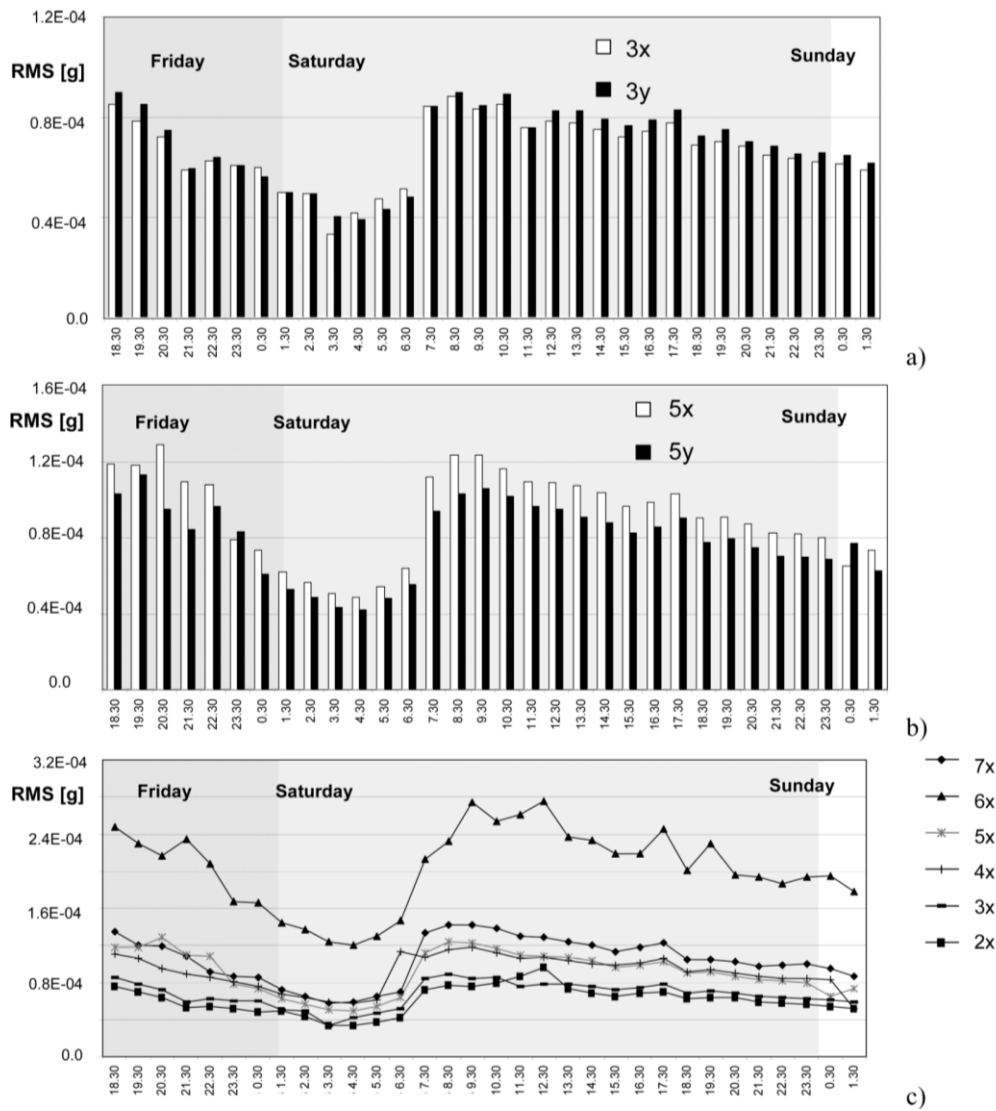


Fig.34. Graphs of the mean acceleration (RMS) at various levels during test 3: a) measures of sensors at the third level; b) measures of sensors at fifth level; and c) measures of sensors at all levels in direction x .

During the night of Friday values decrease until a minimum at about 4a.m., then increase with peaks between 7.30a.m and 11.30a.m. and finally the values lightly

decrease. Regarding the behaviour of the various levels, the trend is regular and uniform for all sensors and the acceleration increases along the height, except for the sensor at the seventh level, showing lower values with respect to the s one. This was probably due to the position of sensors at the last level that were not aligned with the other ones and in particular nearer to the barycentre of the section, so that the torsional effects couldn't be well registered at this level.

4.5.4 Variability of dynamic parameters during the test

An interesting item to check the reliability of the values of frequencies associated to the modal shapes is the monitoring of the frequency values during the day. In Figs.35a-b the frequencies of the first and second modal shapes are reported for the duration of approximately 24hours (during Test 3).

The continuous monitoring of both modal shapes showed increasing values from 8a.m. until 2p.m., a constant value for a couple of hours and then a decreasing until the evening. This phenomenon is due to the dependence of the frequencies on the temperature which increases during the day. However the variations are minimal, consisting in a maximum scatter of 1.4% and 1.6% for mode I and mode II respectively, meaning an absolute error on the determination of the frequency of 0.004Hz for the first two modes due to temperature variation. Analogously, the variability of the modal shapes has been checked by monitoring the values of the relative displacement (normalized respect to the highest level, the seventh at +57.0m) for period of about 24hours (during Test 3).

In Figs.36a-b the normalized values of displacement, δ , are reported for each monitored level for mode I and II respectively. These results showed that variations with respect to the mean behaviour are sporadic and random with an absolute error on the first two modal shapes of 0.01, meaning that during the day they are practically constant.

The scattering is low because the dynamic sources acting on the structure (traffic and wind) produce random vibrations meaning that they are

characterized by no specific frequency or constant value of excitation at a fixed value of frequency.

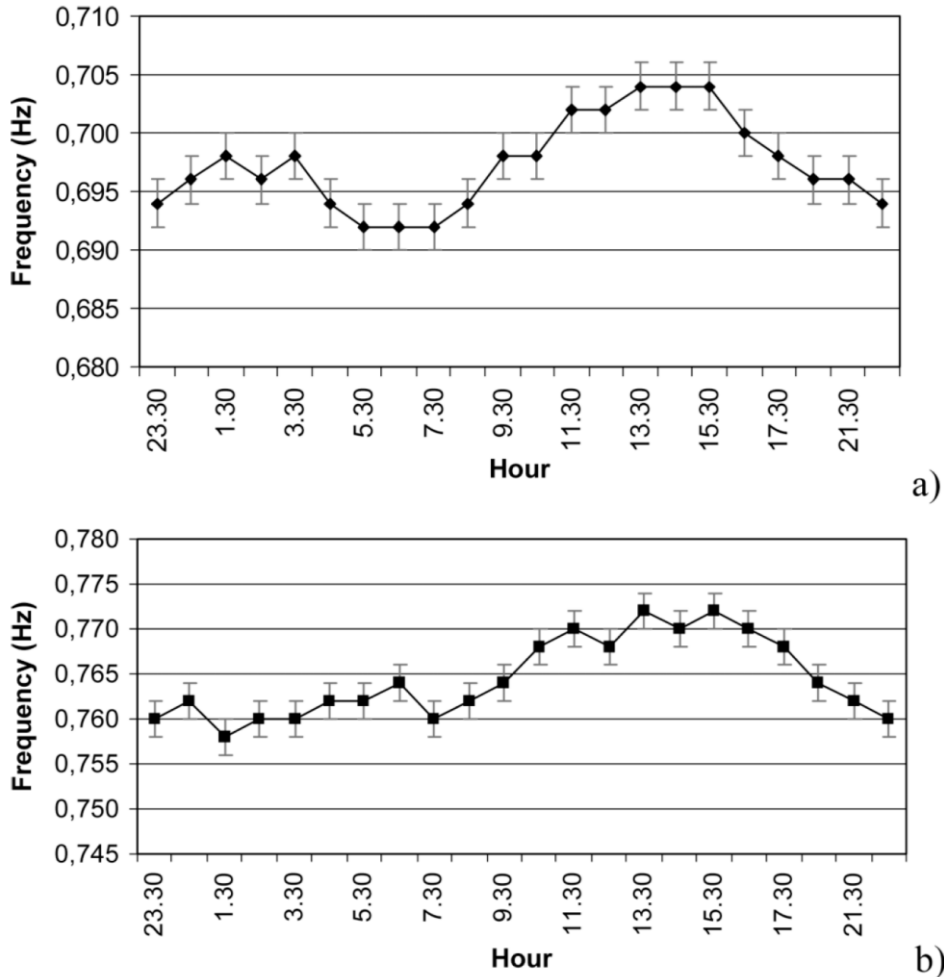


Fig.35. Graph of the daytime variability of natural frequencies: a) mode I; and b) mode II.

Results of various inquire lead us to suppose that the Bell Tower was originally built separately from the other buildings, particularly from the church, and that

it was successively surrounded. This probably means that the small restraining effects produced by the other buildings on the modal shapes in x direction (more significant respect to y direction where only some floors of the cloister could have a restraining effect) can be observed for a low dynamic source. However when a strong severe dynamic action like a seismic event occurs, the Bell Tower probably will show a behaviour more similar to a cantilever.

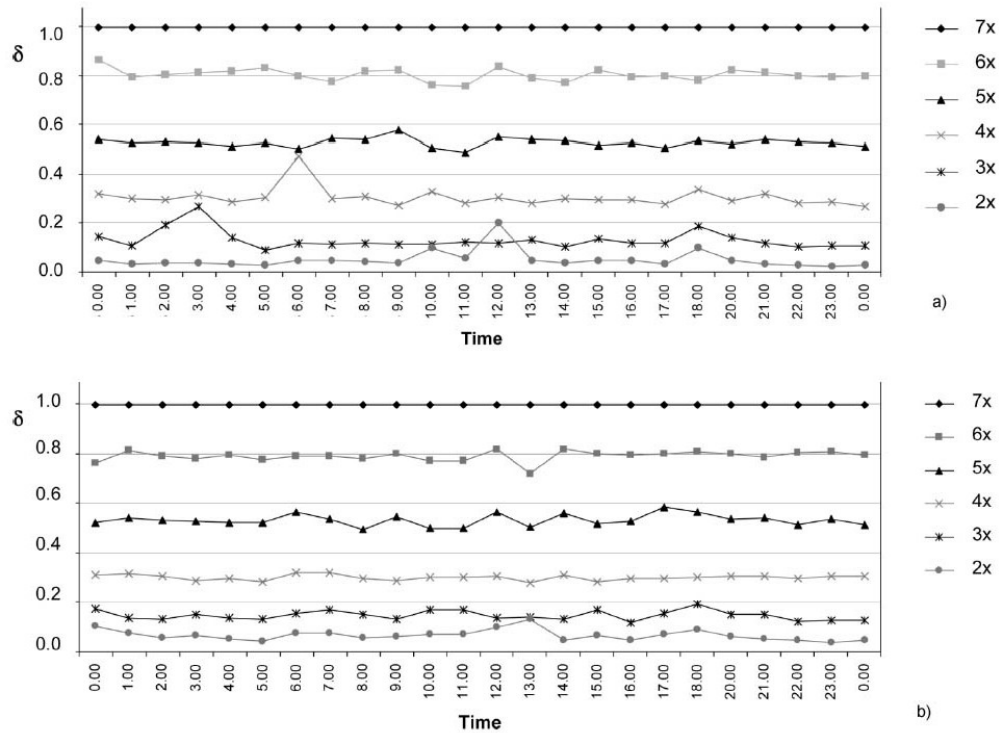


Fig.36. Graph of the daytime variability of normalized values, d , of modal shapes: a) mode I; and b) mode II.

4.6 REFERENCES

- [1] Lourenço P.B., Roque J.A., 2006. “*Simplified indexes for the seismic vulnerability of ancient masonry buildings*”. Construction and Building Materials 20: 200–208.
- [2] Dell’Erba L., 1923. “*Il tufo giallo napoletano. Studio scientifico e tecnico esteso alle cave e alle frane*”. Ed. Pironti, Napoli (in Italian).
- [3] Ceroni F., Pecce M., Manfredi G., Marcari G., Voto S., 2004. “*Analisi e caratterizzazione meccanica di murature di tufo*”, 15° congresso CTE, Bari, 905-914 (in Italian).
- [4] Burattini E., Fiengo G., Guerriero L., 1994. “*Murature tradizionali napoletane: problemi di datazione e formazione di una base di conoscenza*” in Multimedia - Beni culturali e formazione (a cura di G. Gisolfi), Salerno (in Italian).
- [5] Ceroni F., Voto S., 2008. “*Historical, architectonic and structural investigations to conserve and rehabilitate heritage buildings: General tools and applications to case study*”. In Proceedings of International Conference HERITAGE 2008 — World Heritage and Sustainable Development. Vila Nova de Foz Co^ a, Portugal, May 7–9, 2008. Green Lines Institute, 581–590.
- [6] Binda L., Gatti G., Mangano G., Poggi C., Sacchi G., Mandriani, 1992. “*The collapse of the Civic Tower of Pavia: a survey of the materials and structure*”. Masonry International, 1, Stoke on Trent.
- [7] Ceroni F., Pecce M., Voto S., and Manfredi, G. (2009). “*Historical, architectural and structural assessment of the Bell Tower of Santa Maria del Carmine.*” Int. J. Archit. Heritage: Conservation, Analysis, and Restoration.
- [8] Centro Nazionale delle Ricerche (CNR), 1973. “*Determinazione del peso di volume di miscele di aggregati lapidei con bitume o catrame*”, Bollettino Ufficiale del CNR, VII (IV Norme Tecniche, N. 40): I–II (in Italian).
- [9] Reese R. T., Kawahara W. A., 1993. “*Handbook on structural testing*”. Bethel, CT: Society for Experimental Mechanics.
- [10] Zhang L., Brincker R., Andersen P., 2005. “*An overview of operational modal analysis: major development and issues*”. In Proceedings of 1st International Operational Modal Analysis Conference (IOMAC). Copenhagen, Denmark, April 26–27, 2005.
- [11] Brincker R., Zhang L. M., and Andersen P., 2000. “*Modal identification from ambient responses using frequency domain decomposition*”. In Proceedings of 18th International Modal Analysis Conference (IMAC). San Antonio, TX, February 7 –10, 2000. IMAC, 625–630.

-
- [12] Ivorra S. and Pallare' s F. J., 2007. "*A masonry bell-tower assessment by modal testing*". Proceedings of the 2nd International Operational Modal Analysis Conference. Copenhagen, Denmark, April 30– May 2, 2007. IOMAC, CD-ROM.
- [13] Benedettini F., Gentile C., 2007. "*Ambient vibration testing and operational modal analysis of a masonry tower*". In Proceedings of the 2nd International Operational Modal Analysis Conference. Copenhagen, Denmark, April 30–May 2, 2007. IOMAC, CD-ROM.
- [14] Rainieri C., Fabbrocino G., Cosenza E., and Manfredi G., 2007. "*Implementation of OMA procedures using LABVIEW: Theory and application*". In Proceedings of the 2nd International Operational Modal Analysis Conference. Copenhagen, Denmark, April 30 –May 2, 2007. IOMAC, CD-ROM.
- [15] Ivorra S. and Pallare' s. J. F, 2006. "*Dynamic investigations on a masonry bell tower*". Engineering Structures 28:660–667.

Chapter V

Analysis of the structural behaviour of the Carmine Bell Tower

5.1 STRUCTURAL BEHAVIOUR OF THE BELL TOWER

The structural behaviour of the Bell Tower and consequently the selection of the analysis methodologies must be analyzed following two hypothesis connected mainly to the efficacy of the connection of the orthogonal walls. If the four orthogonal walls constituting the structure may be assumed to be integral because of a correct strong connection of the angles, the analysis model may assume a close cross section of the Bell Tower structure, despite it being hollow. Consequently finite element modelling may be used with different levels of complexity dependently on assuming a mono, bi or three-dimensional discretization. Additionally either dynamic or static analysis can be made, both in a linear and non linear field. The modelling of the Bell Tower as monolithic structural body was accomplished utilizing different types of analysis. In particular linear analysis under gravity loads, modal dynamic analysis and non linear static analysis (pushover) have been performed. The pushover analysis is particularly interesting to assess the performances of the structures subjected to

seismic actions. It's based on the non linear static analysis of the structural behaviour even if it is then correlated with the dynamic characteristics of the construction. The results of the analysis on the whole structure are shown in the following paragraph. They indicate that basically the performance of the structure holds a sufficient safety degree versus the design earthquake. It has been evaluated with respect to the values of peak ground acceleration expected for the site and D types soils (poor) according to OCPM 3431 [1]. Anyway this assumption is not exhaustive for assessing the structural safety. In fact if the hypothesis of good connection of orthogonal walls in the corners is not verified, the collapsing condition could be dependent not on a global crisis of the structure, but on the development of local out-of-plane mechanism due to the lack of connection of the single masonry walls. Such mechanisms represent a typology of collapse typical of the masonry structures. Surely it's very insidious in the subject structure. We can't be sure that for the Bell Tower the frame constraints represented by the floors at the different levels be effective like in the ordinary buildings. Additionally the presence of numerous tie-bars and steel strands put in place with previous interventions shows that the problem was already evident to past time technical people that connected the walls with those bars. With reference to the efficacy of the pre-existent tie-bars and strands, the in situ tests showed a high degree of corrosion of the bars, failure phenomena in correspondence of their heads and a tension condition that is indicative of their inefficacy. So, after the global analysis of the structure gave satisfying indications on the Bell Tower safety, the developments of possible local out-of-plane mechanisms were investigated and the solutions to avoid their activation were evaluated.

5.2 GLOBAL ANALYSIS OF THE STRUCTURE

5.2.1 The FEM model

Numerical simulation of the structural behaviour of masonry buildings can be performed according to several approaches synthetically classifiable in three modelling strategies (Lourenço, 2002) [2]:

- Detailed micro-modelling assuming masonry units and mortar joints as continuous elements and unit-mortar interfaces as discontinuous elements;
- Simplified micro-modelling where units are represented by continuous elements, while mortar joints and unit-mortar interfaces by discontinuous ones;
- Macro-modelling where all the components are smeared in a homogeneous continuum.

This last approach was followed to perform finite element modelling of the Bell Tower. Previously the Bell Tower has been modelled in a very simplified way as a one-dimensional element with a variable section (four simplified sections along the entire height) according to a cantilever scheme performed by the SAP2000 CSI commercial software (version 9.0) [3]. This has been made in order to collect preliminary information about the structural behaviour (maximum compressive stresses, main natural frequencies and modal shapes) (Fig.1).

Based on the detailed geometrical and structural survey developed *in situ*, a 3D finite element modelling of the structure has been performed with the DIANA TNO commercial software (release 8.1) [4] using bricks and shell elements and considering a homogeneous and isotropic material, both for tuff and clay brick masonry.

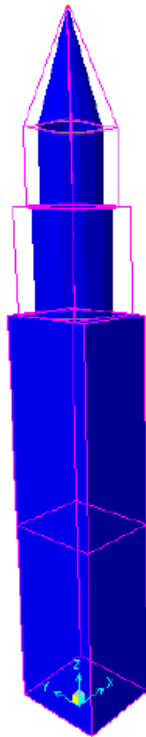


Fig.1. Modelling of the Tower by SAP 2000

In order to establish reliable equivalent homogeneous values of unit weight for the masonry to be introduced in the numerical model, parametric analysis under gravity loads were developed. Starting from the experimental values related to single stones, the unit weight of masonry was varied and the stress distribution in the Tower due only to its weight was compared to the experimental one recorded by single flat-jacks. This means that stress in the investigated portion of wall is assumed uniform along the thickness, even if, particularly for the faced tuff masonry, it could be very heterogeneous along a given section. However this procedure appears to be the simplest available to calibrate reasonably the unit weight and the related approximation should be not significant for the global behaviour of the structure. Finally the values of unit weight assessed basing on the analysis under gravity loads, as showed in the

following, have been:

Unit weight:

- 1200 kg/m³ for the tuff masonry from elevation +0.0m up to +9.0m;
- 1100 kg/m³ for the tuff masonry from +9.0m up to + 40.0m;
- 1600 kg/m³ for the brick masonry.

The mean compressive strength of masonry was estimated at about 1.4MPa for tuff and 2.4MPa for clay bricks, while for the elastic modulus reasonable values obtained by the experimental in situ tests were 530 and 850MPa, respectively, for tuff and clay brick masonry. The experimental values of masonry strength are conservative with respect to values suggested by the technical literature and by the new Italian codes (OCPM 3431, 2005; NTC, 2008) [1&5] that correlate the design strength to the masonry typology to the knowledge level of the examined structure through a confidence factor. These values are at least 50% lower than the limits of the ranges suggested by national codes, even if are comparable to experimental outcomes of laboratory tests on panels made of similar tuff masonry (Marcari et al., 2007) [6].

For the case of the Bell Tower, if an intermediate knowledge level is assumed, the national codes (OCPM 3431, 2005; NTC, 2008) [1&5] allow to assume as compressive strength the mean value of the following ranges: 1.2-1.8MPa and 2.7-4.2MPa respectively for tuff and clay brick masonry in good condition according to OCPM 3431 and 2.1-3.6MPa and 3.6-6MPa according to the more recent NTC 2008[5]. In both cases, these values are divided by a confidence factor of 1.2. This procedure leads to strength values greater than the experimental ones, that therefore have been assumed for the verifications.

For the tensile strength, lacking any experimental reference and with safety assumptions, 5% of the compressive strength (Augenti, 2000) [7] has been considered (0.070MPa for tuff, 0.120MPa for clay bricks). Moreover these values are comparable with the ones (0.066MPa and 0.143MPa) suggested by

the most conservative national code (OCPM 3431, 2005) [1] according to the masonry typology and to the confidence factor, as previously described.

The elastic modulus values were assumed higher than the flat jack readings and the sonic test results (530MPa for the tuff, 850MPa for the bricks) because have been assessed basing on parametric analysis by comparing the experimental and theoretical dynamic behaviour of the structure, as it will be illustrated in details in the following. Updating leads to estimate the elastic modulus as 900MPa and 1200MPa respectively for tuff and clay masonry. That differ appreciably from the initial ones (increasing of 40-60%), but are nearer to the ranges suggested by national codes (OPCM 3431, 2005) [1].

For the linear elastic component of the constitutive law, the same elastic modulus has been used for compressive and tensile loading, adopting an isotropic behaviour with a Poisson's modulus of 0.15.

The compressive behaviour after the peak is characterized by a linear softening branch up to a fixed strain (0.004 for tuff and 0.005 for clay bricks), after which a residual strength value (30% of peak strength) is kept constant without limiting the ultimate strain in order to simulate in the equivalent continuum the displacement capacity related to slips along the mortar joints (Lourenço, 2000) [2]. The tension behaviour is defined linear until the peak strength using the same value of elastic modulus of compression. After the peak a linear softening branch is assumed up to a maximum strain (0.00040 for tuff and 0.00055 for clay bricks, which have been estimated as 10% of the strain corresponding to the beginning of the plastic field in compression) as typical of brittle materials (Lourenço, 2000) [2].

A crack model based on multidirectional approach has been adopted to represent the non-linear behaviour of the masonry. After reaching the maximum tensile strength, the post-peak behaviour is modelled by a linear softening branch up to a maximum strain value. The yielding criterion of Von Mises is adopted as plasticity model.

For performances in tension a multidirectional smeared crack damage model is assumed, where cracks form if the principal stresses overcome the tensile

strength and the angle between two following cracks overcomes a threshold value. Moreover due to cracking of material, the shear stiffness is reduced by a shear retention factor (assumed equal to 0.5, DIANA, 2002b) [8].

In the following paragraph three types of analysis are developed that have been performed with the 3D model:

- Linear static analysis for gravity loads. It has been developed first to adjust the unit weight values of masonry starting from the experimental values of the stones through single flat-jacks test results comparison, and then to estimate the safety condition of the tower under gravity loads;
- Linear modal analysis to adjust the elastic modulus of masonry and the constraint effect of surrounding buildings comparing with the experimental dynamic identification;
- Non-linear static analysis to estimate the safety condition of the tower under seismic actions.

5.2.2 Linear analysis for vertical loads

Linear analysis under gravity loads are a useful instrument to verify the accuracy of the geometrical layout and the reliability of the values of unit weight by comparing theoretical stress distributions with the experimental data obtained *in situ*. After verification of the experimental results and assessment of the model, the theoretical stress distribution in the entire structure can be attained. So that, if a 3D model is used, local problems related to stress concentration can also be evidenced and taken into account for the rehabilitation design. Moreover, knowledge of material strength, estimated by *in situ* surveys, allows assessing the safety degree of the structure under gravity loads. This safety factor is usually conservative, because the experimental *in situ* strength is not the one correspondent to the complete crushing of the investigated masonry portion. In fact the *in situ* test with flat-jacks is usually

stopped before the slope of the experimental stress-strain relationship becomes horizontal, in order to restore the integrity of masonry after the test.

Based on the geometrical survey and the mechanical characterization tests accomplished on the Bell Tower, a finite element modelling of the structure subject only to static loads was developed. Only the load associated with the weight of the structure was considered. Historical inquiries showed that originally the Tower was built separately from the church and earlier than the other surrounding buildings (Fig.2), while nowadays they appear contiguous. It seems reasonable to assume that the original gap was simply filled in the past and that no structural connection was added between the two buildings and the other ones. So, the constraint effects, if any, can be considered due to contact phenomena only.

Relatively to the interactions with the surrounding structures, two configurations were considered:

- Configuration A: ignores the influence of all surrounding structures, so that the Tower is bind at the basement and modelled as a cantilever;
- Configuration B: takes into account the effect of the adjacent buildings for the initial +19.0m, a level that corresponds to the last floor surrounded by the other buildings. In this second configuration, the effect of contiguous buildings has been simulated by horizontal supports in x direction for the sides confining with the church and the Brotherhood and in y direction for the side bordering the monastery/cloister.

In particular on the side bordering the Church two horizontal displacement constraints were assumed in correspondence of the two floors of the Church (at the organ elevation and the covering floor) to simulate their presence. Other horizontal displacement constraints were assumed all along the height of the Bell Tower up to the Church covering floor elevation (around +19.0m) to simulate the action of a transversal wall of the church. On the side bordering the cloister, horizontal constraints were set at three different elevations correspondent to the positions of the cloister and the monastery floors. On the

side bordering the Brotherhood horizontal constraints were set at two elevations correspondent to the floors. Constraints were modelled by fixed horizontal supports in the x direction for the sides adjoining the church and the friary and by fixed horizontal supports in the y direction for the side adjoining the monastery/cloister.

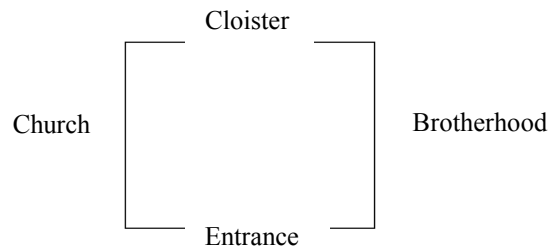


Fig.2. Plan layout of the structures interacting with the Bell Tower

The Tower has been modelled in 3D with the DIANA commercial software through brick elements (HX24L, DIANA, 2002a, [4]) for the first +57.0m until the level where the pear dome starts. The thickness of the masonry walls was modelled utilizing three-dimensional elements with an approximately rectangular shape (the in plan dimension are as average around 0.5m with heights variable between 0.5m and 1.5m). This geometry allowed to model with good accuracy the variability of walls thickness along the height of the Tower and to introduce the openings. The pear dome has been modelled by shell elements (Q20SH, DIANA, 2002a, [4]) (Fig.3) with a mean dimension of 0.40m x 0.70m. For both element typologies some geometrical limits (internal angles between sides in the range 40°-140° and maximum shape ratio lower than 10) have been maintained in order to have reliable calculation efficiency. The floors were modelled by shell elements following the shape of vaults and slabs assessed by the geometric survey, while the RC stairs were not considered in this phase. The material behaviour was assumed to be linear elastic, utilizing the same value for the tension and compression elastic modulus, assuming the

hypothesis of isotropic behaviour.

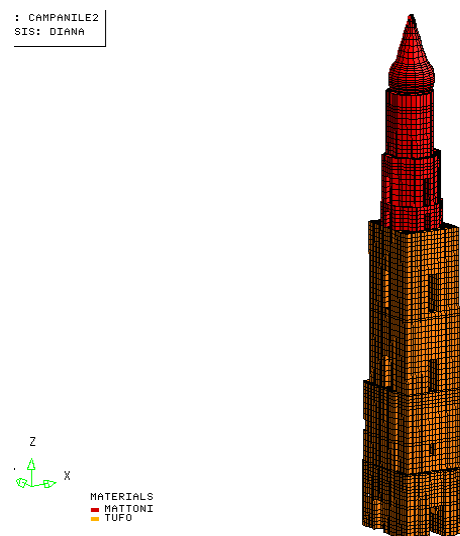


Fig.3. 3D Model of the Bell Tower realized with DIANA

Table 1 shows a comparison between the experimental results obtained with single flat jack tests and the correspondent values derived from the numerical model in the same points of the structure for configurations A and B. Generally the theoretical values are lower in the configuration B and overestimate the experimental values at the lower levels with errors variable between 10% and 30%, while are very similar at the higher levels made with clay bricks.

The tension state was more severe in the cantilever assumption. The theoretical values in the cantilever configuration (A) are greater than the restrained one (B) up +19.0m, while become comparable at higher elevation. In both cases theoretical values overestimate the experimental ones, particularly at the lower levels, even if the unit weight of masonry has been reduced vs the single stones. At the higher levels made of clay bricks the experimental and theoretical results are similar. This means that the estimated values of unit weight are reliable for the clay brick and more uncertain for tuff masonry, as expected due to the greater non-homogeneity of this type of faced masonry (presence of voids,

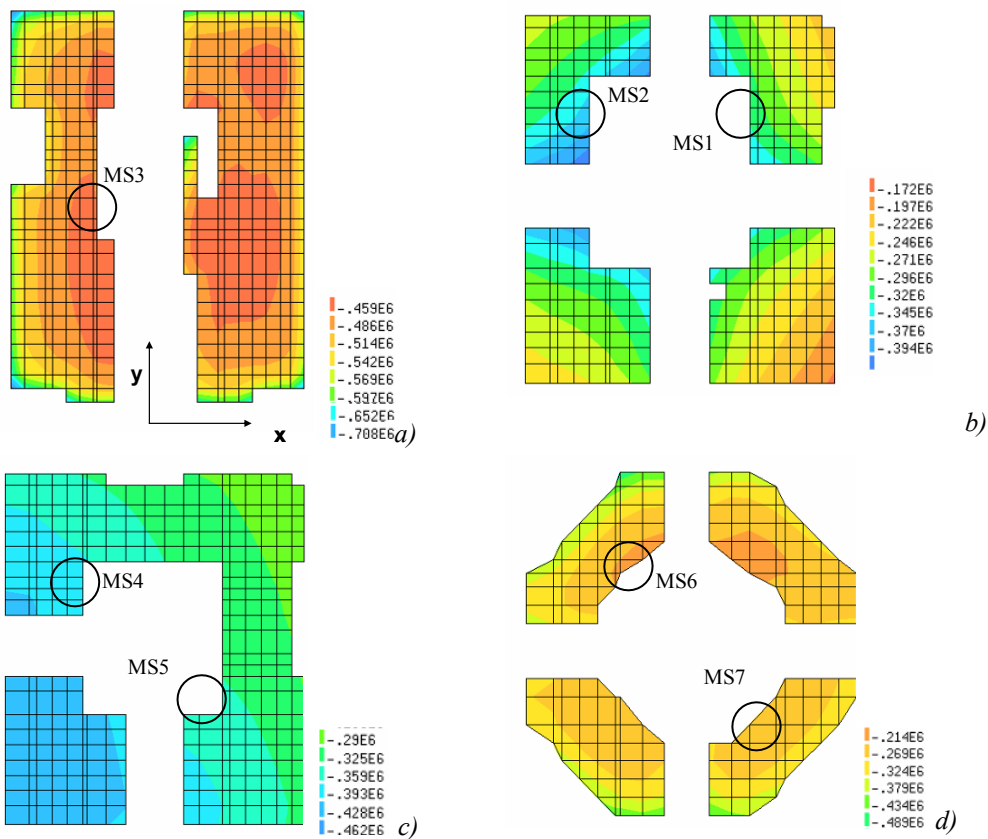
mortar, filling materials inside the two wall faces). However the assessed values of unit weight are lower than the ones suggested by Italian codes (16-18kN/m³ (OPCM 3431, 2005; NTC, 2008) [1&5]).

Table 1. Comparison between experimental and theoretical normal stresses.

Flat-jack	Level	Material	Experimental Stress [MPa]	FEM Configuration B [MPa]	FEM Configuration A [MPa]	SAP Configuration A [MPa]
MS1	+8.70m (first level)	Tuff	0.35	0.33	0.45	0.40
MS2	+8.70m (first level)	Tuff	0.30	0.33	0.42	0.40
MS3	+0.0m (entrance)	Tuff	0.35	0.46	0.55	0.51
MS4	+19.0m (second level)	Tuff	0.26	0.35	0.40	0.31
MS5	+19.0m (second level)	Tuff	0.26	0.31	0.30	0.31
MS6	+40.0m (fourth level)	Clay bricks	0.17	0.19	0.15	0.17
MS7	+40.0m (fourth level)	Clay bricks	0.17	0.21	0.20	0.15

In Figs.4 the stress map (compressive stresses are assumed negative) at the levels, where the single flat-jack tests were made, is reported for the configuration B. The static analysis of the structure under its own weight showed that the normal stresses are slightly increasing along the bisecting line of plane x-y in the direction of the Tower front side (left corner of plan sections) especially at lower levels (+0.0-+19.0m, Figs.4a-b-c). This effect dampens at higher levels (+40.0m, Fig.4d) and is probably due to the

eccentricity of the upper part of the structure that progressively reduces toward the top.



Figs.4. Normal stress distribution at different levels: a) +0.0m, b) +8.7m, c) +19.0m, d) +40.0m

This implies that the forepart of the Bell Tower partially lays on the church. At higher elevations it's always found a compression stress higher on the north-west axis on the façade side correspondent to the cloister location. This trend fades down with the elevation increase, since there is a drop of the value of the masses laying on the lower levels. The stress distribution shows that higher stresses are localized at the lower level (the maximum is 0.68MPa at the ground

level, Fig.4a). High stresses are recorded in the corners along the perimeter or in correspondence of windows, openings, where high stress concentrations can locally develop.

In Fig.5 the stress distribution along the entire Tower is reported. It is highlighted that the highest stresses are localized at the lower level with a mean value of 0.5MPa. At the higher levels, where the section shape becomes octagonal and the walls are made of clay bricks, the stresses are lower, about 0.15MPa as average. This was predictable considering that the higher part of the Tower has several openings compared to the basement that is more massive.

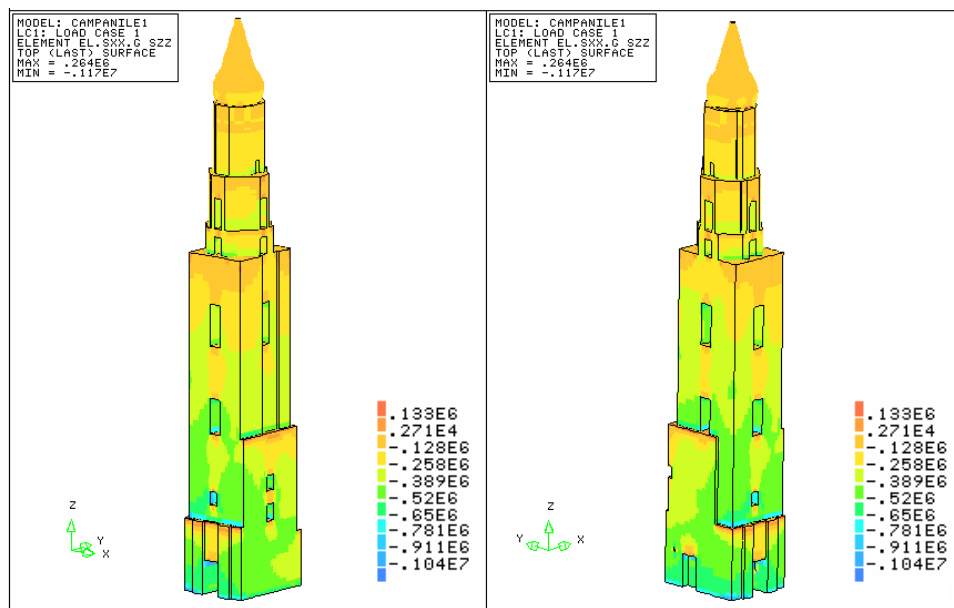


Fig.5. Normal stress distribution in the Tower

Referring to the conservative values of compressive strength given by experimental *in situ* tests (1.4MPa for tuff and 2.4MPa for clay-bricks masonry), the theoretical stress distribution showed that, except for some singular points, the maximum normal stresses are in the range of 35% of the strength for tuff and 6-7% for clay brick and, despite the slight eccentricity of

the structure, no tension stress appears in the distribution.

5.2.3 Modal dynamic analysis

The *in situ* dynamic tests can be helpful not only to experimentally identify the structural behaviour in presence of dynamic actions, but also to adjust the values of elastic constants, the unit weight of masonry assembly and the constraint effects. Therefore, based on the comparisons between experimental evidence (principal modal shapes, natural frequencies) and predictions given by linear dynamic models, the above-mentioned characteristics can be well assessed. This is essential to study the dynamic response under seismic actions and to subsequently develop non-linear models, as discussed in the next section. In particular, FE modelling is a useful support to develop parametric linear modal analyses to assess the values of the material mechanical parameters influencing the dynamic response, since it allows to verify the reliability of those obtained by *in situ* tests (double flat jacks and sonic tests). Furthermore, in many cases historical buildings are not isolated structures, but are embedded in a complex of constructions, often not coeval and homogeneous, making it difficult to identify the mutual interactions. In this case the comparisons between the experimental dynamic characterization and the theoretical one predicted by linear FE models allow showing the effect of the surrounding buildings, analyzing the influence of several constraint conditions on the modal shapes and natural frequencies.

A dynamic modal analysis of the Tower has been developed by the 3D finite element model previously introduced, assuming a linear elastic behaviour for all materials. The values of natural frequencies and the modal shapes obtained by the experimental dynamic identification have been compared with the results of linear dynamic analysis developed for the 3D FE model of the Tower according to various boundary conditions. Several analysis have been aimed to confirm or assess the values of unit weight and Young's modulus of masonry and to clarify the constraint extent supplied by the adjacent buildings.

The dynamic modal analysis was accomplished for different configurations to define the one that better simulates the real behaviour of the structure as shown by the in situ dynamic test. In addition to the configurations A (cantilever scheme) and B (presence of fixed constraints in correspondence of the points of interaction with the surrounding structures), previously introduced for modelling the behaviour under gravity loads, two additional configurations were considered. These two new configurations take also into account the effects of lateral buildings. Historical records demonstrate that the different structures were originally built independently, this mean that there is an uncertainty associated to the extent of constraint due to the adjacent structures. Consequently it was assumed that if there is an interaction, this cannot be represented by fixed constraints, as the experimental modal shape shows, but by a constraint that considers the characteristics of deformability of the bordering elements. This is why the fixed constraints were substituted by springs in one case and in another case they were modelled as portions of elements belonging to adjacent buildings (Fig.6).

- Configuration C: the effects of lateral buildings are modelled by elastic constraints (springs) instead of fixed supports, in the hypothesis that the interaction depends on deformability properties of the adjacent elements and those of the materials filling the gap.
- Configuration D: parts of the lateral buildings adjoining the Tower are partially included in the 3-D model of the structure.

A parametric analysis varying the value of elastic modulus of materials has been also developed in parallel with the evaluation of the restraint effect. The process of model updating (Gentile and Saisi, 2004 [9]; Zingone and Valente, 2005 [10]; Wang and Aldar, 1994 [11]) was performed by optimizing the differences between experimental and numerical eigenfrequencies and mode shape components, choosing the elastic modulus of the materials and the constraint extent offered by the surrounding buildings as tuning parameters.

Updating leads to estimate the elastic modulus as 900MPa and 1200MPa respectively for tuff and clay masonry that differ appreciably from the initial ones (40-60% increase), but are closer to the ranges suggested by national codes [OPCM 3431, 2005] [1]).

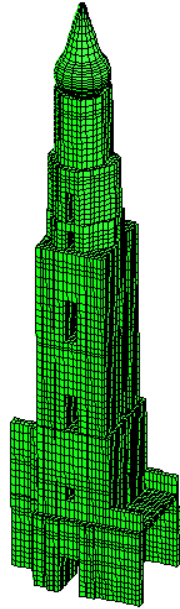


Fig.6. Partial modelling of surrounding buildings

In Table 2 frequencies (f) and periods (T) of the first five vibration modes are listed for the described boundary conditions, showing how the frequencies decrease when the structure is less restrained. Moreover slight differences can be observed between configurations B and D, both taking into account the presence of surrounding buildings through fixed supports or partial modelling (maximum difference of 10-12% for the first 4 modes), while a significant scatter is evident between cantilever (A) and fixed configuration (B) especially for the first two modes (32-27%).

The best fitting with experimental values is given by the configuration with fixed restraints (B), showing a perfect agreement for the first two modes, a

maximum frequency discrepancy of 17% on the 3rd and 4th modes and 28% on the torque mode; also models C and D show a good agreement (i.e. for model D the maximum scatter is 10-12% for the first two modes, 3% for the 3rd and 4th modes, and 8% for the torque one).

Table 2. Experimental vs. theoretical dynamic characterization of the Tower

Mode	Type	Experimental results		Numerical FEM Analysis by DIANA			
		f [hz]	T [s]	(A)	(B)	(C)	(D)
				f [hz]	f [hz]	f [hz]	f [hz]
1	Flex x	0.69	1.45	0.47	0.69	0.66	0.62
2	Flex y	0.76	1.32	0.56	0.77	0.74	0.67
3	Flex x	2.28	0.44	1.88	2.60	2.43	2.31
4	Flex y	2.35	0.43	2.11	2.75	2.61	2.42
5	Torsional	2.76	0.36	2.85	3.54	3.33	2.97

In Figs.7 the modal shapes corresponding to the first five vibration modes obtained by the 3-D model are reported for configurations A (Fig.7a) and B (Fig.7b). In Figs.8&9 the normalized theoretical and experimental modal shapes corresponding to the first four vibration modes are compared considering the different boundary configurations that were examined. The first two flexural modes are able to involve the larger part of the mass of the structure. About 75% for the constraints configuration with lateral buildings (D) and 84% for the cantilever scheme (A). Very low mass percentages are involved in the third and fourth modes (2.9% for configuration D and 5.5% for configuration A).

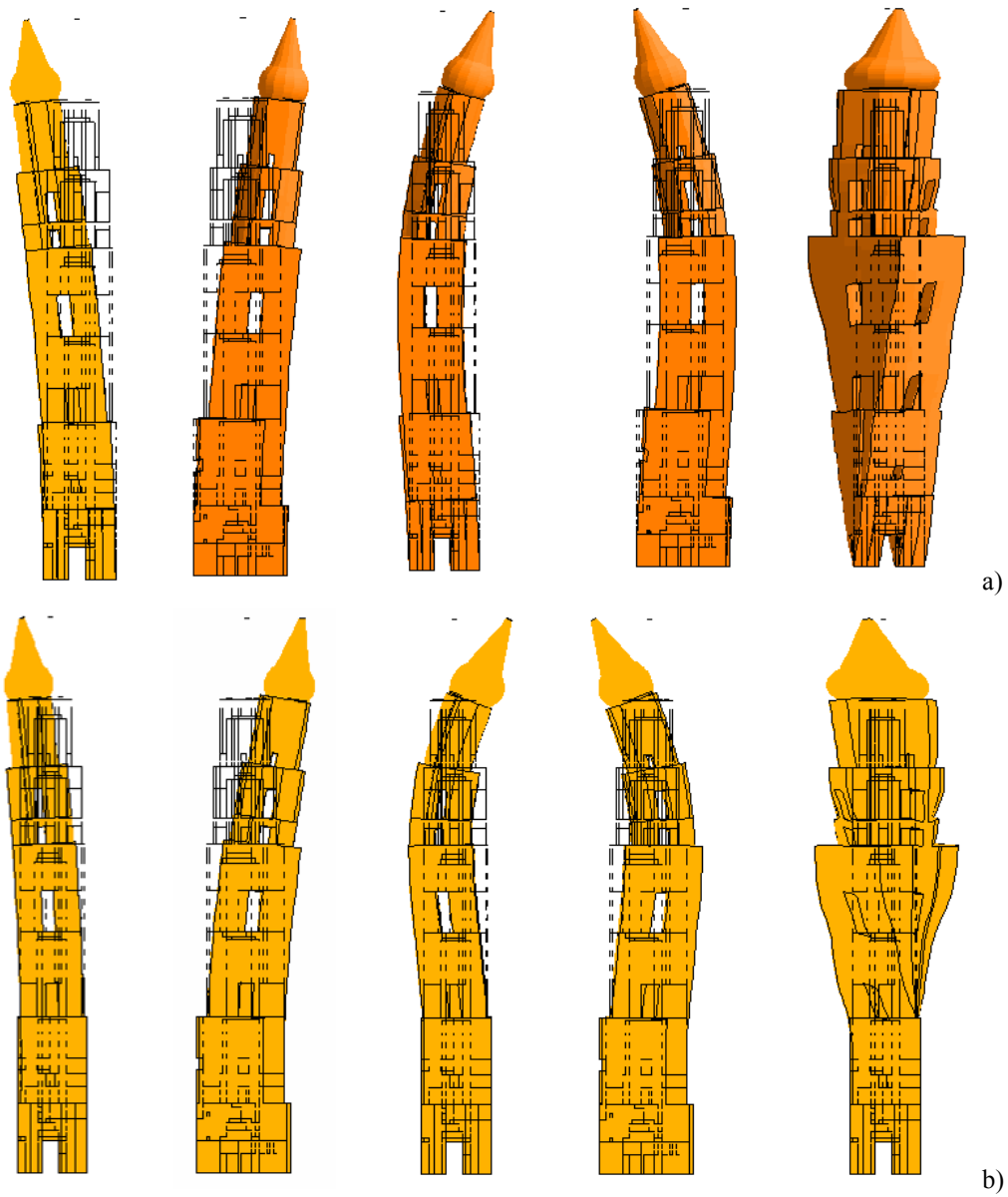


Fig.7. Deformation modal shapes of the first five vibration modes modelled by DIANA: a) configuration A; b) configuration B.

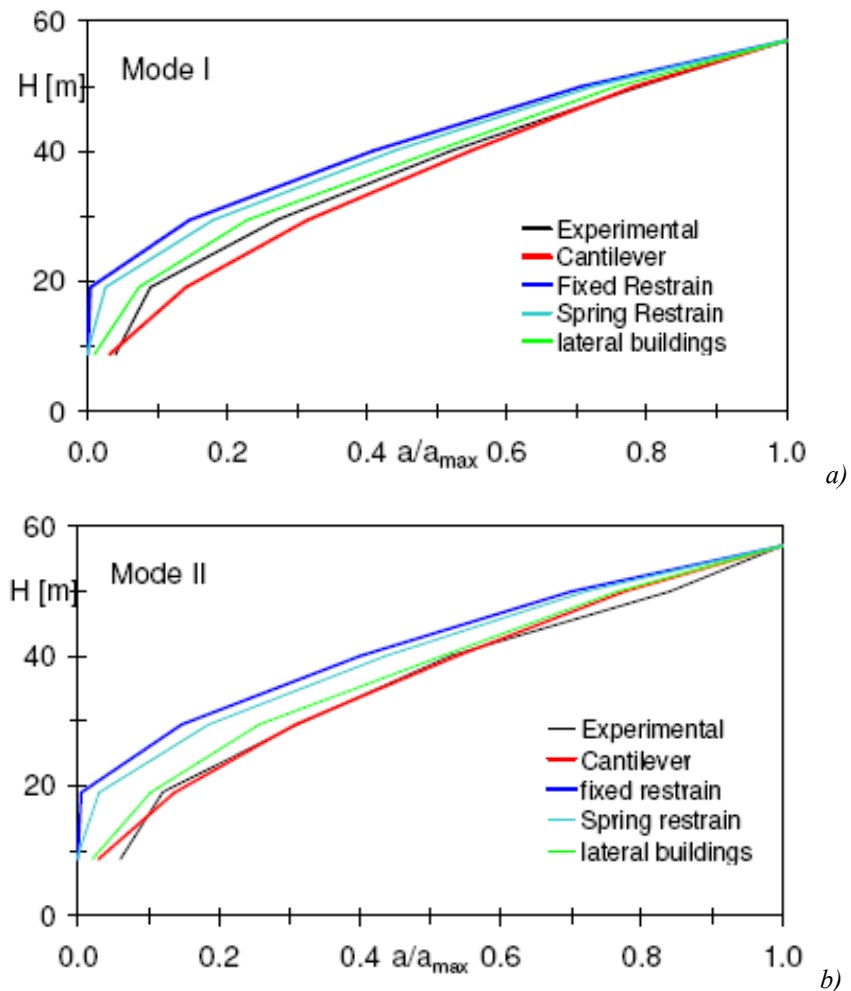


Fig.8. Comparison between the experimental and the theoretical modal shapes in terms of normalized acceleration: a) Mode I, b) Mode II

When a strong dynamic action occurs, as an earthquake, probably the effectiveness of these kinds of restraints is reduced and the Tower behaves like an isolated element. Furthermore this is also confirmed by various inquiries that lead to suppose that the Tower was originally built separately from the other buildings, particularly from the Church, and that it was surrounded successively. The comparisons show that the experimental behaviour is more

similar to the theoretical one predicted by models neglecting or minimizing the effects of lateral buildings (models A and D), while it is not well replicated by the model B, that gives the best agreement in terms of frequencies. This leads to assume that the best fitting, in terms of both frequencies and modal shapes, is attained by the configuration where the lateral buildings are partially included in the model (model D).

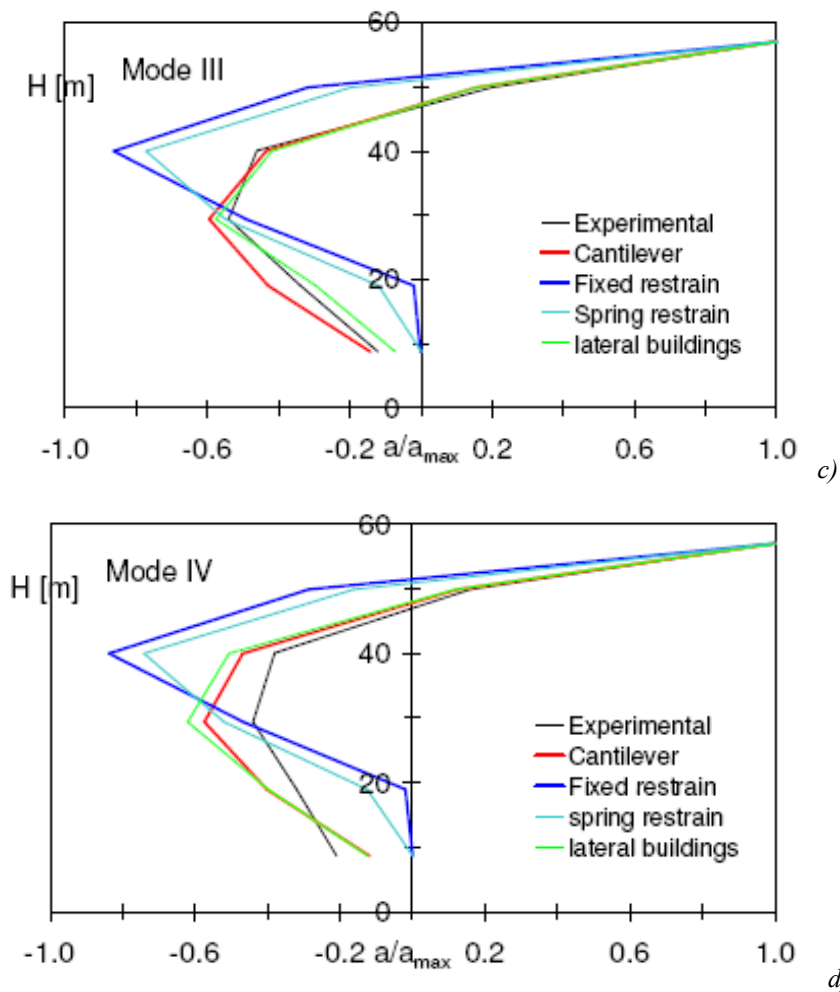


Fig.9. Comparison between the experimental and the theoretical modal shapes in terms of normalized acceleration: c) Mode III, d) Mode IV

In conclusion the comparison between the experimental and theoretical dynamic behaviour of the Tower has pointed out significant effects of the surrounding buildings on the frequencies (the experimental values point to a constrained behaviour rather than a cantilever model) and minor effects on the modal shapes that are lightly less deformable with respect to the cantilever scheme. However, historical inquiries clarified that the church and tower were originally separate and that successively they were connected only by filling the gap between the northern walls of the tower and the church, while the other constructions were built later. Therefore it can be assumed that the constraints offered by surrounding buildings are weak, probably unilateral (or depending on the tensile strength of the filling materials) and effectively active in the operational conditions used for the dynamic identification. On the contrary, these constraints should not be considered under seismic actions, usually characterized by accelerations greater than the environmental ones, so that a cantilever scheme (model A) will be adopted for the following non-linear analysis.

5.2.4 Non linear static analysis and push-over

5.2.4.1 Evaluation of the displacement capacity

Non-linear analysis is needed to assess the safety condition of the structure in order to plan interventions in accordance with the maintenance requirements (ICOMOS Recommendations, 2005) [12].

Seismic assessment of existing buildings under design earthquake actions at ultimate state can be performed by analysis based on non-linear modelling of the structural behaviour. Indeed, assuming a non-linear behaviour of materials, it is possible to evaluate the capability of the structure to dissipate energy in the post-elastic field. In general, for towers and tall structures, due to their lower geometrical complexity, also linear analysis and simplified models can supply interesting and reliable information (DPCM, 2007) [13]. For the case of the

Bell Tower of Santa Maria del Carmine, experimental dynamic behaviour showed that the main modal shapes are substantially independent of one another. Therefore non-linear static analysis can provide significant results about the seismic behaviour of the structure.

In particular, push-over analysis, that is a specific procedure to analyse non-linear behaviour under seismic actions, was performed. This procedure takes into account the dynamic behaviour of the building, through the application of a load distribution similar to the dominant modal shapes, which have been assessed by linear dynamic modelling and experimental identification. The static scheme considered for the non linear static analysis assumes the constraints applied only on foundation (scheme of the Bell Tower considered as a cantilever beam). This choice was made since the modal shapes are pretty close to a cantilever beam as pointed out by the numerical modal analysis. There is an effect dependent on the constraints at intermediate elevations between +0.0 and +19.0m mainly in terms of frequencies. Though, it's quite limited, probably because of the reduced levels of acceleration induced by the environmental dynamic stresses. In the presence of a significant dynamic action, like the one due to the design expected quake, probably the effectiveness of constraints is waved by and the structure behaves like being insulated. Additionally from the standpoint of the stresses induced on the structure the cantilever scheme is conservative. With the aid of the non linear static analysis it can be evaluated the performance of the structure under the actions of a static distribution of horizontal forces. Generally, like in this case, the reaction of the structure to an horizontal action is highlighted through a curve where the shear force acting in foundation. (applied resultant of the horizontal load distribution), is shown as a function of the displacement of a control point of the structure. The force distribution was assumed, for both directions of the quake action, similar to the former modal shapes relative to the cantilever scheme (Fig.10). Table 4 shows a summary of the mechanical characteristics of the materials previously discussed and utilized in the modelling.

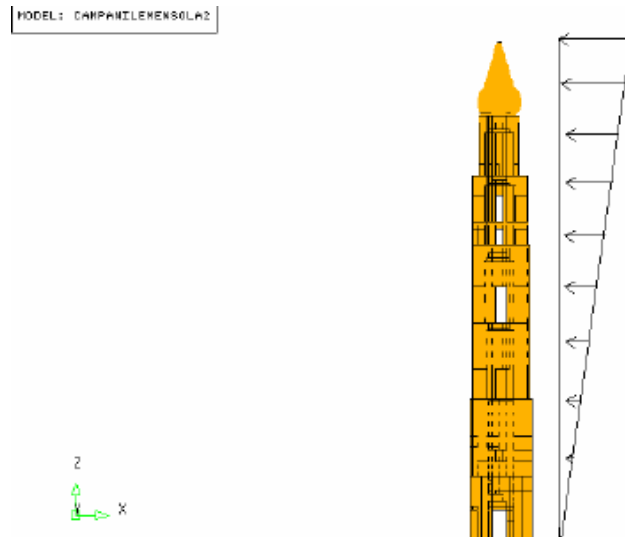


Fig.10. Distribution of the horizontal forces along x direction

Table 4. Mechanical and physical characteristics of the materials

Parameters	Tuff	Brick
Elastic Module E (MPa)	900	1200
Poisson Module	0.15	0.15
Unit weight	1200	1600
Tension resistance (MPa)	0.07	0.12
Fracture Energy Gt (N/m)	1.65	3.65
Ultimate tension deformation	0.040%	0.055%
Post peak tension law	Hordijk	Hordijk
Compressive strength of the masonry	1.4	2.4
Post peak compression law	Linear	Linear
Residual resistance (% resistenza di picco)	30%	30%
Deformation in correspondence of the residual resistance	0.4%	0.5%

Based on the previous considerations, the push-over analysis (Magenes, 2000) [14] was developed modelling the Tower according to the cantilever scheme.

Horizontal seismic actions were applied separately along the two main directions, X and Y, according to a “modal” pattern, where the load distribution along the height is proportional to the first and second modal shapes of the cantilever configuration (A). The importance factor γ_I , (from OCPM 3431, 2005) [1] used to increase the seismic demands for particularly important buildings and redefined for cultural heritage in DPCM, 2007 [13] according to the artistic relevance and the final destination of the structure under evaluation, was taken equal to 1.0, in order also to optimize the assessment procedure. The top of the cover dome (+67.6m) has been assumed as control point of displacements of the horizontal force resultant divided by the entire mass of the structure that represents a sort of spectral acceleration.

In Fig.11, the capacity displacement curves are reported for all directions ($\pm X$, $\pm Y$). For each direction the analysis stopped when the axial-flexural failure of the base section occurs (Fig.12a), leading to different values of maximum force (0.08–0.11 g) according to the direction of pushing force. It must be underlined that in the X direction the maximum displacement is about 1200mm, while for the Y direction it is about 500mm, confirming the higher deformability of the structure in the X direction as already highlighted by the modal analysis (Ceroni, Voto et al., 2009) [15].

In Figs.12 the normal stress distribution along the entire Bell Tower is reported at the maximum shear force applied along the +X direction. The tension stress distribution (shown by the positive values in Fig.12a) develops from the base of the Bell Tower up to elevation +41.4m, in correspondence of the change of the cross section from rectangular to octagonal. The structure collapse is due to the achievement of the crisis value of combined compressive and bending stresses in correspondence of the base cross section of the Bell Tower. Both compression and tension stresses overcome the relative peak resistance. Consequently a significant portion of the section at the base of the Tower presents a stress state located on the degrading branch of the post peak softening curve.

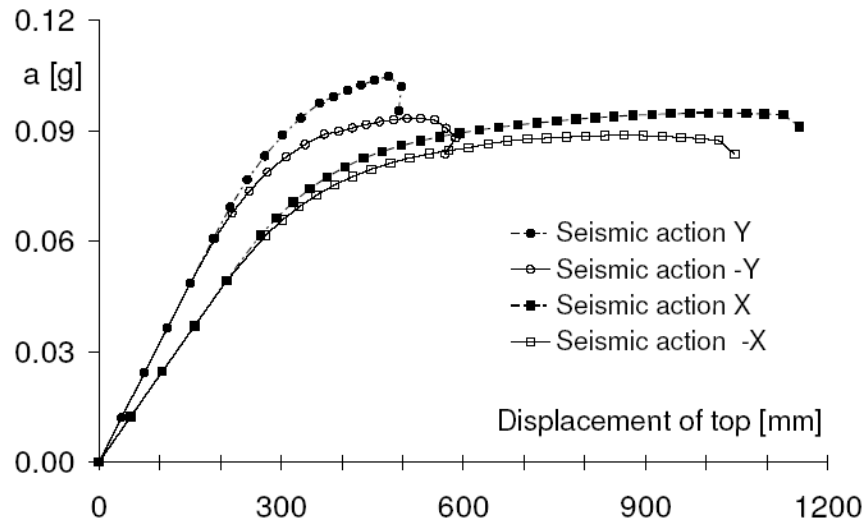


Fig.11. Maximum shear–displacement relations for seismic action in X and Y direction.

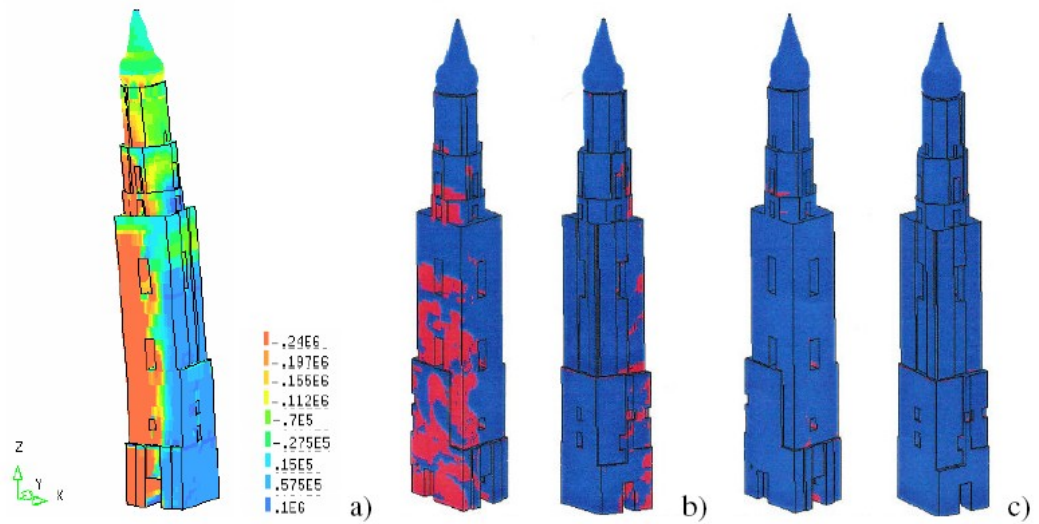


Fig.12. a) Distribution of principal stresses along the Tower for the maximum shear force in +X direction (stress in $N/m^2=10,6MPa$); b) Distribution of tensile stresses greater than $0.07MPa$; c) Distribution of tensile stresses greater than $0.1MPa$

In Figs.12b-c, the distributions of tensile stresses exceeding the tensile strength of tuff (0.070MPa) and clay brick (0.120MPa) masonry are red coloured to evidence the most critical fields. The figures indicate that the tension stresses correspondent to the maximum applicable shear force overcome the value of the peak resistance of the material in the part of the Bell Tower from +0.00 up to +30.00m, correspondent to the part made with tuff. No particular emergency situation appears to exist for the brick part.

5.2.4.2 Evaluation of the displacement demand

The key concept which the non linear static seismic analysis is based on indicates that the strength and displacement capacity of a structure is represented by a curve (capacity curve) matching the resisting horizontal force, i.e. shear load at the base and the displacement of a control point of the building (either a point on the roofing, or at a 2/3 of the height, that with a linear distribution of the forces would represent its centroid). Therefore the curve is an “intrinsic” characteristic of the structure, which is not dependent on the seismic input and may be seen as a tool to reduce the answer of a multi-degree of freedom complex system. The capacity displacement curves can be used to assimilate the behaviour of a complex system with multi degrees of freedom (MDOF system) to that of a simple equivalent non-linear oscillator (SDOF system). Hence in the push-over procedure after the first step leading to the definition of the capacity curve, the maximum displacement capacity of the structure (MDOF system) has to be compared with a target displacement, d_t , calculated according to the code indications (OCPM 3431, 2005, Eurocode 8-Part 1, 2005) [1&16]. To this aim the second step consists in defining the capacity displacement curve (F^*-d^*) of the equivalent SDOF system. This is usually assumed to have a bilinear plot with the significant point established making equal the area under the bilinear curve and the area embedded by the capacity curve of the real structure (Eurocode 8–Part 1, 2005) [16].

On such capacity curve it's possible to compare the displacement capacity of the structure with the displacement demand (target displacement). This latter one, expressed in terms of answer spectrum and evaluated in accordance with the Standard (OCPM 3431, 2005, Eurocode 8–Part 1, 2005) [1&16], represents the displacement that the structure is supposed to sustain under the design seismic action.

The displacement demand is evaluated with reference to the definition of an equivalent one degree of freedom oscillator and plotting a “characteristic force” F^* vs the displacement d^* bilinear curve that envelops an area equal to that of the real structure capacity curve (Fig.13).

The mass and the period of the equivalent oscillator are defined by (1):

$$m^* = \sum m_i \phi_i^2 \quad T^* = \pi \sqrt{\frac{m^*}{k^*}} \quad \Gamma = \frac{\sum \phi_i}{\sum m_i \phi_i^2} \quad (1)$$

Where:

Φ is the vector representative of the first vibration mode of the structure along the direction considered for the seismic action, normalized to the value of the component relative to the check point;

Γ is a transformation factor associated to the first modal shape;

k^* is the secant stiffness of the equivalent system obtained making equal the areas highlighted in Fig.13.

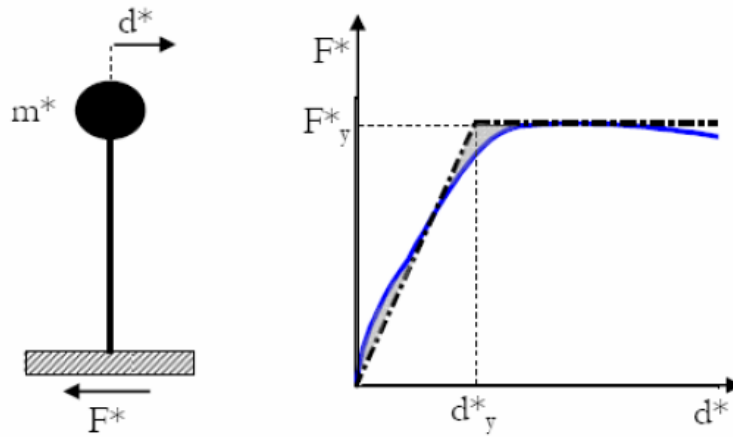


Fig.13. Equivalent oscillator and relationship force F^* vs bilinear displacement d^*

The applied force F^* and the displacement d^* of the one degree of freedom system are associated to the correspondent parameters of the real structure by the relationships (2):

$$F^* = \frac{F_b}{\Gamma} \quad \text{and} \quad d^* = \frac{d_n}{\Gamma} \quad (2)$$

where F_b and d_n are, respectively, the base shear force and the control node displacement of the MDOF system and Γ is the transformation factor.

The coordinates of the yielding point of the equivalent bilinear system may be defined as:

$$F_y^* = \frac{F_{bu}}{\Gamma} \quad d_y^* = \frac{F_y^*}{k^*} \quad (3)$$

where F_{bu} is the ultimate resistance of the structure.

As in the case under analysis, if the period T^* is high enough to be greater than the value T_c , (OCPM 3431, 2005) [1] function of the foundation soil properties

beyond which the coordinates of the spectrum decrease, the displacement demand, d_m^* of the inelastic system (the oscillator) is assumed equal to the displacement of an elastic system, $d_{e,m}^*$ with the same period T^* .

In particular this displacement is computed as coordinate of the elastic spectrum in correspondence of the period T^* , $S_{De}(T^*)$. The spectrum of the elastic answer of the displacement is obtained as direct transformation of the spectrum of the elastic answer of the accelerations, $S_e(T^*)$:

$$d_m^* = d_{e,m}^* = S_{De}(T^*) = S_e(T^*) \times \left(\frac{T^*}{2\pi} \right)^{\gamma} \quad (4)$$

The elastic spectrum displacement of the accelerations $S_e(T^*)$ is computed in correspondence of the period T^* in accordance with the expressions given by the National Standards (OCPM 3431, 2005) [1].

On the contrary if T^* is less than T_c , the displacement of the one degree of freedom inelastic system is larger than the displacement of the elastic system with the same period by an amplification coefficient that considers the ratio between the elastic answer force ($S_e(T^*) \times m^*$) and the yielding force of the equivalent system (F_y). The displacement demand requested to the real structure, on the basis of the (2), is $d_m = \Gamma d_m^*$

5.2.4.3 Comparison between displacement capacity and displacement demand

For the site under analysis, two values of the expected maximum acceleration at bedrock (Peak Ground Acceleration, PGA) have been considered:

- $a_{g,475} = 0.168g$, that is the value with an occurrence probability of 10% in 50 years, corresponding to a return period of 475 years;
- $a_{g,2475} = 0.280g$, that is the value with an occurrence probability of 2% in 50 years, corresponding to a return period of 2475 years;

All these values are based on the recent detailed seismic hazard reference map of Italy (Meletti and Montaldo, 2007) [17]. In particular for existing structures the values $a_{g,475}$ and $a_{g,2475}$ have to be used to develop, respectively, verifications at the Limit State of Significant Damage (LS SD) and Limit State of Near Collapse (LS NC) (Eurocode 8-Part 3, 2005b) [18]. The first verification is usually performed for existing structure, while the latter one for new ones.

In all verifications the worst type of foundation soil is assumed, based on the geotechnical properties of the site (type D soil, (Eurocode 8-Part 1, 2005a) 16]. The target displacements for the equivalent SDOF system, d_t^* , are 226.0mm and 376.0mm respectively for a return period of 475 and 2475 years. These values, multiplied by the participation coefficient related to the first modal shape, $\Gamma=1.71$, give the effective target displacements for the structure, d_t , equal to 386.0mm and 643.0mm. The structure shows different values of its displacement capacity dependently on the loading direction: 1126.0mm, 1020.0mm, 498.0mm and 572.0mm respectively for +X, -X, +Y, -Y directions. With reference to the Limit State of Significant Damage (return period of 475 years) the minimum safety factor is 1.29 (+Y direction) and the maximum is 2.91 (+X direction), therefore the structure is verified; on the contrary with reference to the Limit State of Near Collapse (return period 2475 years), the tower is verified for both $\pm X$ directions (safety factors 1.75 and 1.59), while it is not verified for either $\pm Y$ directions (safety factors 0.77 for +Y and 0.89 for -Y).

In Fig.14 the capacity displacement curves of the SDOF system and of the real structure, normalized to Γ , are shown for the directions with the lowest safety factors (-X, +Y, -Y).

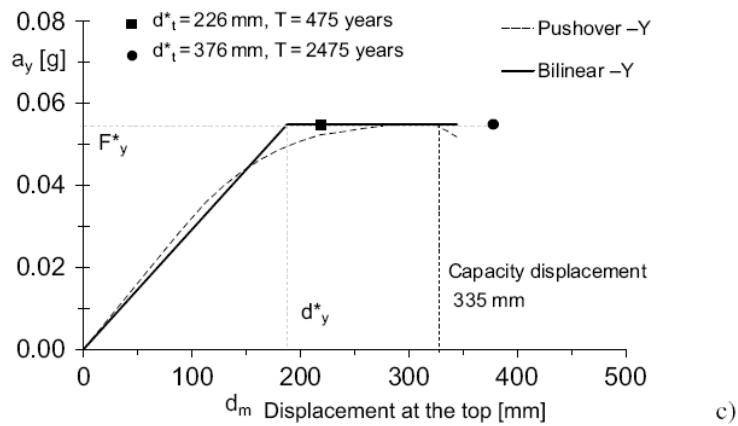
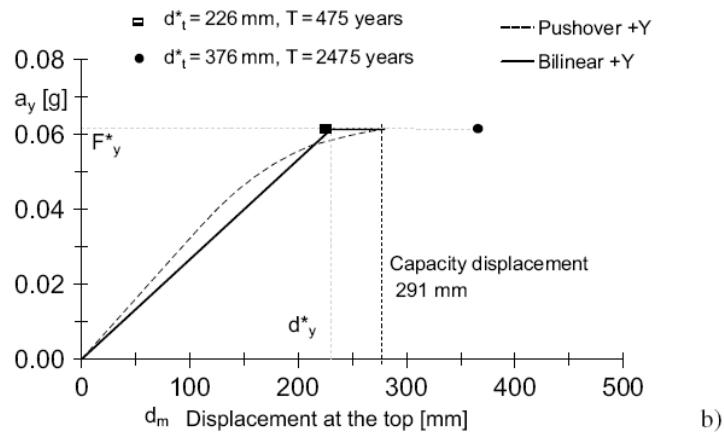
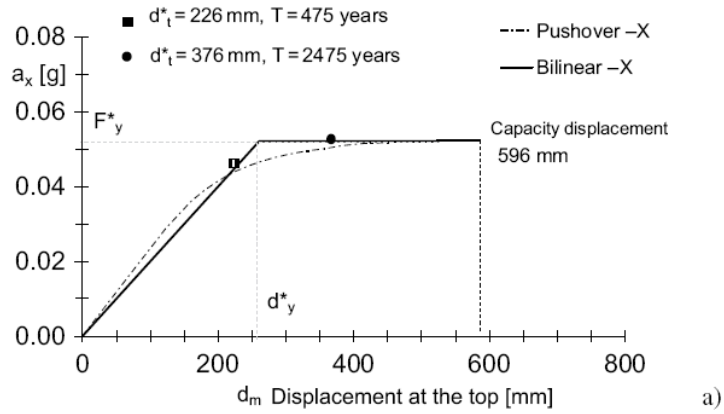


Fig.14. Capacity displacement curves of real structure and SDOF system normalized to $\Gamma=1.71$: a) Direction -X; b) Direction +Y; c) Direction -Y.

In summary, a comparison in terms of displacement between the capacity of the structure and the requested demand, estimated on the basis of the seismic level of the site, let us consider the Bell Tower to have sufficient resistant capability and ductility necessary to absorb the design seismic actions. Finally it's necessary to underline that the modelling was accomplished assuming the Bell Tower being a monolithic structural body, considering that at all levels the orthogonal wall constituting the structure are integral for the correct connection of the corners: this allowed to utilize a model of analysis that assumes a compact cross section of the structure. Anyway this approach is not exhaustive in the evaluation of the structural safety. In fact if the assumption of good connection is not verified, the collapse condition could be due not to a global crisis of the structure, but to the development of local tilting mechanisms of the single masonry panels because of the lack of suitable constraints.

5.3 ANALYSIS OF LOCAL MECHANISMS

Ancient masonry buildings are frequently subject to local failure because single parts can be involved in out-of-plane mechanisms, activated by horizontal actions when the connections among them and/or with the horizontal elements are lacking or no longer effective. This means that the seismic response of a masonry building is strictly influenced by the constraint degree represented by the connections between vertical and horizontal elements. A lack of constraints could make the structure sensitive to local out-of-plane mechanisms and incapable of reacting to the seismic input with a global response. This implies a potential vulnerability in relation to local mechanisms that can involve not only the out of plane collapse of the single masonry panels, but wider portion of the building (tilting of complete badly connected walls, tilting of upper walls in presence of different height building, partial collapse in the corner buildings of the constructions). It's mandatory to assess the safety of the building with reference to such mechanisms. Based on the empirical observation of these phenomena, in the past a very common and simple solution to avoid local mechanisms and attain a global behaviour was represented by insertion of steel tie rods (bars, cables, wires).

All the numerical analyses previously described were developed for the Bell Tower in the hypothesis that walls are well connected in the corners, meaning that no local mechanism could be activated out of the plane. Indications that these local phenomena can actually happen are evidenced by the presence of several steel chains and reinforced injections realized in the past often after seismic events. Consequently, detailed examination of the existing steel chains was performed to evaluate their efficiency in avoiding eventual out-of-plane mechanisms, and then mechanisms in various locations were analyzed.

Generally, the safety conditions of a structure with respect to out-of-plane mechanisms can be simply evaluated by an equilibrium limit analysis regarding

the masonry parts of the building susceptible of being involved in the mechanism and assumed to behave as rigid blocks.

5.3.1 Typologies of local mechanisms of masonry structures

The global behaviour of a masonry structure in presence of seismic actions is highly influenced by the extent of connections among both vertical and horizontal structural elements. Lack of connections among orthogonal wall and between walls and horizontal elements doesn't give the building the capability of a global answer to the seismic input. On the contrary they can cause the initiation of local mechanisms and kinematic motions of collapse because of the independent behaviour of the walls. In this case the predominant behaviour is the out of plane one. Consequently inserting elements that improve also locally the scarfing among the walls or improving their connections with the horizontal structures, reduce the possibility of initiating out of the plane displacements. For example the vulnerability vs out of plane mechanisms may be reduced transforming the out of plane answer of the façade in an answer within the plane of the orthogonal walls (Fig.15). In this way the façade is made integral with the orthogonal walls.

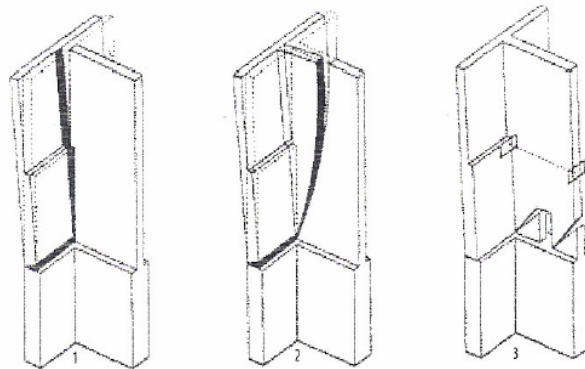


Fig.15. Tilting mechanisms of the façade: 1) without scarfing; 2) with scarfing; 3) with insertion of tie-bars

Often the vulnerability vs the out of plane mechanisms is very high on portions of walls that are not well constrained and orthogonal to the action of the seism (Fig.16a). In this case the insertion of tie-bars increase the level of constraint of orthogonal walls vs the seismic action, involving the walls parallel to the earthquake into the resistant mechanism (Fig.16b). Additionally the presence of tie-bars and/or reinforced concrete kerbstones opposes the spreading apart of the inside walls. This generally implies an increase of the compression of the story bands with an increase of their bending resistance (Fig.16c).

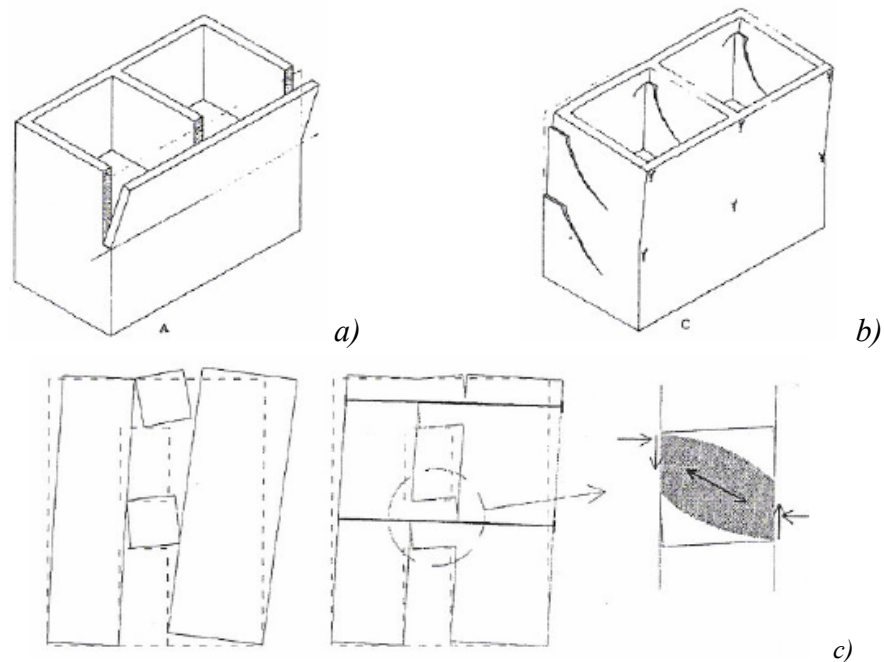


Fig.16. Collapse mechanisms: a) without tie-bars and b) with tie-bars b); c) effect of the tie bars on the story bands

Very often morphological and geometrical peculiarities may be determinant in the initiation of global and local collapse mechanisms. Irregularities and discontinuities in the planimetry, in the altimetry and material lack of homogeneity may cause spots or preferential lines of initiation of such

mechanisms. The following figures show several examples of some mechanisms that can be activated because of particular geometrical configurations. Fig.17 shows a variation of the global tilting of a portion of a façade of the building favoured by the presence of an altimetry discontinuity due to a leaning body of lower height. The presence of in plan discontinuities such as the one in Fig.18 implies a trend to tilting of the added body because of the hammering of the main building and of the eventual bad scarfing of the two bodies masonry. Fig.19 highlights an example of partial tilting of the walls of the façade over and under the level of a floor badly scarfed to the vertical walls. The pushing action of the roofing elements on the underlying walls may favour the initiation of local tilting mechanisms of portions of walls (Fig.20)

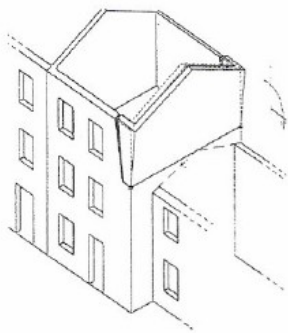


Fig.17. Partial tilting of the façade because of irregularities in the elevation

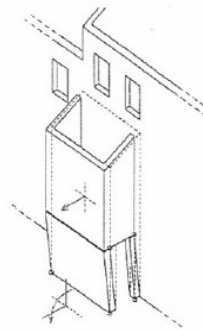


Fig.18. Tilting due to in-plan irregularities

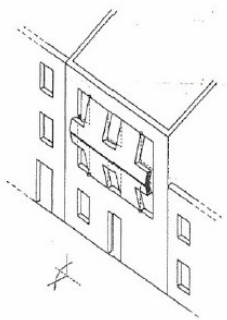


Fig.19. Partial tilting in correspondence of badly connected floors

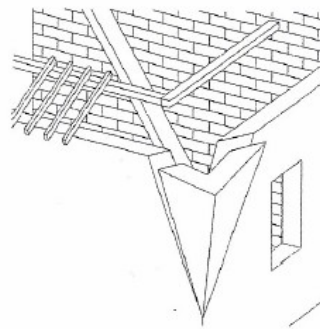


Fig 20. Partial tilting due to the pushing roofing structure

The identification of collapse mechanisms must be based on a careful study of the structure under evaluation. Fig.21 shows some typical kinematic motions for buildings without particular altimetry and planimetry discontinuities. They're differentiated by the location of the cylindrical hinge, localized, for each mechanism in correspondence of the floor elevation and considering the tilting of the upper wall only. Clearly these movements may not be exhaustive since it's necessary also to verify the initiation of more complex or localized mechanisms due to some peculiarity of the building under examination. If the masonry walls are constituted only by one facing, a monolithic behaviour can be assumed. On the contrary for faced wall masonry (quite often for the historical buildings) it must be verified also the potential of differentiated tilting of the two facing if not well connected. The involvement in the generic kinematic motion of portion of main inside walls orthogonal to the main façade walls is dependent on the extent of scarfing in the angles and by the effectiveness of the constraint represented by the horizontal structure.

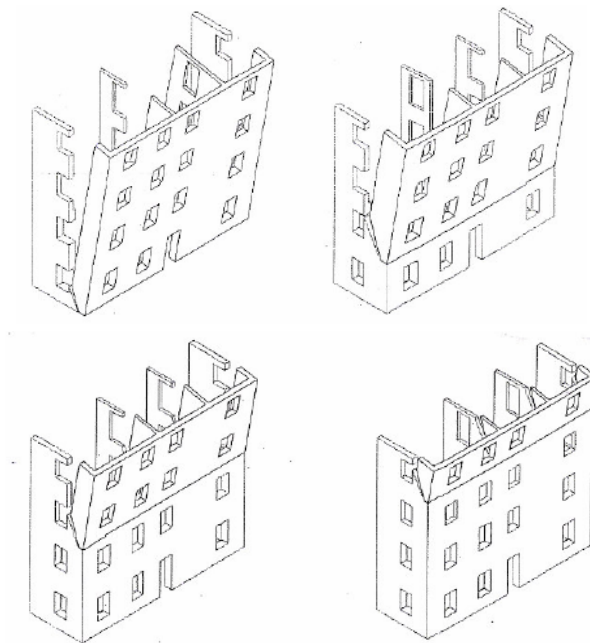


Fig.21. Examples of kinetic motions of the façade

5.3.2 Identification of local mechanisms in the Bell Tower

Masonry buildings are often subjected to partial collapses due to seismic actions and to the loss of balance of portions of walls. Verifying those mechanisms make sense if a certain degree of integration of the masonry wall is guaranteed, to prevent local collapses due to desegregation of the masonry.

Local mechanisms in the masonry walls are mainly due to actions perpendicular to their plane. Checks of these local mechanisms of damage and collapse (within and out of the plane) may be accomplished through the balance limit analysis, following the approach of the kinematic motion based on the selection of the collapse mechanism and the assessment of the horizontal action originating this motion. The application of this checking methodology implies the analysis of the local mechanisms considered significant for the construction. They may be assumed based on either the acquaintance with seismic behaviour of similar structures, already damaged by earthquake or considering the presence of cracked areas, even if not due to seismic actions. Additionally it's necessary to consider the quality of connections of the masonry structures, the masonry texture, the presence of tie-bars, interactions with other elements of the construction or adjacent buildings.

For each possible local mechanism considered significant for the building, a part of the construction must be transformed in a labile system (kinematic chain). It's necessary to determine (through fracture planes due to the low tension resistance of the masonry) rigid bodies capable of relative rotation or sliding.

Generally for the application of the methods it's assumed:

- No tension resistance of the masonry
- Lack of sliding among the blocks
- Infinite compression resistance of the masonry

The safety conditions of a structure vs the out-of-plane mechanisms can be

simply evaluated by an equilibrium limit analysis regarding the masonry parts of the building susceptible of being involved in the mechanism and assumed to behave as rigid blocks.

All the numerical analyses previously described were developed for the Bell Tower in the hypothesis that the walls are well connected in the corners, meaning that no local out of the plane mechanism could be activated. Indications that these local phenomena can actually happen are evidenced by the presence of several steel chains and reinforced injections realized in the past often after seismic events. Consequently, detailed examination of the existing steel chains was performed (Ceroni, Voto et al., 2009a) [2] to evaluate their efficiency in avoiding eventual out-of-plane mechanisms, and then mechanisms in various locations were analysed. Based on the in situ survey, several steel chains were considered ineffective due to evident damage status (corrosion, failure at anchorage) as described in Chapter IV.

Because of the particular geometrical, architectural and structural configuration of the Bell Tower, the following precautionary assumptions were taken to verify the initiation of possible local tilting mechanisms:

- Inefficacy of the angles as constraint all along the height of the panel vs the out of plane displacement of the panels assumed to be independent
- Inefficacy of the floors as constraint at the top and at the bottom of the single panels

It has been assumed that the only kinematic motion that make possible the tilting are those of the single panels recognized between the two floors. The possibility of multiple tilting of panels belonging to consecutive levels was excluded. In fact each floor singles out very well in correspondence of its elevation system of panels with different geometric characteristics that make quite improbable the possibility of causing the tilting of the whole façade or a portion of it (Fig.21). Reasonably it can also be excluded a tilting mechanism derived from the formation of a hinge in an intermediate position of the single panels (Fig.19). In fact there are neither particular geometrical discontinuities along the height of the panels, nor there are stresses so elevated to cause the

formation of a hinge. Assuming the very conservative hypothesis that the walls are not laterally connected to each other and that the floors give no restraining effect at the top and bottom, the masonry panels behave as single blocks susceptible to collapse out of the plane under horizontal actions.

Masonry panels were geometrically identified according to the level of floors and the distribution of openings. It was assumed that each panel can have an out-of-plane mechanism independent of the adjacent ones, such that, extracted from the structure, it is assumed simply supported on its base, subject to vertical and horizontal loads and susceptible to rotate vs the basement (point A Fig.22).

The kinematic equilibrium of the panel is warranted, if the total stabilizing moment is greater than the de-stabilizing one, given that both are calculated with reference to the rotation point at the basement of the block. The balance of each element is verified assuming equal the contributions of such moments computed vs the tilting point at the basis of each panel.

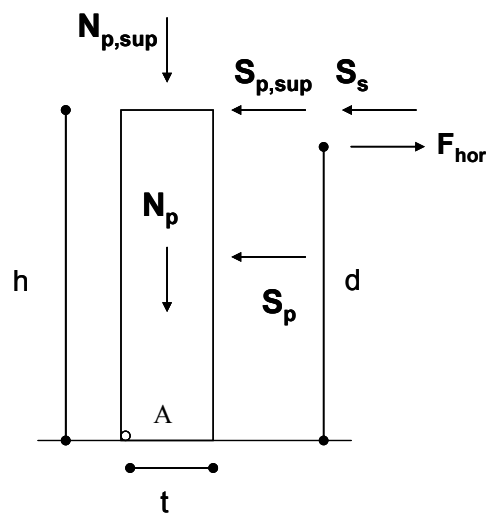


Fig.22. Scheme of the actions active on a rigid body

The complete or partial out-of-plane mechanism of a façade along the entire height was excluded, because each floor defines at each level a system of panels with a well defined geometrical order and independent of those at bottom and top levels. The possibility of a kinematic hinge developing at the middle of each panel was also excluded, because stresses in the element are lower than the compressive strength of the masonry.

Referring to Fig.22, stabilizing contributions are given by:

- Panel weight, N_p , applied in the centre of gravity;
- Upper panel weight, $N_{p,sup}$, applied at the top of the panel;
- Any contribution of existing steel chains or bars, F_{hor} ;

Instead the in-stabilizing contributions are:

- Pushing horizontal force due to the seismic action related to the mass of the panel, S_p , applied at mid height;
- Pushing horizontal force due to the seismic action related to the mass of the upper panels, $S_{p,sup}$, applied at the top of the panel;
- Pushing horizontal force due to the seismic action related to the mass of the floors, S_s , applied at the top of the panel.

The masonry volume above an opening has been half assigned to each adjacent panel and added in the contribution $N_{p,sup}$.

This equilibrium analysis was carried out for the panels above the +19.0m level, which is the last one surrounded by the adjacent buildings and partially restrained, and up to the +57.0m level where the dome starts. The geometry of masonry panels has been individuated based on the position of floors, distribution of openings, and direction of seismic action. Starting from Level 3 at +19.0m, the last level where the tower is surrounded by other buildings, four systems of panels have been defined in the following height ranges: +19.0-+29.0, +29.0-+40.0, +40.0-+49.0, and +49.0-+56.0m and the effective geometry

has been regularized.

At each level, the actual geometrical configurations have been simplified by obtaining transformed configurations (Fig.22), identifying the resistant panels according to the direction of seismic action. As an example, for Levels 3 and 4 subjected to a seismic action acting in the X direction, the panels are identified considering their length parallel to the X axis (Figs.23a and b). The volume of material over the opening was considered as a mass fifty-fifty leaning on the panels aside the opening.

The check to tilting of the single panels were started from elevation +19.0m, that is the last partially constrained level of the Bell Tower for the presence on three of its side of the church, the Brotherhood building and the cloister. For such levels Fig.23 show the original plans, their geometrical scheme and the determination on the plan view of the panels resistant to seismic actions supposed acting orthogonally on the panels under evaluation.

For the portion of the Bell Tower where the plan shape becomes octagonal, the equilibrium of walls has been checked considering the seismic action acting orthogonally to them. Four similar panels have been defined at Level 5 (Fig.23c), while for Level 6 three panels have been identified (Fig.23d).

5.3.3 Verification of mechanisms according to the Italian Seismic Code

With reference to the evaluation of the actions the Standard OPCM 3431 [1] considers for new construction buildings the possibility to develop out of the plane checks of the masonry panels evaluating the acting stresses according a linear static analysis (point 8.1.5.2). This refers the same equivalent forces proportional to the masses utilized for the verification of non structural elements (point 4.9). The seismic action is calculated according to the approach coming from Eurocode 8 (2005a) [16] for non structural elements. In particular a kinematic linear analysis has been developed according to the limit equilibrium analysis, the acceleration, a^*_0 , that causes an out-of-plane mechanism in whatever masonry panel of the structure should be greater than the acting calculated value based on a linear distribution of acceleration along the height of the structure (OPCM 3431, 2005; Eurocode 8–Part 1, 2005a) [1&16]:

$$a^*_0 > \frac{a_g \cdot S \cdot \gamma_a}{q_a} \cdot \left[1.5 \cdot \frac{Z}{H} + 1 \right] \quad (5)$$

where:

Z: is the height of the centre of gravity of each panel above ground level;

H: is the total height of the structure (+67.00m);

q_a : behaviour reducing factor, that can be assumed equal to 2, in analogy with out-of-plane verifications of non structural elements (OPCM 3431, 2005; Eurocode 8 Part 1, 2005a) [1&16];

γ_a : is the importance factor of the element assumed equal to 1 as in the global analysis (Eurocode 3, 2004) [19];

$S=1.35$ is the amplifying factor corresponding to the worst soil typology (type D, Eurocode 8 – Part 1, 2005a, DPCM 2008) [16&13];

a_g : is the expected peak ground acceleration.

The distribution of the accelerations given by (5) was utilized to evaluate the stresses in accordance with a linear static analysis. Hence the horizontal seismic forces acting on each panel can be calculated as:

$$F_a = W_a \cdot \frac{a_g S}{q} \cdot \left[1.5 \cdot \frac{Z}{H} + 1 \right] \quad (6)$$

with W_a the seismic weight of each masonry panel considered.

Relationship (6) corresponds to a linear distribution of accelerations, and then of forces, along the height of the structure. The initial value at basement level is the peak ground acceleration that is then amplified as the height increases. This means that the seismic input propagates along the height without damping effects, where each block is independent of the others and the first is independent of the soil.

If the peak ground acceleration, a_g , with an occurrence probability of 2% in 50 years with return period of 2475 years ($a_{g,2475} = 0.28g$, Limit State NC) is assumed, the equilibrium is not verified at any analyzed level and in particular the worst condition is attained in panels between levels +19.0m-+29.0m (especially panel 3Y shown in the lateral view of Fig.24a and in the plan view of Fig.25a). In Fig.25b the regularized geometry of panels between +19.0m and +29.0m is reported. Panel 3Y shows the lowest ratio of stabilizing to destabilizing moment (0.60), so that, in order to achieve safety, additional horizontal forces $\Delta F_{hor} = 1100kN$ in the X direction and $\Delta F_{hor} = 880kN$ in the Y direction are needed. Contribution of existing undamaged steel tie rods has been taken into account considering a maximum working tensile stress of 250MPa.

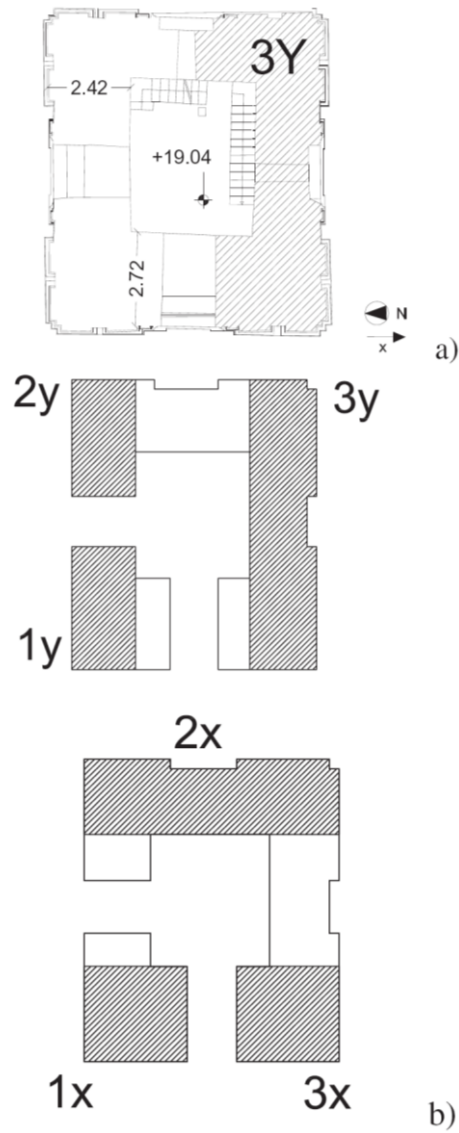
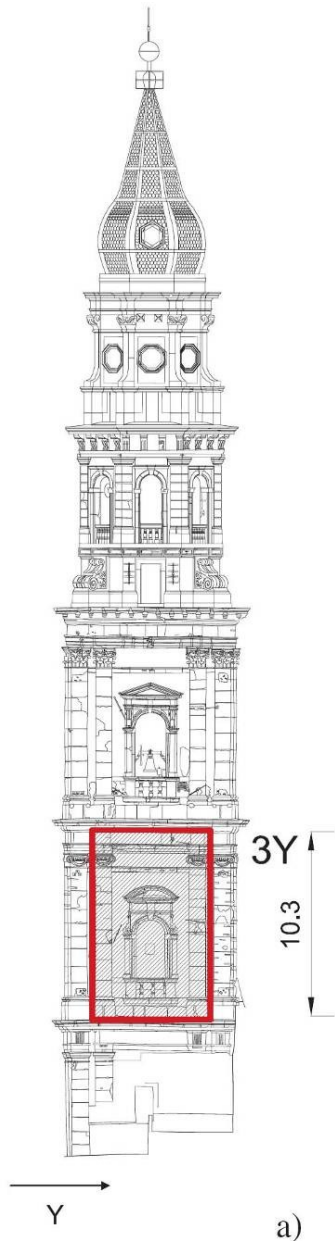


Fig.24. Lateral view of the Tower with panel 3Y evidenced

Fig.25. Tuff panels between +19.0–+29.0 m: 1) original plan view; 2) schematic reproduction of resistant panels in X and Y directions.

At the upper levels, following a similar approach, lower forces are required. The safety condition deteriorates on the assumption that all the chains and steel tie rods used in the walls are ineffective; under this hypothesis the maximum total tensile force required between +19.0m–+29.0m becomes $F_{\text{hor}} = 1830\text{kN}$.

Verifications at the Limit State of Significant Damage (LS SD), performed assuming the peak ground acceleration with an occurrence probability of 10% in 50 years ($a_{g,475} = 0.168\text{g}$) and considering active the existing undamaged chains, showed that only the walls between the 4th (+40.0m) and 5th (+49.0m) floors and between 5th and 6th (+57.0m) floors need additional equilibrating forces of 100kN and 80kN, respectively. In Table 5 the thickness and width of each identified panel between the two following levels are reported and the requested additional tensile forces to satisfy the equilibrium are indicated.

Table 5. Instabilizing loads at the Bell Tower top levels

Panel	Wall thickness (m)	Width (m)	$a_g=0.280g$ F_t (kN)	$a_g=0.168g$ F_t (kN)
<i>Level 3(+19.00m) and 4(+29.00m)</i>				
3X	2.9	3.1	<i>326</i>	— ^a
1X	2.9	3.1	<i>326</i>	— ^a
2X	2	7.7	<i>880</i>	— ^a
2Y	2	3.7	<i>414</i>	— ^a
1Y	2	3.9	<i>456</i>	— ^a
3Y	1.8	9.2	<i>1103</i>	— ^a
<i>Level 4(+29.00m) and 5(+40.00m)</i>				
1X	2.9	3.1	<i>125</i>	— ^a
4X	2.9	3.1	<i>125</i>	— ^a
2X	1.5	3.1	— ^a	— ^a
3X	1.5	3.1	— ^a	— ^a
2Y	1.6	3.7	<i>329</i>	— ^a
1Y	1.6	3.9	<i>88</i>	— ^a
3Y	2.1	3.7	<i>412</i>	— ^a
4Y	2.1	3.9	<i>177</i>	— ^a
<i>Level 5(+40.00m) and 6(+49.00m)</i>				
1	1.8	2.9	<i>253</i>	<i>80</i>
2	1.4	3.5	<i>265</i>	<i>100</i>
3	1.4	3.3	<i>247</i>	<i>90</i>
4	1.6	3.7	<i>310</i>	<i>100</i>
<i>Level 6(+49.00m) and 7(+56.00m)</i>				
0	0.9	2	<i>150</i>	<i>80</i>

Note: Italic font is used to indicate the largest demand force values in both X and Y directions at each level.

^a Not required

5.4 REFERENCES

- [1] OPCM 3431 - Ordinanza del Presidente del Consiglio dei ministri [2005] “*Primi elementi in materia di criteri generali per la classificazione sismica del territorio nazionale e di normative tecniche per le costruzioni in zona sismica*”, Document no.3431 (in Italian).
- [2] Lourenço P.B., 2002. “*Computations on historic masonry structures*”, Progress in structural engineering and materials, 4(3), 301-319.
- [3] SAP 2000 CSI, Design manuals – Version 9.0, Computers and Structures, Inc., Berkeley, California, USA
- [4] DIANA finite elements analysis, User’s manual – Release 8.1 - Element Library, TNO Building and Construction Research, Department of computational Mechanics, A.A. Delft, the Netherlands, 2002a.
- [5] Min.LL.PP, DM 14 Gennaio, 2008. “*Norme Tecniche per le Costruzioni (NTC)*”, Gazzetta Ufficiale della Repubblica Italiana, 29, (in Italian).
- [6] Marcarì G., Manfredi G., Prota A., Pecce M., 2007. “*In-plane shear performance of masonry panels strengthened with FRP*”, Composites – Part B: Engineering, Elsevier, 38, 887-901.
- [7] Augenti N., 2000. “*Il calcolo sismico degli edifici in muratura*”, Casa editrice UTET Libreria Srl, (in Italian).
- [8] DIANA finite elements analysis, 2002b. User’s manual – Release 8.1 - Material Library, TNO Building and Construction Research, Department of computational Mechanics, A.A. Delft, the Netherlands.
- [9] Gentile C., Saisi A., 2004. “*Dynamic-based F.E. model updating to evaluate damage in masonry towers*” Proc. of IV SACH Structural Analysis of Historical Construction, Padova, Italy.
- [10] Zingone G., Valente G., 2005. “*Methodology and techniques for seismic protection of the monumental patrimony, Seismic Prevention of Damage*”, WIT Press Part. VI, Chapter 17.
- [11] Wang D., Haldar A., 1994. “*Element-level system identification with unknown input*”, Journal of Engineering Mechanics, 120(1).
- [12] ICOMOS Recommendations [2005] *International Council on Monument and sites, Recommendations for the analysis, conservation and Structural restoration of Architectural Heritage*, Document approved in the Committee meeting in Barcelona on 15th June 2005.

- [13] DPCM 12/10/2007, Direttiva del Presidente del Consiglio dei Ministri 12/10/2007, 2007. “*Direttiva del Presidente del Consiglio dei Ministri per la valutazione e la riduzione del rischio sismico del patrimonio culturale con riferimento alle norme tecniche per le costruzioni*”, published on Gazzetta Ufficiale della Repubblica Italiana n. 24, 29/01/2008 (in Italian).
- [14] Magenes G., 2000. “*A method for pushover analysis in seismic assessment of masonry buildings*”, *Proc. of 12th World Conference on Earthquake Engineering*, Auckland, New Zealand, CD-ROM.
- [15] Ceroni F., Pecce M., Voto S., Manfredi G., 2009a. “*Historical, architectural and structural assessment of the Bell Tower of Santa Maria del Carmine*”, *International Journal of Architectural Heritage: Conservation, Analysis, and Restoration*, Francis Taylor, Vol. 3, No. 3, 2009.
- [16] European Committee for Standardization, (CEN 2005a). “*Design of structures for earthquake resistance. Part 1: General rules, seismic actions and rules for buildings*”. EN 1998-1:2005, Eurocode 8, Brussels, Belgium.
- [17] Meletti C., Montaldo V., 2007. “*Stime di pericolosità sismica per diverse probabilità di superamento in 50 anni: valori di a_g* ”, Progetto DPC-INGV S1, Deliverable D2, <http://esse1.mi.ingv.it/d2.html> (in Italian).
- [18] European Committee for Standardization (CEN 2005b). “*Design of structures for earthquake resistance. Part 3: Assessment and retrofitting of building*”. EN 1998-3:2005, Eurocode 8, Brussels, Belgium.
- [19] ENV 1993-1-1, Eurocode 3, 2004. Design of steel structures - Part 1-1: General rules for buildings.

Chapter VI

Rehabilitation works

6.1 DESIGN OF SEISMIC THREAT REHABILITATION

This study has showed that according to the value of a_g assumed for safety verifications, the extent of the structural problems is related to both local and global behaviour aspects. Particularly the Tower is not safe with reference to the local behaviour both at the Limit State of Significant Damage and Near Collapse. On the contrary with reference to the global behaviour, only at the LS of NC in the Y direction the Tower doesn't result safe (minimum safety factor 0.77).

Furthermore the retrofitting design should lead to a seismic upgrading of the Bell Tower respectful of the “low impact” requirements provided for masonry heritage buildings (ICOMOS Recommendations, 2005) [1] and representing the most suitable balance between the accepted safety level and the minimum interference on the architectural order of the structure. This means that the optimal and well-balanced solution will consist in the design of a retrofitting intervention aiming at solving only the local equilibrium problems. Therefore in order to have the requested additional stabilizing forces, to avoid local out-of-plane mechanisms and to warrant a global “box” behaviour of the structure, the

upgrading intervention should be represented by adding new tie rods made of innovative materials for panels between fourth and fifth floors and fifth and sixth floors, Cosenza and Iervolino, 2007 [2]).

The rehabilitation work foresees the application of tie bars in substitution of the actual steel damaged ones, in order to pick up the assessed normal loads and to guarantee the necessary connections among the orthogonal walls and secure the global behaviour of the structure under seismic loads.

In particular a key requirement was to reduce as much as possible the invasively effect of the stabilization work, in accordance with the recent “Guidelines for the assessment and reduction of the seismic threat to the cultural heritage structures correlated to the construction standards” [3] as for OCPM 3431 [4]. Table 1 shows the normal loads necessary to verify the balance condition of each single panel vs out-of-plane mechanisms.

Table 1. Verification of the balance vs the tilting loads

Level [m]	Panel	Normal load [t]
+19.0-+29.4	3X	0.0
+19.0-+29.4	1X	0.0
+19.0-+29.4	2X	0.0
+19.0-+29.4	2Y	0.0
+19.0-+29.4	1Y	0.0
+19.0-+29.4	3Y	0.0
+29.4-+40.0	1X	0.0
+29.4-+40.0	4X	0.0
+29.4-+40.0	2X	0.0
+29.4-+40.0	3X	0.0
+29.4-+40.0	2Y	2.0
+29.4-+40.0	1Y	0.0
+29.4-+40.0	3Y	1.0
+29.4-+40.0	4Y	0.0
+40.0-+49.9	1	8.0
+40.0-+49.9	4	10.0
+40.0-+49.9	2	9.0
+40.0-+49.9	3	10.0
+49.9-+57.0	1	8

Walls between levels +40.0m and +49.0m are presently connected by two systems of four ties represented by steel bars (diameter of 40mm). The first four bars are positioned orthogonally to each other at +41.7m (Figs.1a-b, 2), have an external anchorage made of a vertical steel bar and show no significant corrosion problems, so that their contribution has been taken into account in the structural checks. Furthermore in situ tests highlighted that they are subjected to tensile stresses ranging between 41.5MPa and 71.5MPa.

At +48.3m the second system is made of four steel bars (diameter 40mm) placed orthogonally (Figs.1a-b and 2). They have an external anchorage made of a horizontal steel bar. As previously described, those ties are characterized by evident corrosion phenomena and don't seem to bear any load as confirmed by tensile stresses measured in two of them; therefore their contribution has not been considered in the checks. At a level of +55.6m there is only one system of six orthogonal steel bars (average diameter of 35mm) (Figs.1a-b,3) characterized by evident corrosion phenomena and damaged conditions of the anchorage; therefore these ties have not been considered in the checks .

The four tie rods in a west-east direction (along Y axis) are coupled two by two. Each group of two has an external anchorage made of a steel squared plate (side 400mm). In the other direction, two single rods with a similar anchorage are present. All these ties have an intermediate blocking system used in the past probably to preload them (Fig.5). In situ tests evidenced that: the two north-south ties detached from the walls are unloaded; those most corroded in a west-east direction bear a stress of about 100MPa; the others are subjected to tensile stresses ranging between 26MPa and 46MPa. Appendix X summarizes the distribution of the existing bars and the assessment of their functional status.

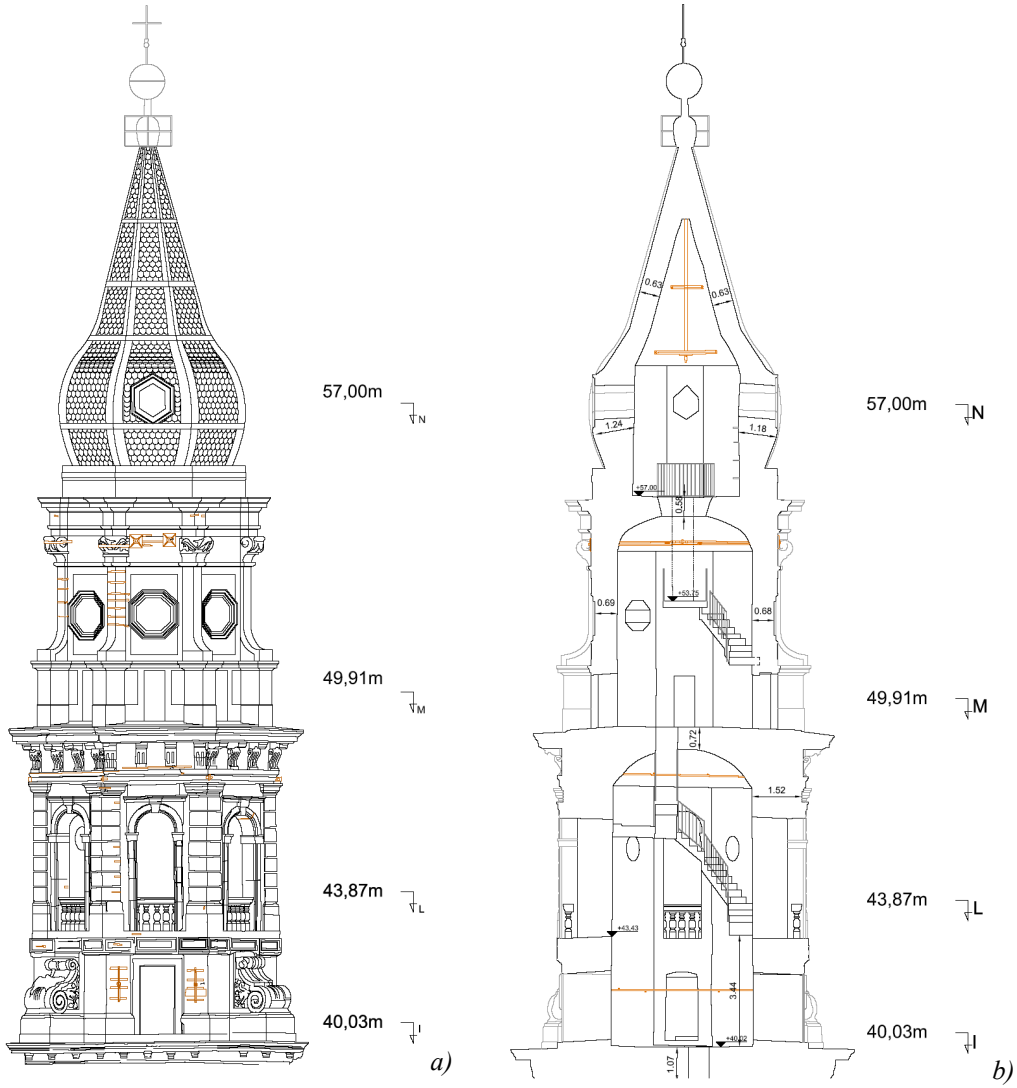


Fig.1. a) West view of upgraded portion of Tower; b) Vertical north-south section



Fig.2. Steel tie bar system +41.7m



Fig.3. Steel tie bar system +48.3m



Fig.4. Steel tie bar system +55.6m

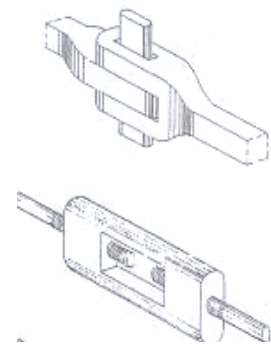


Fig.5. Blocking system

6.1.1 Design and installation of the new ties

Based on the results of the numerical analysis, tie-bars were located in correspondence of two of the four evaluated levels. In order to realize a low invasive rehabilitation work that in this case also represents the final demonstration of a multidisciplinary study on the Bell Tower (Ceroni, Voto et al. 2009a; 2009b) [5&6] according to recent indications on historical masonry heritage structures (ICOMOS 2005; DPCM 2008) [1&7]. It was planned to remove the existing damaged ties and replace them with new ties arranged according to the same layout and using the same existing holes. In particular to guarantee higher durability of the intervention the necessary tie-bars have been manufactured in GFRP (Glass Fiber Reinforced Plastic). This material is characterized by a good chemical inertia, elevated mechanical properties and reduced unit weight (the ratio between its tension strength and specific gravity may be as high as seven times the correspondent specific property of steel). Additionally the utilization of these bars drops down the environmental sensitivity problems the existing bars were affected by in the past.

6.1.1.1 Choice and design criteria of innovative material for new ties

The observed damage status in the existing steel ties (Fig.6) has clearly underlined the need of realizing new ties made of materials having high durability and chemical inertia to corrosion phenomena, which are favourably increased in the windy and seaside environment characterizing the Bell Tower. The corrosion phenomena detrimentally affecting steel elements govern the effective life of a structure and its maintenance costs. In structural engineering durability this property is related to the effective life of the construction and is strictly influenced by the conditions of the working environment. In the case of cultural heritage masonry buildings the issue to warrant a high durability is more relevant due to the intrinsic value of the construction that has to be preserved as long as possible. So preferably materials with higher durability should be used. Therefore, it was planned to realize the new ties at two levels in

the Bell Tower, using GFRP materials for their superior mechanical and chemical properties and for the reduced weight, making both transportation and installation operations easier. GFRP ties have higher durability (Ceroni et al. 2006) [8] compared to those metallic ties usually adopted in ancient masonry buildings (Necevska-Cvetanovska and Apostolska 2008) [9] and often seriously damaged by corrosion phenomena. The selected upgrade solution complies well with the philosophy of “minimal intervention–maximal protection” (IZIIS, RZZSK, GCI 1991–1994) [10,11&12]; (ICOMOS, 2005: Linee Guida, 2005) [1&3]. A similar philosophy has driven the design of the strengthening of a masonry synagogue using innovative materials as reported by Paret et al. (2008) [13].



Fig.6. Problems of tie-bars detachment

Usually GFRP elements show a linear elastic behaviour until failure. For GFRP materials the Young modulus varies in the range 15.000-40.000MPa and the tensile strength is variable between 200MPa and 700MPa. Considering that the unit weight of these materials is very low (about 17-20kN/m³), it can be observed that the ratio of tensile strength to unit weight can also be 7-8 times greater than steel. A critical aspect for applications in which the GFRP elements

should be pre-stressed is related to the end anchoring system, due to the low shear strength.

For application to the Bell Tower, a specific system of ties and end anchorage has been designed. This system is made out of Glass Fibre Reinforced Plastic (GFRP) tie-bars and an anchoring end fitting made in steel and aluminium to let the tie-bar accomplish their connecting action under loads that tilt the walls out of their plane. To make transportation and assembling of the ties at the higher levels of the Tower easier (+48.3m and +55.6m), each tie was made of GFRP laminates having a square cross section of 40 x 9mm (Fig.7) in order to reduce the inertia of the section and make the arrangement of laminates into rolls possible.

Due to the building yard convenience, it's proposed to make the tie-bars by coupling rectangular shape 30 x 6mm bars that will be made available in 2.0m diameter rolls of predefined length. This way the maximum weight of each roll is around 5kg and this simplifies the handling and the positioning. Laminates are made of epoxy resin fibre reinforced with glass roving (fiber volume percentage of 65%) and one or more of them constitute a single tie.

The anchorage system (Figs.7-8) is realized at both ends of the rod by an aluminium header (red coloured in Fig.7) with a conic drilling accommodating a wedge shaped aluminium element (light blue coloured in Fig.7) that will block the GFRP laminates of the tie-bars. At both ends of the tie a squared stainless steel plate (40.0cm side for 5th level and 30.0cm side for the 6th one) made of AISI 304 corrosion resistant steel (CRES) is applied with four stainless M16 steel bolts connecting the anchorage system to the masonry wall. Those plates allow a distributed transmission of the force that the tie rods should provide exceptionally under seismic actions and to warrant in serviceability conditions the uniform transfer of the preload imposed at the time of installation. The idea to apply a light preload to the tie rods came from the need of aligning the laminates during the installation and warrants an active constraint effect to the walls also in service conditions.

To preload the tie-bars, the anchorage system provide four M16 CRES (Corrosion Resistant Steel) bolts on one side, fastened to correspondent nut

welded on an opposite plate (dimensions 150 x 150 x 10mm). The application of a torque to the bolts by a dynamometric wrench transfers tension load to the bars and to the Fibre/Glass composite bars. The existing steel bars in correspondence of elevation +49.0m and +56.0m were removed.

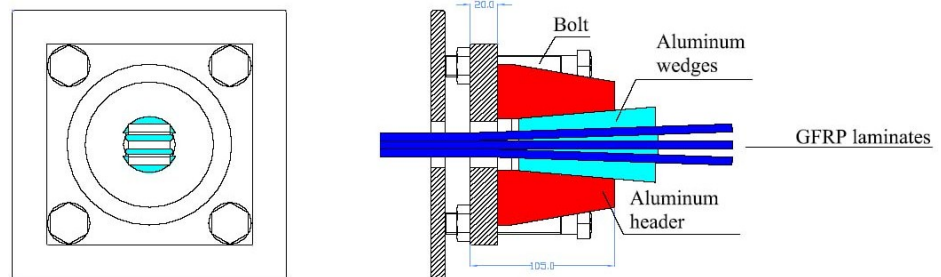


Fig.7. Anchorage system for used GFRP ties



Fig.8. Inox steel anchorage head

This removal was accomplished by cutting the bars inside, removal of the outside anchorage (either longitudinal bar or plate) and subsequent sliding of the bars.

Preliminary tests showed that this type of anchorage did not perform well if the tie is made of only one laminate. For this reason, ties with a minimum of two

laminates have been considered. To verify the stability of end fitting anchoring and the resistance of the GFRP laminates, laboratory tests were accomplished on tie bars made out of either two or three laminates. The failure mode was always by tension stress in the GFRP laminates, confirming the effectiveness of the anchoring system to avoid sliding of the bars. Based on these preliminary tests the above mentioned laminate thickness of 40mm was determined as optimal to prevent crushing due to localized stresses at the anchorage. Therefore, two systems made of two and three laminates were tested in tension to check both the tensile strength of laminates and the slipping strength of the anchorage. In each experimental test tensile failure of glass fibres was observed without slipping of the anchorage.

The safety failure resistance coefficient of the glass fibres indicated by the manufacturer has been set in accordance with the Instructions CNR DT 203/2006 [14]. In particular the partial safety factor is 1.5 while the environmental drop off factor has been set to 0.8, corresponding to a dry exposure condition for glass fibres, with a global safety factor of 1.9. There is no drop off due to long endurance loads, so the corresponding conversion factor was assumed to be equal to 1.0. It's assumed that the bars are not subjected to loads extended in time. In fact they are loaded in presence of seismic actions, do not carry permanent loads. The design failure loads resulted is being equal to 250kN and 160kN for systems with three and two laminates, respectively. These two systems have been designed to satisfy the checks at Levels 5 and 6. The design has been carried out based on the following criteria:

- Have a minimum of two laminates per tie;
- Thickness of each laminate of 40.0mm;
- For ties with two laminates, ensure that one laminate is able to carry the entire design load;
- For ties with three laminates ensure that if one is not effective, the other two would be able to withstand the design load.

Criteria 3 and 4 were used in order to be conservative with respect to a new system for which long-term data on the performance are not yet available and

also considering the importance of the structure. It is noted that the major influence on the cost is due to the anchorage rather than to the number of laminates; therefore, for this case to be conservative it was not determined to have a significant cost increase. Based on the above criteria:

- To connect panels between +40.0m-+49.0m a minimum tensile load of 10t is required for each new tie rod (Table 1), a system of four orthogonal elements, each of them made of three GFRP laminates with a design load of 25t, has been planned to replace the existing ones just below the fifth floor(Fig.9, Fig.10).
- Analogously between +49.0m-+56.0m the minimum required load for each panel is 8t (Table 1), so that four orthogonal elements made of two GFRP laminates (design load 16t) will substitute the existing six ones just below the sixth floor. (Fig.9, Fig.11).

It's clear that the design strength of the installed tie bars plentifully overestimate the loads required by the balance analysis of the panels: in fact we preferred to utilize bars made by more than one laminate. This was chosen to cut down the risk of laminates sliding within the anchorage block and to avoid the efficacy of system relying on one element only. Elevated safety coefficients were assumed also to cover the uncertainties associated with the installation procedures applied on site.

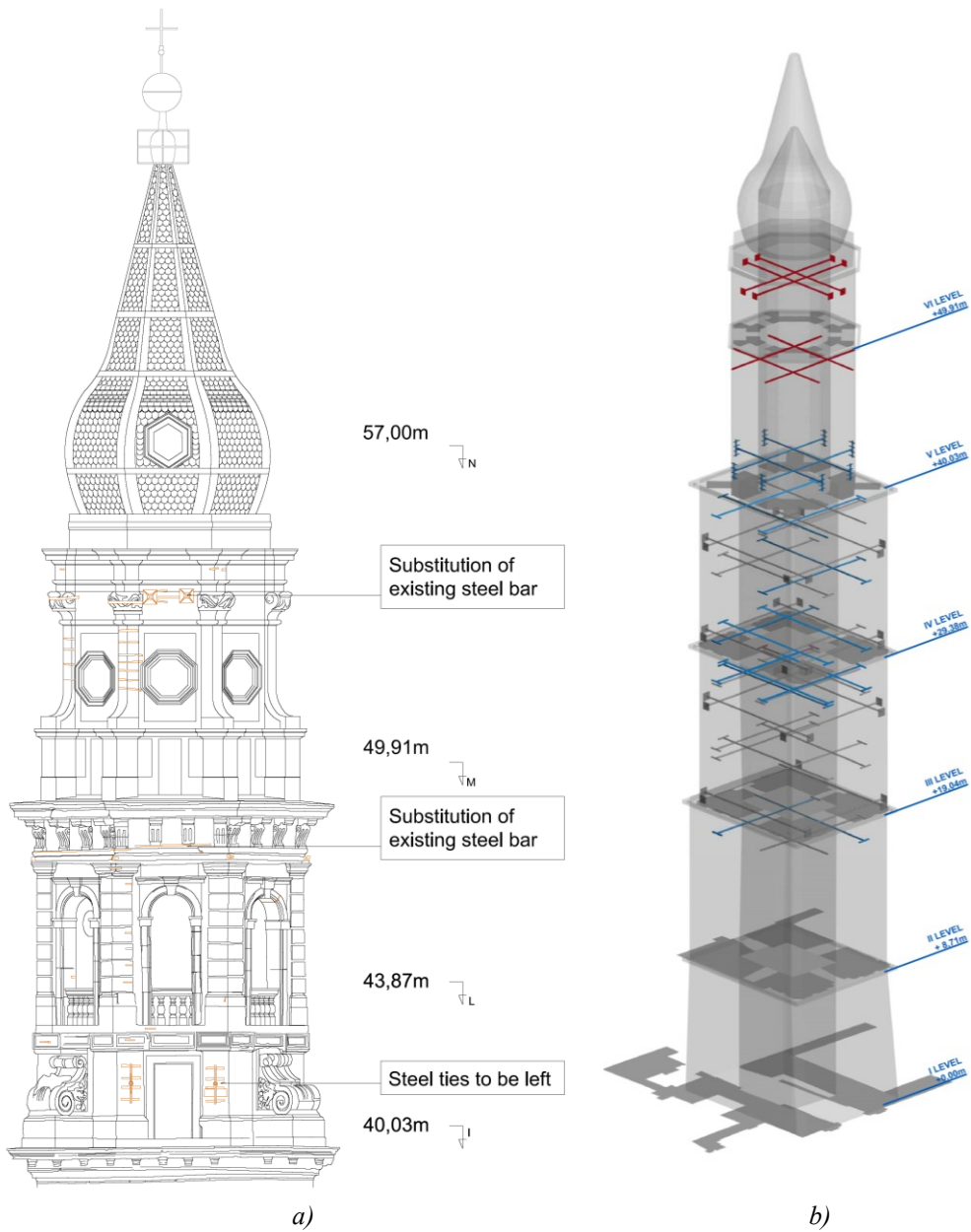


Fig.9. a). West view of upgraded portion of Tower; b) 3D model representative of the tie-bar network system present in the Tower. The new Glass Fibre bars are highlighted in red.

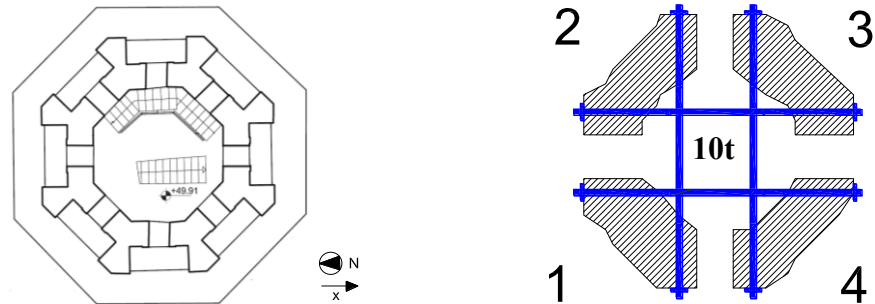


Fig.10. Plan lay out of the bar system to locate under the fifth frame almost at elevation +49.0m, in substitution of the pre-existing bars

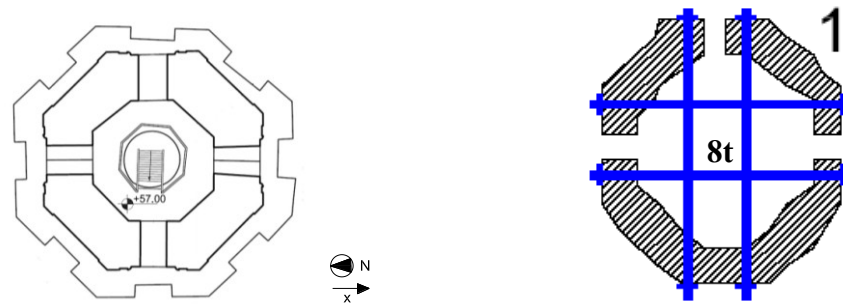


Fig.11. Plan lay out of the bar system to locate under the sixth frame almost at elevation +55,6m in substitution of the pre-existing tie-bars

6.1.1.2 The scaffolding

Following the design of the rehabilitation work of the Carmine Bell Tower, the building yard was set up. In particular it has been mounted an outside scaffolding to allow the access to the levels where to implement the rehabilitation work (Fig.12). It has been mounted also an inside scaffolding (Fig.13) to be able to work at the different levels of the existing bars. Before putting in place the new glass fibre bars, the existing ones in steel were removed at level +49m and +56m. The removal was accomplished cutting the bars inside, removing the outside anchorage (either longitudinal bars or plate) and then slipping off the bars.

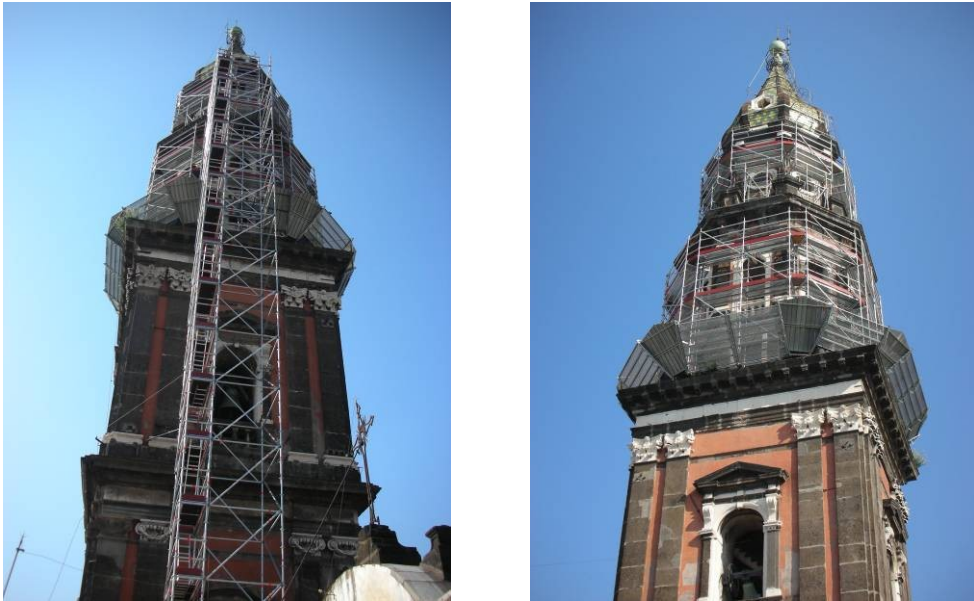


Fig.12. Outdoor scaffolding set up on the four sides of the Bell Tower



Fig.13. Scaffolding set up inside the Bell Tower

6.1.1.3 Sequence of Installation of New Ties

After internally cutting the existing steel bars, the external anchorages made of longitudinal steel bar (at +48.3m) or of a steel plate (at +55.6m) were removed (Fig.14a) and then the bars pulled out. Then, the new ties have been inserted in the same holes of the old ones (Fig.14b). The portions of the ties passing through the walls have been protected by a plastic tube (Fig.14c) to avoid the problem that the mortar, later used to fill the holes and refine the wall surfaces, could be in contact with the ties; this allows the tie to slip along the tube in the case of reloading interventions (Fig.14d). Once the ties have been inserted into the holes, the anchorage systems were positioned at both ends. First the squared stainless steel plates have been applied on the external masonry walls (side 40mm for the fifth level and 30mm for the sixth level, Figs.15a-b). On the fixed edge of each tie-bar, the two aluminium wedges were first put into the headpiece. Then aluminium straps were put between the laminates to separate them and apply a shimming avoiding them to slip within the headpiece. The bars were snubbed with a dynamometric wrench applying torque load to the four bolts alternatively (Fig.15f). The preload (variable in the range 30MPa–40MPa corresponding to about 10% of the ultimate strength of the ties given by the experimental test) was applied to each tie. With respect to this last aspect, it is observed that, when the damaged existing steel ties were cut, they suddenly shortened, indicating the presence of a certain level of tensile stress probably due to the reduction of cross section due to corrosion and to the tendency of the walls at higher levels to move out-of-plane.

The procedure of assembling and snubbing the locking system is reported in Figs.15 (a-g). Finally, in order to protect the ends of each tie, an aluminium covering cup (Fig.15h) was installed upon completion of the preloading procedure; this was done to prevent the cuts at the ends from being directly exposed to fibers in an external environment and then determine the detrimental effects related to the loss of integrity of the interface between the resin and fibers (Ceroni et al. 2006) [7]. The final internal view of the installed ties is

shown in Fig. 15i.

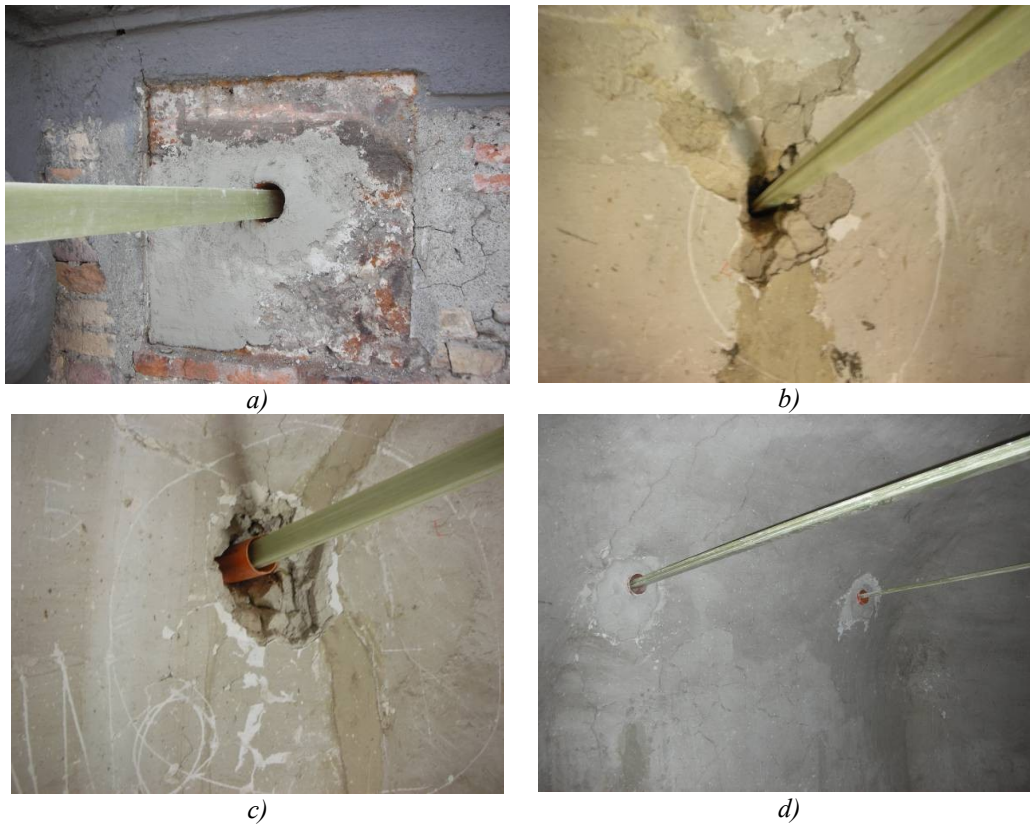


Fig.14. Installation of the new tie-bars: a)removal of the eternal existing steel plate; b) positioning of the new tie bar in the existing holes; c) positioning of the plastic tube to protect the ties; d) hole finishing



a)



b)



c)



d)



e)



f)



g)



h)



i)

Fig.18. Application of the anchoring end fitting and pre-load : a-e) Installation of the end fitting; f) Pre-load application ; g) tie-bars snubbing; h) Final view of the end fitting .

6.1.1.4 Monitoring system

Particularly for cultural heritage buildings proper management is required in order to perform long-term maintenance and conservation of the historical, cultural, and architectural value (ICOMOS 2005, DPCM 2008) [1 and 6]. For this reason, after the realization of an intervention, both the efficiency of the system realized and the response of the structure to the usual and exceptional actions should be checked over time. The effectiveness of a rehabilitation work could decrease with time due to phenomena of decay or relaxation in the constituent materials. Additional reasons for that decrease could be dependent on modifications in the loads acting on the structural elements due to wrong

operations or collapse of components of the structure for accidental event. In this case situations even worse than the original ones could be originated and the rehabilitation work could be not effective, even harmful. Monitoring the stabilization system after its installation may become a useful tool to assess in the short and long period the answer of the structure to the operation and its effectiveness versus normal and accidental actions. Indirectly it's possible to monitor in this way the stresses which the structure is subjected to in the years and evaluate the possibility to accomplish a new rehabilitation work with corrective actions.

For the Bell Tower of “Santa Maria del Carmine” a basic monitoring of the intervention was designed with the objective of checking the stress level in the GFRP ties over time starting from the snubbing values set up in the initial phase of the assembly. Therefore, prior to preloading, four strain gauges have been glued on the external laminates of each tie. The measured strain during the preloading phase allowed calculating the corresponding stress under the assumption of linear elastic behaviour of GFRP. Stress and related force values were then checked and compared to those obtained from the values of the torque key. Considering the uniformity of the laminate surfaces and loading conditions along them, strain gauges seemed to be the best solution to monitor the ties over time, starting from the initial value of the preload stress, in order to check long-term phenomena or anomalous load conditions. In fact the analysis of the existing bar showed the presence of corrosion phenomena that in some cases caused a reduction of the cross section with a drop in the loading capacity of the bar in presence of horizontal actions coupled to disjunctions of the bar in correspondence of the anchorage points or wall interfacing. This is the reason why the intervention has been planned with a partial substitution of the existing decayed steel bars with fibreglass ones, and integration with glass fiber bars where the preexisting ones were not sufficient to guarantee the stability of the walls supposed not being connected in the presence of horizontal actions. The new bar have been applied with a light pretension load to guarantee them to be working also in the presence of a light horizontal force. Monitoring the

tensional status which the bars will be subjected to, is a useful tool to evaluate their efficiency in the time.

The monitoring of the tensional status in the bars is realized through the measurements of the deformations. In fact the glass fibre material has an elastic linear behaviour up to failure. So through the knowledge of the elasticity module, the correspondent tensional status can be easily assessed. Deformations are determined through electrical extensometers that return local deformation values where applied. With glassfibers bars, extensometers appear to be particularly suitable because of the low surface roughness that facilitate their application and due to the uniformity of tensional status along the bars. This guarantees the reliability of the results even with a limited number of measurements. In correspondence of the two levels where the rehabilitation work was accomplished, each laminate the tie bars are made of, was instrumented with two extensometers (except the central one of the tie realized with three laminates) before snubbing (Figs.16a-b). The measurement of the deformation during the snubbing operation allowed to evaluate (under the assumption of linear elastic behaviour with a Young Modulus $E= 40.000\text{MPa}$), the applied tension that will be the reference value for the measurements that will follow in the years. For each one of the two levels where the intervention will be made, the bars to add or to substitute won't be less than four. Consequently for each level it's foreseen to have 16 measurement points. To that purpose it's foreseen to install signal acquisition modules, each one capable to acquire many channels contemporary. The elongations measurements can be coupled environmental data reading, like temperature and humidity level. In fact the intervention will be accomplished in a partially open structure where climatic excursions may be significant during the following seasons, so to cause thermal deformation in the bars. The so designed monitoring trough strain gauges have been connected to an electronic data acquisition unit (Fig.16c), scheduled to register all the measurements four times a day at the same time and to record them on an internal memory card, from which the data can be periodically downloaded.

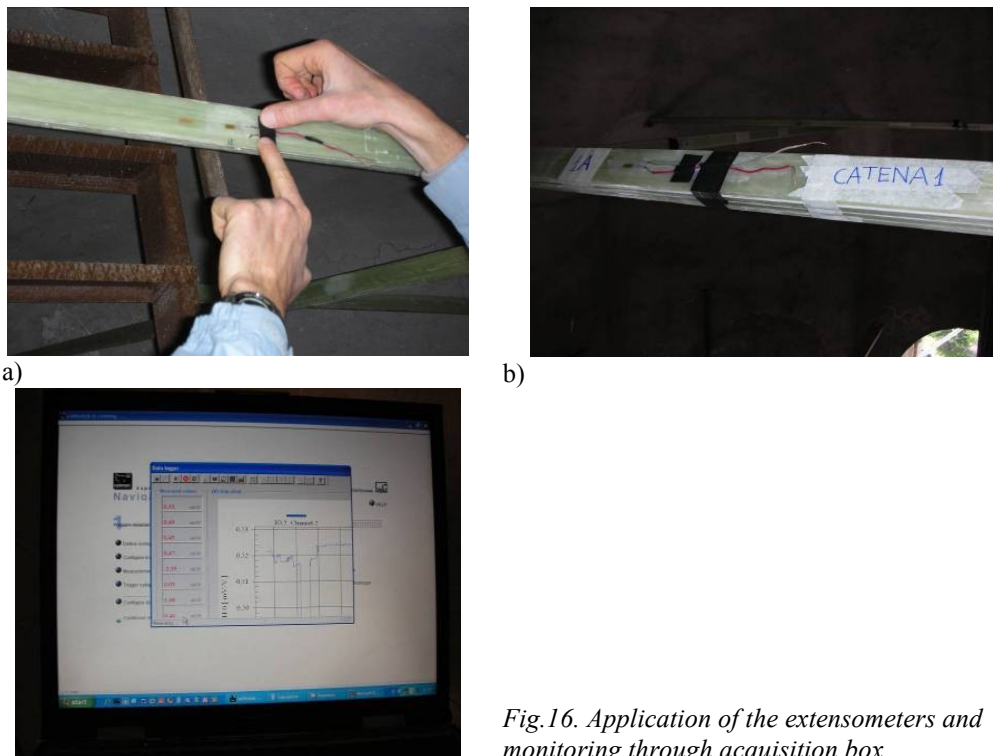


Fig.16. Application of the extensometers and monitoring through acquisition box

Furthermore, the acquisition unit in the tower is connected to a Global System for Mobile (GSM) connections modem that allows implementing an alert service message system that, if a strain gauge overcomes the set threshold, it sends a warning message to a mobile phone or a PC connected to a GSM modem. Measurements of strain along the laminates have been coupled to measurement of temperature at the two floors where the new ties have been installed in order to check if daily or seasonal temperature variations could cause thermal strain in the ties, which in this case are installed in an “open” structure. Since the bar intervention is meant to adapt the structure to support possible seismic actions, that by definition have an accidental character, the

sampling interval of the measurements can be conveniently assumed to be daily.

6.2 RESTORATION OF NON STRUCTURAL ELEMENTS

Possible rehabilitation works (Fig.16) to eliminate the decay phenomena shown on the outside facing of the Carmine Bell Tower (Table 1, Chapter III) are indicated in the following:

Materials	Symbology	Phenomenon description
Peperino		Fault
Planned Operations		
CLEANING	Preparation by thorough cleaning with small tools and sorghum brushes. Following spray of atomized de-ionized and/or distilled water at low pressure.	  
CONSOLIDATION	A global consolidating treatment will be applied by low pressure sprinkling highly penetrating acrylic resins.	 
PROTECTION:	Final protecting treatment by brush application of a silicon water-repellent resin.	 
Materials	Symbology	Phenomenon description
Marble		Detachment
Planned Operations		
CLEANING	Preparation by thorough cleaning with small tools and sorghum brushes. Following spray of atomized de-ionized and/or distilled water at low pressure.	  
CONSOLIDATION	A global consolidating treatment will be applied by low pressure sprinkling highly penetrating acrylic resins.	 
PROTECTION:	Final protecting treatment by brush application of a silicon water-repellent resin.	 
Materials	Symbology	Phenomenon description
Plaster		Detachment
Planned Operations		
CLEANING	Thorough cleaning with wiping rags, sorghum brushes is accomplished. In case, a local cleaning will follow using small tools. At the end powder and water spray will be removed by vacuum suction.	  
CONSOLIDATION	Surfacing and styling of the support joints will be made. A global consolidating treatment will follow by low pressure	  

	sprinkling of highly penetrating acrylic resins.			
PROTECTION:	A final protecting treatment will be made by brush application of a water repellent silicon resin.			

Materials	Symbology	Phenomenon description
Peperino		Presence of vegetation

Planned Operations

CLEANING	The elimination of the infesting weed will start with a controlled eradication (i.e. mechanical eradication that doesn't cause any alteration to the masonry materials). Spray application of a bio cider compatible with the support. A thorough cleaning with small tools, rags and sorghum brushes will follow. Final vacuum suction of all residues.			
PROTECTION:	Final protecting treatment by brush application of a silicon water-repellent resin.			

Materials	Symbology	Phenomenon description
Peperino		Patina

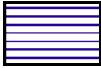
Planned Operations

CLEANING	A generalized cleaning operation will be implemented by low pressure spraying of atomized de-ionized and/or distilled water. More persistent debris will be removed by small tools. Residues will be eliminated by vacuum suction. Plentiful rinsing will follow.			
PROTECTION:	Final protecting treatment by brush application of a silicon water-repellent resin in water solution.			

Materials	Symbology	Phenomenon description
Peperino		Surface deposit

Planned Operations

CLEANING	A generalized cleaning operation will be implemented by low pressure spraying of atomized de-ionized and/or distilled water. More persistent debris will be removed by small tools. Residues will be eliminated by vacuum suction. Plentiful rinsing will follow.			
PROTECTION:	Final protecting treatment by brush application of a silicon water-repellent resin in water solution.			

Materials	Symbology	Phenomenon description
Marble		Surface deposit
Planned Operations		
CLEANING	A generalized cleaning operation will be implemented by low pressure spraying of atomized de-ionized and/or distilled water. Residues will be eliminated by vacuum suction. Plentiful rinsing will follow.	  
PROTECTION:	Final protecting treatment by brush application of a silicon water-repellent resin in water solution.	  
Materials	Symbology	Phenomenon description
Plaster		Tie-bar and strand sockets, brackets
Planned Operations		
CLEANING	A generalized cleaning operation will be accomplished by brushing and sanding. Linking and puttying of cracks and/or joints.	  
PROTECTION:	Final protection is supposed to be brush applied rust preventer based on polyurethane resin because of its high elastic characteristics, chemical and mechanical resistance.	
Materials	Symbology	Phenomenon description
Peperino		Cracking
Planned Operations		
CLEANING	A generalized cleaning operation will be implemented by low pressure spraying of atomized de-ionized water.	  
CONSOLIDATION	Localized puttying of small cracks or fissures by suitable knives and carbide lime mortar charged with acrylic resin, marble powder and micron size silica. Generalized consolidation by brush application of acrylic resins.	
PROTECTION:	Final protection treatment by brush application of a water repellent silicon resin in water solution.	

Materials	Symbology	Phenomenon description
Marble		Cracking
Planned Operations		
CLEANING	A generalized cleaning operation will be implemented by low pressure spraying of atomized de-ionized water.	   
CONSOLIDATION	Localized puttying of small cracks or fissures by suitable knives and carbide lime mortar charged with acrylic resin, marble powder and micron size silica. Generalized consolidation by brush application of acrylic resins.	
PROTECTION:	Final protection treatment by brush application of a water repellent silicon resin in water solution.	
Materials	Symbology	Phenomenon description
Peperino		Deformation
Planned Operations		
CLEANING	After the removal of stones, a thorough cleaning operation of the substrate must be accomplished by rags, sorghum brushes. In case it may follow a localized cleaning operation by small tools. Vacuum sucking of powder and sprayed water.	        
CONSOLIDATION	Surfacing and styling of the support joints will be accomplished. After that a consolidating global treatment will be applied by low pressure sprinkling of highly penetrating acrylic resins.	
PROTECTION:	Final protection treatment by brush application of a water repellent silicon resin in water solution.	

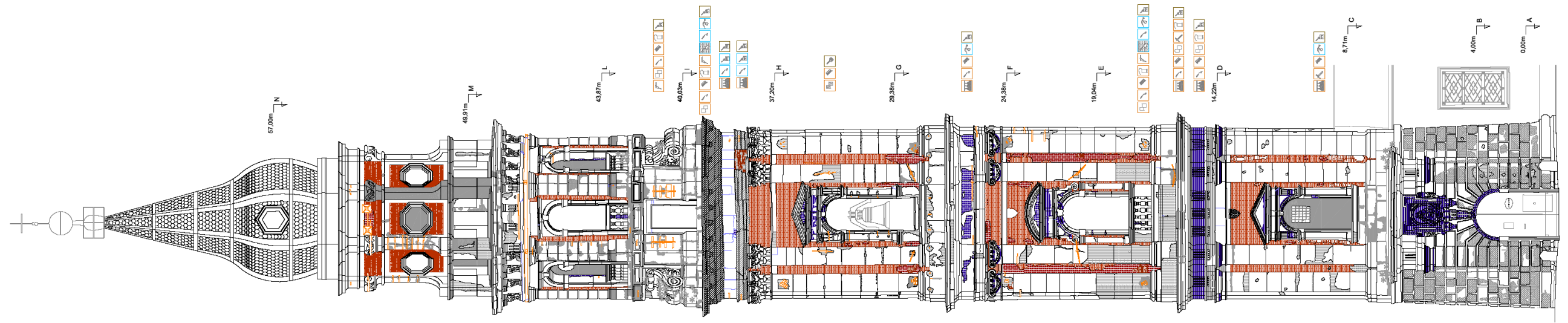


Fig.16. Different cases of decay

6.2 REFERENCES

- [1] ICOMOS Recommendations, 2005. *International Council on Monument and sites, Recommendations for the analysis, conservation and Structural restoration of Architectural Heritage*, Document approved in the Committee meeting in Barcelona on 15th June 2005.
- [2] Cosenza E., Iervolino I., 2007. "Case Study. Seismic retrofitting of a medieval bell tower by FRP", *ASCE Journal of Composites for Construction*, Vol. 11, No. 3: 319-327, 2007.
- [3] *Linee Guida per la valutazione e riduzione del rischio sismico del patrimonio culturale con riferimento alle norme tecniche per le costruzioni*, Luglio 2006 (in Italian).
- [4] OPCM 3431, 2005. Ordinanza del Presidente del Consiglio dei ministri - *Primi elementi in materia di criteri generali per la classificazione sismica del territorio nazionale e di normative tecniche per le costruzioni in zona sismica* (in Italian).
- [5] Ceroni F., Pecce M., Voto S., Manfredi G. 2009a. "Historical, architectural and structural assessment of the Bell Tower of Santa Maria del Carmine". *Int. J. Archit. Heritage: Conservation, Analysis, and Restoration*, in press.
- [6] Ceroni F., Pecce M., and Manfredi G., 2009b. "Modelling and seismic assessment of the Bell Tower of Santa Maria del Carmine: Problems and solution.". *Neurosci. Res.* (N Y), in press.
- [7] Direttiva del Presidente del Consiglio dei Ministri, DPCM 2008. "Direttiva del Presidente del Consiglio dei Ministri per la valutazione e la riduzione del rischio sismico del patrimonio culturale con riferimento alle norme tecniche per le costruzioni" Rome (in Italian).
- [8] Ceroni F., Cosenza E., Manfredi G., and Pecce M., 2006. "Durability issues of FRP rebars in reinforced concrete members". *Cem. Concr. Compos.*, 28(10), 857–868.
- [9] Necevska-Cvetanovska G., Apostolska R. (2008). "Consolidation, rebuilding and strengthening of St. Clement's church, St. Panteleymon, Plaoshnik, Ohrid". *Eng. Struct.*, 30(8), 2185–2193.
- [10] Institute of Earthquake Engineering and Engineering Seismology (IZIIS), 1991–1994. "Seismic strengthening, conservation and restoration of churches dating from the Byzantine period (9th–14th century) in Macedonia". First phase of investigations Vol. 1–6, Rep. No. ISIIS 500-76-91/(1-6).
- [11] Republic Institute for Protection of Cultural Monuments (RZZSK), 1991–1994. "Seismic strengthening, conservation and restoration of churches dating from the Byzantine period (9th–14th century) in Macedonia". Second phase of investigations Vol. 7–10, Rep. No. ISIIS 92-71/(7-10).

- [12] Getty Conservation Institute (GCI). “*Seismic strengthening, conservation and restoration of churches dating from the Byzantine period (9th–14th century) in Macedonia*”. Third phase of investigations Vol. 11–12, Rep. No. ISIIS 94-68/(1, 2), 500-76-91/(1-6).
- [13] Paret T. F., Freeman S. A., Searer G. R., Hachem M., Gilmartin U.M. (2008). “*Using traditional and innovative approaches in the seismic evaluation and strengthening of a historic unreinforced masonry synagogue*”. Eng. Struct., 30(8), 2114–2126.
- [14] CNR DT 203-2006, “*Istruzioni per la Progettazione, l’Esecuzione ed il Controllo di Strutture realizzate con Calcestruzzo armato mediante Barre di Materiale Composito Fibrorinforzato*”. (in Italian).
Council National Research (CNR 2006). “*Guide for the design and construction of concrete structures reinforced with fiber-reinforced polymer bars*”. CNR DT 203-2006, (<http://www.cnr.it/sitocnr/Englishversion/CNR/Activities/RegulationCertification.html>).

Chapter VII

Conclusion

The activities developed in this work suggest a typical procedure to approach the analysis of monumental buildings applicable to masonry structures made of different materials, independently of their location. The knowledge and analysis procedure followed for the Bell Tower of “Santa Maria del Carmine” to design and install a strengthening structure, represents an example of the multidisciplinary approach necessary to rehabilitate heritage structures. In fact this work implies synergies among complementary expertise to better this work from multiple standpoints. Historical inquiries, geometrical and material surveys, damage assessment and in situ tests must be developed in parallel to define the structural configuration, inclusive of the component materials and their assembling and to assess the global behaviour under static and dynamic actions. The study of the Tower showed the paramount role played by historical, archival, and architectural research to investigate the vicissitudes which the structure was subjected to, the ancient construction techniques and building materials and the interventions made in the past. These inquiries, associated with information from visual observation, surveys, and in situ tests, allow obtaining a well organized framework of understanding. The design of the upgrading work is the last step of a detailed study of the construction,

developed through several in situ investigations and theoretical inquiries by 3D finite-element modelling.

The seismic analysis of the Bell Tower addressed the following issues, typical of heritage masonry buildings:

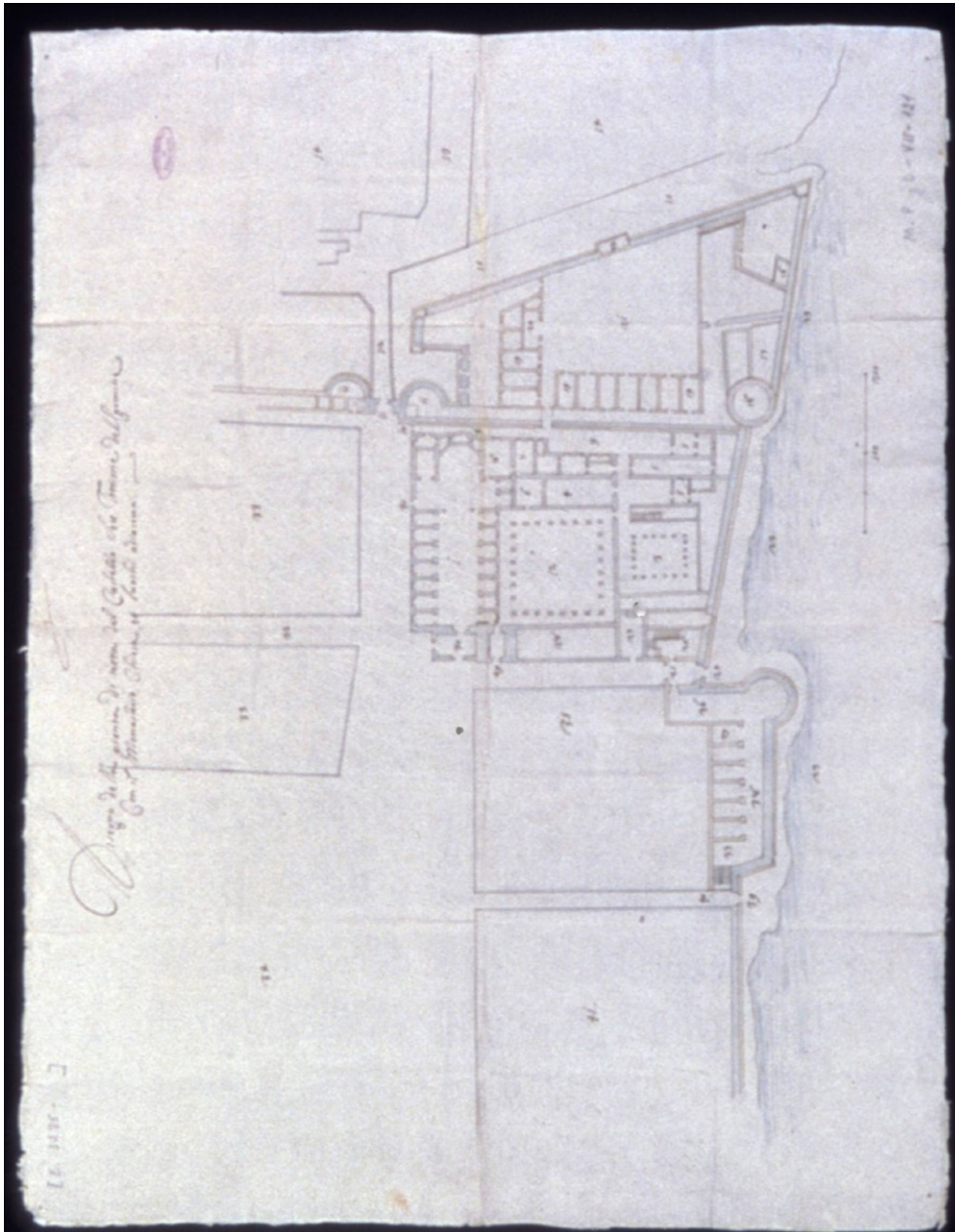
- in situ tests and surveys needed to identify the mechanical properties of the masonry and to define dimensions, shape and constraint conditions of the structural elements;
- experimental vs. theoretical dynamic identification that is useful to assess the constraint conditions and the elastic parameters in order to develop a reliable model aimed at estimating the structural performances under seismic actions;
- development of a push over analysis adopting non-linear models for materials that allows to estimate the extent of structural safety under seismic actions assuming a global behaviour of the structure;
- local verifications considering out-of-plane mechanisms of masonry walls, that often represent the weak point for safety.

The specific results collected about the Bell Tower of Santa Maria del Carmine have highlighted the significance of the comparison between theoretical linear dynamic analyses and experimental identification in order to assess the boundary conditions of the structure.

Linear analysis showed that the Tower is largely safe under gravity loads; non-linear analysis, that appeared a reliable method to estimate the seismic performances of the structure, showed that the tower is safe at the Limit State of Significant Damage in all directions, while this is not verified at the Limit State of Near Collapse in the Y direction. Finally, local verifications about the development of out-of-plane mechanisms of masonry walls completed the global analyses and highlighted conditions of instable equilibrium for several masonry panels both at Limit State of Significant Damage and Near Collapse. All this means the need of a retrofitting intervention. The collected results

allowed identification of the weakness of the structure as a possibility that masonry walls are involved in local out-of-plane failure mechanisms, due to the ineffective connections between vertical and horizontal structural elements. The consolidating technique of intervention represented by insertion of tie-bars connecting opposite walls to avoid such mechanisms was chosen. An innovative solution has been introduced by installing tie rods made of GFRP laminates coupled to an aluminium/stainless steel end anchorage system in order to preserve them from the corrosion phenomena that evidently affected the existing ones. In this case, the selection of FRP was very appropriate to ensure high durability of an open-air installation near the sea, to exploit the high strength of the material, and to take advantage of its low weight which minimized transportation and installation costs. The design procedure introduces the concept that for construction characterized by a very long use life, such as the ancient heritage buildings, it is preferable to use more durable materials, and that all-in intervention has to be compatible with both the low impact criterion and safety requirements resulting in “minimal intervention-maximal protection.” In order to check the effectiveness of the ties over time, a continuous strain monitoring system has also been installed. Each step of the study presented herein is essential to assess the constituent materials, their assembly and the global model of the structure for static and dynamic actions.

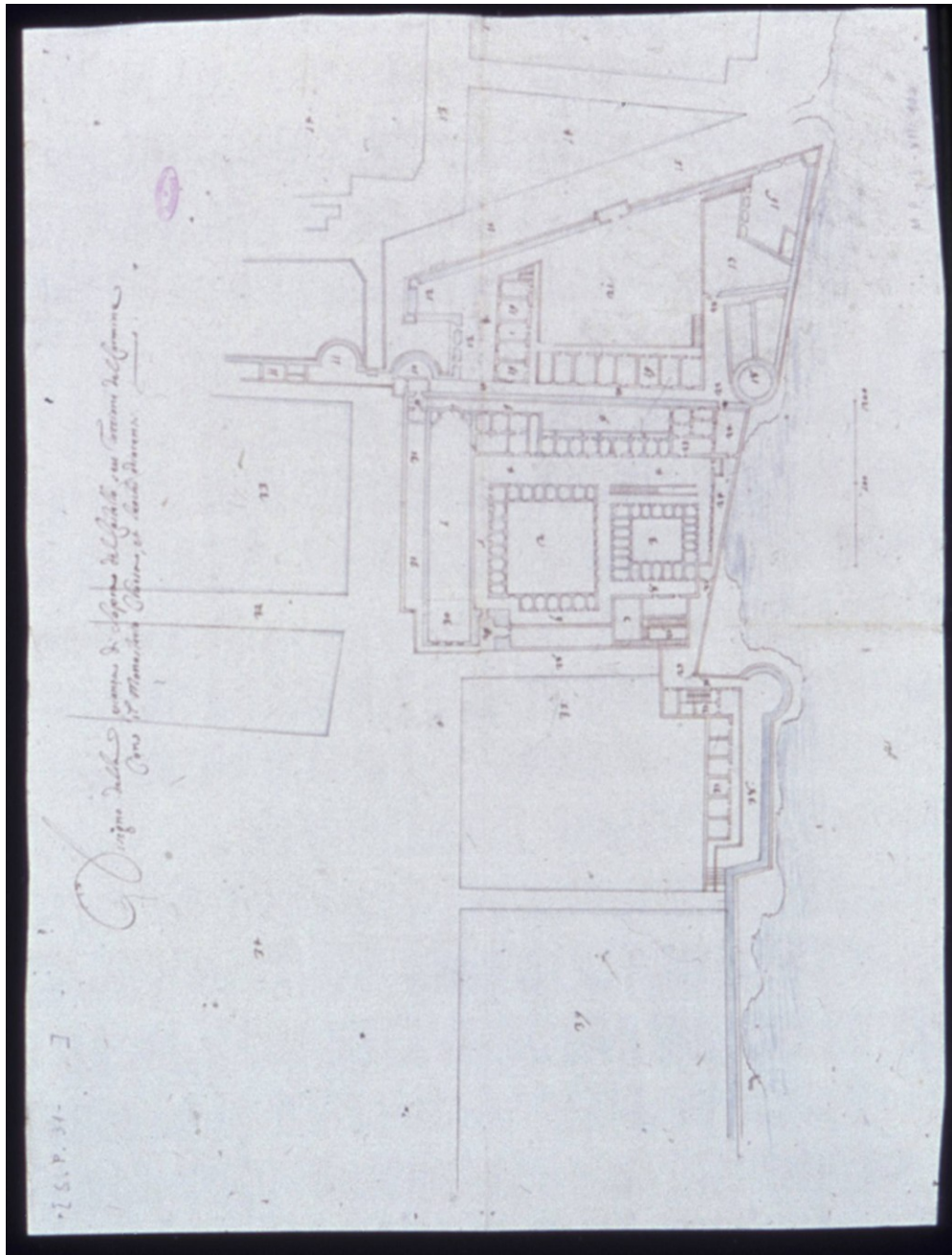
Appendix I



Declaration of the survey of the first level of the Castle on the Carmine Stronghold with the monastery, church, and places adjacent. Simancas Archive, Spain, legajo 3285, ano 1662

Legend

1. Carmine Church
2. Larger Cloister
3. Smaller Cloister
4. Refectory
5. Kitchen, oven, cellar
9. Passage behind the church and monastery separating the Stronghold from the Monastery
10. “Carrese” Gate
11. “Carmine” Gate
12. Bridge that goes over the city walls
13. “Borgo Loreto” street
18. “Stendardo” Stronghold
24. “Marina del Carmine” Gate
- 26. Stairs to be built in a free area close to the Parish to go to the upper level.**
27. Parish
28. Oratory
29. Monastero’s door
32. “Lavinaio” Street



Declaration of the survey of the second level of the Castle on the Carmine Stronghold with the monastery, church, and places adjacent. Simnacas Archive, Spain, legajo 3285, ano1662

Legend

1. Carmine Church roof
2. Larger Cloister
3. Smaller Cloister
4. Large Dormitory
- 5. Walkway over the dormitory taking to the Church in correspondence of the Organ door and Choir**
6. Additional walkway
16. High standing ground to be built in the outside corner of the Stronghold
17. Additional lower ground
18. “Stendardo” Stronghold
20. Strada da farsi dietro dette case del quartiere et dietro la muraglia da farsi per difesa di esse
21. Baluardo Stronghold parade ground
- 26. New stairs to be built close by the Parish to have connection with the Bell Tower**
- 29. Bell Tower**
- 31. Walkway over the Chapels around the Church and Choir to allow to get to the Bell Tower**

ARCHEIVO SIMANCAS
 M-3285-50

Don J. M. de Campuzos
 Ego J. M. de Campuzos

In conformita' dell'ordine datosi nella uggia et accenn fatto
 de Vo. a J. M. de Campuzos gen. D. Vicenzo D'Amalia
 Generale Gio. Gio. Maria Torancacho M. de Campuzos del
 Corp. Grand Carnero et il M. de Campuzos Don
 Gio. de Monroy J. de Val Cayfallo seu Comand.
 del Cammino a rinnovare il stato di dett. Torreone,
 et li luochi che al posto occupano li soldati chertanno
 Presidiati per la difesa di quello et vorriano fare
 riflessione di potere dividere in qualche modo
 li soldati dal habitazione de frati senza pero
 che resti indifeso il Posto in conformita dell'
 ordine dato da Vo. perche a senso fatto
 piu disegno et discorso sopra il luoco del Vo.
 et sudetti di offenimo che il stato di detto
 Torreone del modo come si ritrova hoggi non
 ha forme di fortezza et sia aguto che da
 milta parti ui si puo' entrare et poterlo
 difeso quanto piu viene occupato da soldati
 tanto piu stara' sicuro supplendo al mancanti.
 Nelle forme del luoco la quantita' et valore della
 militia, pero' hauidosi a fare la sudetta divi-
 sione per disoccupare li dormitorij et celle de
 frati et rinnovare la communication che

16

di guardia del quale si possono
 guarnire le fontanelle et vande,
 et la porta del Monasterio et
 d'altre, et fare la fabrica della
 grida nel Vacuo acob la Parro-
 chia et arco fare le cauna et
 amare li dormitorij verso la
 marina verso il passo del bacione
 et innanzi la casa del S. Gio. una
 et fare il Corridore coperto sopra
 le stampe dell' Infermeria et
 venire la communicatione con il
 Campanile et la Circumvallatione
 attorno il Monasterio in
 ragione con la Compagnia delle Case,
 de ducat. due mila in circa 2000 —

Che Oltre insieme tutte quelle partite
 fanno la somma de ducat. dodici
 Milia et ottocento 12800 —

Et quello e quanto possiamo riferire
 al V. S. et facendoli Vicereale li P. I. M.
 Napoli li 16 de Mayo 1662
 D. V. S.

Donat Roberto Caputo, Andrea Michi Puchiatto

30

Obras a realizar en el Torreón del Carmen, para separar las habitaciones de los religiosos de las de los soldados, antecedentes sobre las fortificaciones de Nápoles (1), Archivo de Simancas, España, legajo 3285 - 48, año 1662

Work to be done in the Carmine Stronghold to separate the Friars Housing from the soldiers barracks, within Naples fortification, Simancas Archive, Spain, 3285-48, 1662

Appendix II

- Moscarella P.T., *Chronistoria del Carmine Maggiore di Napoli*, Scritta dal Pier Tommaso Moscarella fino al 1589 e continuata da altri fino al 1825
- D'Engenio Caracciolo C., "*Napoli Sacra, oltre la vere origini*", In *Napoli per Ottavio Feltrano*, ad istantia de Stefano Monleuiero, 1623
- Sasso C.N., "*Storia de' monumenti di Napoli e degli architetti che gli edificavano*", Naples 1856
- Ceva Grimaldi F., "*Della città di Napoli dal tempo della sua fondazione sino al presente*", Stamperia e Calcografia, Naples 1875
- Nobile G., "*Descrizione della città di Napoli e delle sue vicinanze*", vol. II, Stabilimento Tipografico del Cav. Gaetano Nobile, Naples 1863
- D'aloè S., "*Storia della Chiesa di Napoli provata con monumenti*", Naples 1869
- Galante A., "*Guida Sacra della Città di Napoli*", Fibrebo, Naples 1873
- Domenico, C., "*Il Santuario della Bruna o la Chiesa del Carmine Maggiore*", Fibreno, Naples 1875
- Capasso B., "*Sulla circoscrizione civile ed ecclesiastica e sulla popolazione della città di Napoli dalla fine del secolo XIII fino al 1809*", In "*Atti dell'Accademia Pontaniana*" vol. XV, Stamperia della Regia Università 1883
- D'Aloè S., "*Catalogo di tutti gli Edifici Sacri della città di Napoli e suoi sobborghi*", Archivio Storico per le Province Napoletane Forni Editore, Bologna 1883
- Folinea E., "*Progetto Generale per la bonifica dei fondaci e dei quattro quartieri Porto, Pendino, Mercato, Vicaria*", Naples Real Stabilimento dei fondaci e dei quattro quartieri Porto, Pendino, Mercato, Vicaria, Real Stabilimento topografico Comm. Francesco Giannini & figli, Naples 1884
- Filangieri G., "*Chiesa e Convento del Carmine Maggiore in Napoli*", Descrizione storica e artistica, Tipografia dell'Accademia Reale delle Scienze, Naples 1885

- De Blasiis G., *“Le case dei Principi Angioini nella piazza di Castelnuovo”*, In Archivio Storico per le provincie napoletane pubblicato a cura della Società di Storia Patria Naples presso Federico Furchheim, Libraio, Naples 1886-1887
- D’Ambra R., *“Napoli Antica Illustrata”*, Naples 1889
- Sigismondo G., *“Descrizione della città di napoli e i suoi borghi, Sal Bolognese”*, A. Forni, Naples 1989
- Di Giacomo S., *“Le Chiese di Napoli: Santa Maria del Carmine maggiore”*, Napoli Nobilissima Per 40 vol. I,ff. 1-2, 4 Gen/Feb-Apr 1892 pp. 18-32, p. 56-60, p. 97, Naples
- De La Ville Sur-Yllon, L., *“Dal Carmine a Revigliano”*, Napoli Nobilissima Per 40 II, fasc. XII, Naples 1893
- Capasso B., *“La casa e la famiglia di Masaniello”*, Collezione napoletana di storia e d’arte n°1 Editore Dott. Gennaro Giannini, Naples 1919
- Serra L., *“Note sullo svolgimento dell’architettura barocca a Napoli”*, Napoli Nobilissima n.s. II (1921-22)
- Quagliarella P. T., *“Guida storico-artistica del Carmine Maggiore, Napoli”*, Taranto 1932
- Franciosi A., *“Le Chiese di Napoli”*, D’Auria, Naples 1936
- Chierici G., *“Architettura religiosa a Napoli nei secoli XVII e XVIII”*, Rivista Palladino I, Milan 1937
- Pane R., *“Architettura dell’eta’ barocca a Napoli”*, E.P.S.A., Naples 1939
- Doria G. , *“Le strade di Napoli”*, Saggio di toponomastica storica, Ricciardi, Naples 1943
- Gleijeses V., *“La Piazza Mercato in Napoli”*, Del Delfino, Naples 1943
- Pane R., *“Napoli Imprevista”*, Torino 1949
- Doria G., *“Napoli e il suo golfo”*, Touring Club Italiano, Milan 1961
- Doria G., *“Settecento Napoletano”*, ERI, Edizioni Rai Radiotelevisione Italiana, Milan 1962

- Doria G., *“Napoli e dintorni. guida storico-artistica”*, E.S.I., Naples 1966
- Pisa G., *“Il Carmine Maggiore”*, Fede-Storia-Arte, Naples 1938
- Procino G., *“Il Vesuvio e la Vergine del Carmine”*, A.C.M, Naples 1964
- Doria G., *“Storia di una capitale, Napoli dalle origini al 1860”*, Milano, Riccardo Ricciardi, Naples 1967
- Ferrajoli F., *“Napoli monumentale. dall’Anticaglia a San Giovanni a Mare”*, F. Fiorentino, Stamperia Napoletana, Naples 1968
- Gleijeses V., *“Le piazzette di Napoli”*, Delfino, Naples 1969
- Strazzullo F., *“Architetti e ingegneri napoletani dal ‘500 al ‘700”*, Edition di Gabriele e Mariateresa Benincasa, Naples 1969
- Venditti A., *“Fra’ nuvolo e l’architettura napoletana tra cinque e seicento”*, L’Orsa Maggiore, Lecce 1969
- Monaco G., *“Piazza Mercato: sette secoli di storia”*, in Nuova collana di Storia Napoletana diretta dal Gaetano Capasso, Athena Mediterranea, Naples 1970

- Galasso G., *“Napoli spagnola dopo Masaniello”*, Edizione Scientifica Italiana, Naples 1972
- Wittkower R., *“Arte e architettura in Italia 1600-1750”*, Torino 1972
- De Seta C., *“Storia della città di napoli dalle origini al settecento”*, Laterza, Naples 1973
- Gleijeses V., *“La nuova guida storico-artistica-monumentale-turistica”*, Società Editrice Napoletana S.r.l., Naples 1973
- Venditti A., *“Urbanistica e architettura angioina”*, Edizioni Scientifiche Italiane, 1973
- Celano C., Chiarini, G. B., *“Notizie del bello dell’antico e del curioso della città di Napoli”*, Edizioni Scientifiche Italiane, Naples 1974
- Monaco G., *“Cinque secoli di storia della parrocchia di Masaniello”*, Laurenziana, Naples 1974

- Blunt A., *“Neapolitan Baroque and Rococo Architecture”*, London 1975
- Monaco G., *“Santa Maria del Carmine detta “la bruna” Storia-Culto-Folklore”*, Laurenziana, Naples 1975
- Gleijeses V., *“Nuovissima Guida di Napoli e dintorni”*, SEN, Naples 1977
- Pane R., *“Il Rinascimento nell’Italia Meridionale”* II Edizioni di Comunità, Milan 1977
- Delli S., *“Le piazze di Napoli”*, Newton Compton, Rome 1978
- Pane R., *“L’architettura del Rinascimento”*, in AA.VV. *Cultura Materiale*, cit. *“La voce della Campania”* a. VII n°12,17, Naples 1979
- De Seta C., *“Napoli”*, Laterza, Naples 1981
- Cinque G., *“Da Santa Maria del Principio all’Incoronata di Capodimonte”*, Città di Maria, Laurenziana, Naples 1982
- Alisio G., *“Napoli nel Seicento, Le vedute di Francesco Cassiano de Silva”*, Electa, Naples 1984
- Cantone G., *“Napoli Barocca e Cosimo Fanzago”*, Banco di Napoli, Naples 1984
- Cantone G., *“Civiltà’ del Seicento a Napoli”*, Naples 1984
- Gleijeses V., *“I quartieri di Napoli”*, Società Editrice Napoletana S.r.l., Naples 1984
- Pane R., *“Seicento napoletano”*, Edizioni di Comunità, Milan 1984
- Nappi E., *“Contributi a Giovan Giacomo Conforto”*, Naples
- *Nobilissima* Vol. XXIV, fasc. I-II sett.-dic. 1985 ff. 173-183 Vol. XXV, fasc. V-VI gen.-apr. 1986 ff. 40-44
- Pavone M. A., *“Napoli scomparsa nei dipinti di fine Ottocento”*, Newton Compton Editori, Rome 1987
- Tintoretto F., *“Introduzione allo studio delle piazza del centro antico e storico”*, Università degli studi, DPU, Naples 1987
- Battista P., Gentile S., Guida, E., Lattuada, P., Rubino, G.E., *“Il Mercato di Napoli: il presente del passato”*, Giannini, Naples 1988

- AA.VV., *“Ricerche sul ‘600 napoletano”*, Edizioni L&T, Milan 1988
- Pane G., Valerio V., *“La città di Napoli tra vedutismo e cartografia”*, Grimaldi & C. editori, Naples 1988
- Amato Santa Maria U., *“Cupole e Campanili di Napoli”*, Tipografia Laurenziana, Naples 1989
- Buccaro A., *“Architettura e gli spazi urbani: i tre fori napoletani”*, In Agorà anno II giugno/luglio 1989 n° 4
- Amirante G., Guglielmelli A., *“Architettura napoletana tra ‘600 e ‘700”*, Edizioni Scientifiche Napoletane, Naples 1990
- Amirante R., *“Napoli architettura e città, II Seminario Internazionale di Progettazione”*, La Buona Stampa S.p.a, Ercolano (Na) 1990
- Divenuto F., *“Napoli Sacra nel XVI secolo”*, Edizioni Scientifiche Italiane, Naples 1990
- Gambardella A., *“Piazza Mercato a Napoli: architettura e sviluppo urbano del borgo orientale”*, Sagep, Genova 1990
- Gleijeses V., *“Chiese e palazzi della città di Napoli”*, La Botteguccia, Naples 1991
- Alisio G., *“Napoli nell’Ottocento”*, Electa, Naples 1992
- Cantone G., *“Barocco Napoletano”*, Istituto Poligrafico e Zecca dello Stato, Libreria dello Stato, Roma 1992
- Miele M., *“Personalità di Fra’ Nuvolo”*, in incontri di studio su Fra’ Nuvolo, Naples 1994
- Regina V., *“Le Chiese di Napoli”*, Newton Compton Editori, Roma 1995
- Alisio G., *“Concorso per Piazza Mercato”*, Electa, Naples 1996
- Di Mauro L., *“Mura e torri di Napoli”*, Electa, Naples 1997
- Cajati C., Pastore R., *“Il chiostrò e la piazza: il Mercato da Sant’Eligio al Carmine”*, Giannini, Naples 1998
- Achille M., *“Le fortificazioni nel Regno di Napoli, note storiche”*, Giannini, Naples 1998
- Vladimiro V., *“Piante e vedute di Napoli dal 1486 al 1599”*, l’origine

- dell'iconografia urbana europea, Electa, Naples 1998
- A cura dei Padri Carmelitani Carmine Maggiore, *“La Bruna e il Carmine di Napoli”*, Naples 2001
 - Ferraro I., *“Atlante della Città storica, quartieri bassi e risanamento”*, Clean, Naples 2004

All the texts reported are in Italian.

Appendix III

Il primo ottobre 1905 fu firmato il contratto
 per l'organo strumentale pneumatico
 tubolare

Il 27 Maggio 1906 fu pagato l'Appalta-
 tore sig. Raffaele Servillo per i lavori
 fatti nel coro, che venne accostato
 al muro della facciata della chiesa
 e fu abolita la comunicazione col
 corridoio del vecchio Castello. Detto
 appaltatore ebbe L. 162.00

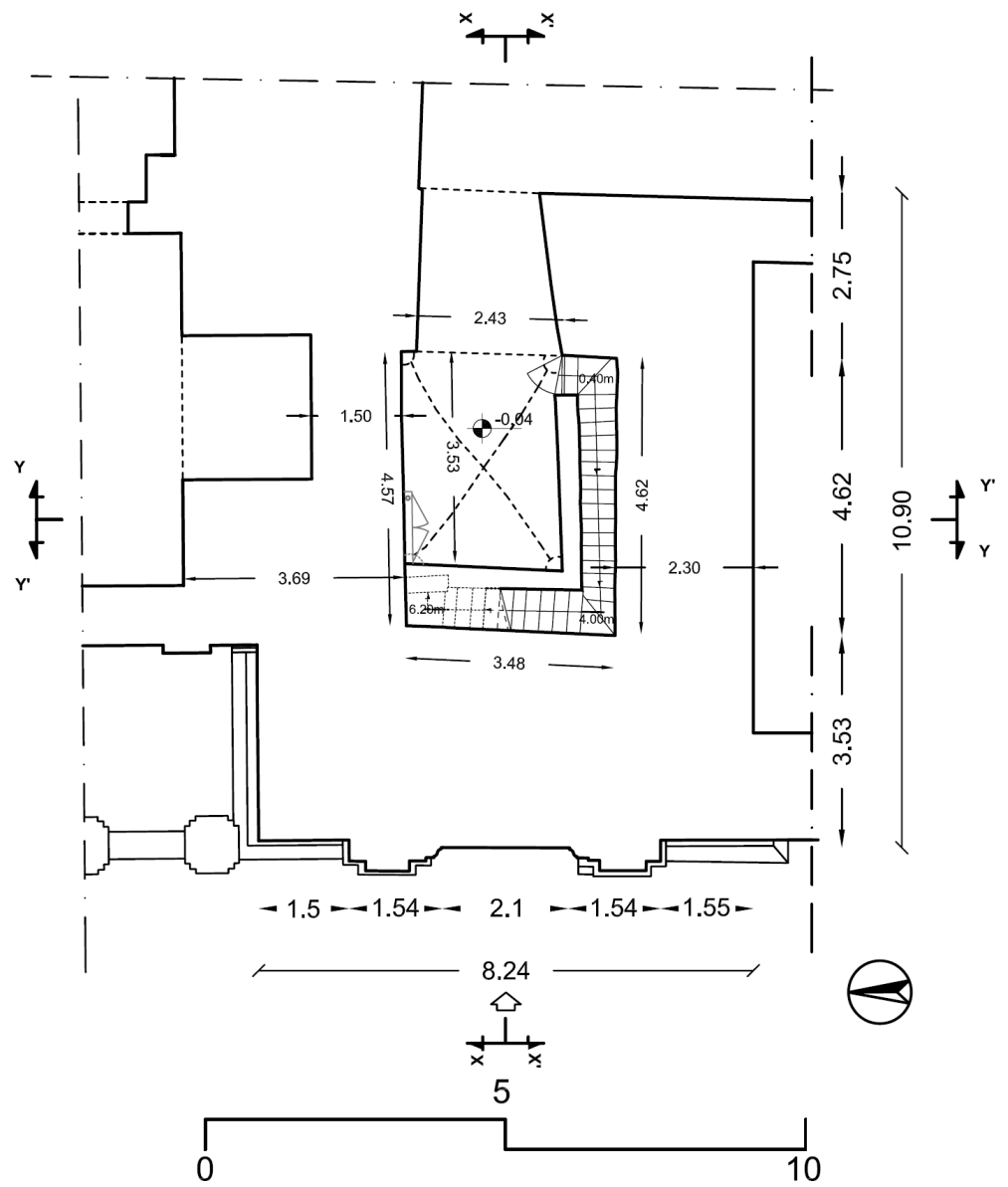
Il 31 Maggio 1906 furono pagate
 le rotarie di ferro ^{di tipo disposto} per rinforzare il
 pavimento del coro, su cui doveva pog-
 giare la gran massa dell'organo
 e costarono L. 588.90

Dopo questi lavori fu necessario
 riattare tutto il coro, e per que-
 sto riattamento si è pagato al fa-
 legname Raffaele Nota L. 1469.00

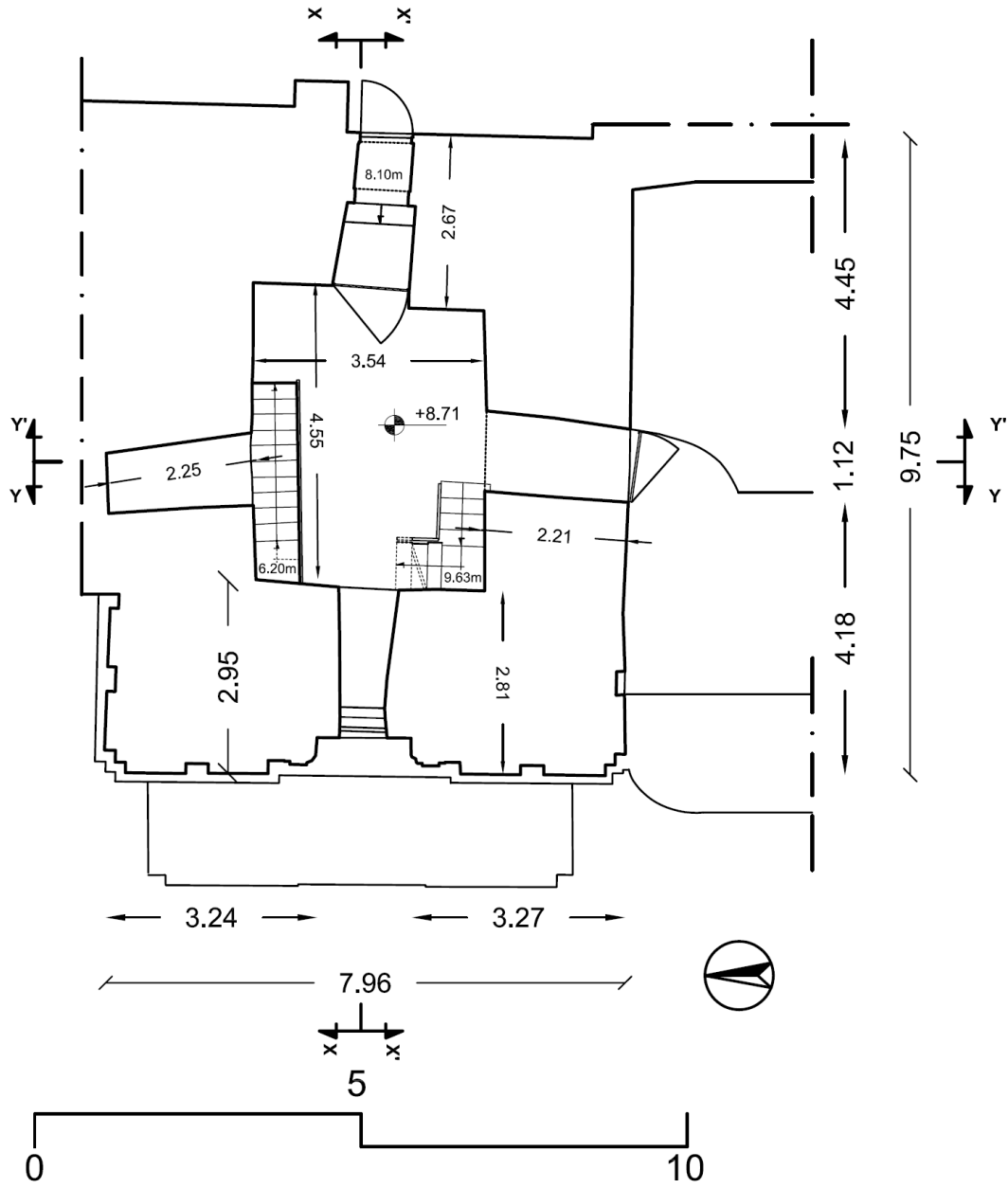
2219.90

...On May 27 it was cut the connection by the corridor to the old castle

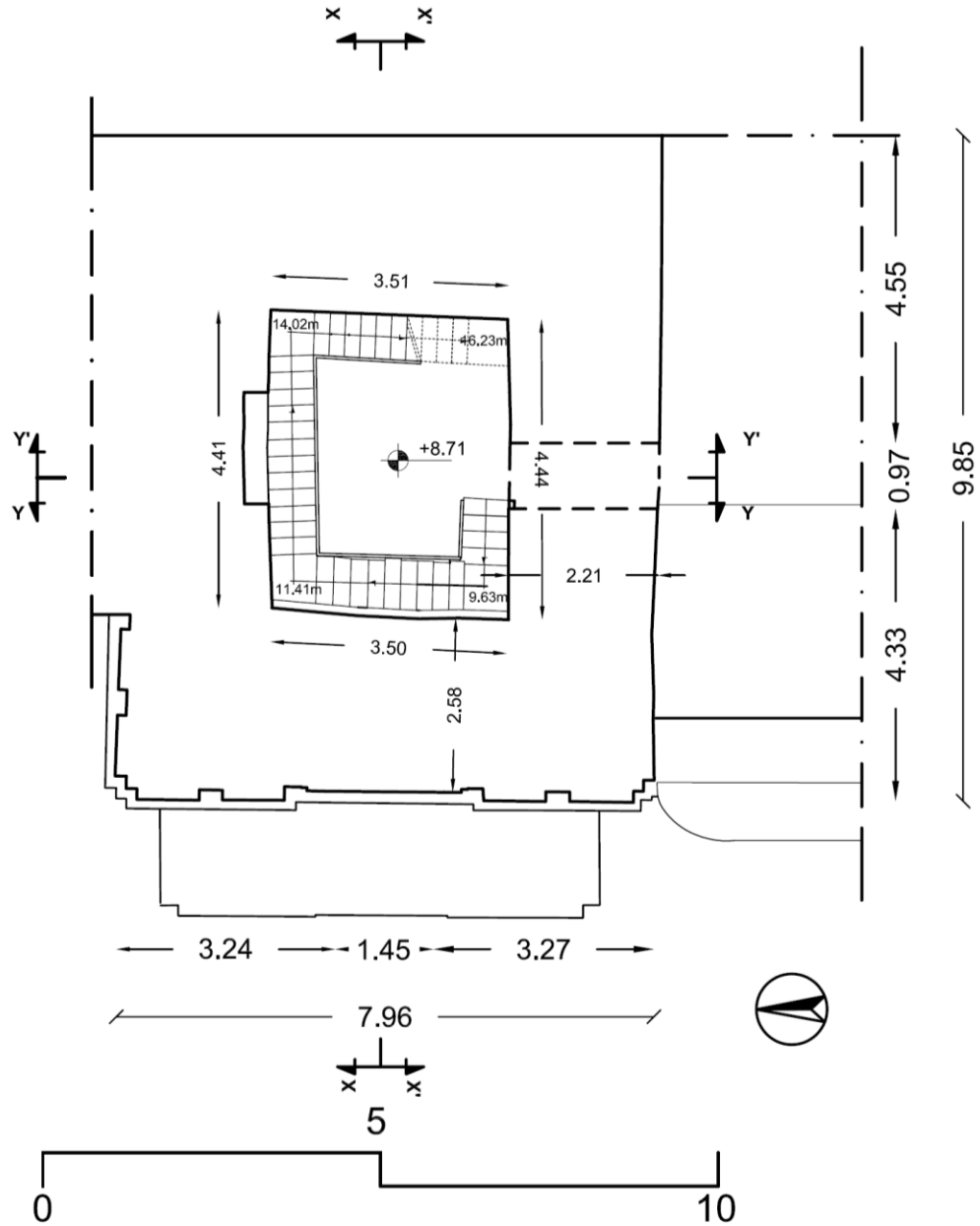
Appendix IV



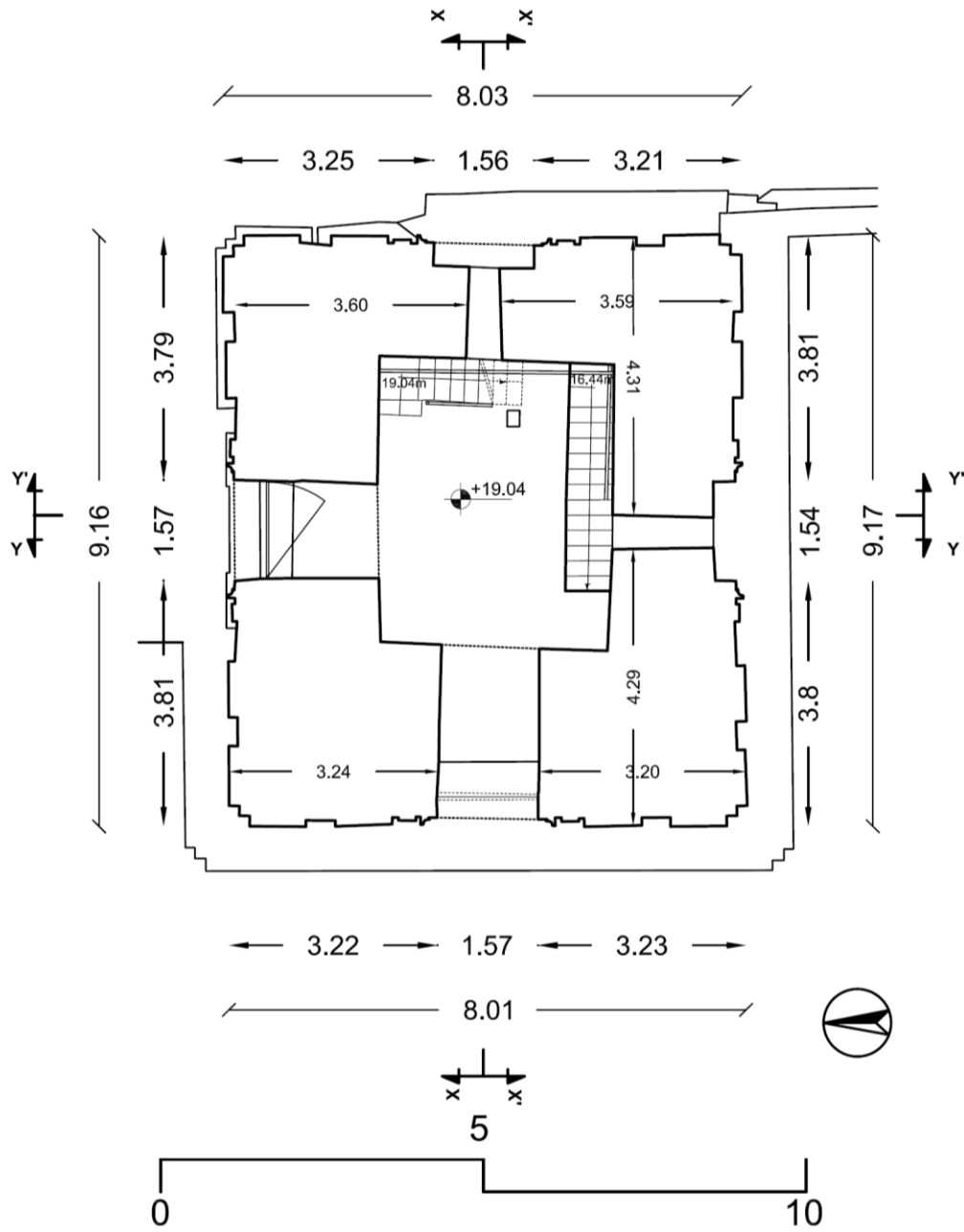
I level, +4.00m (section BB)



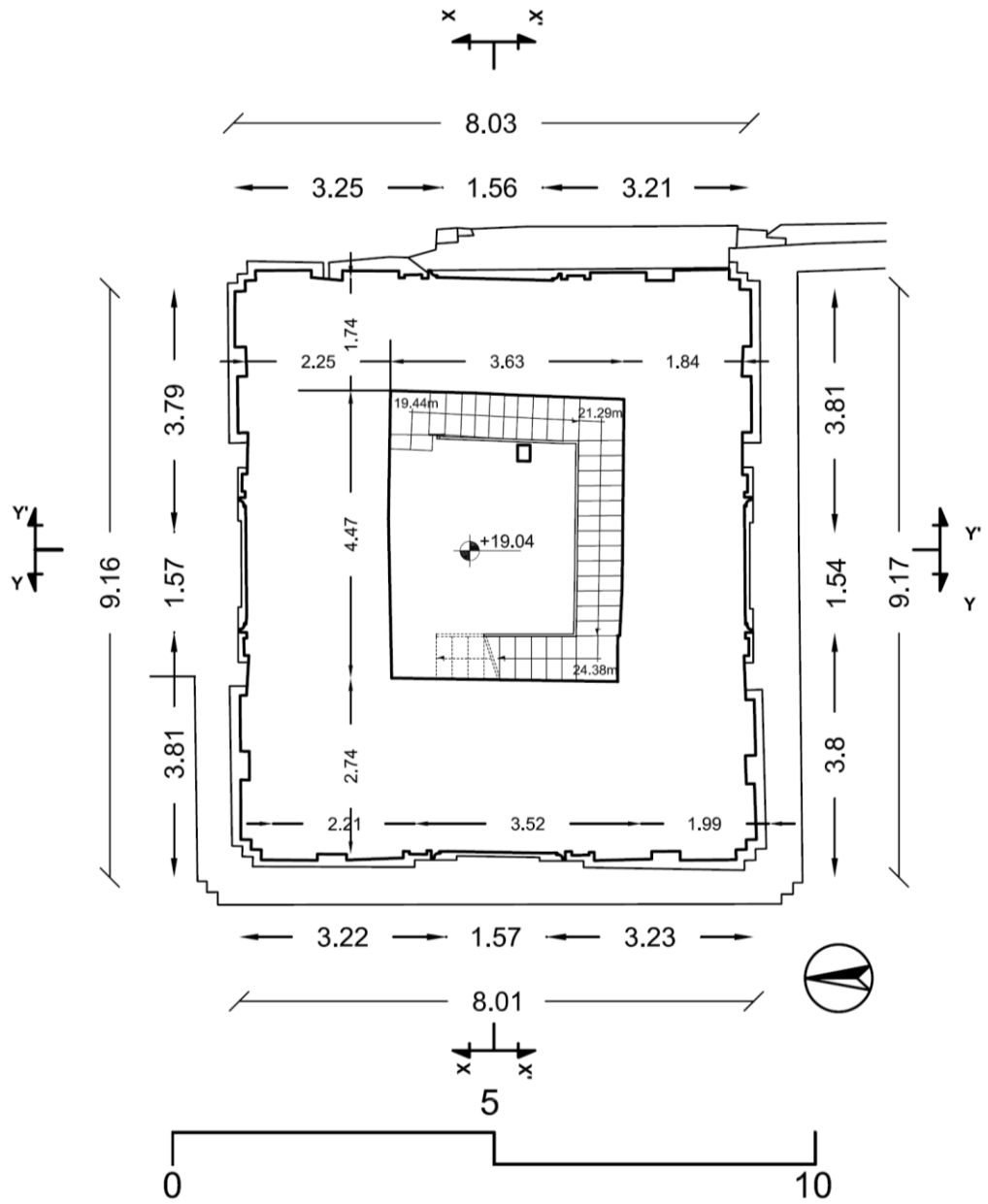
I level, +8.71m (section CC)



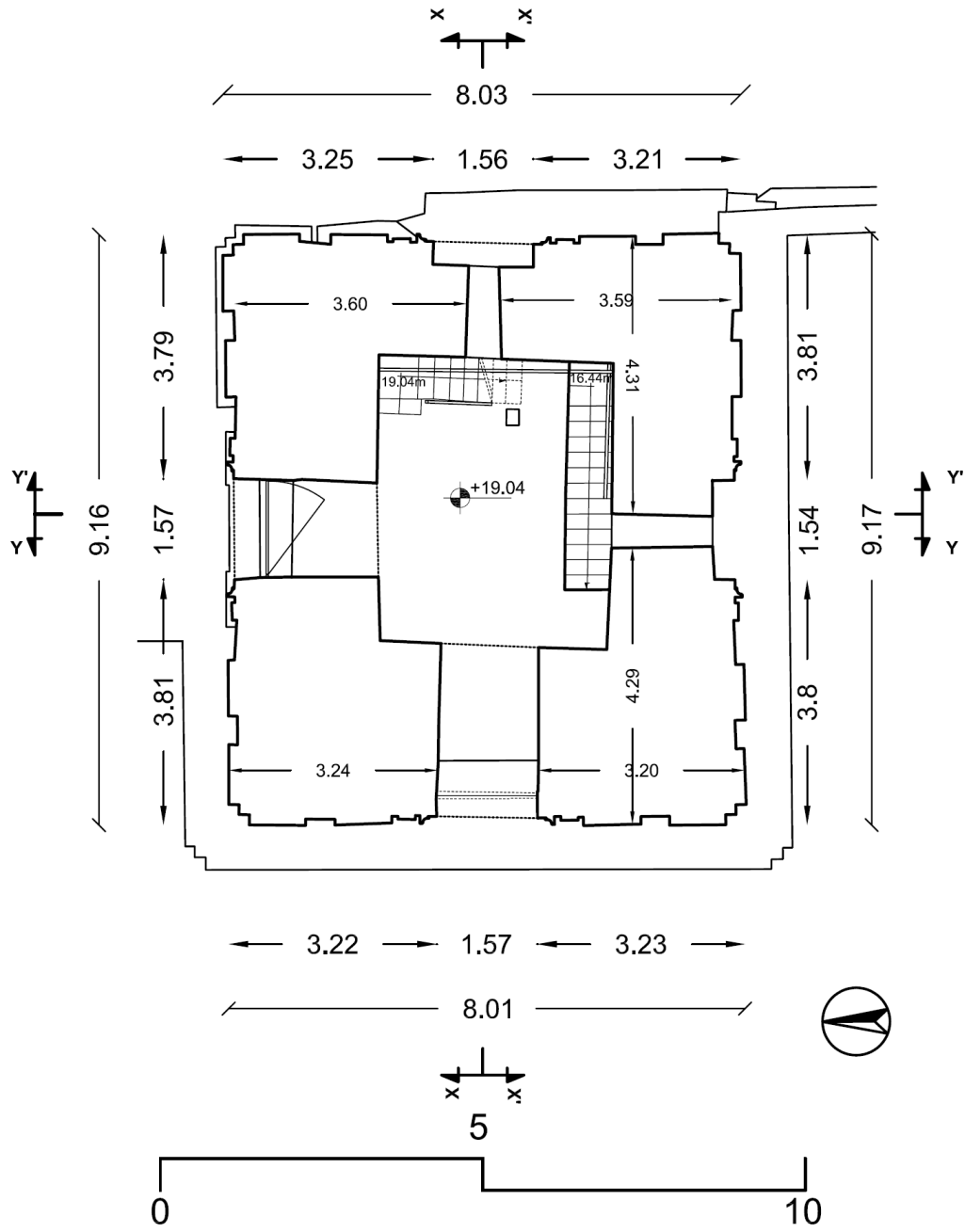
I level, +14.22m (section DD)



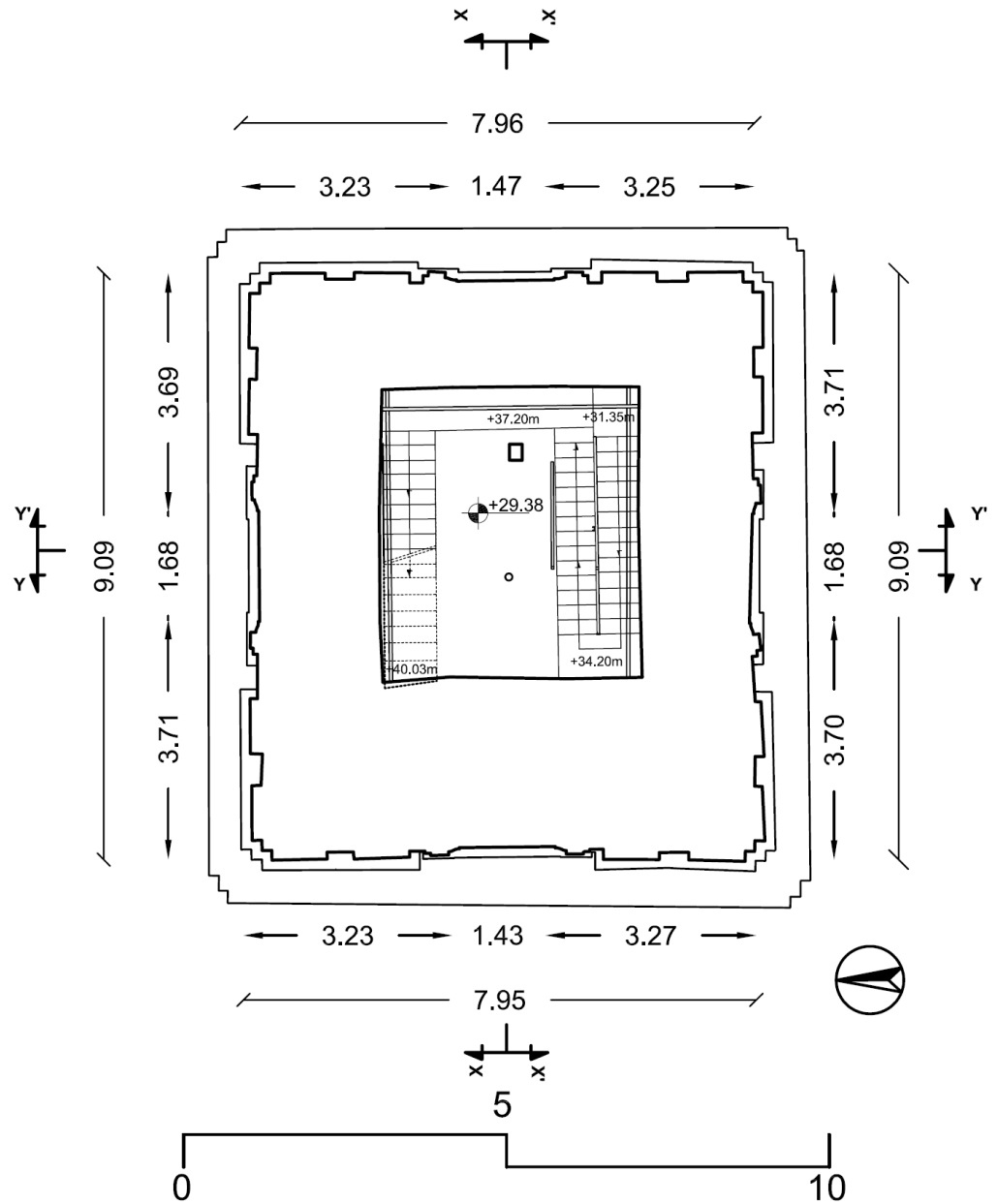
II level, +19.04m (section EE)



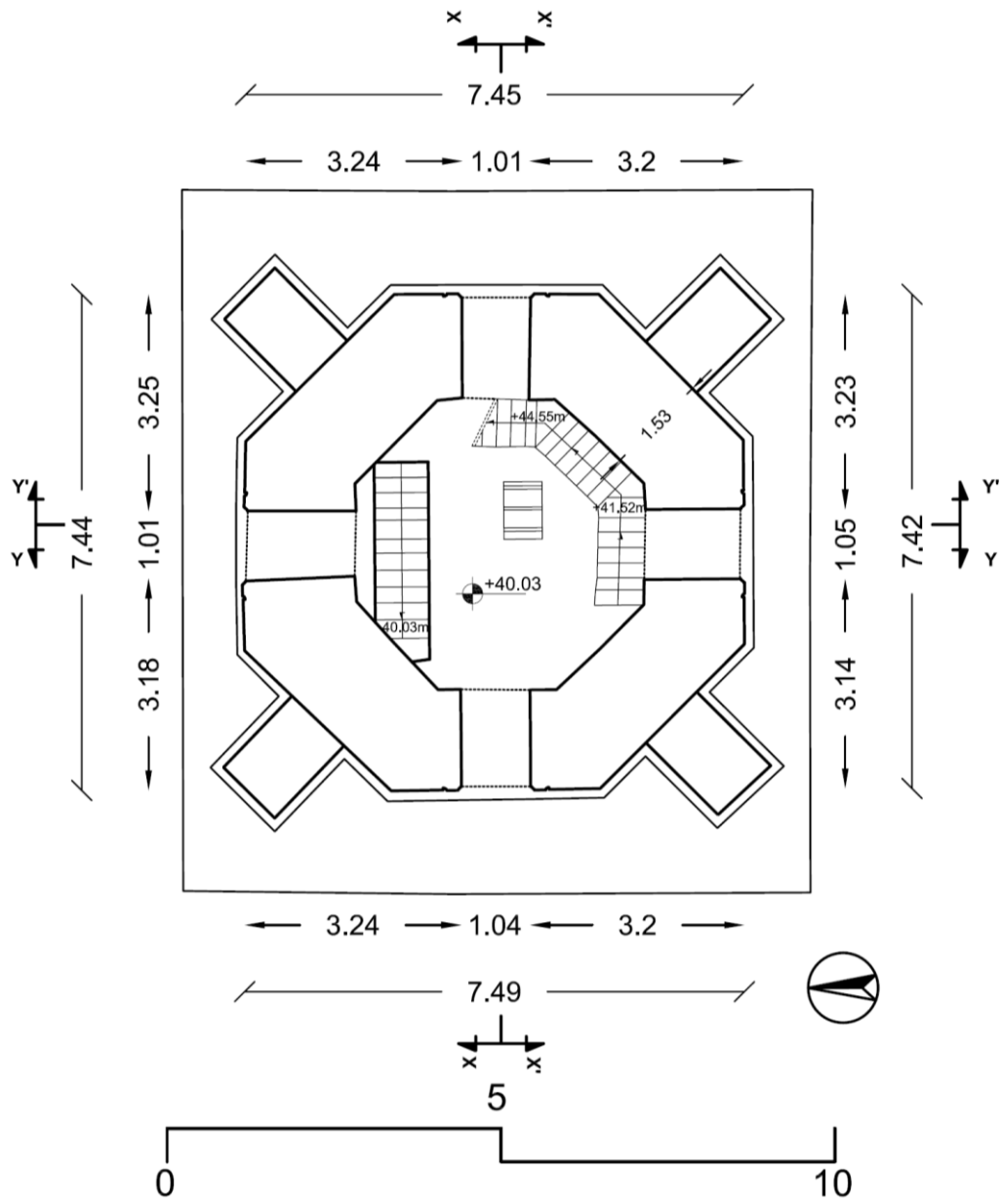
II level, +24.38m (section FF)



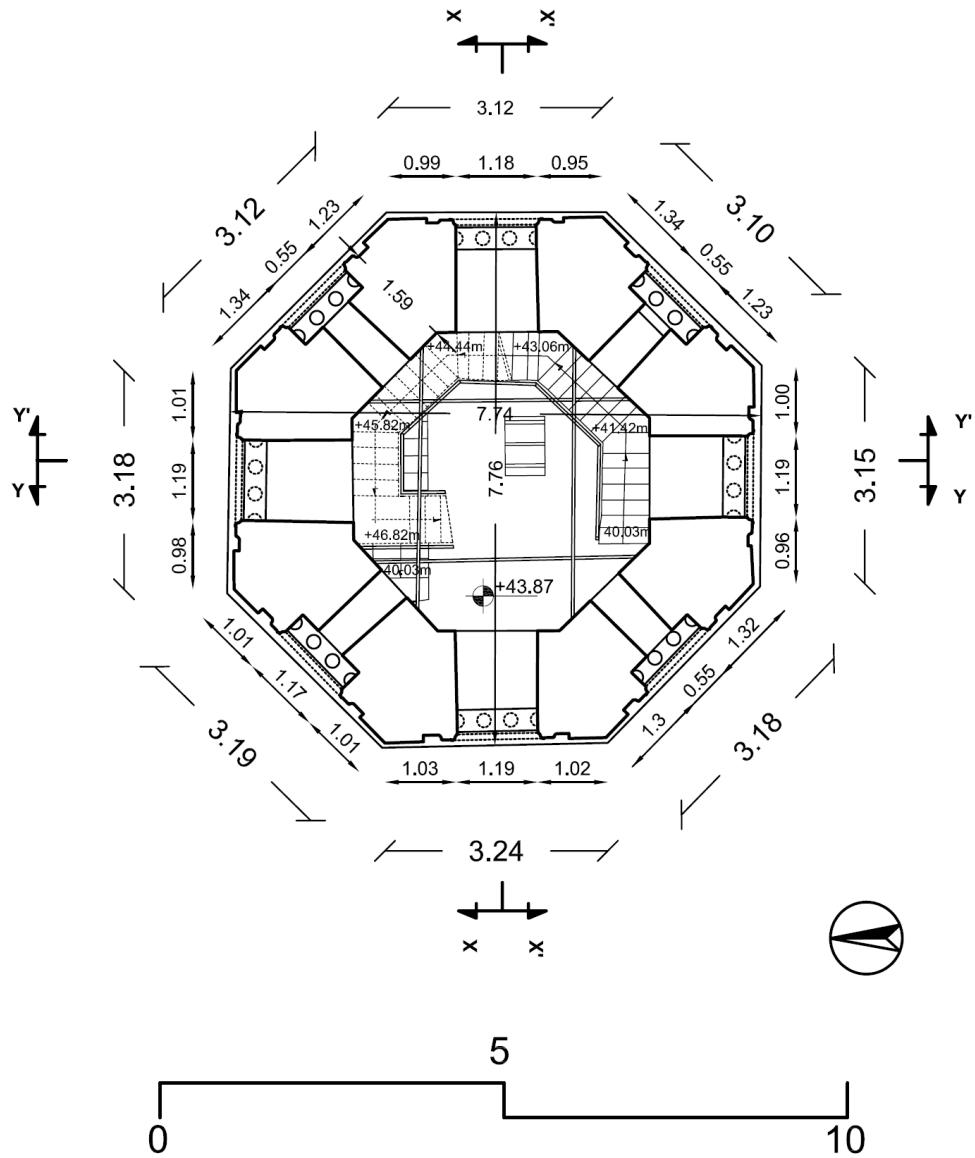
III level, +29.38m (section GG)



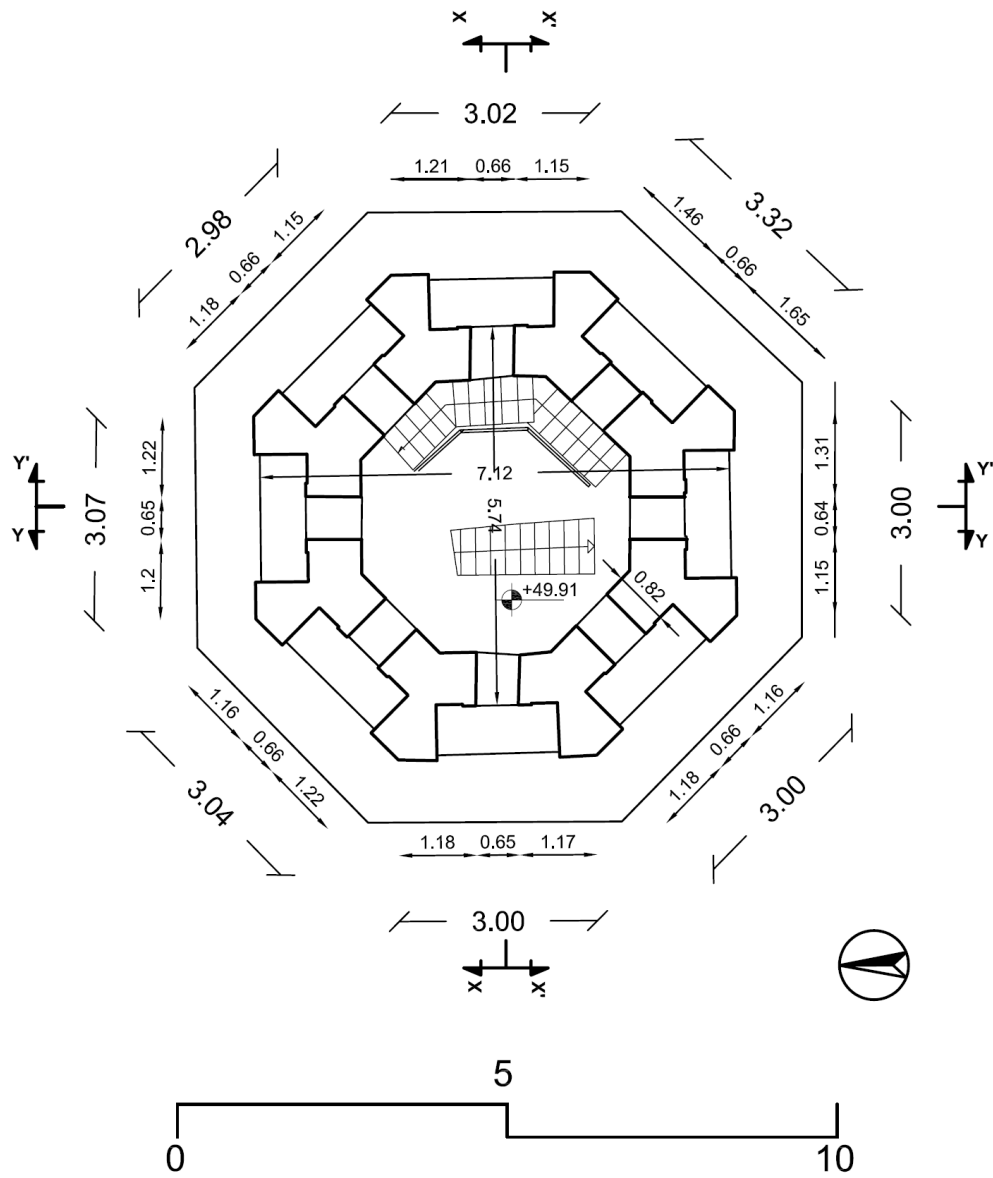
III level, +37.20m (section HH)



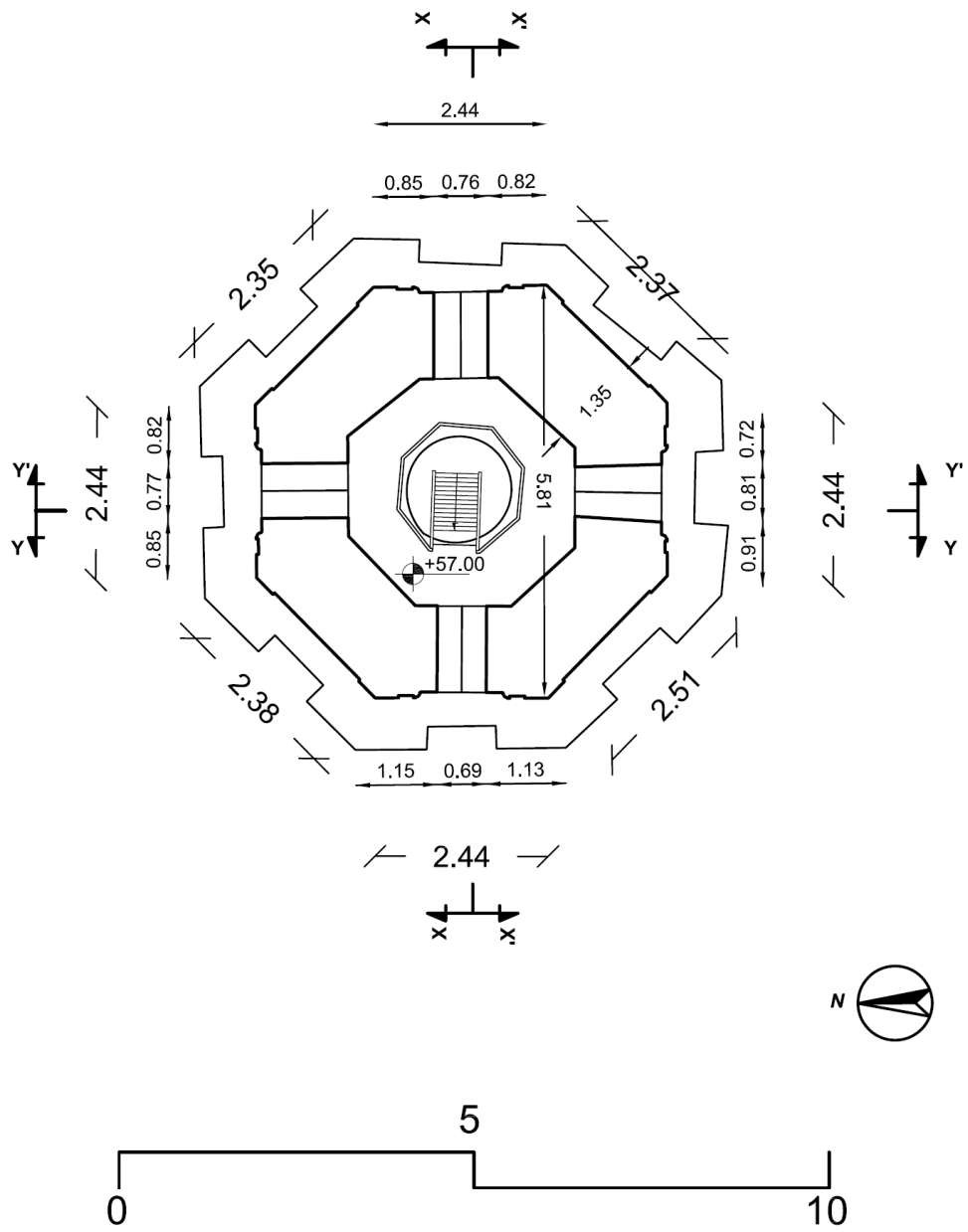
IV level, +40.03m (section II)



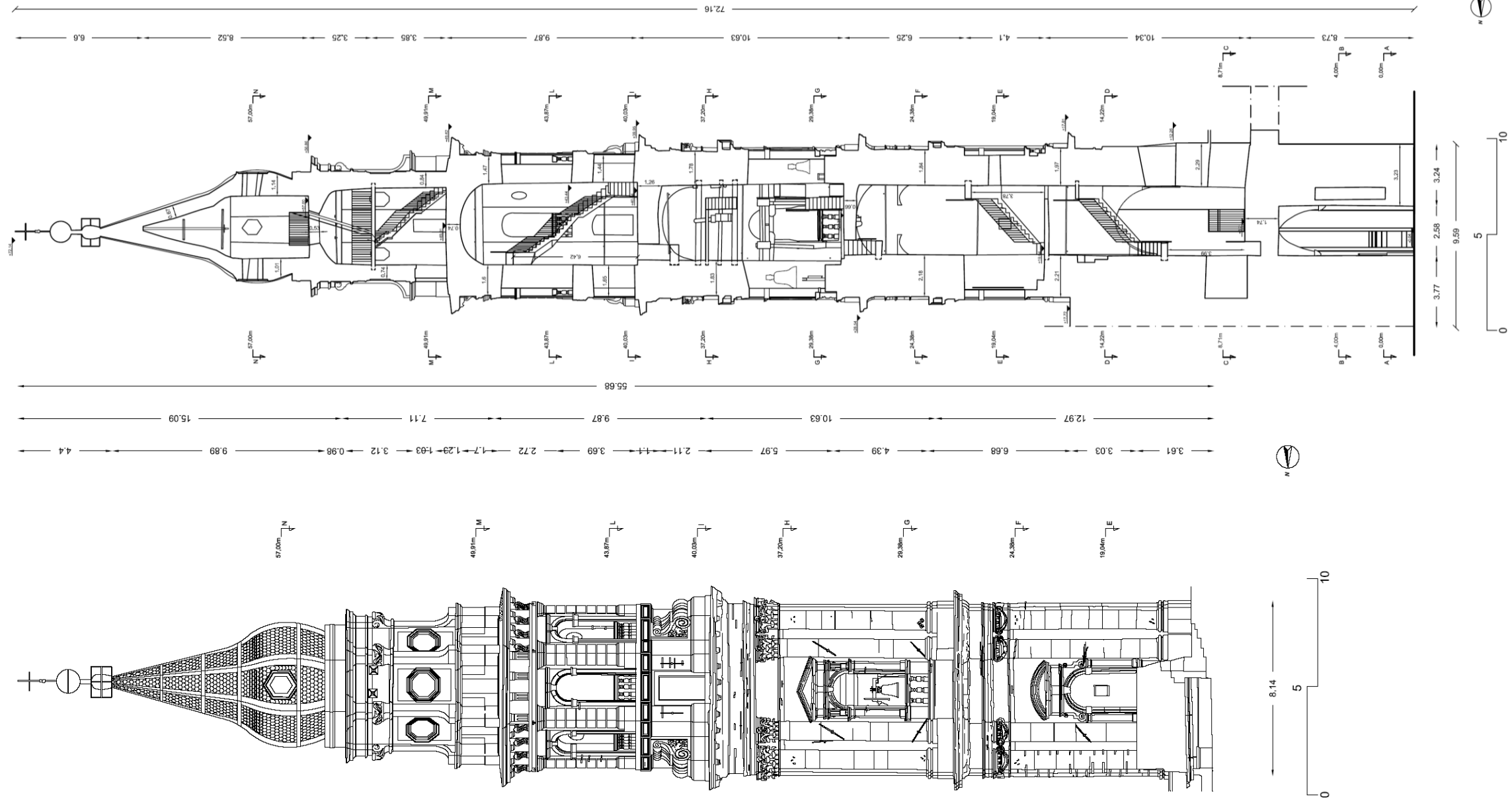
V level, +43.87m (Section LL)



VI level, +49.91m (Section MM)

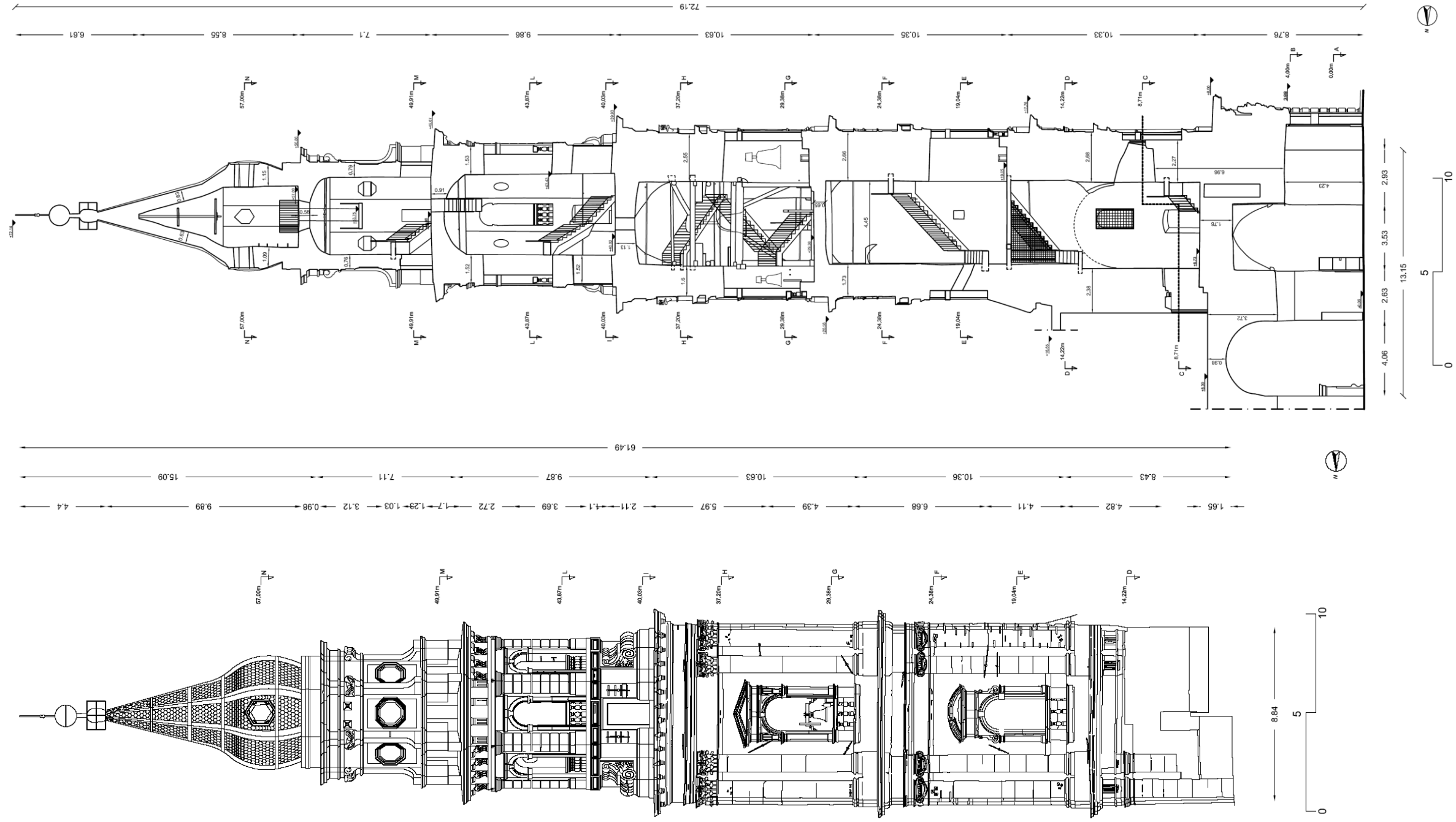


VII level, +57.00m (Section NN)



Longitudinal Section Y-Y

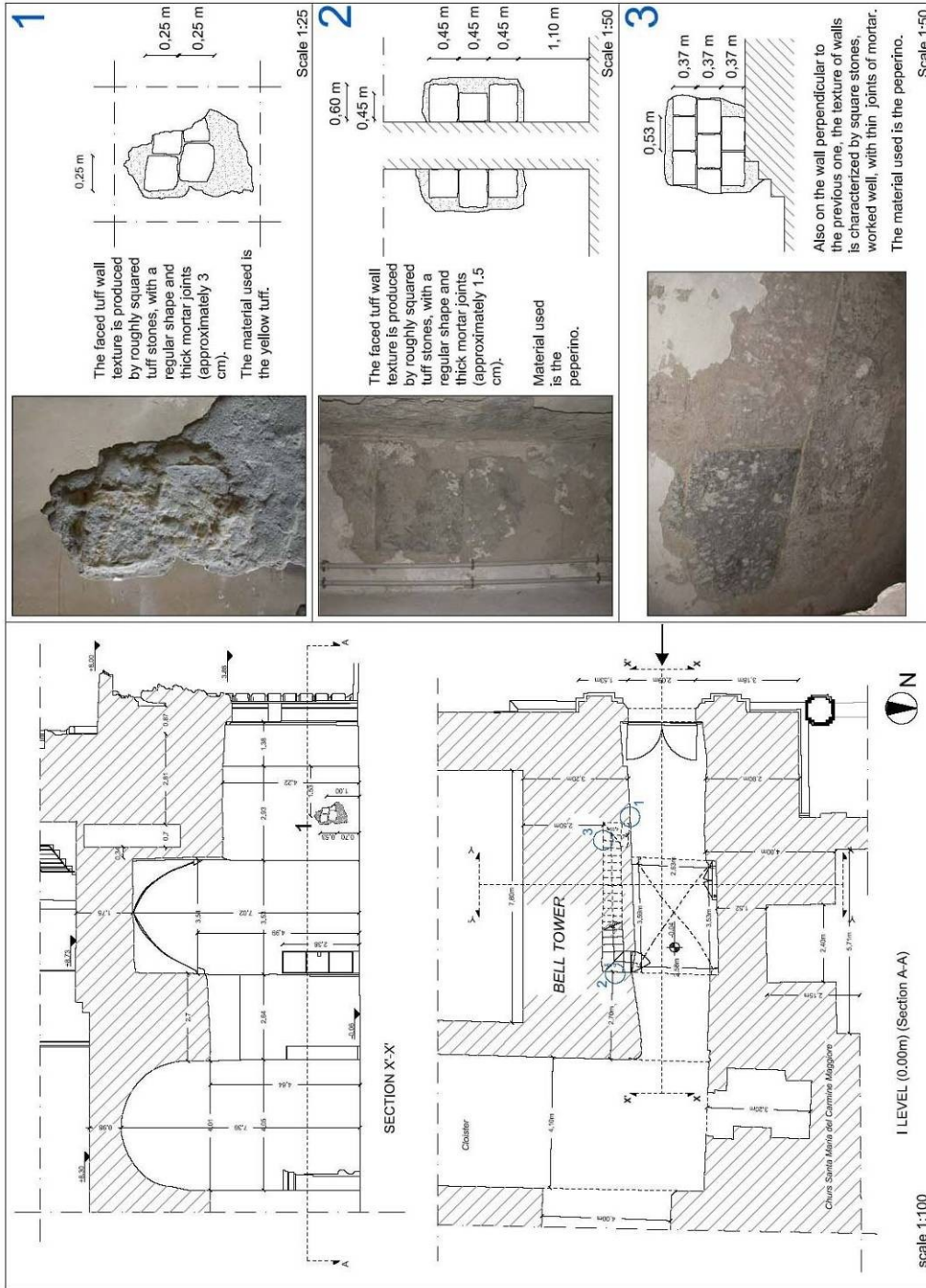
East Facade

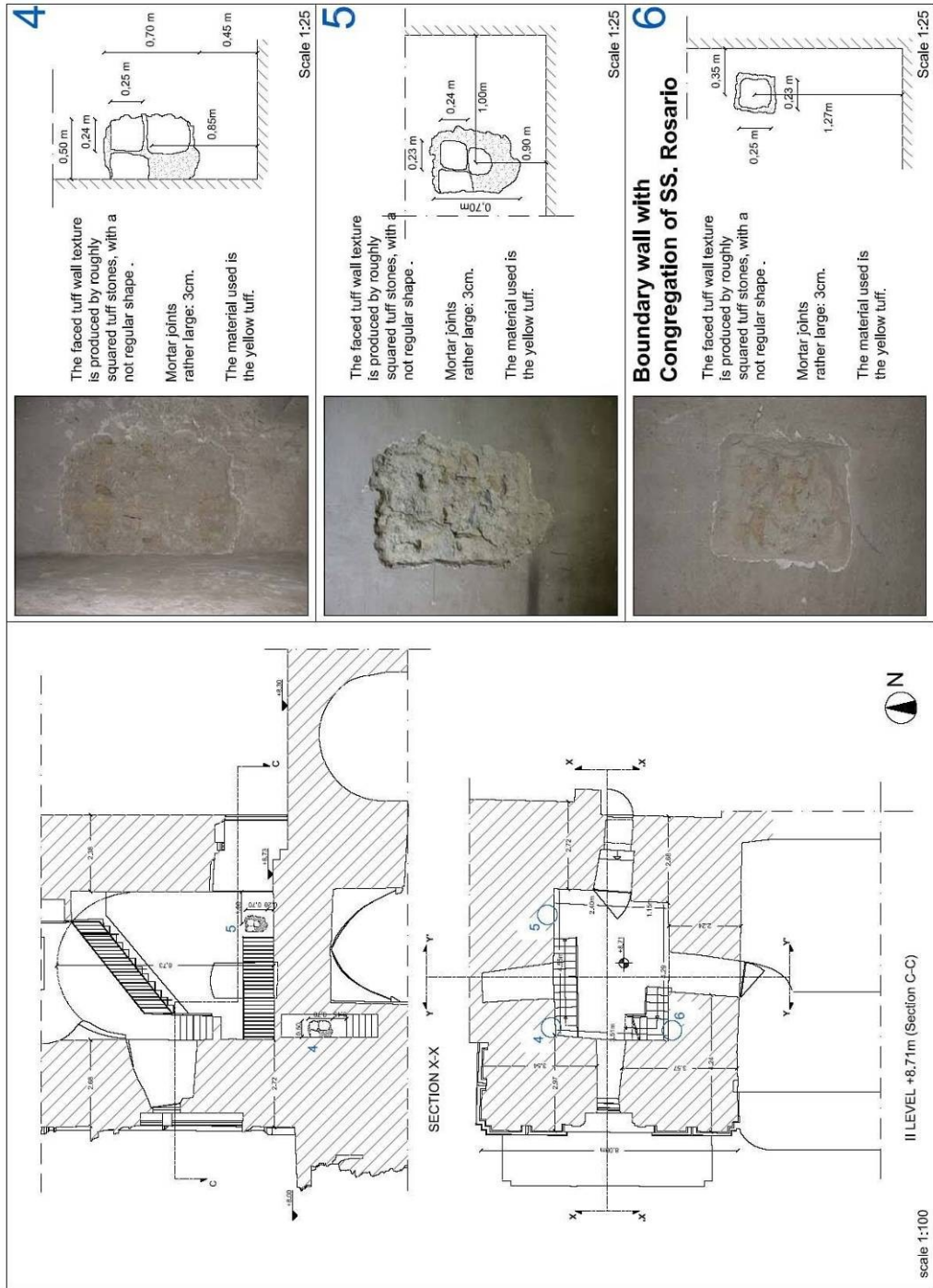


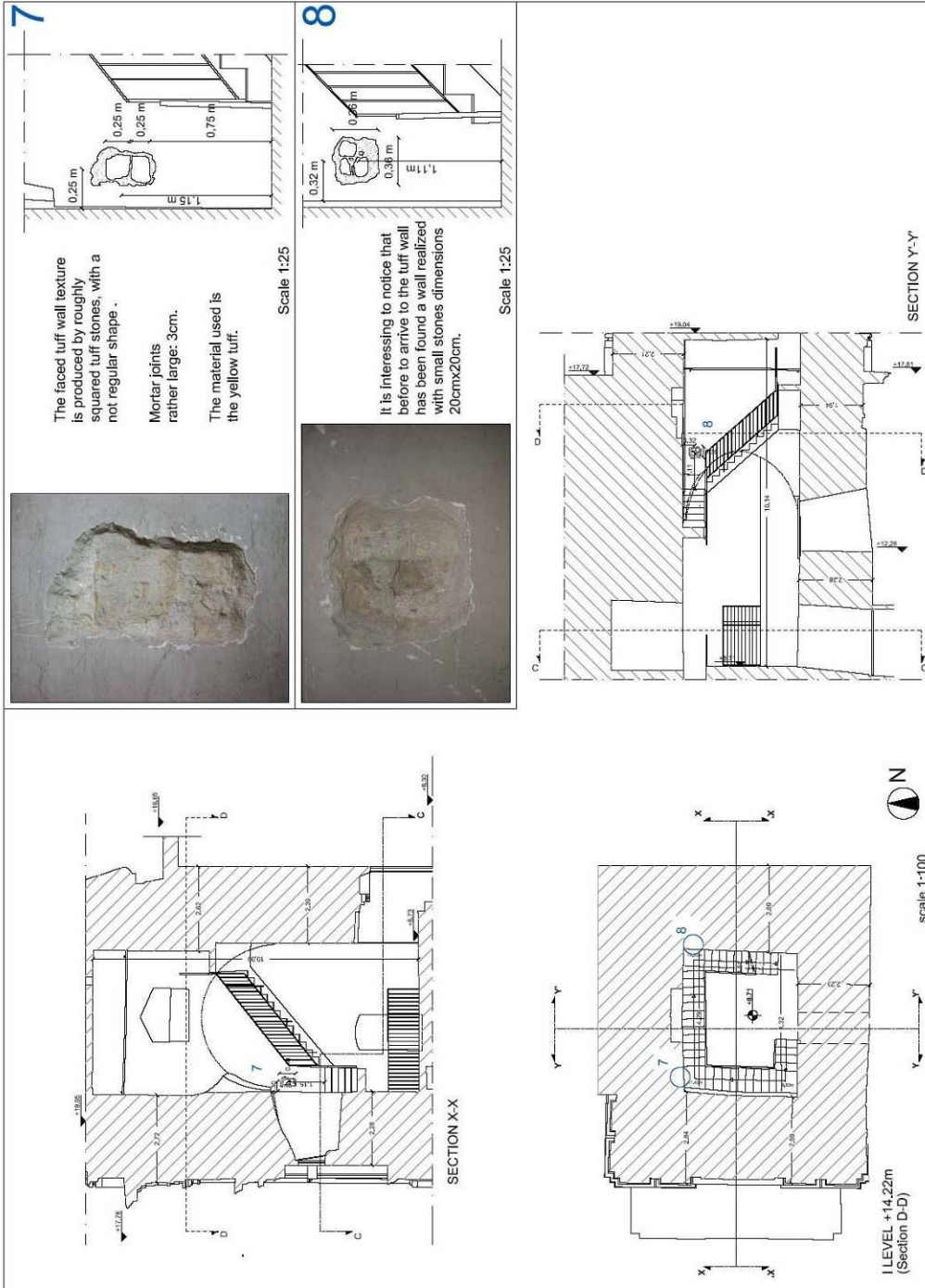
Longitudinal Section X'-X''

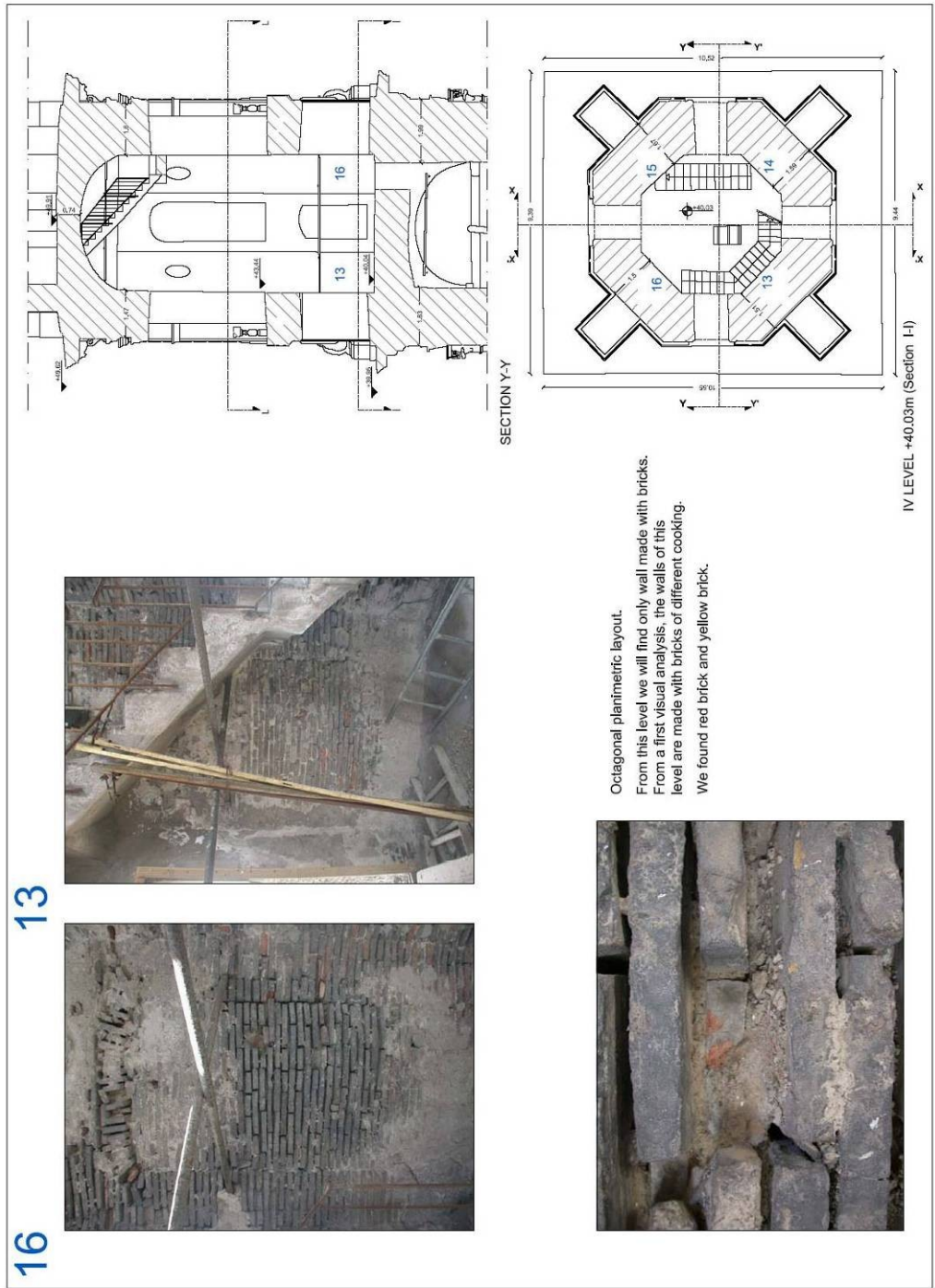
South Facade

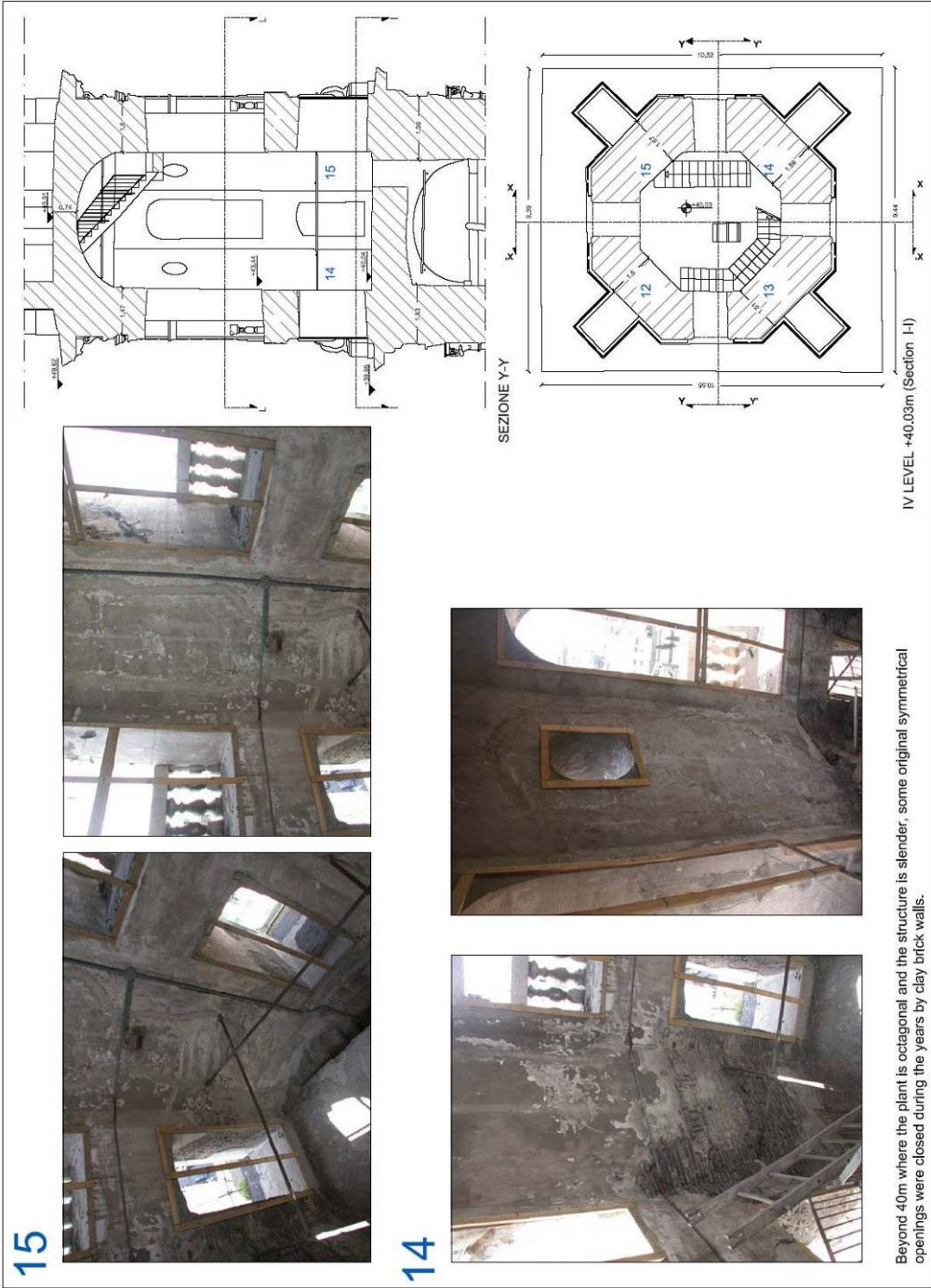
Appendix V



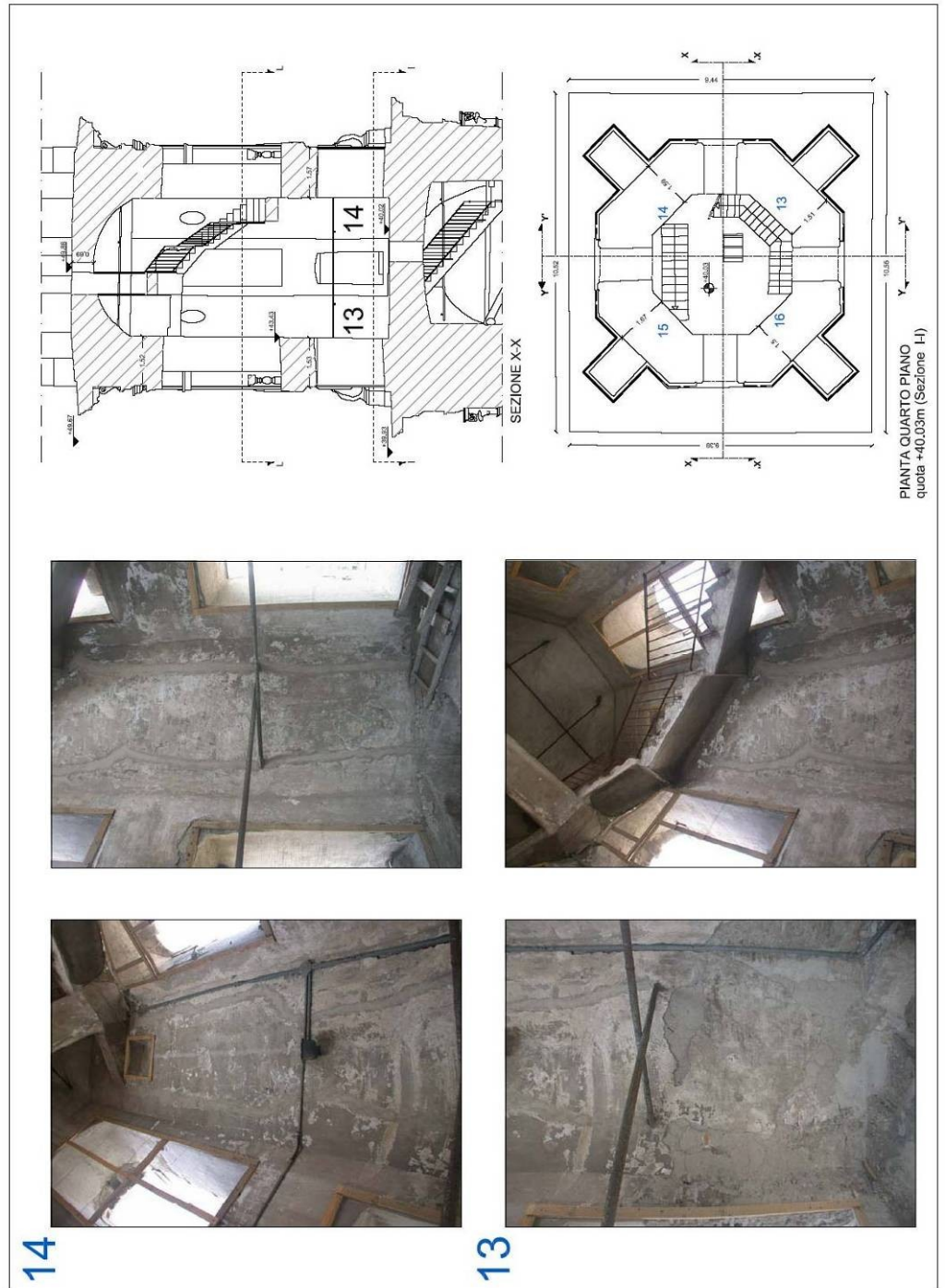




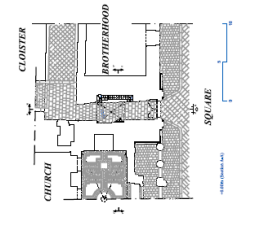
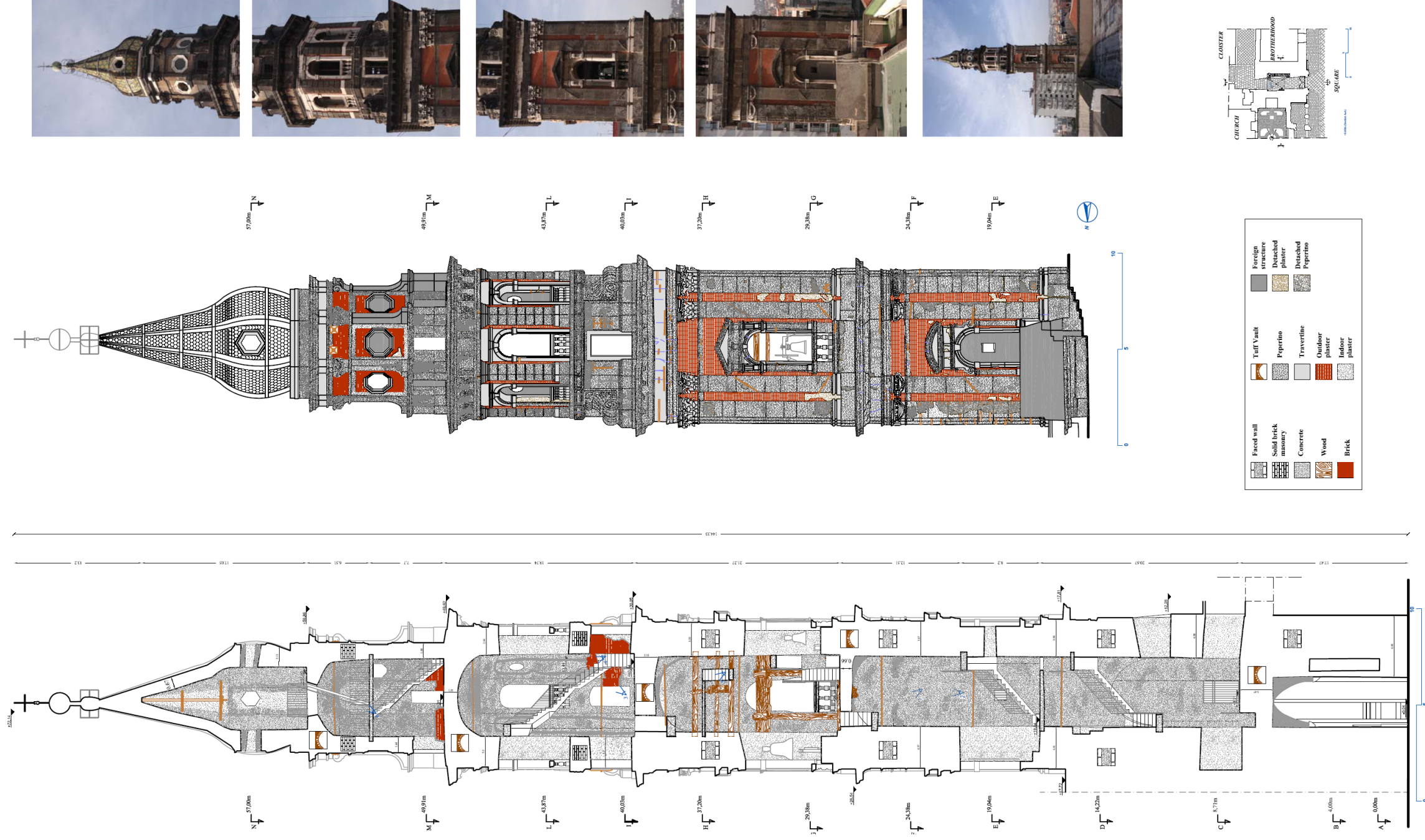




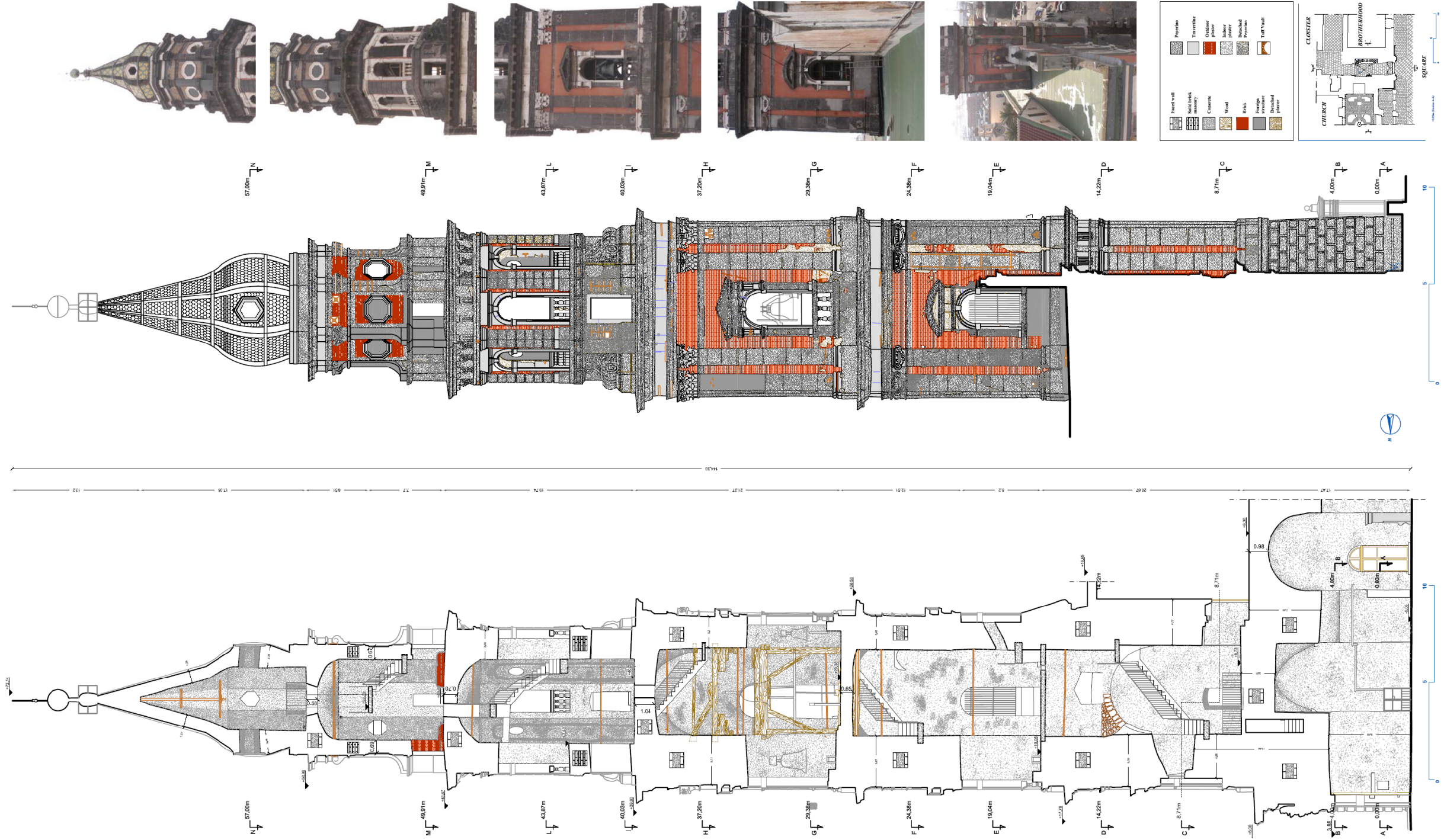
Beyond 40m where the plant is octagonal and the structure is slender, some original symmetrical openings were closed during the years by clay brick walls.



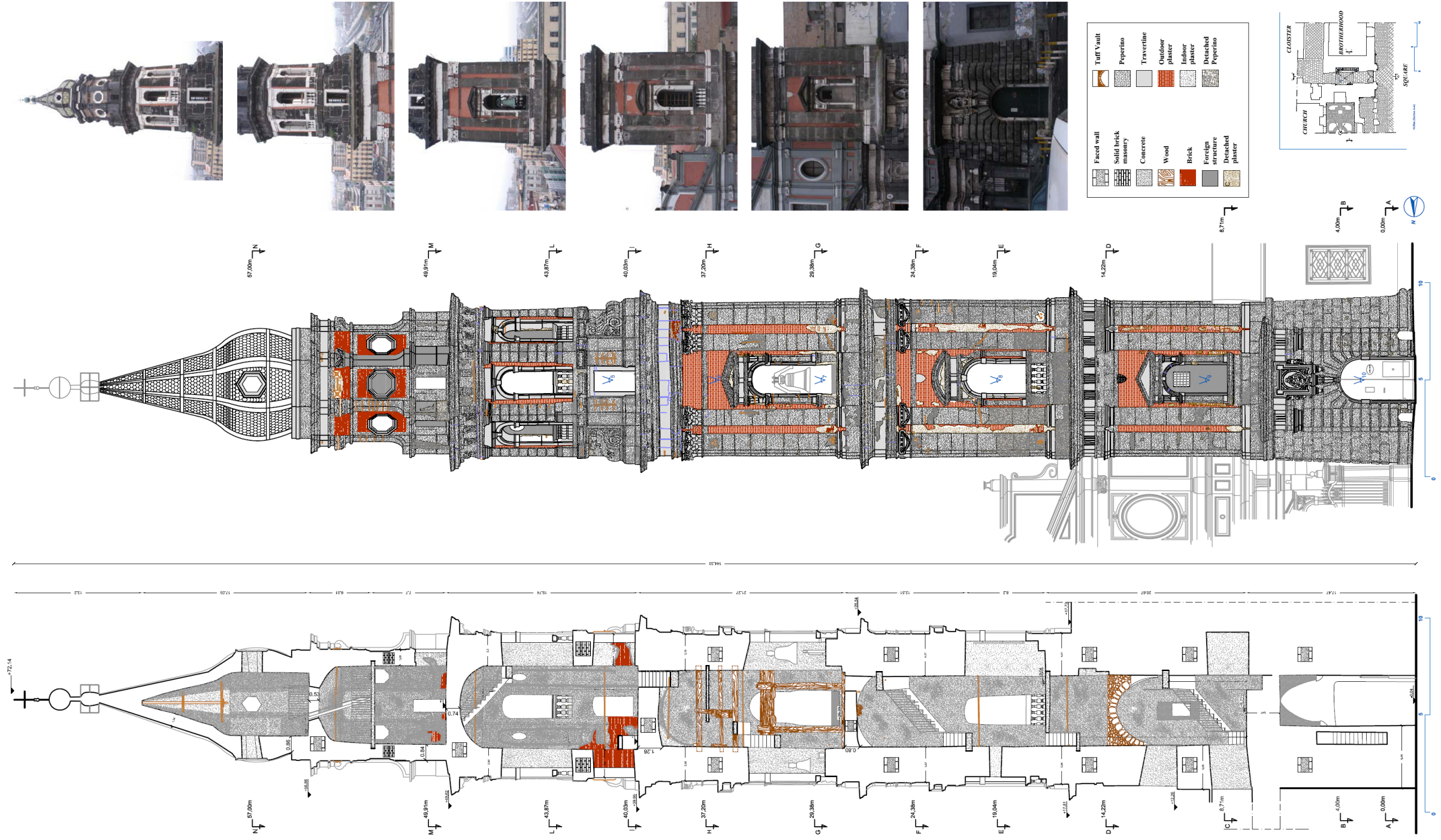
Appendix VI



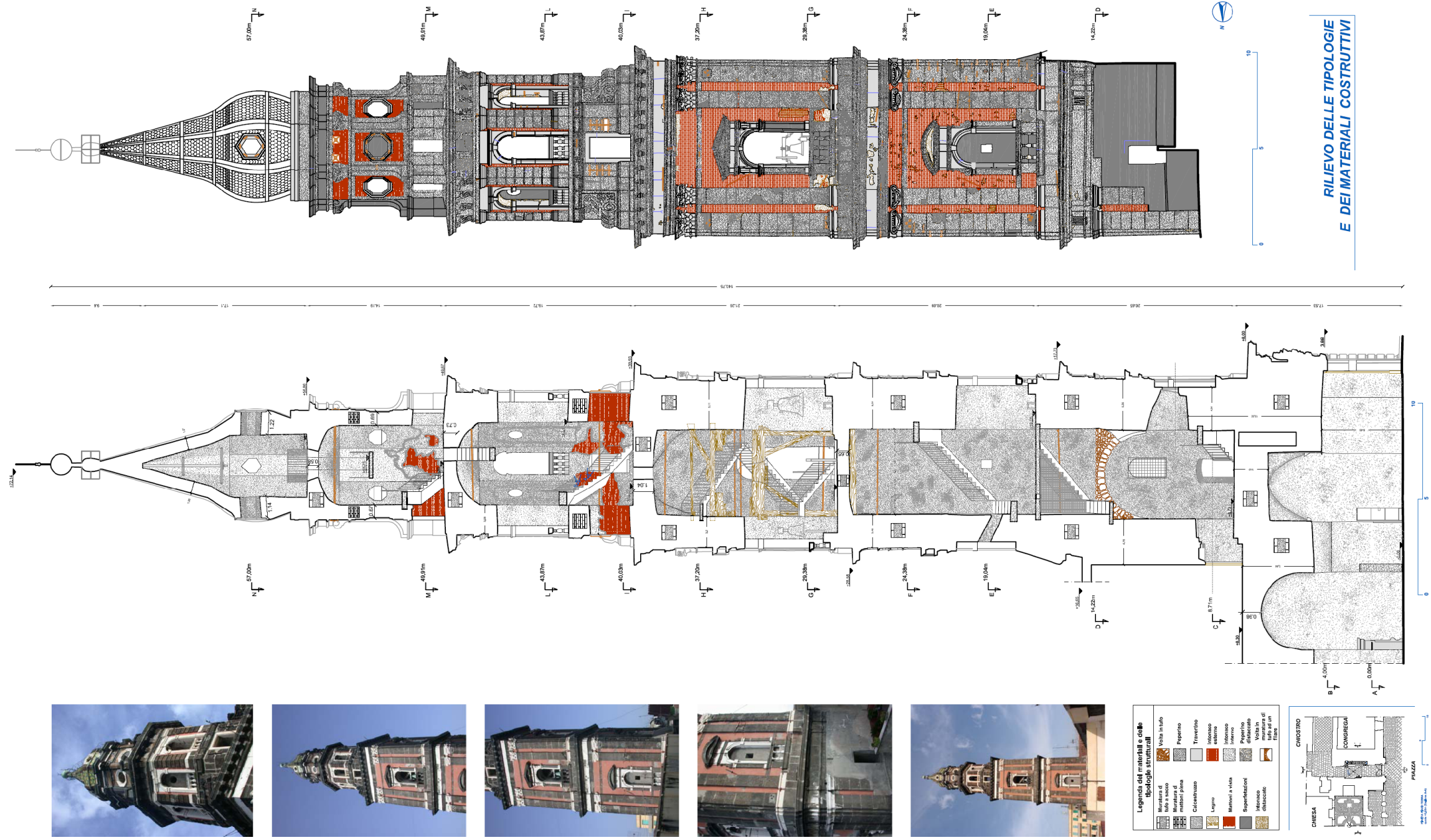
Longitudinal section Y-Y and East facade



Longitudinal section X'-X' and North facade



Longitudinal section Y-Y and West facade



Longitudinal section Y-Y and South facade

Appendix VII

Drawing's legend

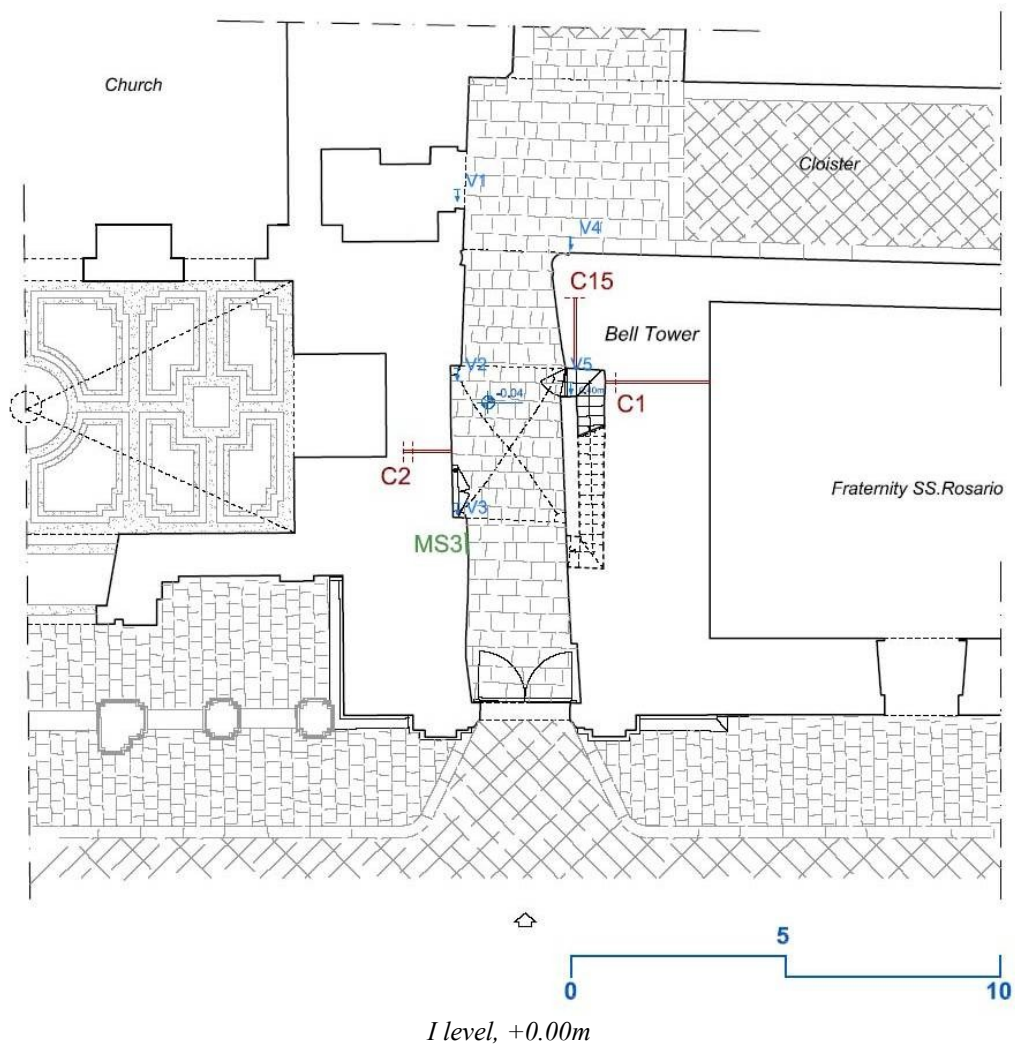
C: Coring

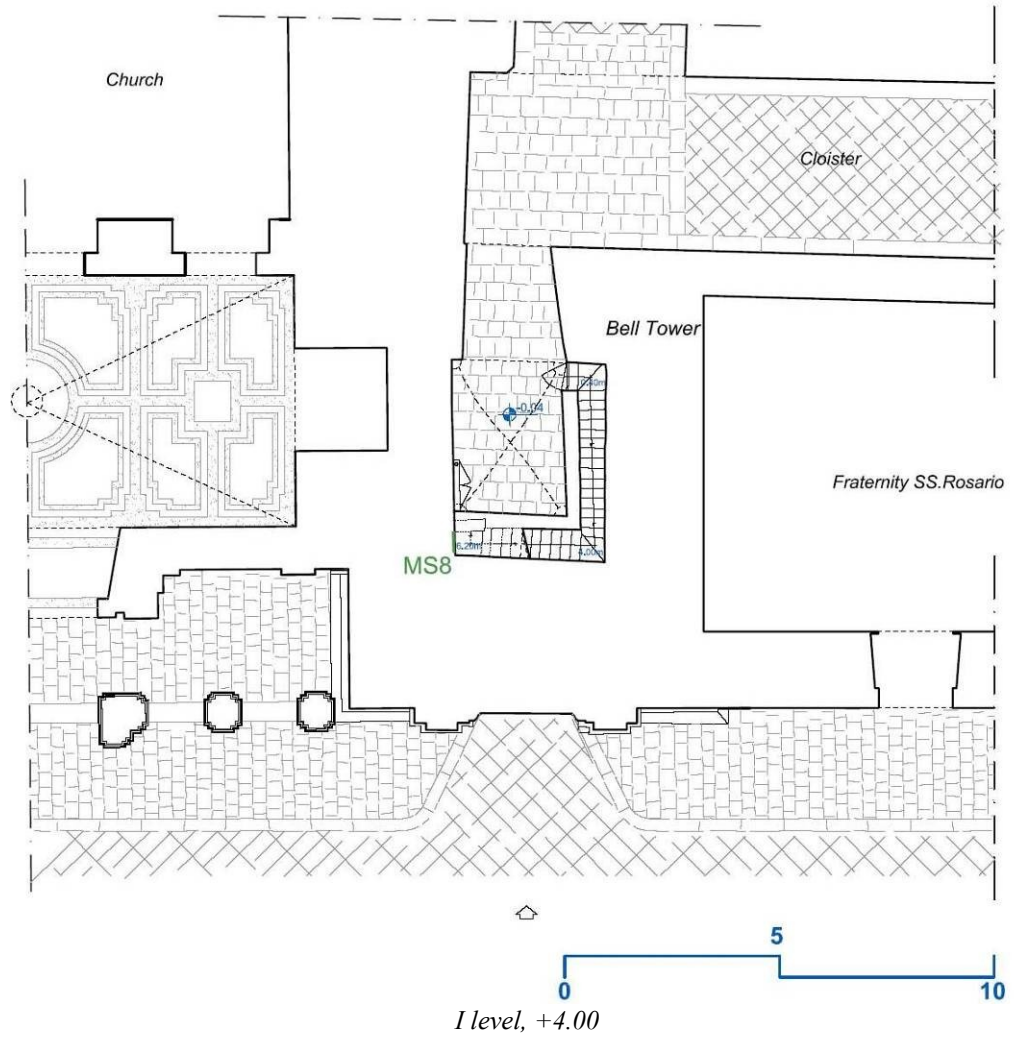
MD: Double flat jack

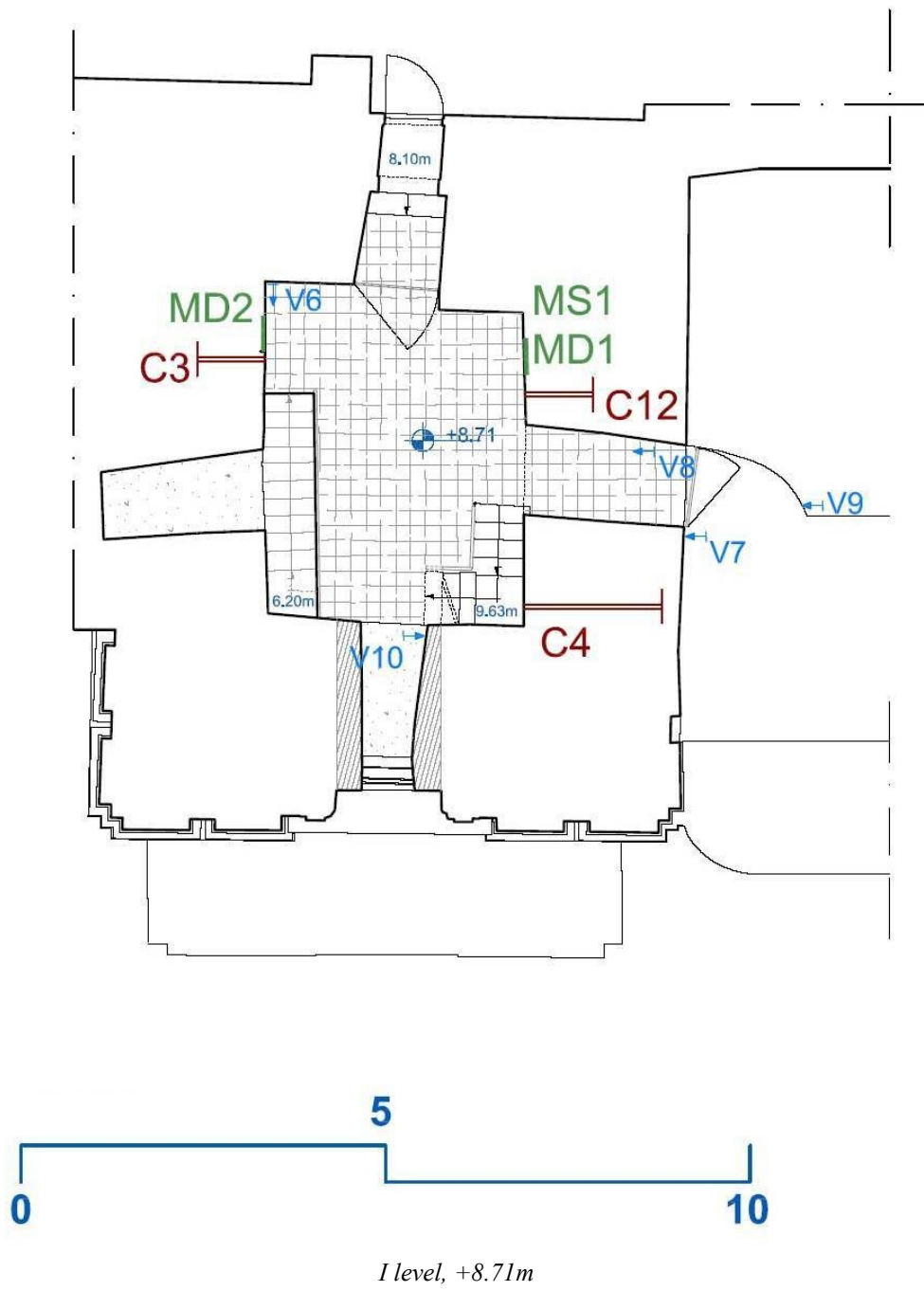
MS: Single flat jack

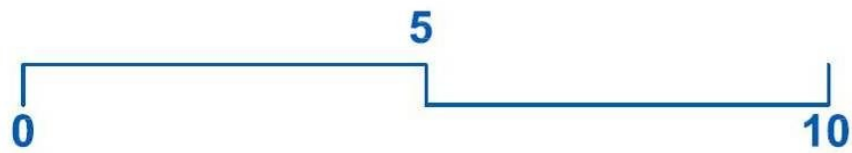
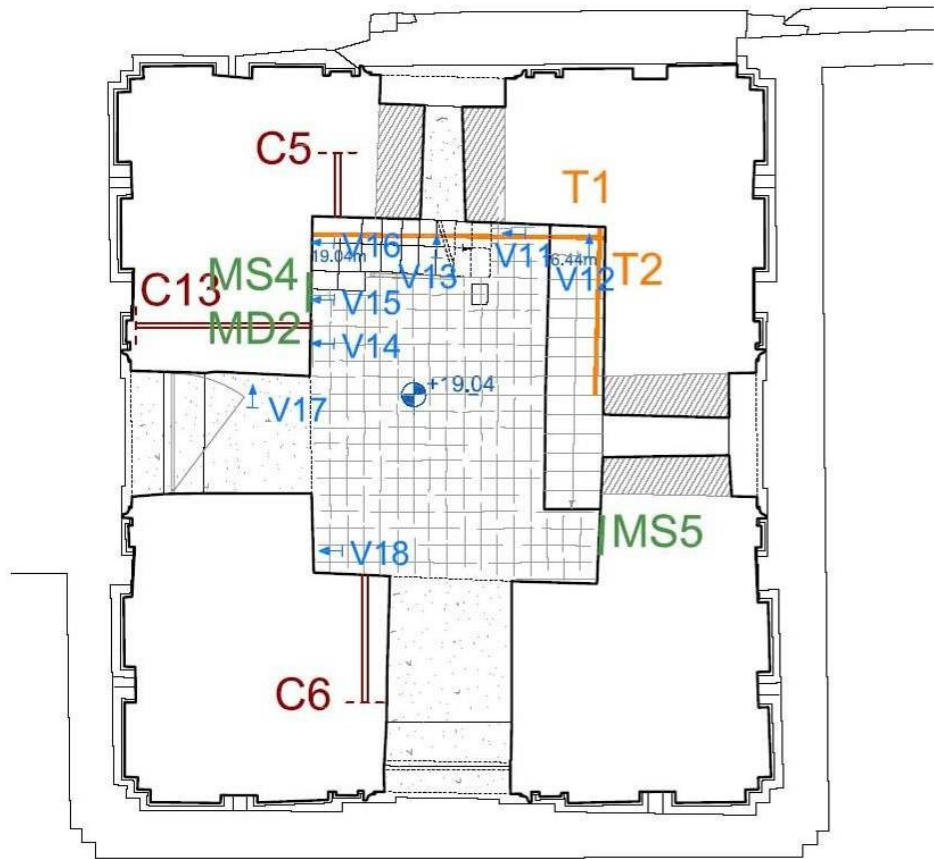
V: Waves inquires

T: Bar

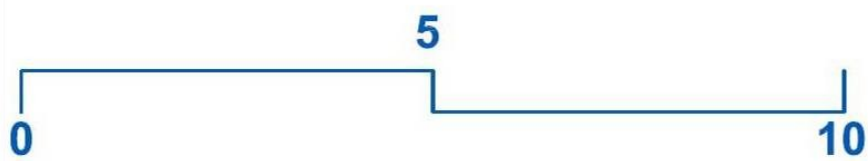
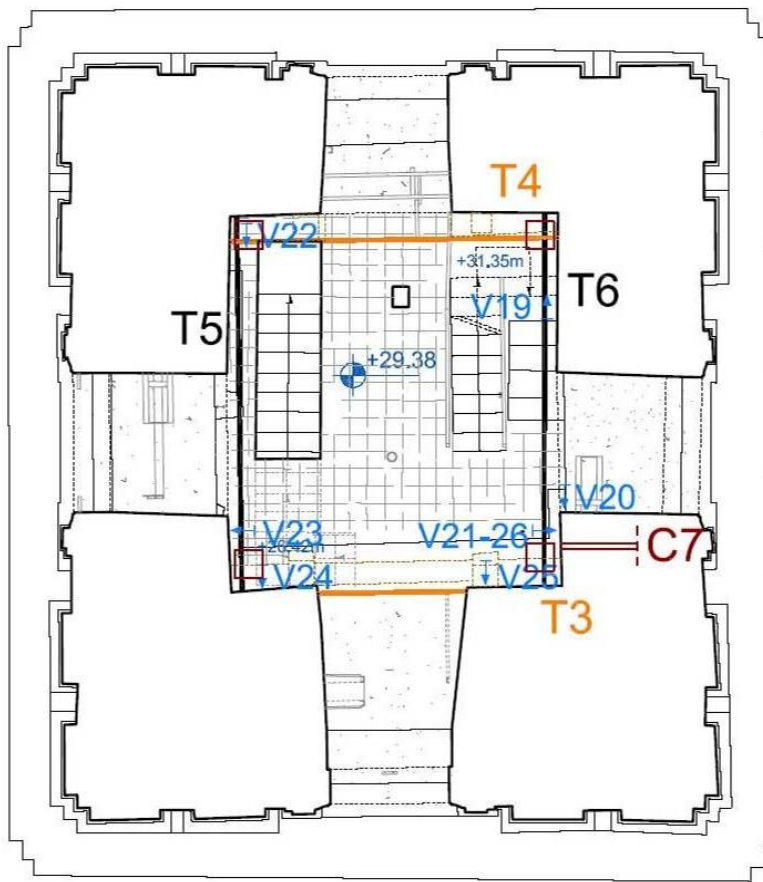




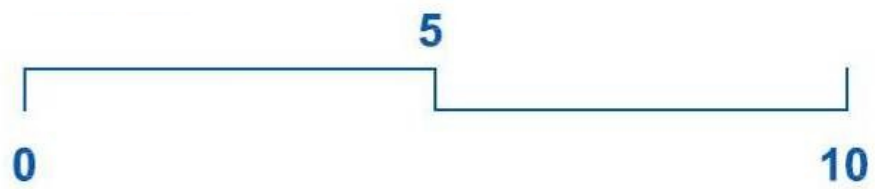
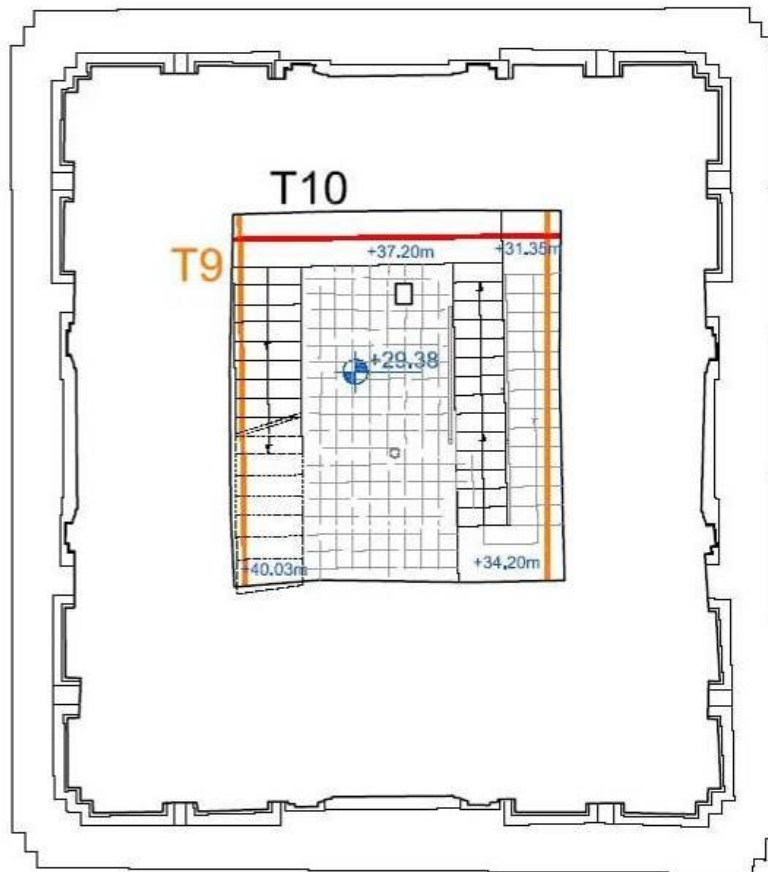




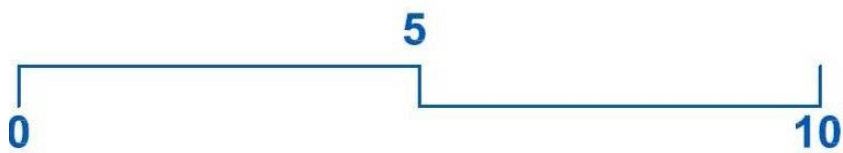
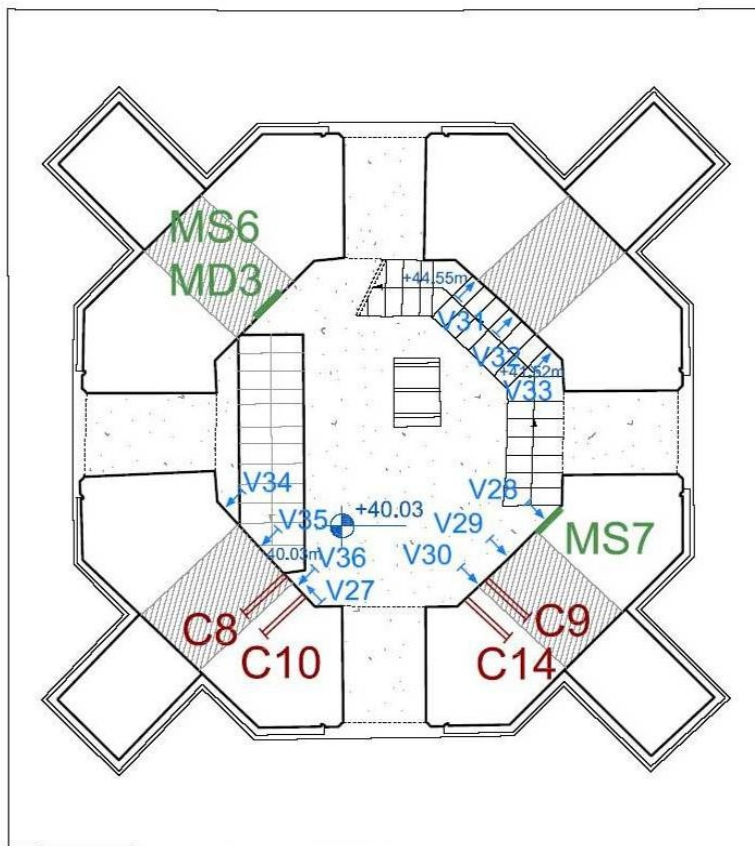
II level, +19.04m



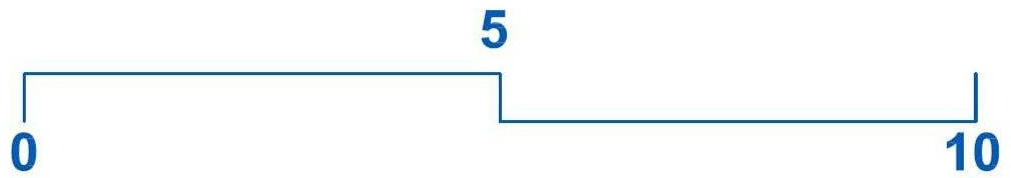
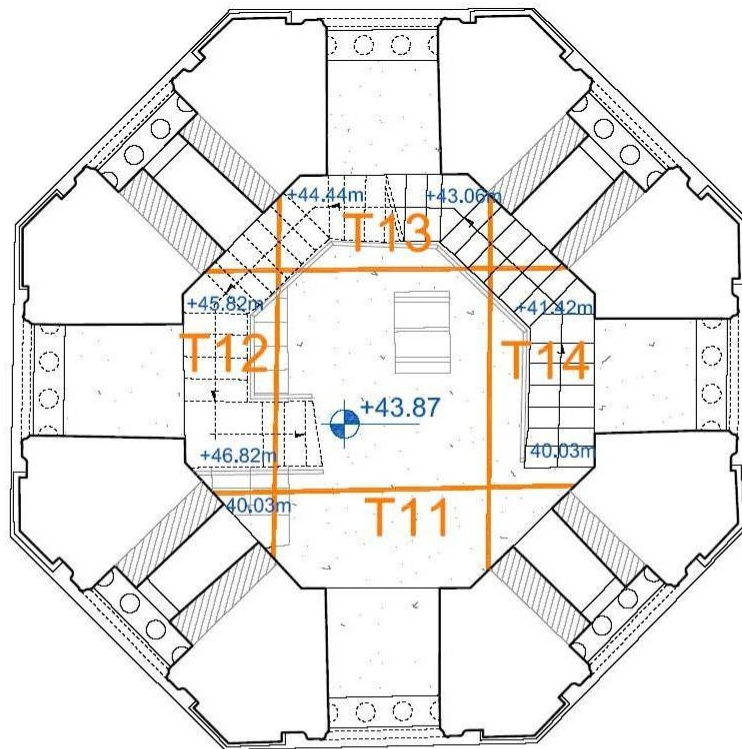
III level, +29.38m



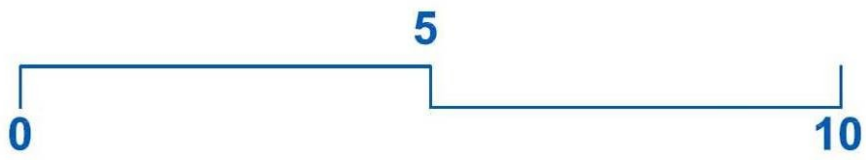
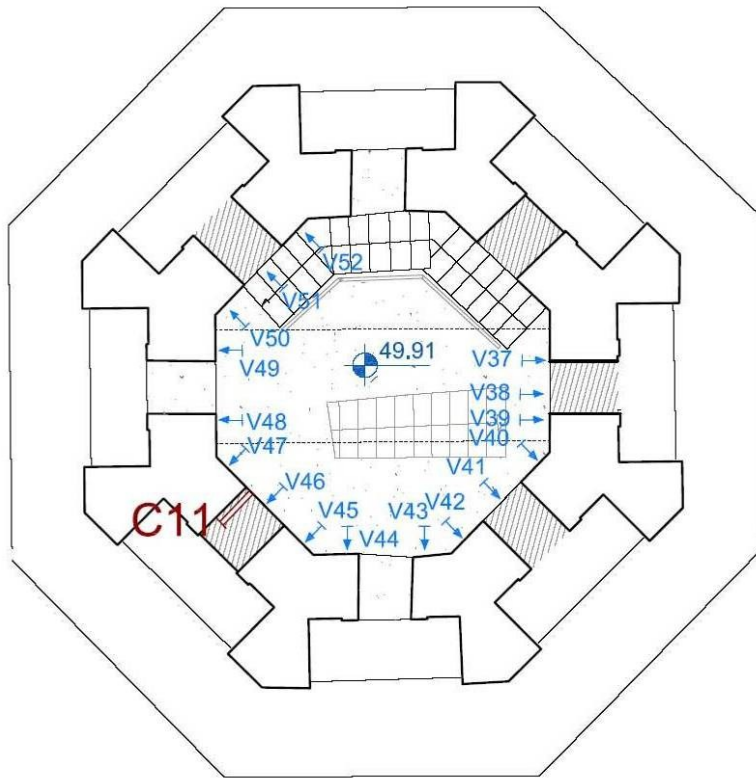
III level, +37.20m



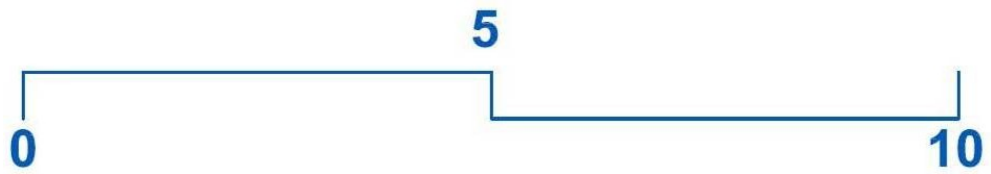
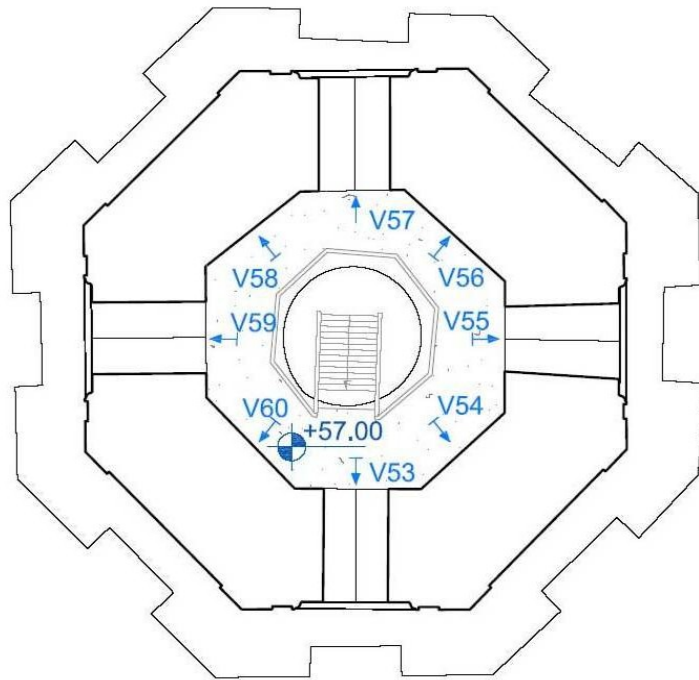
IV level, +40.03m



V level, +43.87m



VI level, +49.91m



VII level, +57.00m

Appendix VIII

	Location	Level (m)	Distance (m)	Longitudinal wave's time (ms)	Longitudinal wave's speed (m/s)	Transversal wave's time (ms)	Transversal wave's speed (m/s)
V1/1	North wall: +1,50 Horizontal	1,50	12,40	16,00	775	-	-
V1/2		1,50	3,70	6,40	578	-	-
V1/3		1,50	7,20	10,40	692	-	-
V2/1	North wall: +1,50 Horizontal	1,50	3,60	4,00	900	-	-
V2/1		1,50	8,50	11,20	759	-	-
V3	North wall: +1,50 Horizontal	1,50	4,90	6,30	778	-	-
V4	East wall: +1,50 Horizontal	1,50	2,65	2,20	1205	-	-
V5	South wall: +1,50 Horizontal	1,50	7,90	8,00	988	-	-
V6	North wall: +10,20 Horizontal	1,50	2,25	3,60	625	4,60	489
V7	South wall: +10,20 Horizontal	1,50	2,25	2,80	804	-	-
V8	South wall: +10,20 Horizontal	1,50	2,00	2,80	714	-	-
V9/1	South wall: +10,20 Horizontal	1,50	7,00	10,40	673	-	-
V9/2		0,50	7,00	17,20	407	-	-
V9/3		1,80	7,00	10,40	673	-	-
V10/1	West wall: +11,50 Horizontal	2,70	3,90	8,00	488	-	-
V10/2		2,70	4,00	Not connected walls		-	-
V11/1	East wall: +18,60 Horizontal	-1,50	3,80	6,80	559	-	-
V11/1		-1,50	4,00	7,60	526	-	-
V12	South wall: +18,60 Horizontal	-1,50	1,90	3,04	625	-	-
V13/1	East wall: +19,60 Horizontal	0,50	2,05	3,12	657	-	-
V13/2		1,00	2,05	3,62	566	-	-
V14/1	North wall: +20,70 Horizontal	1,30	2,20	3,60	611	-	-
V14/2		1,30	2,35	4,00	588	-	-
V15/1	North wall: +20,70 Horizontal	1,30	0,70	2,00	350	-	-
V15/2		1,30	1,06	2,16	491	-	-
V15/3		1,30	1,41	2,88	490	-	-
V15/4		1,30	1,76	2,96	595	-	-

	Location	Quote (m)	Distance (m)	Longitudinal wave's time (ms)	Longitudinal wave's speed (m/s)	Transversal wave's time (ms)	Transversal wave's speed (m/s)
V15/5	North wall: +20,70	1,30	2,11	4,00	528	-	-
V15/6	Horizontal	1,30	2,47	3,00	823	-	-
V16/1	North wall: +20,70	1,00	2,25	3,80	592	-	-
V16/2	Horizontal	1,00	2,35	4,20	560	-	-
V17/1	North wall: +20,70 Horizontal	1,30	3,80	3,20	1188	-	-
V17/2		1,30	3,60	4,40	818	-	-
V17/3		1,30	3,80	5,60	679	-	-
V18	North wall: +20,70 Horizontal	1,30	2,15	6,00	358	-	-
V19	South wall: +31,30 Horizontal	0,50	1,90	2,40	792	-	-
V20/1	South wall: +30,20	0,50	0,80	1,40	571	-	-
V20/2	Horizontal	2,50	0,80	1,76	455	-	-
V21	South wall: +33,50 Vertical	0,50	4,10	4,24	967	5,12	801
V22	North wall: +30,75 Horizontal	0,60	1,35	Discontinuity		-	-
V23	Nord wall: +31,50 Vertical	0,30	2,10	1,70	1235	-	-
V24	West wall: +31,40 Vertical	0,30	2,00	2,00	1000	-	-
V25	West wall: +31,55 Vertical	0,30	2,15	2,40	896	-	-
V26	South wall: +31,60 Vertical	0,50	2,20	2,30	957	-	-
V27/1	South-west wall: +40,10 Horizontal	Up doorbeam	1,50	2,24	670	-	-
V27/2		Up doorbeam	1,50	2,24	670	-	-
V27/3		On the doorbeam	1,50	2,48	605	-	-

	Location	Level (m)	Distance (m)	Longitudinal wave's time (ms)	Longitudinal wave's speed (m/s)	Transversal wave's time (ms)	Transversal wave's speed (m/s)
V27/4	South-west wall: +40,10 Horizontal	Under the doorbeam	1,50	1,80	833	-	-
V27/5		Under the doorbeam	1,50	1,60	938	-	-
V27/6		Under the doorbeam	1,50	1,60	938	-	-
V28	South-west wall: +40,50 Vertical	0.40	2,70	4,00	675	-	-
V29	South-west wall: +40,50 Vertical	0.40	2,70	3,84	703	-	-
V30	South-west wall: +40,50 Vertical	0.40	2,70	4,00	675	-	-
V31	South-east wall: +40,50 Vertical	0.40	3,30	4,96	665	-	-
V32	South-east wall: +40,50 Vertical	0.40	3,30	4,40	750	-	-
V33	South-east wall: +40,50 Vertical	0.40	3,30	4,98	663	-	-
V34	North-west wall: +40,50 Vertical	0.40	2,20	3,12	705	-	-
V35	North-west wall: +40,50 Vertical	0.40	2,20	3,76	585	-	-
V36	North-west wall: +40,50 Vertical	0.40	2,20	2,88	764	-	-
V37	South wall: +50,20 Vertical	0,20	1,80	2,96	608	-	-
V38	South wall: +50,20 Vertical	0,20	1,80	2,72	662	-	-

	Location	Elevation (m)	Distance (m)	Longitudinal wave's time (ms)	Longitudinal wave's speed (m/s)	Transversal wave's time (ms)	Transversal wave's speed (m/s)
V39	South west wall: +50,20	0,20	1,80	2,40	750	-	-
V40	Vertical	0,20	1,80	2,48	726		
V41	South west wall: +50,20	0,20	1,80	2,40	750	-	-
V42	Vertical	0,20	1,80	2,48	726	-	-
V43	West wall: +50,20	0,20	1,80	2,24	804	-	-
V44	Vertical	0,20	1,80	2,00	900	-	-
V45	North west wall: +50,20	0,20	1,80	2,32	776	-	-
V46	Vertical	0,20	1,80	2,88	625	-	-
V47	North west wall: +50,20	0,20	1,80	2,32	776	-	-
V48	Vertical	0,20	1,80	2,16	833	-	-
V49	North wall: +50,20	0,20	1,80	2,00	900	-	-
V50	Vertical	0,20	1,80	2,40	750	-	-
V51	North east wall: +50,20	0,20	1,80	2,06	874	-	-
V52	Vertical	0,20	1,80	2,08	865	-	-
V53	West wall: +50,20	0,20	1,70	2,88	590	-	-
V54	Vertical	0,20	1,70	3,12	545	-	-
V55	South west wall: +57,20	0,20	1,70	3,12	545	-	-
V56	Vertical	0,20	1,70	2,96	574	-	-

	Location	Elevation (m)	Distance (m)	Longitudinal wave's time (ms)	Longitudinal wave's speed (m/s)	Transversal wave's time (ms)	Transversal wave's speed (m/s)
V57	East wall: +57,20 Vertical	0,20	1,70	4,56	373		
V58	North east wall: +57,20 Vertical	0,20	1,70	2,24	759		
V59	North wall: +57,20 Vertical	0,20	1,70	2,40	708		
V60	North east wall: +57,20 Vertical	0,20	1,70	2,24	759		

Appendix IX

n°	level	direction	N	D	Area	sigma	Elettrogalvanic measurements		
	m		[kg]	[mm]	[cmq]	[kg/cmq]	[amp]	[milliVolts]	[amp x mlliVolts]
22	55,8	y	5396	38,5	11,6	463,5	0,0030	5879	17,6
21	55,8	y	3038	32,0	8,0	377,7	0,0030	6031	18,1
20	55,8	x	0	35,0	9,6	0,0	0,0310	4712	146,1
19	55,8	y	0	36,0	10,2	0,0	0,0190	5017	95,3
18	55,8	y	2221	33,0	8,6	259,7	0,0090	5001	45,0
17	55,8	x	7518	31,0	7,5	996,1	0,0230	5634	129,6
16	48,6	x	-36	40,0	12,6	-2,9	0,0190	5439	103,3
15	48,6	y	158	40,0	12,6	12,6	0,0080	7627	61,0
14	42	y	6816	40,0	12,6	542,4	0,0040	5308	21,2
13	42	x	8996	40,0	12,6	715,9	0,0030	5644	16,9
12	42	y	7170	40,0	12,6	570,6	0,0020	5628	11,3
11	42	x	5224	40,0	12,6	415,7	0,0020	6010	12,0
10	38,7	x	-47	42,0	13,9	-3,4	0,0050	5233	26,2
9	38,7	y	2079	40,0	12,6	165,4	0,0020	6638	13,3
8	34,7	x	1582	40,0	12,6	125,9	0,0070	6001	42,0
7	34,7	y	5234	43,0	14,5	360,4	0,0100	4763	47,6
6	30,5	y	-342	51,0	20,4	-16,7	0,0009	7899	7,1
5	30,5	y	690	51,0	20,4	33,8	0,0010	4980	5,0
4	30,5	x	8026	50,0	19,6	408,8	0,0007	7248	5,1
3	27,5	y	3767	42,0	13,9	271,9	0,0010	4937	4,9
2	18	y	6260	42,0	13,9	451,8	0,0007	8003	5,6
1	18	x	8346	42,0	13,9	602,4	0,0004	8321	3,3
max						996,1	0,0310	8321	146,1
min						-16,7	0,0004	4712	3,3

Appendix X

Tie bars checked	n°	Floor	Typology	Diameter	Level [m]	Dir.	Wall	Anchoring	Tension Stress
	1	+0.0-+19.0m	Tie-bar		+17.8	NS	West	Horizontal steel bar	
T1	2	+0.0-+19.0m	Tie-bar	42	+17.8	NS	East	Horizontal steel bar	602
T2	3	+0.0-+19.0m	Tie-bar	42	+17.8	EO	North	Not visible	452
	4	+0.0-+19.0m	Tie-bar		+17.8	EO	South	Horizontal steel bar	
	5	+19.0-29.0m	6 strands	7 ϕ 4	+19.5	NS	West	Plate	
	6	+19.0-29.0m	6 strands	7 ϕ 4	+19.5	NS	East	Plate	
	7	+19.0-29.0m	6 strands	7 ϕ 4	+19.5	EO	North	Plate	
	8	+19.0-29.0m	6 strands	7 ϕ 4	+19.5	EO	South	Plate	
	9	+19.0-29.0m	Tie-bar		+22.5	NS	West	Inclined steel bar	
	10	+19.0-29.0m	Tie-bar		+22.5	NS	West	Not visible	
	11	+19.0-29.0m	Tie-bar		+22.5	NS	East	Inclined steel bar	
	12	+19.0-29.0m	Tie-bar		+22.5	EO	North	Inclined steel bar	
	13	+19.0-29.0m	Tie-bar		+22.5	EO	South	Inclined steel bar	
	14	+19.0-29.0m	6 strands	7 ϕ 4	+25.5	NS	West	Plate	
	15	+19.0-29.0m	6 strands	7 ϕ 4	+25.5	NS	East	Plate	
	16	+19.0-29.0m	6 strands	7 ϕ 4	+25.5	EO	North	Plate	
	17	+19.0-29.0m	6 strands	7 ϕ 4	+25.5	EO	South	Plate	
	18	+19.0-29.0m	Tie-bar	42mm	+28.6	NS	West	Horizontal steel bar	
	19	+19.0-29.0m	Tie-bar	42mm	+28.6	NS	East	Horizontal steel bar	
T3	20	+19.0-29.0m	Tie-bar	42mm	+28.6	EO	North	Horizontal steel bar	272
	21	+19.0-29.0m	Tie-bar	42mm	+28.6	EO	South	Horizontal steel bar	
	22	+29.0-39.0m	6 strands	7 ϕ 4	+30.2	NS	West	Plate	
	23	+29.0-39.0m	6 strands	7 ϕ 4	+30.2	NS	East	Plate	
	24	+29.0-39.0m	6 strands	7 ϕ 4	+30.2	EO	North	Plate	
	25	+29.0-39.0m	6 strands	7 ϕ 4	+30.2	EO	South	Plate	
	26	+29.0-39.0m	Tie-bar	50mm	+30.2	NS	West	Inclined steel bar	
T4	27	+29.0-39.0m	Tie-bar	50mm	+30.2	NS	East	Inclined steel bar	409
T5	28	+29.0-39.0m	Tie-bar	50mm	+30.2	EO	North	Inclined steel bar	34
T6	29	+29.0-39.0m	Tie-bar	50mm	+30.2	EO	South	Inclined steel bar	-17
T8	30	+29.0-39.0m	Tie-bar	40mm	+34.6	NS	West	Inclined steel bar	
	31	+29.0-39.0m	Tie-bar	40mm	+34.6	NS	East	Inclined steel bar	
	32	+29.0-39.0m	Tie-bar	40mm	+34.6	EO	North	Steel bar inclinata	

T7	33	+29.0-39.0m	Tie-bar	40mm	+34.6	EO	South	Inclined steel bar	360
	34	+29.0-39.0m	6 strands	7 ϕ 4	+36.0	NS	West	Plate	
	35	+29.0-39.0m	6 strands	7 ϕ 4	+36.0	NS	East	Plate	
	36	+29.0-39.0m	6 strands	7 ϕ 4	+36.0	EO	North	Plate	
	37	+29.0-39.0m	6 strands	7 ϕ 4	+36.0	EO	South	Plate	
	38	+29.0-39.0m	Tie-bar		+38.4	NS	West	Horizontal steel bar	
T10	39	+29.0-39.0m	Tie-bar	42mm	+38.4	NS	East	Horizontal steel bar	-3
T9	40	+29.0-39.0m	Tie-bar	40mm	+38.4	EO	North	Horizontal steel bar	165
	41	+29.0-39.0m	Tie-bar		+38.4	EO	South	Horizontal steel bar	
T13	42	+39.0-49.0m	Tie-bar	40mm	+41.7	NS	West	Vertical steel bar	716
T11	43	+39.0-49.0m	Tie-bar	40mm	+41.7	NS	East	Vertical steel bar	416
T12	44	+39.0-49.0m	Tie-bar	40mm	+41.7	EO	North	Vertical steel bar	571
T14	45	+39.0-49.0m	Tie-bar	40mm	+41.7	EO	South	Vertical steel bar	542
T16	46	+39.0-49.0m	Tie-bar		+48.3	NS	West	Not visible	
	47	+39.0-49.0m	Tie-bar	40mm	+48.3	NS	East	Not visible	-3
T15	48	+39.0-49.0m	Tie-bar	40mm	+48.3	EO	North	Not visible	13
	49	+39.0-49.0m	Tie-bar		+48.3	EO	South	Not visible	
T17	50	+49.0-56.0m	Tie-bar	31	+55.5	NS	West	Plate	996
T20	51	+49.0-56.0m	Tie-bar	35	+55.5	NS	East	Plate	0
T19	52	+49.0-56.0m	Tie-bar	36	+55.5	EO	North	Not visible	0
T18	53	+49.0-56.0m	Tie-bar	33	+55.5	EO	North	Plate	260
T21	54	+49.0-56.0m	Tie-bar	32	+55.5	EO	South	Plate	378
T22	55	+49.0-56.0m	Tie-bar	38	+55.5	EO	South	Not visible	464